UAB
Universitat Autònoma de Barcelona

Development of the Industrial Process to Manufacture a Highly Potent Active Pharmaceutical Ingredient

Ronnie Andrés Miranda Salinas

ADVERTIMENT. L'accés als continguts d'aquesta tesi doctoral i la seva utilització ha de respectar els drets de la persona autora. Pot ser utilitzada per a consulta o estudi personal, així com en activitats o materials d'investigació i docència en els termes establerts a l'art. 32 del Text Refós de la Llei de Propietat Intel·lectual (RDL 1/1996). Per altres utilitzacions es requereix l'autorització prèvia i expressa de la persona autora. En qualsevol cas, en la utilització dels seus continguts caldrà indicar de forma clara el nom i cognoms de la persona autora i el títol de la tesi doctoral. No s'autoritza la seva reproducció o altres formes d'explotació efectuades amb finalitats de lucre ni la seva comunicació pública des d'un lloc aliè al servei TDX. Tampoc s'autoritza la presentació del seu contingut en una finestra o marc aliè a TDX (framing). Aquesta reserva de drets afecta tant als continguts de la tesi com als seus resums i índexs.

ADVERTENCIA. El acceso a los contenidos de esta tesis doctoral y su utilización debe respetar los derechos de la persona autora. Puede ser utilizada para consulta o estudio personal, así como en actividades o materiales de investigación y docencia en los términos establecidos en el art. 32 del Texto Refundido de la Ley de Propiedad Intelectual (RDL 1/1996). Para otros usos se requiere la autorización previa y expresa de la persona autora. En cualquier caso, en la utilización de sus contenidos se deberá indicar de forma clara el nombre y apellidos de la persona autora y el título de la tesis doctoral. No se autoriza su reproducción u otras formas de explotación efectuadas con fines lucrativos ni su comunicación pública desde un sitio ajeno al servicio TDR. Tampoco se autoriza la presentación de su contenido en una ventana o marco ajeno a TDR (framing). Esta reserva de derechos afecta tanto al contenido de la tesis como a sus resúmenes e índices.

WARNING. The access to the contents of this doctoral thesis and its use must respect the rights of the author. It can be used for reference or private study, as well as research and learning activities or materials in the terms established by the 32nd article of the Spanish Consolidated Copyright Act (RDL 1/1996). Express and previous authorization of the author is required for any other uses. In any case, when using its content, full name of the author and title of the thesis must be clearly indicated. Reproduction or other forms of for profit use or public communication from outside TDX service is not allowed. Presentation of its content in a window or frame external to TDX (framing) is not authorized either. These rights affect both the content of the thesis and its abstracts and indexes.

Faculty of Science

Department of Chemistry

Ph.D. in Chemistry

Ph.D. Thesis

Development of the Industrial Process to Manufacture a Highly Potent Active Pharmaceutical Ingredient

Ronnie Andrés Miranda Salinas

2024

Thesis Director

Dr. Joan Pau Bayón Rueda

Department of Chemistry

Universitat Autònoma de Barcelona

Company Supervisor

Mr. Albert Corominas Tarruella

Moehs Ibérica S.L.

Ph.D. Thesis presented by Ronnie Andrés Miranda Salinas to obtain the degree of Doctor by Universitat Autònoma de Barcelona

Directed and reviewed by

Dr. Joan Pau Bayón Rueda

Reviewed by

Mr. Albert Corominas Tarruella

Acknowledgements

The success and final outcome of this thesis required the guidance and assistance from many people and I fell really privileged to have worked with all of them along the completion of my project. All that I have learned and which is reflected in this project is due to the support of all my mates and I would not forget to thank them.

This doctoral thesis has been performed from April 2021 to May 2024 in R&D department of Moehs Ibérica S.L. in collaboration with the Chemistry department of the Universitat Autònoma de Barcelona (UAB) under the supervision of Albert Corominas Tarruella and the direction of Dr. Joan Pau Bayon Rueda. I would like to thank for the dedication, patience, help and guidance and also for the knowledge transmitted during these years.

Also a special gratitude to Moehs' R&D Director Helena Camps and Product Life-cycle Manager Isabel Lloveras to render me the opportunity to work with them in this amazing and challenging project.

Thank you Agencia de Gestió d'Ajuts Universitaris i de Recerca (AGAUR) of Generalitat de Catalunya for the funding and the trust placed and the training received.

I have a special mention to Adria Vernet, Guiu Perez, Blanca López and Laura Badia for all good moments lived together, which have been a part of my life becoming my second family. I also would like to extend my sincere esteem to all staff in the laboratory for their support.

A special thank to my family to their unconditional support, specially to Irene for her patience and support in the most difficult moments. To my parents to whom I owe to be the person I am today.

To my grandmother, chemical engineer and my second mother. You awoke my passion for science since I was too young to understand it. I'm sure you would be proud to read my thesis. I have no words to thank you such a treasure you gave me. Rest in peace.

"*It may seem that science is a method of providing answers to basic questions. However, history shows us that when a really big step is taken in knowledge is when we realize what was the correct way to formulate those questions."*

Beyond The Stars. Photographing A Black Hole

Table of Contents

Abbreviations and acronyms.....Page I

Structure index.....Page IV

Chapter 1. General introduction.....Page 1

1.1 Company introduction.....Page 3

1.2 Highly Potent Active Pharmaceutical Ingredients.....Page 4

1.3 α_2-adrenergic receptors agonist for sedation.....Page 6

1.4 State of the art for the synthesis of a HPAPI for sedation.....Page 8

1.5 Project strategy.....Page 17

Chapter 2. Optimization of the current synthesis.....Page 21

2.1 Obtention of the starting material **19**.....Page 22

2.2 Synthesis of the ketone **21**.....Page 23

2.2.1 Studies on the formation of Grignard **20**.....Page 24

2.2.2 Studies on the deprotonation of imidazole **19**.....Page 26

2.2.3 Studies on the formation of Imine-magnesium intermediate complex **54**.....Page 27

2.2.4 Studies on the hydrolysis of imine-magnesium complex **54**.....Page 28

2.2.5 Studies on the purification and precipitation of ketone **21**...Page 28

2.3 Synthesis of the alkene **14**.....Page 30

2.3.1 Studies on methyl addition to ketone **21**.....Page 31

2.3.2 Studies on the dehydration of tertiary alcohol **22**.....Page 32

2.4 Asymmetric hydrogenation of the alkene **14**.....Page 33

2.4.1 Study on the influence of the concentration in the asymmetric hydrogenation of alkene **14**.....Page 34

2.4.2 Study on the influence of the temperature in the asymmetric hydrogenation of alkene **14**.....Page 34

2.4.3 Design of Experiments study.....Page 35

2.5 Obtention of the enantiopure alkane *S*-**8**.....Page 37
2.5.1 Studies on the precipitation of diastereomeric tartrate salt **39**.....Page 37
2.5.2 Studies on the crystallization of diastereomeric tartrate salt **39**.....Page 41
2.5.3 Study on the base release of enantiopure alkane *S*-**8**.....Page 42
2.6 Obtention of the final product *S*-**15**.....Page 43

Chapter 3. Process industrialization.....Page 49
3.1 Process Safety studies.....Page 49
3.1.1 Secondary reactions study.....Page 50
3.1.2 Main reaction study.....Page 52
3.1.3 Process criticality assessment.....Page 53
3.1.4 Manufacturing process safety evaluation.....Page 55
3.2 HPAPI Unit design.....Page 60
3.2.1 HPAPI Unit facilities.....Page 61
3.2.2 HPAPI Unit Risk Management.....Page 64
3.3 Process validation.....Page 65
3.3.1 Industrial obtention of ketone **21**.....Page 65
3.3.2 Industrial obtention of alkene **14**.....Page 69
3.3.3 Industrial obtention of the enantiopure alkane *S*-**8**.....Page 71
3.3.4 Industrial obtention of the final product *S*-**15**.....Page 74
3.3.5 General results and conclusions of the process validation..Page 75
3.4 Regulatory affairs.....Page 76

Chapter 4. New synthetic approach.....Page 81
4.1 Route of synthesis improvements.....Page 81
4.2 Synthesis of the ketone **21**.....Page 82
4.2.1 Change proposal studies.....Page 83
4.2.2 Ketone **21** related compounds evaluation.....Page 85
4.3 Synthesis of alkene **14**.….....Page 87

4.4 Asymmetric hydrogenation of alkene **14**.....Page 88
4.4.1 Effect of solvent in the asymmetric hydrogenation of alkene **14**.....Page 91
4.4.2 Effect of pH in the asymmetric hydrogenation of alkene **14**.....Page 94
4.4.3 Effect of the metal source in the asymmetric hydrogenation of alkene **14**.....Page 95
4.4.4 Effect of ligand in the asymmetric hydrogenation of alkene **14**.....Page 97
4.4.5 Effect of imidazole substitution in the asymmetric hydrogenation of alkene **14**.....Page 103
4.4.6 Effect of metal cocatalyst in the asymmetric hydrogenation of alkene **14**.....Page 110
4.4.7 Study on the functionalization of imidazole regioselectivity.....Page 113
4.4.8 Synthesis optimization of Boc functionalized alkene **68**....Page 118
4.4.9 Summary of asymmetric hydrogenation of Boc functionalized alkene **68**.....Page 120
4.5 Synthesis of enantiopure alkane *S*-**8**.....Page 121
4.5.1 Direct resolution of alkane *S*-**8**.....Page 121
4.5.2 New resolution strategy from Boc functionalized alkene **68** hydrogenation.....Page 130
4.5.3 Resolution mechanism of the direct crystallization method.....Page 132
4.6 Scale-up trial.....Page 133
4.6.1 Summary of the new optimized process.....Page 139
4.7 Nitrosamines Drug Substance Related Impurities (NDSRIs).....Page 141
4.8 General conclusions.....Page 144
4.9 Next steps.....Page 145
4.10 Bibliography.....Page 146

Chapter 5. Experimenal Methodologies.....Page 157
5.1 Analytical Procedures.....Page 157
5.1.1 Ultra-High Performance Liquid Chromatography.....Page 157
5.1.2 High Performance Liquid Chromatography.....Page 157
5.1.3 High-Resolution Mass spectrometry.....Page 158
5.1.4 Nuclear Magnetic Resonance.....Page 158
5.1.5 Differential Scanning Calorimetry.....Page 158
5.1.6 Potentiometric titration.....Page 158
5.1.7 Single Crystal X-Ray Diffraction.....Page 159
5.1.8 Powder X-Ray Diffraction.....Page 159
5.1.9 Head-Space Gas Chromatography.....Page 159
5.2 Synthesis and characterization of ketone **21** and its related compounds.....Page 160
5.2.1 Synthesis of ketone **21**.....Page 160
5.2.2 Synthesis of ketone **57**.....Page 161
5.2.3 Synthesis of imine **59**.....Page 162
5.2.4 Synthesis of imidazole **19**.....Page 163
5.2.5 Synthesis of aldoxime **51**.....Page 164
5.2.6 Synthesis of amide **18**.....Page 165
5.2.7 Characterization of aryl bromide **33**.....Page 166
5.2.8 Characterization of phenol **62**.....Page 166
5.3 Synthesis of alkene **14** and its related compounds.....Page 167
5.3.1 Synthesis of tertiary alcohol **22**.....Page 167
5.3.2 Synthesis of alkene **14**.....Page 168
5.3.3 Synthesis of Bn functionalized alkene **32**.....Page 169
5.3.4 Synthesis of Ms functionalized alkenes **66** and **79** (Mixture).....Page 170
5.3.5 Synthesis of Cbz functionalized alkene **67**.....Page 172
5.3.6 Synthesis of Boc functionalized alkene **68**.....Page 172
5.3.7 Synthesis of Fmoc functionalized alkene **69**.....Page 174
5.3.8 Synthesis of MC functionalized alkene **70**.....Page 175

5.3.9 Synthesis of N_T-Me functionalized alkene **73**.....Page 176
5.3.10 Synthesis of N_π-Me functionalized alkene **74** (From mixture)….....Page 176
5.3.11 Synthesis of N_T-Et and N_π-Et functionalized alkenes **75** and **76** HCl (Mixture).....Page 177
5.4 Synthesis of the enantiopure alkane *S*-**8** and its related compounds.....Page 178
5.4.1 Boc functionalized alkene **68** asymmetric hydrogenation..Page 178
5.4.2 Synthesis of tartrate **39**.....Page 179
5.4.3 Synthesis of enantiopure alkane *S*-**8**.....Page 180
5.4.4 Synthesis of N_π-Me enantiopure alkane **77**.....Page 182
5.4.5 Synthesis of N_π-Et enantiopure alkane **80** (HCl).....Page 182
5.5 Synthesis of the final product *S*-**15**.....Page 183
5.6 NMR spectra of compounds.....Page 185
5.6.1 NMR spectra of **18**.....Page 185
5.6.2 NMR spectra of **19**.....Page 186
5.6.3 NMR spectra of **33**.....Page 187
5.6.4 NMR spectra of **51**.....Page 188
5.6.5 NMR spectra of **21**.....Page 189
5.6.6 NMR spectra of **57**.....Page 190
5.6.7 NMR spectra of **62**.....Page 191
5.6.8 NMR spectra of **14**.....Page 192
5.6.9 NMR spectra of **22**.....Page 193
5.6.10 NMR spectra of **32**.....Page 194
5.6.11 NMR spectrum of **66**.....Page 195
5.6.12 NMR spectrum of **79**.....Page 195
5.6.13 NMR spectra of **67**.....Page 196
5.6.14 NMR spectra of **68**.....Page 197
5.6.15 NMR spectra of **69**.....Page 200
5.6.16 NMR spectra of **70**.....Page 201
5.6.17 NMR spectra of **73**.....Page 202

5.6.18 NMR spectra of **74**.....Page 203
5.6.19 NMR spectra of **75**.....Page 204
5.8.20 NMR spectra of **76**.....Page 205
5.7.21 NMR spectra of *S*-**8**.....Page 206
5.7.22 NMR spectra of **39**.....Page 207
5.7.23 NMR spectra of **77**.....Page 208
5.7.24 NMR spectra of **80**.....Page 209
5.7.25 NMR spectra of *S*-**15**.....Page 210

Abbreviations, acronyms and structure index

Abbreviations and acronyms

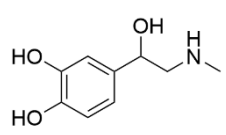
ADT_{24}	Adiabatic Decomposition Temperature at 24 h
AGP	Acid Glycoprotein
API	Active Pharmaceutical Ingredient
BCN	Barcelona
BCU	Bruker Control Unit
BEH	Ethylene Bridged Hybrid (Trademark)
BINAP	Binaphtyl ligands
Boc	*tert*-Butyl Carbamate
cAMP	Cyclic Adenosine Monophosphate
Cbz	Benzyl Carbamate
CbzCl	Benzyl Chloroformate
CCD	Central Composite Design
cGMP	current Good Manufacturing Practices
CHPLC	Chiral High-Performance Liquid Chromatography
CLS	Continuous Liner System
CNS	Central Nervous System
Conv.	Conversion
COSY	Correlated Spectroscopy
C_p	Heat Capacity
CPT	Containment Performance Target
DCM	Dichloromethane, methylene chloride
DIBALH	Diisobutylaluminium Hydride
DMF	Dimethyl Formamide
DMSO-d_6	Deutered Dimethylsulfoxide
DoE	Design of Experiments
DSC	Differential Scanning Calorimeter
DuanPhos	Tetrahydro-biisophosphindolyl ligands developed by Duan Liu and Xumu Zhang[100]
DuPhos	Registered Trademark, in reference to Benzodiphospholane ligands developed by DuPont
e.e.	Enantiomeric excess
eq	Equivalents
ESI	Electrospray Ionization
Et	Ethyl

Et_3N	Triethylamine
EtBr	Ethyl Bromide
EU	European Union
FDA	Food and Drug Administration
Fmoc	Fluorenylmethyloxycarbonyl
FmocCl	Fluorenylmethyloxycarbonyl Chloride
GMP	Good Manufacturing Practices
HMBC	Heteronuclear Multiple-Bond Coherence
HPAPI	Highly Potent Active Pharmaceutical Ingredient
HPLC	High-Performance Liquid Chromatography
HRMS	High Resolution Mass Spectrometry
HS-GC	Head-Space Gas Chromatography
HSQC	Heteronuclear Single Quantum Coherence
HSS	High Strength Silica
ICH	International Council for Harmonisation of technical requirements for pharmaceuticals for human use
MC	Methyl Carbamate
MCF	Metyhl Chloroformate
Me	Methyl
MeI	Methyl Iodide
MGRC	Moehs Group Research Center
MIBK	Methyl isobutyl ketone, 4-methyl-2-pentanone
Ms	Mesyl, methanesulfonyl
MS	Mass Spectrometry
MTSR	Maximum Temperature of the Synthesis Reaction
NDEA	*N*-Nitrosodiethylamine
NDMA	*N*-Nitrosodimethylamine
NDSRI	Nitrosamine Drug Substance-Related Impurity
NMR	Nuclear Magnetic Resonance
NOE	Nuclear Overhauser Effect
NOESY	Nuclear Overhauser Effect Spectroscopy
NorPhos	Trademark, referent to Norbornene diphosphoine
OEB	Occupational Exposure Band
OEL	Occupational Exposure Limit
PDA	Photodiode Array
PHOx	Phosphinooxazoline Ligands

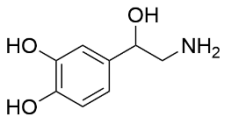
PMC	Plastics Management Corp. was established, known as PMC Global Inc
POx	Registered Trademark, referent to ferrocene-type PHOx ligands
PTFE	Polytetrafluoroethylene
PXRD	Powder X-Ray Diffraction
QC	Quality Control
QDa	Registered Trademark, referent to the quadrupole
R&D	Research and Development
r.t.	Room Temperature, generally 20 - 25 ºC
RoI	Residue on Ignition
RoS	Route of Synthesis
RPN	Risk Priority Number
RTP	Rapid Transport Port
SADABS	SAINT Area Detector Absorption Bruker/Siemens, referent to the software by Bruker and Siemens
SC-XRD	Single Crystal X-Ray Diffraction
SDRX	*Servei de Difracció de Raig-X*
SegPhos	Registered Trademark, referent to Bibenzodioxole bisphosphines
SEM	2-(Trimethylsilyl)ethoxymethyl
SeRMN	Servei de Resonància Magnética Nuclear
SHELXL-2016	Trademark name of auxiliary software for structure refining
SHELXS-86	Trademark name of auxiliary software for structure solution
SMEAH	Sodium bis(2-methoxyethoxy)aluminium Hydride
SMEPAC	Standardized Measurement of Equipment Particulate Airbone Concentration
T3	Trifunctional C18 alkyl-phase
T_b	Boiling Temperature
TBME	*tert*-Butyl methyl ether
TBN	*tert*-Butyl Nitrite
TEOF	Triethylorthoformate
THF	Tetrahydrofuran
TOF	Turn Over Frequency
ToF	Time of Flight
TosMIC	*para*-Toluenesulfonyl Methyl Isocyanate
T_p	Process Temperature
Tr	Trityl, triphenylmethyl

Ts	Tosyl, 4-methylbenzenesulfonyl
TUV	Tungsten Ultraviolet-Visible
UAB	*Universitat Autònoma de Barcelona*
UHPLC	Ultra-High Performance Liquid Chromatography
UHPLC-MS	Ultra-High Performance Liquid Chromatography Mass Spectrometry
UPLC	Registered Trademark, referent to UHPLC
US	United States
USA	United States of America
V	Volumes, referent to mL per g of substrate
ΔT_{ad}	Temperature increase in Adiabatic conditions due to a chemical reaction
ΔT_{atd}	Temperature increase due to Adiabatic Thermal Decomposition

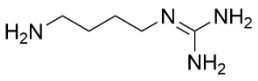
Structure index



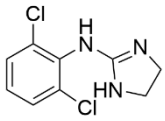
1



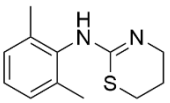
2



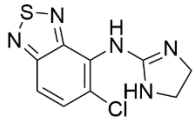
3



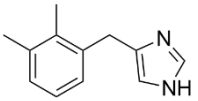
4



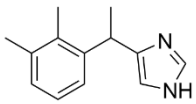
5



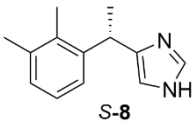
6



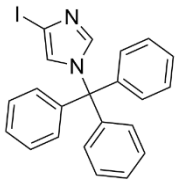
7



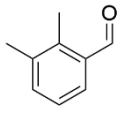
8



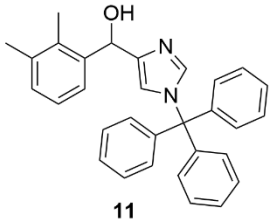
***S*-8**



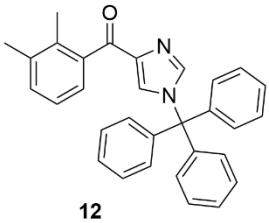
9



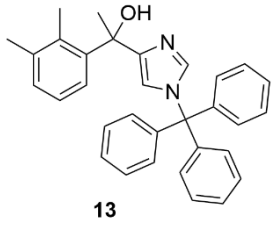
10



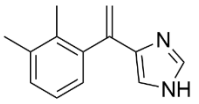
11



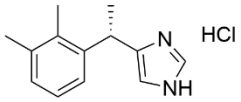
12



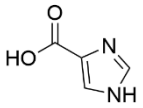
13



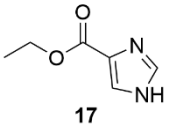
14



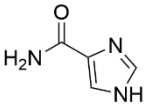
S-**15**



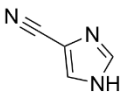
16



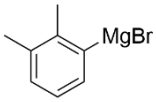
17



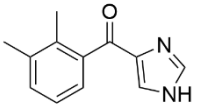
18



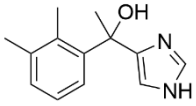
19



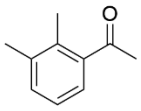
20



21



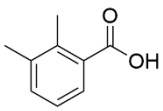
22



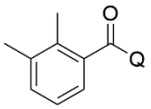
23



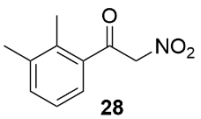
24



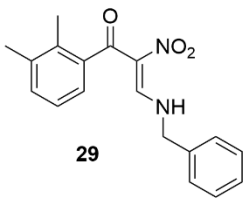
25



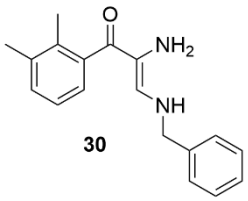
26: Q = Imidazole
27: Q = *o*-nitrophenol



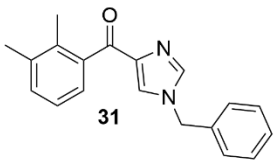
28



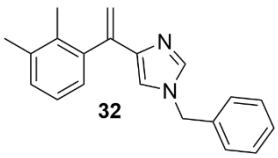
29



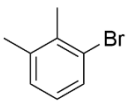
30



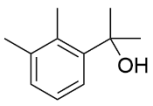
31



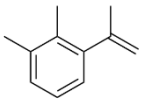
32



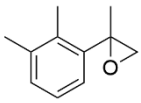
33



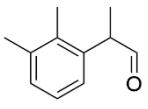
34



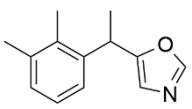
35



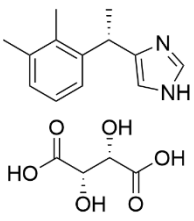
36



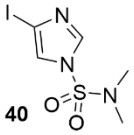
37



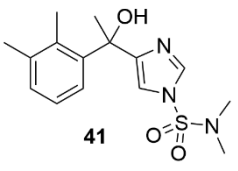
38



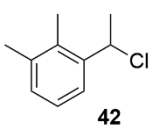
39



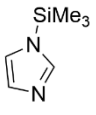
40



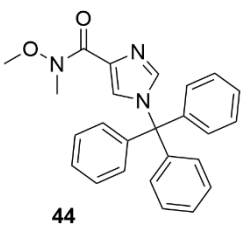
41



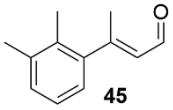
42



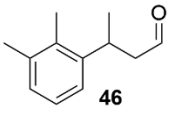
43



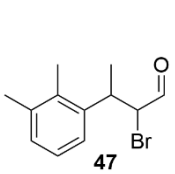
44



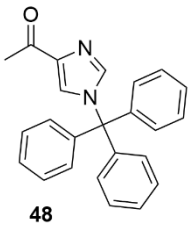
45



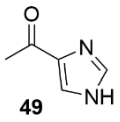
46



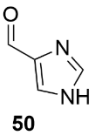
47



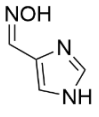
48



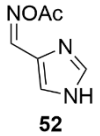
49



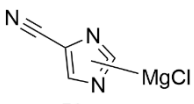
50



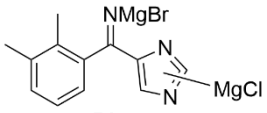
51



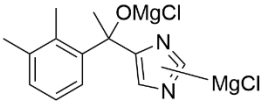
52



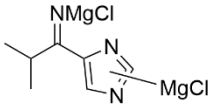
53



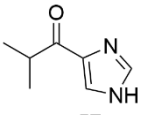
54



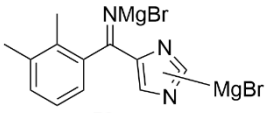
55



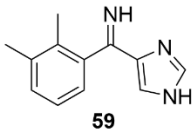
56



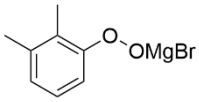
57



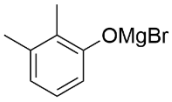
58



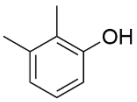
59



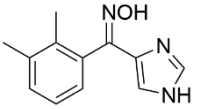
60



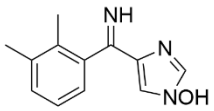
61



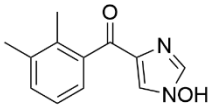
62



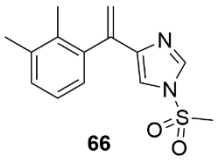
63



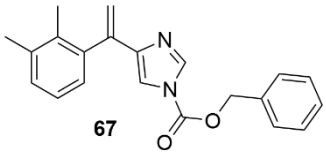
64



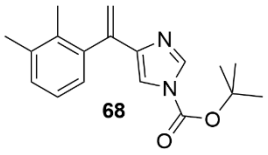
65



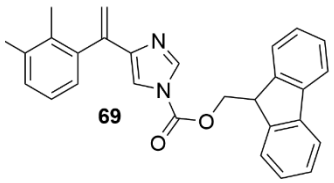
66



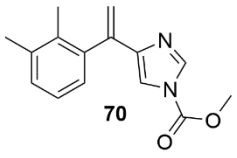
67



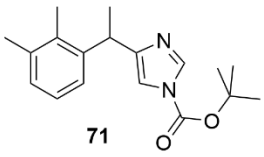
68



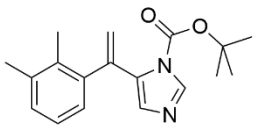
69



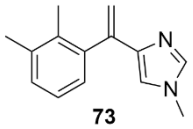
70



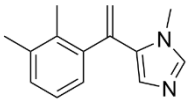
71



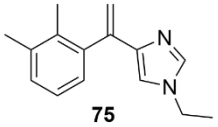
72



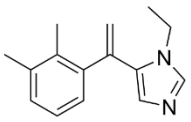
73



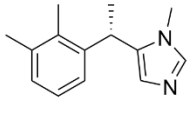
74



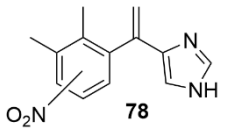
75



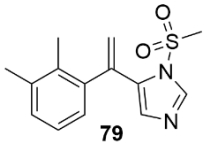
76



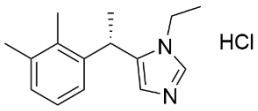
77



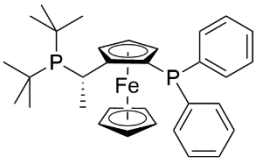
78



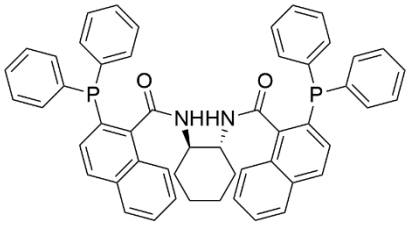
79



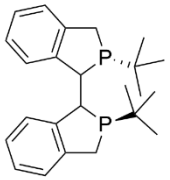
80



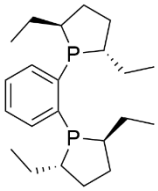
L-1



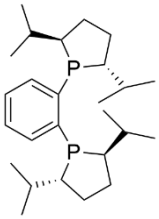
L-2



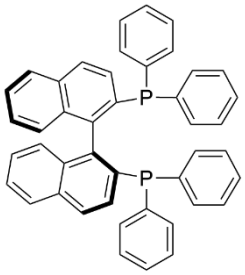
L-3



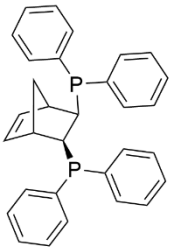
L-4



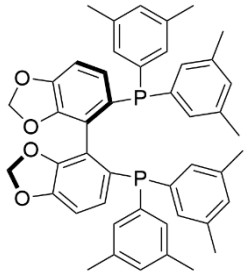
L-5



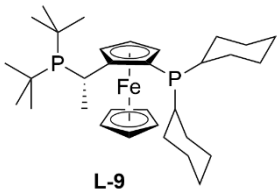
L-6



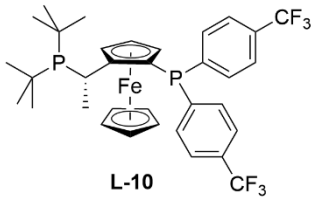
L-7



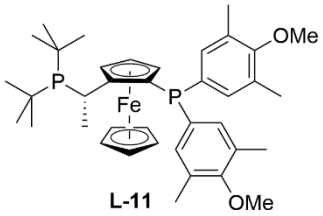
L-8



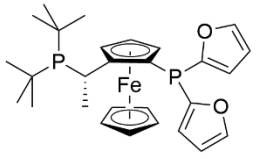
L-9



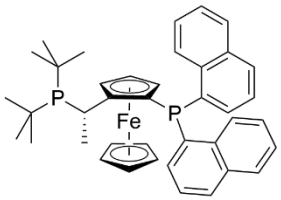
L-10



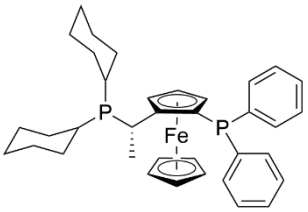
L-11



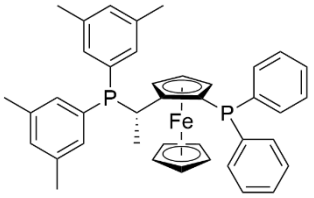
L-12



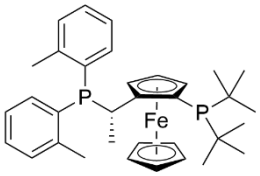
L-13



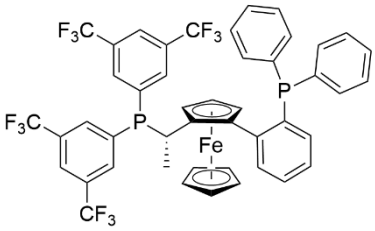
L-14



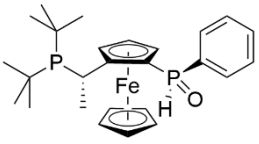
L-15



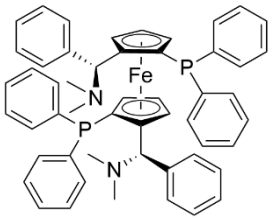
L-16



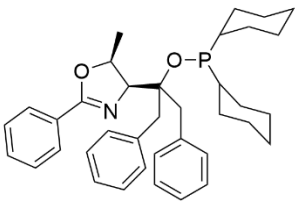
L-17



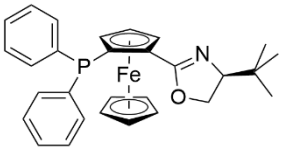
L-18



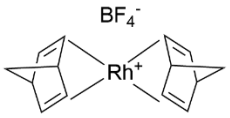
L-19



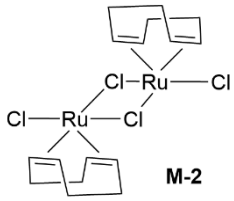
L-20



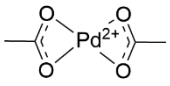
L-21



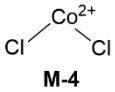
M-1



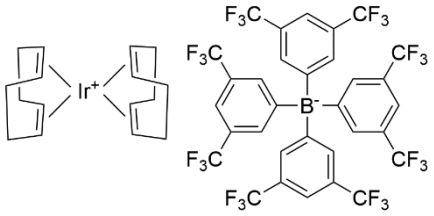
M-2



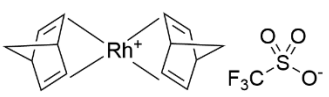
M-3



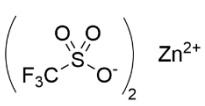
M-4



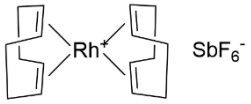
M-5



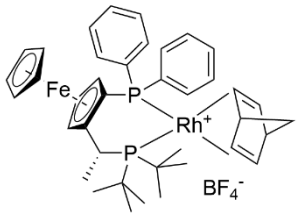
M-6



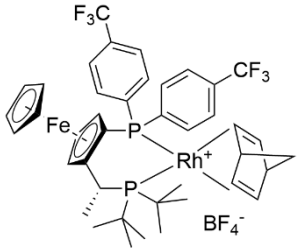
M-7



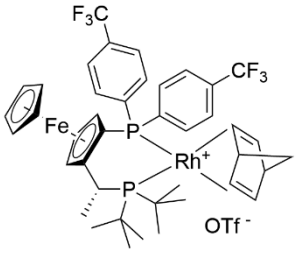
M-8



ML-1



ML-2



ML-3

Chapter 1.
General introduction

Chapter 1. General introduction

Commercializing new drugs is an extremely costly and time-consuming investment for a pharmaceutical company. The story begins with the development of a new drug substance which requires millions of dollars and years of research. Promising results in the early stages of the discovery do not necessarily ensure the success of the new drug substance. Few of the new molecules reach clinical trials and hardly any of them reach the market. The regulations to bring a new drug substance to the market have increased in the last years to ensure the healthcare of the patients. This hardening in the regulation turns into an increase in the investment requirements and manufacturing costs. The success of a new drug product involves multiple departments in a company, and in most cases, this becomes a multiorganizational task.

The association between Fine Chemical companies and Pharmaceutical companies is very common as the regulation concerning each one is not exactly the same. Fine Chemical companies are involved in the manufacturing of the drug substance, commonly referred to as Active Pharmaceutical Ingredient (API). Pharmaceutical companies are responsible for the drug product which is the final product to be commercialized.

The optimization of drug development has become critical for the commercial success of the drug product. On the one hand, the research in the early stages represents about 65 % of the total cost in R&D which increases along the clinical trials until commercialization.[1] The failure of the drug substance means a waste of money invested in the project. On the other hand, the time used in the development is crucial for sales revenue. For the originator, the company who has discovered the new drug entity, the development is performed under patent protection and the time spent reduces the time in which the product can be commercialized under protection. For generic brands, the first company who have the generic version as soon as the patent expires is the one that gains more customers.

Despite the costs of research and development must be reduced, Fine Chemical and Pharmaceutical companies have increased their investment in R&D in the recent years.[1] This is related to the increase in the number of studies and the complexity of them during clinical trials. The sameness of most new drug substances as their first-in-class analogs forces them to demonstrate more accurately the improvements, sometimes slightly, in respect of their approved analogs. The development of an

optimized manufacturing process of a well-known API can generate intellectual property, valuable industrial knowledge, and business opportunities for a company.

Generic versions of a drug product are economical versions of the original ones commercialized by other companies. Generic versions can be sold once the patent protection expires. The development of new manufacturing processes for existing drug products enhance innovation and continuous improvement in the industry. This favors competitiveness in manufacturing costs, which facilitates the population's access to medicines.

The industrial development of a new manufacturing process for a drug substance is divided into 6 different phases (Figure 1). Phase 0 begins at the bibliographic evaluation of the project in which the technical availability is studied. At the same time, all existing routes of synthesis (RoS) and possible new strategies are explored. This involves the in-depth study of all existing patents related and bibliographic analysis of the existing scientific work. Once a new synthetic route is proposed, Phase I is initiated in which the synthetic route is outlined, and some reagents and strategies are defined. Then, Phase II involves the optimization of the selected RoS and in Phase III first scale-up is performed.

When the new synthetic methodology is optimized and scaled, the project begins Phase IV in which a safety process study is performed before the validation of the manufacturing process. At the same time, critical parameters and quality attributes are defined and tested to ensure the robustness of the manufacturing process. This validation must comply with the current Good Manufacturing Practices (cGMP)[2] as defined in the International Council for Harmonisation of Technical Requirements for Pharmaceuticals for Human Use (ICH) guidelines (ICH Q7). Finally, in this phase, the stability studies of the API began.

Phase V involves the industrialization of the drug substance and the elaboration of the Drug Master Files of the API for the regulatory institutions. In this Phase, continuous improvement is performed in the Life-cycle management of the product. This involves further optimization of the manufacturing process, managing manufacturing deviations and updating of the Drug Master File.

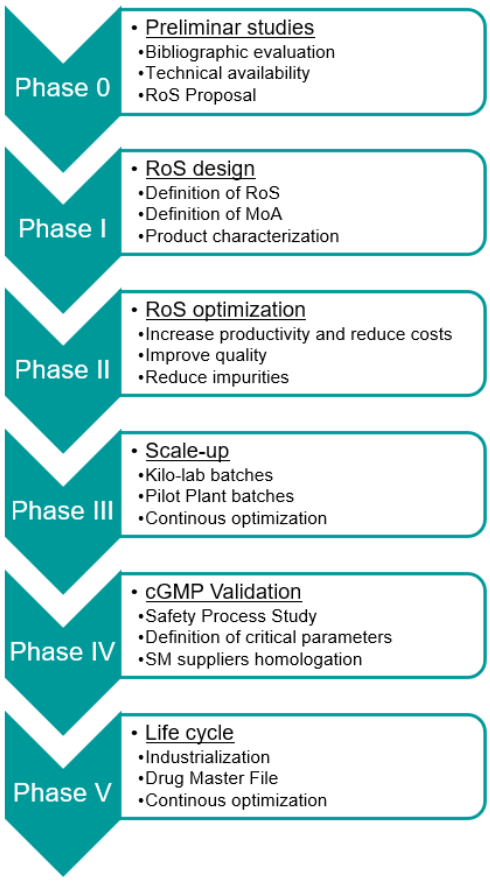


Figure 1. *Phases of the industrial development of a new manufacturing process for an API*

Among others, these steps are essential for the industrial production and commercialization of the product.

1.1 Company introduction

Moehs Group is a dynamic group of companies active in the pharmaceutical ingredients business. The main activity of the Group is manufacturing APIs & Custom Manufacturing for the pharmaceutical industry. Moehs Group has a worldwide presence that covers more than 90 countries,[3] most of them represented by an extensive sales agency network.

Moehs was founded in Barcelona in 1962 by Mr. Melchor Mallasen Ornat from which the company's name is derived: *Mallasen Ornat e Hijos*. In 1980 Moehs became part of the Sanofi group for 15 years as a main manufacturing chemical plant in Spain. In 1995 Moehs was acquired by the PMC American holding company joining other fine chemical companies around Europe. At the beginning of the 21st century, Moehs

reorganized itself as Moehs Iberica, which is the original company, and Moehs Catalana, which is the manufacturing chemical plant. At the same time, Moehs inaugurated a new chemical plant, Moehs Cantabra. During 2005 Moehs acquired Coprima (*Polinyà*) being the third manufacturing site of Moehs group, Benechim (Belgium) and Norchim (France) joined in 2008 and Chemische Fabrik Berg (Germany) in 2009. In the course of 2011, Moehs, shared 50 % of Proteos Biotech (Spain). After the 50th anniversary in 2012, Moehs opened its newest chemical plant Moehs BCN (Castellbisbal) in 2013. During mid-2017, Moehs built up its R&D center called Moehs Group Research Center (MGRC). In the course of 2019, Moehs grew by acquiring 60 % of Zeta Pharmaceuticals company.[3]

Moehs's most recent investment performed has been, in 2021 at the MGRC site, in which a special unit dedicated to the manufacturing of Highly Potent Active Pharmaceutical Ingredients has been built.[3]

1.2 Highly Potent Active Pharmaceutical Ingredients

With the pass of the years, the pharmaceutical industry has developed more and more targeted therapies. Regarding small molecules, those APIs that show a very high selectivity for their pharmacological target and exhibit biological activity at extremely low concentrations, are known as Highly Potent APIs (HPAPIs). The majority of the new HPAPIs developed in the last few years are used in oncology for cancer treatment. Nowadays, around 25 % of the drug products commercialized around the world contain a HPAPI. The main goal of using a HPAPI instead of a conventional API is lower side effects due to their extremely high selectivity.[4]

Despite their advantages and greater market opportunities, HPAPIs present some challenges for the industry, such as the upgrade of their facilities for these new, highly potent drugs. Due to the hazards associated to HPAPI, the manufacturing costs of these compounds is very high. The main difficulty is the need for specialized containment to ensure low levels of exposure to the substance.[4,5]

There is no common definition of HPAPI. However, some statements are used to characterize HPAPIs. Often are defined as active molecules with biological activity at 15 µg/Kg or less. This is often related to the second statement which is a drug substance with a maximum daily therapeutical dose of less than 1 mg. The definition is

extensive to any active molecule with extremely high selectivity to its biological target with the potential to cause toxicity at low doses. Finally, any novel compound of unknown potency and toxicity should be considered also as a HPAPI.[5,6]

The potency of APIs is often indicated by the Occupational Exposure Level (OEL)[6] where the lower the value, the more potent the substance. With the increasing potency, a higher the level of containment that is required. The OEL is described as the maximum concentration in air of a determined substance (generally in µg/m^3 or ng/m^3) to which exposure during 8 h a day does not present any side effect.[7] In order to classify APIs, groups are formed with those with similar OELs and called Occupational Exposure Band (OEB). The most common OEB system behold 5 different bands which OEL limits and common APIs of each band are shown in table 1.[6]

Table 1. *5 bands OEB system and common APIs in each band*

OEB	OEL Limits	Common APIs
OEB 1	> 1000 µg/m^3	Ibuprofen, Naproxen (5000 µg/m^3 both)[8,9]
OEB 2	1000 – 100 µg/m^3	Sofosbuvir (200 µg/m^3)[10]
OEB 3	100 – 10 µg/m^3	Ibrutinib (20 µg/m^3)[11]
OEB 4 (HPAPIs)	10 – 1 µg/m^3	Apixaban (8,3 µg/m^3)[12]
OEB 5 (HPAPIs)	1000 - 10 ng/m^3	Vismodegib (300 ng/m^3)[13]

To work with OEB 1 APIs, a ventilated place is necessary, and gloves are recommended when working with powder. Furthermore, working with OEB 2 and OEB 3 fume hoods are needed, gloves and any other Personal Protective Equipment (PPE) are also mandatory. Moreover, an isolator is needed when working with OEB 4 and OEB 5 HPAPIs. The use of isolators depends on the amount of substance to be handled and the task duration. For low quantities and low task duration, it is possible to work in fume hoods with special restrictions. When working with higher amounts of substances, isolators and laminar flow hoods are compulsorily in combination with other PPE to ensure the least exposure possible.[6]

The molecule of interest for this project is an α_2-adrenergic receptors agonist used for sedation. Its OEL is 600 ng/m^3 so is classified as an OEB 5 HPAPI.[14]

1.3 α_2-adrenergic receptor agonists for sedation

Adrenergic receptors are a class of G-protein-coupled receptors that are activated by adrenaline and noradrenaline, in general by many catecholamines. The 5 main categories of adrenergic receptors are: α_1, α_2, β_1, β_2 and β_3. Specifically, α_2-adrenergic receptors are located mainly in the Central Nervous System (CNS). Adrenergic receptor agonists are a family of drugs that stimulate the response of adrenergic receptors.[15]

α_2-adrenergic receptors activation inhibits the release of norepinephrine from the presynaptic neuron promoting a reduction in the brainstem vasomotor center activity, which is mediated by CNS, leading to a sedative and antihypertensive effect (Figure 2). α_2-adrenergic receptor agonists are frequently used in anesthesia as sedatives and also for muscle relaxation and analgesia.[16]

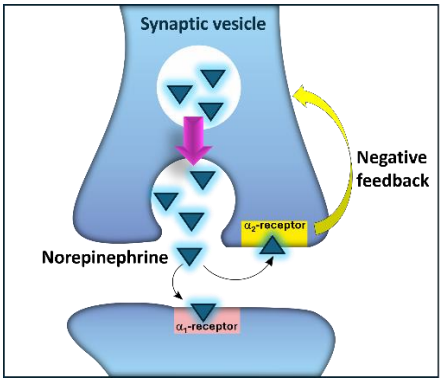


Figure 2. *Representation of release of norepinephrine from presynaptic neuron to α_1-receptor (pink) inhibited by α_2-adergenic receptor (yellow)[16]]*

The α_2-adrenergic receptor is mainly naturally activated by epinephrine and norepinephrine (Figure 3). In 1910 compound **3** was discovered and it was found it could increase blood flow in rabbits.[17] Its structure-activity relationship was studied but needed further research to discover compound **4** in an attempt to develop a nasal decongestion compound.[18] This led to the discovery of good number of biologically active molecules capable to activate adrenergic receptors. During those years compound **5** was discovered and patented for anesthesia, sedation and muscle relaxation.[19] Most recently, in 1996, compound **6** was discovered evidencing a structural similarity to compound **4**.[19,20]

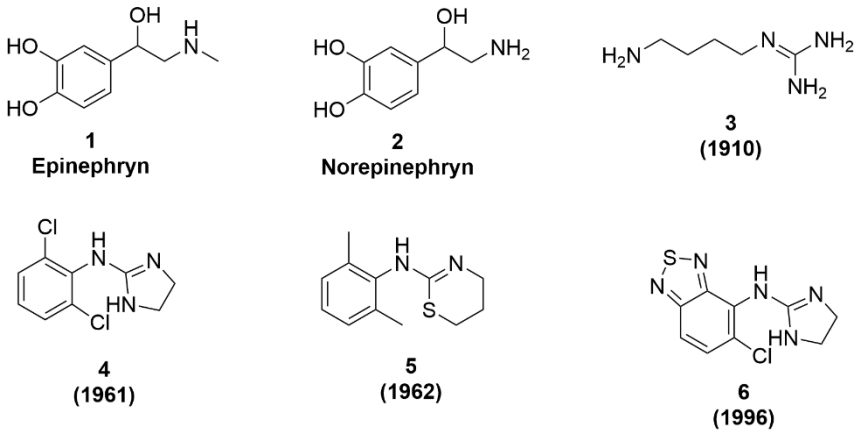


Figure 3. *Relevant α_2-adrenergic receptor agonists*

Compound **7** is an imidazole derivate discovered by Orion Pharma and approved by FDA in 1983 for equine sedation (Figure 4).[21] This compound was the evolution of compounds **4** and **5**.*[22]* Its main side effect is to produce arrhythmia. As it is used as a sedative in surgery, it is commonly used in combination with antibiotics. The combination of compound **7** with sulfonamide-type antibiotics is very dangerous, particularly when administered concurrently. Orion Pharma investigated new chemical entities to increase the activity of the compound and also reduce its side effects.

After years of research, imidazole *rac*-**8** was discovered and commercialized in 1987.[21] It was found that the introduction of the methyl group increases the activity of the compound respect to 7 by more than 6 times.*[22]* The arrhythmia was drastically reduced but bradycardia was noted in clinical trials. However, its high activity allowed the combination with other drugs such as opioids, antibiotics and other analgesics.

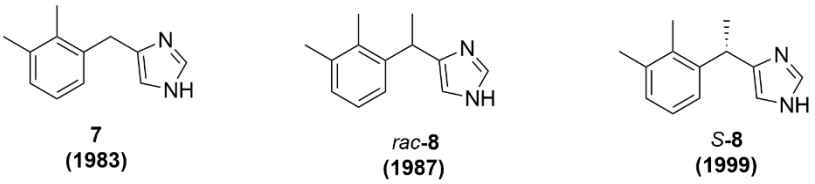


Figure 4. *α_2-adrenergic receptor agonists developed by Orion Pharma*

After 12 years of research, *S*-**8** was discovered and commercialized by Orion Pharma in 1999.*[21]* One of the enantiomers was established as much more active than the other. *S*-enantiomer was reported to be 7 times more active than the racemic version of the drug.*[16,22]* Further research showed that the *R*-enantiomer was inactive toward α_2-adrenergic receptors but in higher concentrations could produce hypertension.*[23]*

Because of that, most of the side effects related to the higher concentration required for its biological activity were reduced.

The increase in biological activity and selectivity makes the final *S*-**8** to be considered as HPAPI. The biological activity and OEL of compounds **7**, *rac*-**8** and *S*-**8** are shown in table 2.

Table 2. *Biological activity and OEL of compounds **7**, rac-**8** and S-**8***

Compound	Biological activity	OEL
7	60 µg/Kg[24]	300 µg/ m^3[25]
rac-**8**	9,63 µg/Kg[24,22]	10 µg/ m^3[26]
S-**8**	1,4 µg/Kg[16,24,22]	0,6 µg/m^3[14]

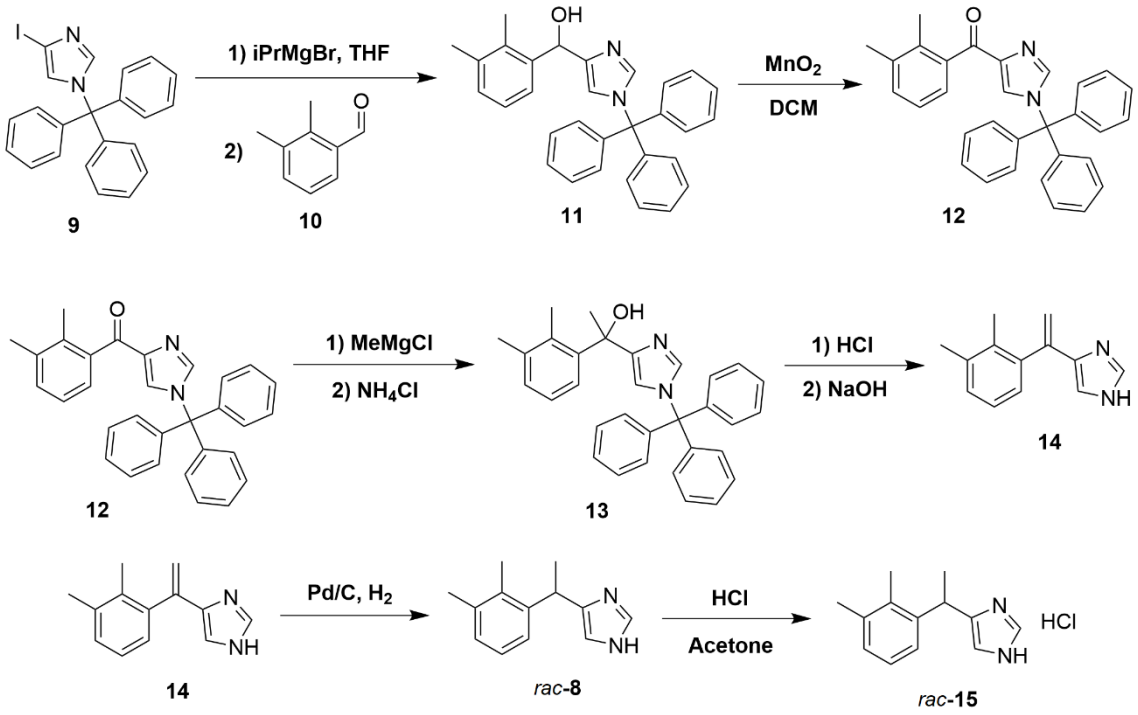
The compound of interest in this project is compound *S*-**8**. The industrial synthesis of this compound will be discussed with all related considerations. Synthetic and analytical procedures will also be presented. In addition, economic, regulatory and intellectual property issues will also be included.

1.4 State of the art for the synthesis of a HPAPI for sedation

Compound **7** was first described and patented by Orion Pharma in 1980[27] in which imidazole derivates were prepared and tested for pharmaceutical compositions. In this patent, a benzyl or benzoyl imidazole intermediate was reported to successfully contribute in the synthesis of compound *S*-**8**. It was not until 1988 that compound *S*-**8** was reported and patented.[28] After the product patent expired (2008), other processes were patented as generic versions allowing the product to reach the market.

In 2009, Grindex, patented a new process using a trityl intermediate as can be observed in scheme 1.[29]

This synthetic route starts with a trityl-protected iodoimidazole **9** which is converted to the corresponding Grignard reagent by halogen-magnesium exchange[30] in the presence of iPrMgBr in THF. Then, the aryl aldehyde **10** is added to afford the corresponding alcohol **11** after the nucleophilic addition.

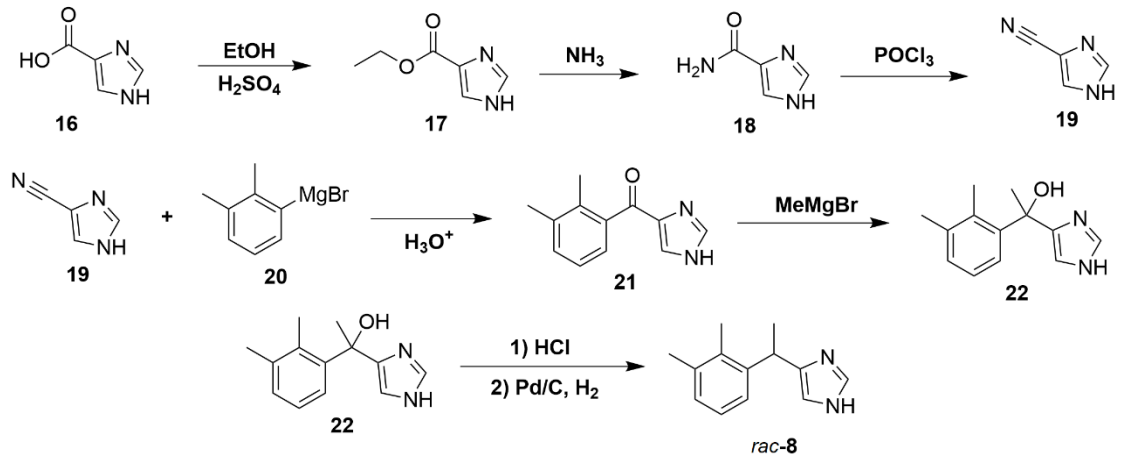


Scheme 1. *Patented Grindex synthesis of compound* ***8***

Alcohol **11** is oxidized to the corresponding ketone **12** in the presence of MnO_2 in dichloromethane (DCM). The resulting ketone is methylated with MeMgCl to yield alcohol **13** which is dehydrated in hydrochloric acid to give the corresponding alkene **14**. Alkene **14** is subsequently reduced with Palladium over carbon (Pd/C) under hydrogen atmosphere to the corresponding racemic alkane *rac*-**8** which is treated with HCl to give its hydrochloric salt *rac*-**15**, after crystallization in acetone.

In 2009, Sinochem patented in China a similar process as shown in Scheme 2.[31] The interesting part of this patent is the direct synthesis of ketone **21** from the nitrile intermediate **19**. However, the synthesis of this nitrile in this specific way is protected until 2029.

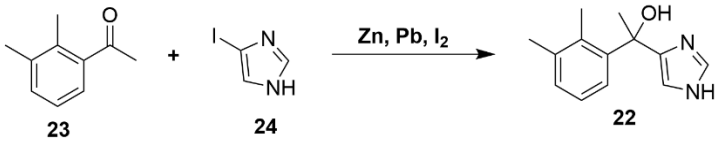
Sinochem synthesis starts with the imidazole carboxylic acid **16** which is converted into the corresponding amide **18** through esterification with ethanol under acid catalysis obtaining the ethyl ester **17** which is subsequently treated with ammonia. Amide **18** is dehydrated to form the corresponding nitrile **19** which is treated with the aryl magnesium bromide **20** to yield ketone **21**.



Scheme 2. *Patented Sinochem synthesis of compound rac-**8***

This is methylated with MeMgBr to obtain the corresponding tertiary alcohol **22**. The alcohol is converted into alkane *rac*-**8** under catalytic hydrogenation with Pd/C and hydrogen chloride under hydrogen atmosphere.

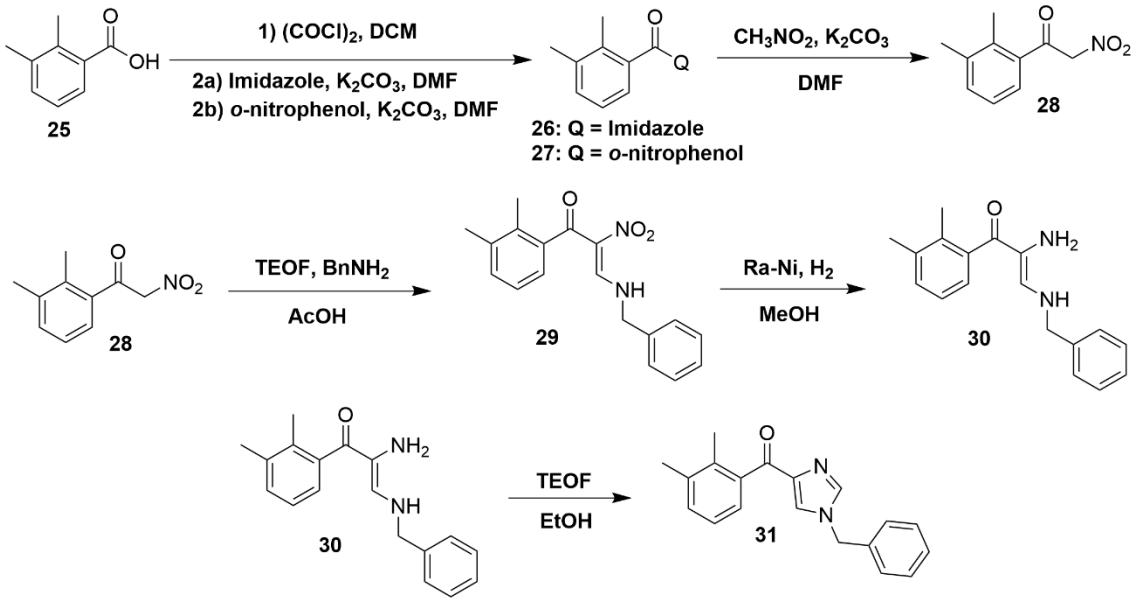
In early 2010, Huaxipharm, patented a process to obtain alcohol **22**[32] with a similar approach to Grindex synthesis[29] (Scheme 3) and ending the synthesis of *rac*-**8** with the Sinochem process.[31] What is interesting in this process is that even using the imidazole as a nucleophile, it is not needed to protect position 1 of the imidazole as reported in Grindex patent[29].



Scheme 3. *Patented Huaxipharm synthesis of compound **22***

Moreover, aryl methyl ketone **23** was commercially available at an acceptable price. The synthesis starts with the iodoimidazole **24** that reacts with zinc under lead catalysis, initiated by iodine to form the corresponding organozinc compound which reacts easily with aryl methyl ketone **23** to yield alcohol **22**.

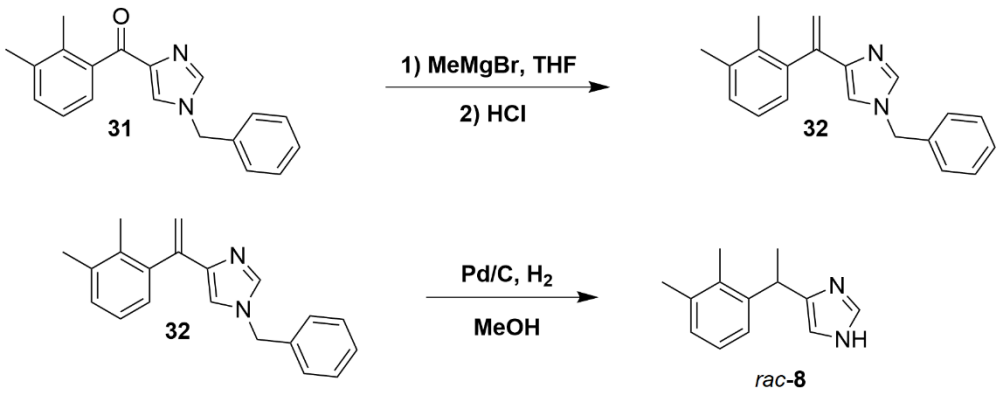
At the end of the same year, I-Tech AB, patented a synthesis which form the imidazole ring during the synthesis as depicted in scheme 4.[33]



Scheme 4. *Patented I-Tech AB synthesis of compound* ***31***

The synthesis starts with the benzylic acid **25** which is converted into the corresponding acyl-chloride in the presence of oxalyl chloride in dichloromethane with the consequent nucleophilic attack of imidazole or *o*-nitrophenol. The resulting activated benzoyl **26** or **27** is treated with nitromethane in DMF in the presence of potassium carbonate to afford the nitro-ketone **28**. Compound **28** is reacted with triethyl orthoformate in the presence of benzylamine to obtain the nitro compound **29** which is reduced to the corresponding amine **30** with Raney-Nickel. The imidazole is synthesized through a ring closing with compound **30** reacting with triethyl orthoformate to yield imidazole **31**.

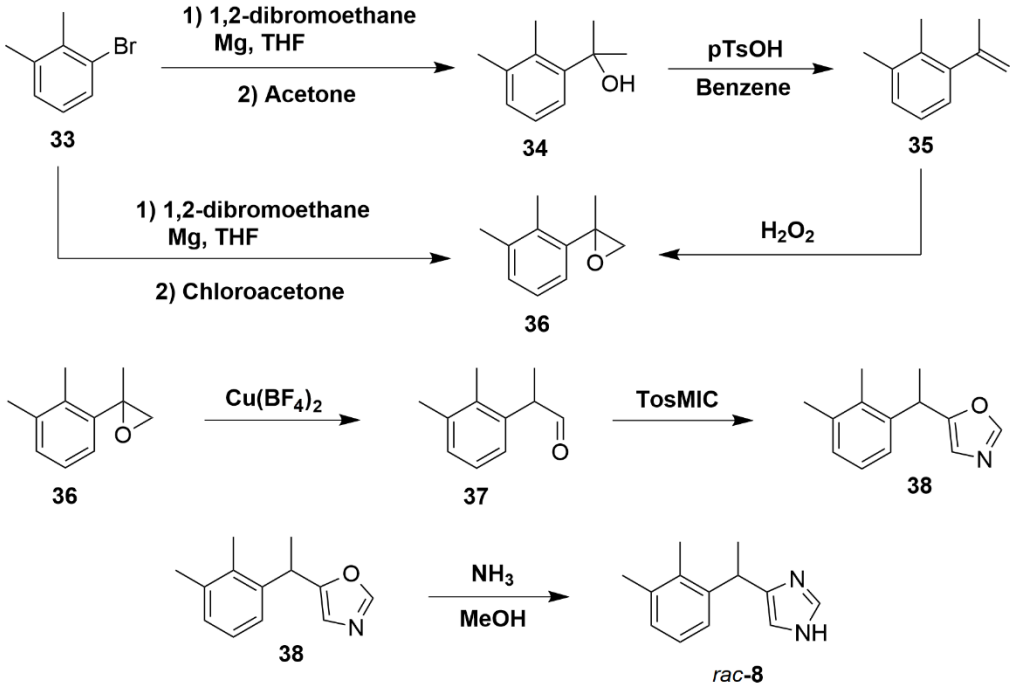
From ketone **31**, the synthesis of racemic compound *rac*-**8** follows the same synthesis as the original synthesis of Orion Pharma[27] as shown in scheme 5.



Scheme 5. *Patented Orion Pharma synthesis of compound rac-****8*** *from compound* ***31***

Ketone **31** is treated with MeMgBr and the corresponding alcohol is dehydrated with hydrochloric acid to obtain alkene **32**. Then, olefin **32** is hydrogenated and deprotected using Pd/C in MeOH to yield compound *rac*-**8**.

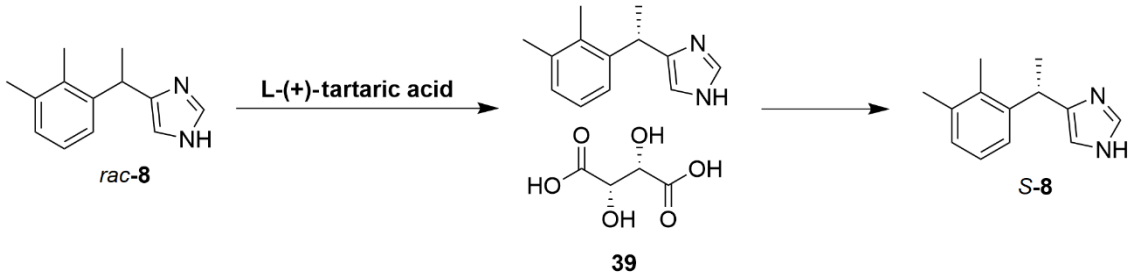
Years later, Lonza patented a process that also builds the imidazole during the synthesis via oxazole conversion to imidazole (Scheme 6).[34,35]



Scheme 6. *Patented Lonza synthesis of compound rac-**8***

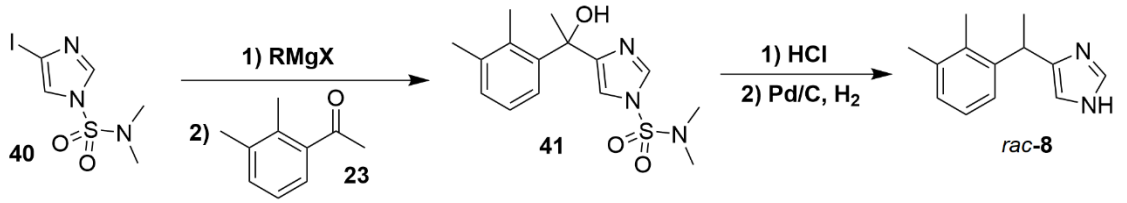
The synthesis starts with the aryl bromide **33** which is converted to the corresponding Grignard reagent **20** through the reaction with magnesium and 1,2-dibromoethane as initiator. Grignard reagent **20** reacts with acetone to give the tertiary alcohol **34** which is dehydrated in the presence of *p*-toluenesulfonic acid to yield alkene **35**. Then, alkene **35** is oxidized to its corresponding epoxide **36**. A direct synthesis for **36** was also described from compound **33** through the reaction with chloroacetone.[36,37] Epoxide **36** is converted into aldehyde **37** with copper(II) tetrafluoroborate under Lewis acid catalysis.[38] The aldehyde is submitted to *p*-toluenesulfonyl methyl isocyanate (TosMIC) to yield oxazole **38** through a 5-*endo-dig* cyclization via a Van Leusen reaction.[39] Finally, the oxazole moiety is converted into the corresponding imidazole with saturated ammonia solution in methanol to yield racemic compound **8**.[40]

Few months later, Edmond Pharma reported the obtention of enantiopure compound *S*-**8** through the resolution of salt **39** after the derivatization of compound **8** with 0,5 molar ratio of L-(+)-tartaric acid (Scheme 7).[41]



Scheme 7. *Patented Edmond Pharma obtention of compound S-**8***

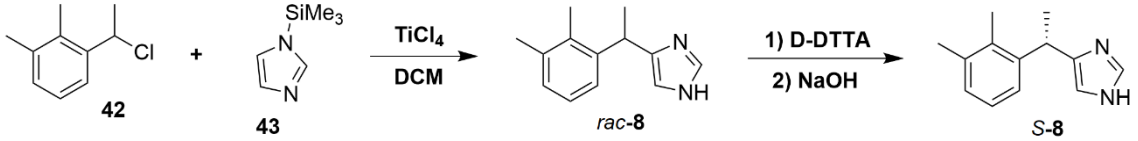
At the end of 2013, Hubei Biopharm patented a very similar process to that of Huaxipharm[32] but starting from protected imidazole **40** (Scheme 8).[42]



Scheme 8. *Patented Hubei Biopharm obtention of compound rac-**8***

The synthesis starts with the 4-iodo-1-(*N*,*N*-dimethylsulfamoyl)imidazole **40** that reacts with an alkyl magnesium halide to form the corresponding Grignard reagent which reacts easily with acetophenone **23** to yield alcohol **41**. This is one-pot dehydrated and hydrogenated to yield compound *rac*-**8**.

At the same time, Huaxipharm patented a new process to obtain compound *S*-**8** (Scheme 9). [43]



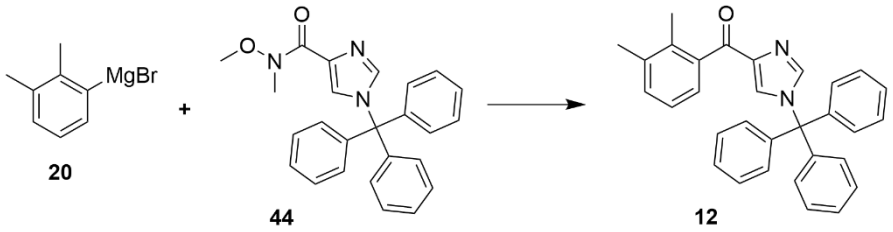
Scheme 9. *Patented Huaxipharm obtention of compound S-**8***

Initially, the silyl-protected imidazole **43** is transformed to compound *rac*-**8** through a Friedel-Craft alkylation with alkyl chloride **42** in the presence of $TiCl_4$. Enantiomers in

racemic **8** are separated as the corresponding diasteriometic salts when treated with D-(+)-ditoluoyl tartaric acid (D-DTTA). Finally, the compound *S*-**8** is recovered in the presence of NaOH.

At the beginning of 2014, Jiangsu Chiatai patented compound *S*-**8** as a perchlorate salt. [44] However, the investigation of novel salts was discontinued around the world despite this patent was granted in China.

At the same time, a very similar process to obtain compound **12** starting from the imidazole carboxamide **44** was patented by Ningbo Team in China[45] and Tianjin Weijie in USA and EU[46] (Scheme 10). Finally, only US Patent of Tianjin Weijie was granted.



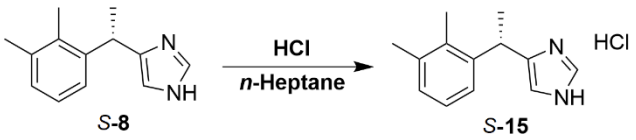
Scheme 10. *Ningbo Team and Tianjin Weijie obtention of compound* ***12***

Both companies claimed the same conditions to obtain compound **12** from Grignard **20** and carboxamide **44** and the subsequent transformation to compounds *rac*-**8** and *S*-**8** in the conditions described by Grindex[29] and Edmond Pharma[41]. However, they described different routes to obtain the carboxamide **44** being this, their key intermediate.

From mid-2014 until late 2015, three different patents were published claiming diverse resolution steps to obtain enantiopure compound *S*-**8**. Anhui Yi Xin Ming claimed a resolution with 1*R*-(-)-camphorsulfonic acid[47], Cisen Pharma with D-glucose in a co-crystal form[48] and Hainan General with L-malic acid[49].

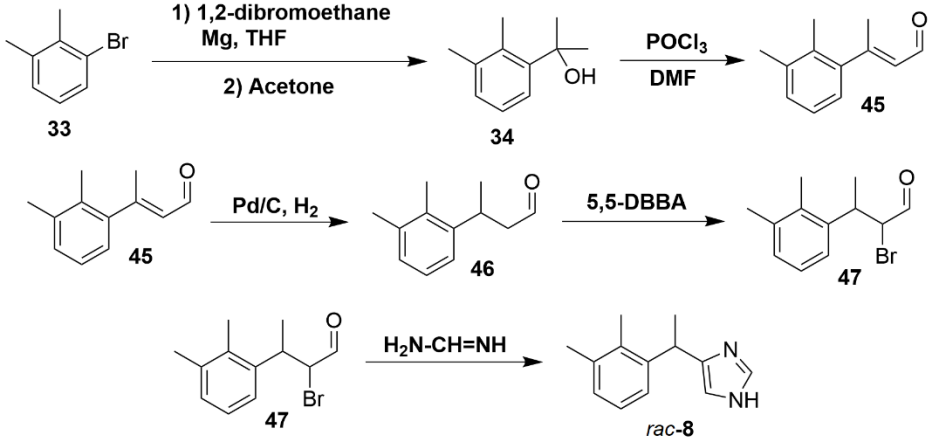
By the end of 2015, Yangtze River Pharmaceutical patented the same synthesis of compound **8** as Huaxipharm but using a *N*-Boc protected imidazole[50] instead of the Silyl-protected that claimed Hauxipharm[43].

At the beginning of 2016, Jiangsu Nhwa patented the obtention of hydrochloride *S*-**15**, the hydrochloride salt of compound *S*-**8**, in its crystalline form C. This form was obtained when crystalized compound *S*-**15** in *n*-heptante (Scheme 11). [51]



Scheme 11. *Jiangsu Nhwa obtention of crystalline form C of compound S-**15***

At the same time, Cambrex described a process[52] based in Lonza's patent.[34,35] The process begins with a Grignard reagent and ends-up forming the imidazole ring (Scheme 12).

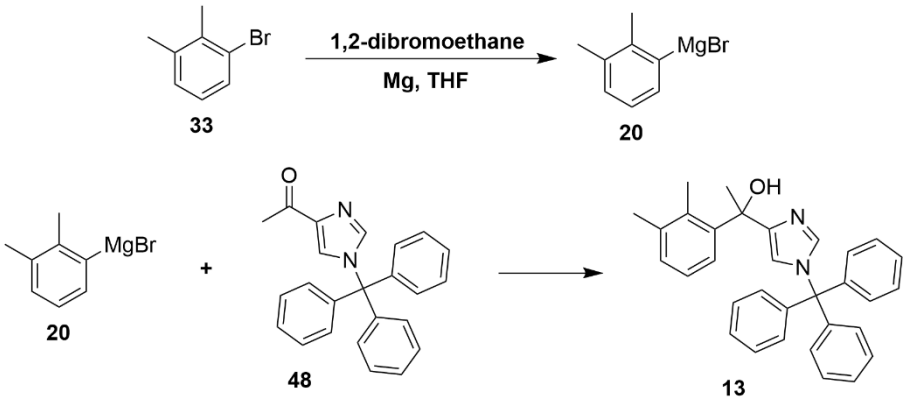


Scheme 12. *Patented Cambrex obtention of compound rac-**8***

The synthesis begins as in Lonza process from aryl bromide **33** to obtain the alcohol **34**. This alcohol is reacted with $POCl_3$ in DMF to obtain the unsaturated aldehyde **45** through a Vilsmeier Haack- type reaction and hydrogenated in the presence of Pd/C under hydrogen atmosphere to yield aldehyde **46**. This is reacted with 5,5-dibromobarbituric acid (5,5-DBBA) to obtain the corresponding 2-bromobutanal **47** which is treated with formamidine to yield compound **8** in a 5-*exo-tet* cyclization.

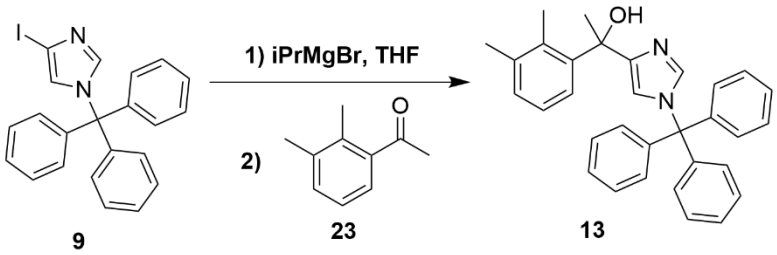
Finally, in 2016 Jiangsu Hengrui patented two very similar processes to obtain alcohol **13** and procced as described by Grindex[29] until the obtention of compound *rac*-**15** (*Scheme 1*). The processes differ in the nucleophile and electrophile moieties and improves Grindex process by introducing the methyl group in the starting reactants.

Instead of using an aldehyde as an electrophile, Jiangsu Hengrui uses a ketone to directly obtain the corresponding tertiary alcohol.



Scheme 13. *First patented Jiangsu Hengrui synthesis of compound* ***13***

In this way, first patented process by Jiangsu Hengrui[53] differs from Grindex patent in that the imidazole **48** is the electrophile (*Scheme 13*). The nucleophile is the xylyl moiety (aryl bromide **33**). The synthesis starts with the Grignard **20** formation from bromide **33**, which is reacted with keto-imidazole **48** to yield the alcohol **13**.



Scheme 14. *Last patented Jiangsu Hengrui synthesis of compound* ***13***

The last patented process of Jiangsu[54] is mostly similar to Grindex patent in terms of the reactivity of the synthons employed. However, the use of aldehyde **10** (Scheme 1) is replaced by a ketone (Scheme 14). Thus, trityl-protected iodoimidazole **9** is converted into the corresponding Grignard reagent by halogen-magnesium exchange[30] in the presence of iPrMgBr. Then, aryl methyl ketone **23** is added to afford the corresponding tertiary alcohol **13** after the nucleophilic addition.

The synthesis of compound *S*-**15** by Moehs will be proposed in next chapters considering all these relevant processes and new relevant references found during the investigation.

1.5 Project strategy

This project was initially developed in Norchim, a Moehs group company. For commercial interest, this project was transferred to the Moehs Group Research Center (MGRC). As time is a critical factor which can determine the success of the project, it was decided to adapt Norchim's manufacturing process to MGRC site facilities. In that process transfer, optimization of the current synthesis was performed. At the same time, new strategies to optimize the manufacturing process even if they involve a new route of synthesis were explored.

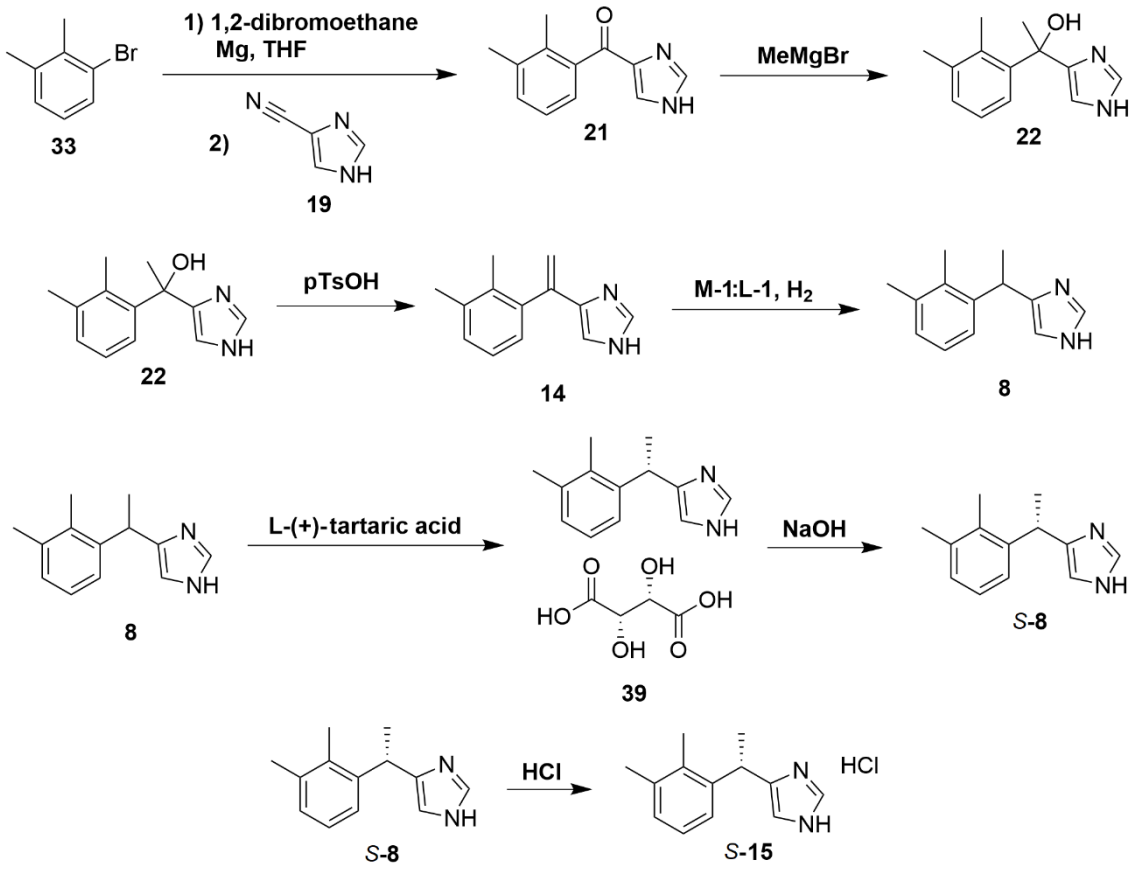
With this strategy, Moehs aimed to gain customers worldwide and, in the future, to be able to change the manufacturing process to another more efficient reducing the initial time for the product to reach the market.

Chapter 2 and Chapter 3 of this project are focused on the adjustment of Norchim's manufacturing process to Moehs' facilities with the optimization of the process and industrialization of the defined process. Chapter 4 is focused on the further development of a new synthetic approach to optimize the existing manufacturing process.

Chapter 2.
Optimization of the current synthesis

Chapter 2. Optimization of the current synthesis

The approach selected for the synthesis of compound *S*-**15** relays on the enantioselective formation of the desired stereocenter by asymmetric hydrogenation of the corresponding alkene group in the presence of a chiral ligand (Scheme 15). The enantiomeric excess of *S*-**8** could then be further improved by resolution through crystallization of the corresponding diastereomeric salt, **39**. The absolute configuration of *S*-**8** was determined by comparison in CHPLC to the certified USP standard.



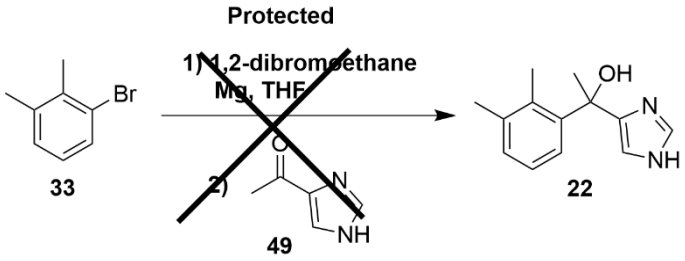
Scheme 15. *Selected synthesis of compound S-**15***

The alkene intermediate **14** at the core of this strategy is obtained by acid-promoted dehydration of the corresponding tertiary alcohol **22**, which can be synthetized via the corresponding ketone **21** in two steps from aryl bromide **33** and imidazole **19**. Imidazole **19** can be easily synthetized from the corresponding aldehyde in three steps one-pot synthesis.

On the basis of this synthetic route, Moehs began to work on the optimization and adaptation to the facilities in the company. All investigations regarding each step of the synthesis will be exposed in the following chapters.

2.1 Obtention of the starting material 19

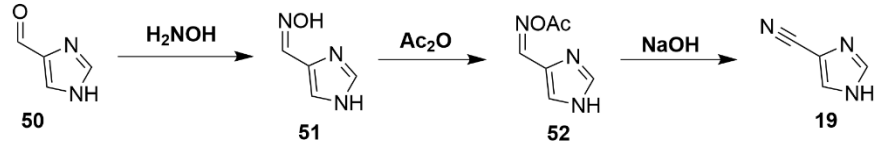
The synthesis of hydrochloride *S*-**15** is divided in 6 steps starting from aryl bromide **33** and the imidazole **19** to give ketone **21** as the first step. Actually, the synthesis of **21** has been attempted employing as electrophiles an aldehyde[29], an amide[45] or nitrile[31]. Among them, the use of nitrile was finally chosen since the corresponding aldehyde required more steps and the amide turned out to be less reactive against nucleophilic addition than the nitrile and could also give rise to secondary polyaddition products.



Scheme 16. *Possible synthesis of tertiary alcohol* ***22***

Alternatively, the use of ketone **21** can be avoided by preparing alcohol **22** via methyl ketone **49**. The obtention of the tertiary alcohol **22** intermediate could be obtained through the corresponding Grignard addition from the aryl bromide **33** to the ketoimidazole **49** (Scheme 16). However, this specific step was protected by Jiangsu Hengrui[53] in their first patent. For this reason, the obtention of the alkene key intermediate **14** must be synthesized in 2 steps via the ketone **21** and methylation starting from the corresponding nitrile **19**.

Norchim developed a new methodology to obtain easily and with very high yield (> 90 %) and purity (> 99,5 %) imidazole **19** (Scheme 17).

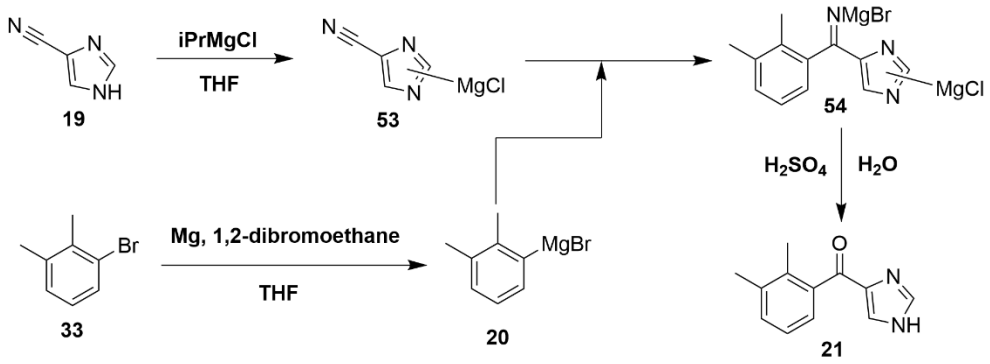


Scheme 17. *Synthesis of imidazole* ***19*** *by Norchim*

The synthesis starts with the formylimidazole **50** reacting with hydroxylamine to obtain the corresponding oxime **51**. Then, **51** is acetylated with acetic anhydride and followed by acetic acid elimination promoted by NaOH to yield the corresponding imidazole **19**. Despite Norchim developed a very efficient process to obtain this key starting material, due to commercial interests, Moehs decided to purchase this compound.

2.2 Synthesis of the ketone 21

The synthesis of the ketone **21** provided by Norchim (Scheme 15) presents some drawbacks in terms of scalability of the process. The most important factor to be focused is on the possibility to decrease the reaction volumes described by Norchim. Besides, safety of the process involved in this modification must be studied.



Scheme 18. *Synthesis of imidazole **21** by Norchim*

The first step in the synthesis was the formation of the Grignard reagent **20** (Scheme 18). The reaction was carried out in a total of 24 volumes of THF (1 volume = 1 mL/ 1 g of substrate) divided in 7 V with the magnesium and 17 V with the aryl bromide **33**. In addition, 3 mol % of the 1,2-dibromoethane was used as initiator.

The second step in the synthesis consisted of the deprotonation of imidazole **19** with 1,3 eq of iPrMgCl in 50 V of THF. Thus, the Grignard reagent formed in the first step, **20**, was added to the deprotonated imidazole complex **53** to yield the imine magnesium salt **54** (Scheme 18). Finally, this imine was hydrolyzed with 4 eq of H_2SO_4 dissolved in 20 V of H_2O. It must be noted that until this point, around 100 V of solvents were used.

Finally, 18 V *n*-heptane was added to the reaction mixture and the formed layers were separated. The aqueous layer was washed with 18 V more of *n*-heptane and next, 13 V of H_2O were added. After separation of the corresponding layers, the aqueous layer

was adjusted to pH 10 with aqueous NH_3. This made ketone **21** to precipitate so the suspension is filtered. The cake was washed 4 times with 11 V of H_2O and twice with 7 V of heptane. The solid obtained was dried under vacuum at 40 ºC for at least 16 h.

2.2.1 Studies on the formation of Grignard **20**

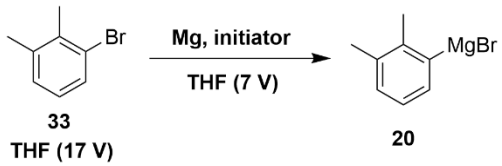
After a verification trial, the study of the synthesis of the ketone **21** is started beginning with the Grignard **20** formation.

This step presented various issues and hitches:

- Excessive reaction volumes: 24 V of THF were used in this step. Reduction of reaction volumes had to be studied. Thus, as the concentration of the reaction mixture increased, the process safety of this step had to be also studied.

- Inefficient reaction activation: The activation with 1,2-dibromoethane required at least 45 ºC and the bubbles formed indicating the reaction activation were difficult to observe.

- Poor safety process in reaction initiation: The reaction is carried out in 24 V which initially only 7 V are used to suspend the magnesium (Scheme 19). As this could facilitate the initiation of the reaction, also could lead to possible runaway of the reaction as the total volume at this moment was lower. For this reason, the distribution of reaction volumes toward magnesium and aryl halide must be studied.



Scheme 19. *Obtention of the Grignard reagent **20** by Norchim. Distibution of the solvent is indicated.*

Grignard formation could be initiated by organometallic hydrides compounds as previously described.[55,56] Also, iodine is a very common initiator for Grignard reactions. However, Moehs has experience with these methodologies and reported not to be so much robust as the initiation with 1,2-dibromoethane. Besides, sodium bis(2-methoxyethoxy)aluminium hydride (SMEAH) and Diisobutylaluminium hydride

(DIBALH) were also considered as possible initiators. It has been reported that the initiation of the reaction using these compounds can occur at room temperature or even colder.

To make safer the reaction, the major part of the solvent to suspend the magnesium was added initially. For this reason, the main decrease of solvent volume could be performed in the dilution of the aryl halide **33**.

The main points to be considered were the ease of identifying the initiation of the reaction and the stability of the more concentrated Grignard solution. Trials with different conditions and results are shown in table 3.

Table 3. *Conditions and results of Grignard formation trials*

Entry	Initiation conditions	THF volumes	Initiation observations	Conversion (%)[a]	Appearance
1	3 mol % of 1,2-dibromoethane at 45 – 50 ºC	7 with Mg 17 with **33**	Difficult to observe bubbles, no visible reaction heat	> 99,0	Fluid solution
2	3 mol % of 1,2-dibromoethane at 45 – 50 ºC	7 with Mg 3 with **33**	Difficult to observe bubbles, no visible reaction heat	> 99,0	Thick solution with jelly precipitate
3	3 mol % of 1,2-dibromoethane at 45 – 50 ºC	14 with Mg 6 with **33**	Difficult to observe bubbles, no visible reaction heat	> 99,0	Fluid solution
4	3 mol % of SMEAH 1 M in THF at 20 – 25 ºC	7 with Mg 17 with **33**	Huge effervescence and color change	98,2	Fluid solution
5	3 mol % of DIBALH 1 M in THF at 20 – 25 ºC	11 with Mg 4 with **33**	Huge effervescence and color change	> 99,0	Thick to jelly solution
6	3 mol % of DIBALH 1 M in THF at 20 – 25 ºC	14 with Mg 3 with **33**	Huge effervescence and color change	> 99,0	Fluid solution

(a) Determined by UHPLC from reaction crude

It was observed a clear difference between activating the reaction with 1,2-dibromoethane and SMEAH or DIBALH. When adding the metallic hydride, a huge effervescence was observed. When adding a small amount of the aryl halide **33** the solution turned black and a strong reaction heat was detected.

When reducing the total reaction volume from 24 V to 10 V, a very thick solution was formed after cooling to room temperature and a jelly precipitate appeared which was attributed to an oversaturation of the solution. Decreasing the reaction volumes down to 15 V, the precipitate disappeared but the whole solution was still very thick or jelly. Finally, decreasing just down to 17 V, a fluid solution was obtained. It must be noted that when cooling the 24 V solution to 0 – 5 ºC, no visible differences were observed whereas when cooling to 0 – 5 ºC the solution at 17 V it turned very thick and a jelly precipitate appeared. This may indicate that the solution at 17 V is near to saturation at room temperature.

Considering these results two changes were applied:

- The reaction volumes were reduced to 17 V (14 V with Mg and 3 V with aryl halide **33**).

- The activator was changed to DIBALH at room temperature.

2.2.2 Studies on the deprotonation of imidazole **19**

The second step involved the formation of imidazole magnesium complex **53**, conducted in 50 V of THF and using 1,3 eq of iPrMgCl (Scheme 18). The main objective at this stage was to minimize reaction volumes. Along with the concentration, temperature became a critical factor of the reaction and the potential formation of impurities was also studied.

After the initial trials, it was observed that the reaction mixture thickened significantly upon concentration, resulting in homogeneity issues within the reactor. Various conditions were tested, and the corresponding results are presented in table 4.

The concentration of the mixture significantly influenced the observed heat released, causing a rise in temperature and concurrently leading to an increase in the formation of impurities (entries 1 compared to 2 and 3). In response to this, the reaction

temperature was lowered 10 ºC compared to the initial range (entries 4 and 5). This adjustment allowed a reduction in the reaction volume from 50 V to 17 V while maintaining an acceptable amount of impurities.

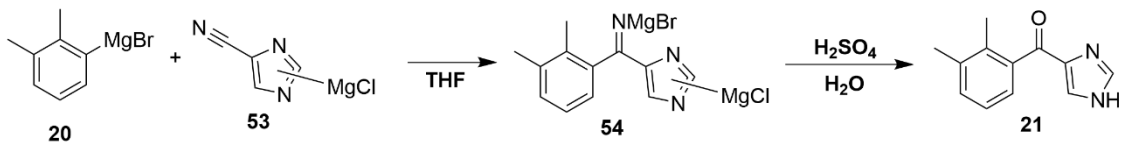
Table 4. *Conditions and results of deprotonation trials*

Entry	THF volumes	T (ºC)	Appearance	Impurities formation[c]
1	50	From -5 to 0[a]	Fluid solution	No
2	10	From -5 to 0[b]	Very thick and not homogeneous	Yes
3	20	From -5 to 0[b]	Very thick but homogeneous	Yes
4	24	From -10 to -5[b]	Very thick but homogeneous	Low
5	17	From -15 to -10[b]	Very thick but homogeneous	Low formation

(a) No exothermic heating was observed. (b) High exothermic heating observed. (c) Determined by UHPLC-MS from the reaction crude

2.2.3 Studies on the formation of imine-magnesium intermediate complex **54**

The only improvement performed in the third step, was the systematization of the THF washings to ensure the complete transfer of the Grignard **20** solution to the imidazole salt, **53**, suspension. All other parameters remained consistent with the Norchim process description, as no significant impacts were observed (Scheme 20). It was observed that increasing the reaction time did not affect conversion, and the reaction evolution was found to decrease at lower temperatures.



Scheme 20*. Obtention of the imine-magnesium complex **54** according to Norchim procedure*

Another improved aspect from Norchim's procedure was the elimination of the residual magnesium from the Grignard reagent. It was only described the treatment of the residual Mg with diluted aqueous HCl. We implemented the addition of 5 V of THF after Grignard transfer to prevent its spontaneous reaction with air exposure. Moreover, as

the reaction of Mg with HCl is highly exothermic, 25 V of water were added to the reaction mixture before the addition of the concentrated acid. After the quenching was completed, a more manageable solution was obtained.

2.2.4 Studies on the hydrolysis of imine-magnesium complex **54**

The fourth step in the synthesis involves the hydrolysis of the complex **54** for the obtention of ketone **21** (Scheme 20). Norchim initially reported performing the hydrolysis at room temperature using 4 equivalents of H_2SO_4 in 20 V of H_2O, completing the reaction in 2 hours. Various trials involving different H_2O amounts were conducted at different reaction times (Table 5):

Table 5. *Conditions and results for the obtention of ketone **21** after the hydrolysis of complex **54***

Entry	H_2O volumes	V % of H_2O in reaction mixture	Reaction conversion (%) over time[a]					
			2 h	3 h	4 h	5 h	6 h	16 h
1	20	20	Quant.					
2	12	19	78,4	96,7	99,9			
3	10	21	78,2	97,9	Quant.			
4	10	18	65,4	88,7	98,1	99,9		
5	6	17	43,6	62,8	80,4	92,3	98,7	Quant.

(a) Determined by UHPLC from the reaction crude

The amount of H_2O selected for this step was 10 V. The addition of more H_2O hindered the separation from the THF in the work-up (entries 1 and 2). However, lower amounts of H_2O increased the reaction time (entry 2 and 5). For this reason, entry 4 conditions were selected.

2.2.5 Studies on the purification and precipitation of ketone **21**

The work-up of the last step in the synthesis of **21** consists in the addition of *n*-heptane to the THF/H_2O mixture to favor the separation of the THF layer from the aqueous phase, where the newly produced ketone is dissolved. The ratio between *n*-heptane and H_2O was maintained as described by Norchim but the total amount was decreased by a factor of 3,6. This reduction was applied to allow the future scale-up to a 30 L reactor. Then the pH was adjusted to 10 with aqueous ammonia precipitating the

desired product. The main problem in this step was the effective removal of the salts formed during the process. For this reason, centrifugation washes were not reduced. To control inorganic impurities, a potentiometric assay was performed to ensure the quality of ketone **21**.

The total volumes of H_2O used in Norchim's precipitation process were 33 V (20 from the reaction and 13 from the work-up). From the last aqueous phase, the following trials were conducted to investigate the precipitation at pH 10:

- Trial 1: pH adjustment at 0 - 10 ºC and the suspension is filtered at room temperature.

- Trial 2: pH adjustment at 0 - 10 ºC. The suspension is heated to 40ºC, cooled to 0 – 5 ºC and filtered.

- Trial 3: pH adjustment at room temperature with a slow addition of ammonia and the suspension is filtered at 0 – 5 ºC.

The aqueous phase presented a turbidity that precipitates as a solid in a few hours. An aliquot of supernatant was filtered and the solid was analyzed without detecting any signal by UHPLC-MS. Therefore, the solid was attributed to the magnesium salts of the process. According to this, other trials were carried out and the conditions and results are shown in table 6:

Table 6. *Conditions and results in the trials for the precipitation of* ***21***

Entry	Filtration	H_2O Volumes	Temp. pH adjust.[a] (ºC)	Heated	Filtration Temp. (ºC)	Assay (%)[b]
1	No	0	0 - 10	No	0 – 5	100
2	No	0	0 - 10	No	r.t.	92
3	No	0	0 - 10	Yes, 40 ºC	0 – 5	89
4	No	0	r.t.	No	0 – 5	92
5	Yes	0	0 - 10	No	0 – 5	100
6	No	0	0 - 10	No	0 – 5	92
7	No	5	0 - 10	No	0 – 5	95
8	Yes	5	0 - 10	No	0 – 5	99
9	Yes	10	0 - 10	No	0 – 5	100
10	Yes	15	0 - 10	No	0 – 5	100

(a) All trials were performed at pH 10. (b) Determined by potentiometric titration

It was observed that Norchim's process did not produce any magnesium salts precipitated after hydrolysis due to the dilution. As the concentration was increased, this precipitate appears. Apparently, increasing H_2O volumes before precipitation could lead a potentiometric assay of about 100 % indicating no residual magnesium salts in the final product. However, to increase the robustness and mitigate the risk of salts in the desired ketone **21** a salts filtration is performed before the work-up and 10 V of H_2O were added after the work-up, right before **21** precipitation.

So finally, precipitation volumes were reduced from 33 to 26 V of H_2O to fill the 30 L reactor allowing to increase batch size. Additionally, the final amounts of solvents and reagents for ketone **21** obtention were adjusted to be measurable by the equipment at this scale.

2.3 Synthesis of the alkene 14

The synthesis of the alkene **14** provided by Norchim presents some inconvenience in terms of time economy. The most important factor to be focused on is the isolation of the alcohol **22**. The process safety involved in this process also must be studied.

The first step in the synthesis reported by Norchim is the methylation of the ketone **21** with 3 eq of MeMgCl in 10 V of THF. After refluxing for 2 hours, the solution is quenched with saturated aqueous solution of NH_4Cl and pH adjusted to 7 with aqueous HCl. Phases are separated, aqueous phase washed with 2 V of EtOAc twice and the organic phases washed with saturated NaCl aqueous solution. The organic phase is distilled, and 8 V of *n*-heptane is charged to the residue. The resulting suspension is centrifugated and washed with 2 V of *n*-heptane twice. The solid obtained is dried at 40 ºC under vacuum for 16 h to give alcohol **22**.

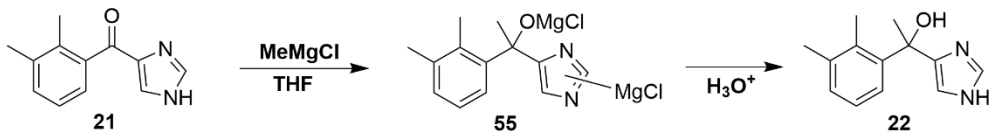
The second step in the synthesis is the dehydration of the tertiary alcohol. The reaction is carried out in 10 V of Toluene in the presence of 10 mol % of pTsOH. After 3 hours at reflux, the solution is cooled and added a $NaHCO_3$ saturated aqueous solution. The resulting suspension is centrifugated and washed with 1 V of H_2O and 1 V of *n*-heptane twice each. The solid is dried at 40 ºC under vacuum for 16 h to obtain the alkene **14**.

As the methyl addition reaction does not generate many side products and the final organic phase containing the alcohol **22** is already distilled, it is feasible to continue to

the next step in a one-pot synthesis approach. Keeping this in mind, the study of the synthesis of the alkene **14** was started.

2.3.1 Studies on methyl addition to ketone **21**

The methyl addition to **21** (Scheme 21) reported by Norchim was carried out at room temperature. However, a very thick suspension is formed leading to a heterogeneous mass with uncompleted conversion. For this reason, the reaction is heated at reflux for 2 h.



Scheme 21. *Obtention of the tertiary alcohol **22** by methylation of ketone **21***

In this step, Moehs doubles the batch size by combining 2 batches of ketone **21**. This increases the total volume to more than the reactor capacity. For this reason, the reaction volumes must be reduced. As it is possible to form a heterogeneous suspension concentrating the reaction, the volumes of THF were reduced from 10 to 8 V. Moreover, the addition of MeMgCl was performed at room temperature while heating, taking advantage of the reaction exotherm to heat the reaction mixture to reflux. Conditions and results of this trials are shown in table 7.

Table 7. *Conditions and results for the trials of methyl addition to **21***

Entry	THF volumes	Conversion (%) at 2 h[a]	Conversion (%) at 3 h[a]
1	10	99,5	Quantitative
2	8	99,4	Quantitative

(a) Determined by UHPLC from reaction crude

As the reaction worked as expected, to increase the robustness of the process, the reaction time was increased from 2 h to 3 h, maximizing the conversion without impurities formation.

Other process parameters as the ones concerning the reaction quenching with NH_4Cl saturated aqueous solution and the amount of NaCl saturated aqueous solution were systematized by dissolving a known amount of NH_4Cl and NaCl in a known amount of

water. Quenching temperature reported by Norchim was 0 – 10 ºC and the temperature proposed by Moehs used was 0 – 30 ºC. No observable differences were observed except quench time which was reduced when increased the temperature range. In this way, the procedure is easier to be performed without compromising quality.

Finally, to investigate the product loss in alcohol **22** isolation, the final organic phase was distilled under vacuum to dryness and the yield was evaluated. Then the product was suspended in *n*-heptane, recovered by filtration and the yield evaluated after drying. A comparison between yields obtained are shown in Table 8:

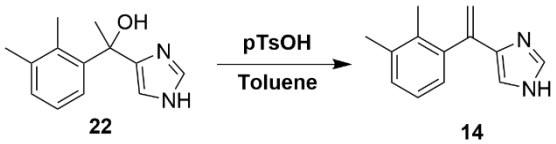
Table 8. *Conditions and results of the obtention of alcohol* ***22***

Entry	Precipitation volumes	Yield (%)
1	8	91
2	N/A	95

The difference in yield could be attributed to the solubility of the alcohol **22** in *n*-heptane. The yield of product to be reacted in the next step is higher when no isolation is performed.

2.3.2 Studies on the dehydration of tertiary alcohol **22**

The second step described by Norchim consists in the dehydration of the alcohol **22** carried out in toluene in the presence of catalytic amounts of pTsOH (Scheme 22).



22 **14**

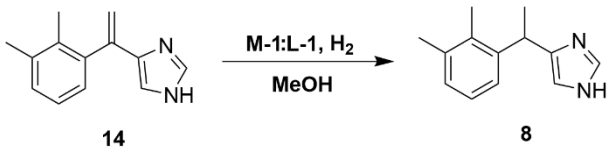
Scheme 22. *Dehydration of the tertiary alcohol* ***22***

It was tried to continue with the dehydration without isolating the alcohol **22**. A toluene stripping was carried out and then 10 V of toluene and 0,1 eq of pTsOH were charged to the distillation residue. The dehydration was performed by heating the reaction mixture to reflux with a Dean Stark apparatus for 3 h. After this time, a 99,9 % conversion was determined by UHPLC-MS. Then, the saturated $NaHCO_3$ aqueous solution was replaced by the solution of 0,5 eq of $NaHCO_3$ in 2 V of H_2O. In these conditions compound **14** crystallized and after heating up to 38 ºC the suspension was

cooled to room temperature to give a solid which was isolated by filtration. The solid was then washed with 1 V of H_2O twice and 1 V of *n*-heptane twice and dried at 40 ºC under vacuum for 16 h. In this way, alkene **14** was obtained with a overall yield of 89,2 % from ketone **21**.

2.4 Asymmetric hydrogenation of alkene 14

Norchim reported the asymmetric catalyzed hydrogenation of the alkene **14** with a rhodium complex bearing a Josiphos ligand. This reaction is carried out in 46 V of MeOH at 45 – 50 ºC under 10 bar of H_2 for 12 h. The only hydrogenator for this batch size accessible for us was Norchim's hydrogenator of 60 L and 30 bar of pressure. Originally, Norchim filled the reactor to around 30 L.



14 **8**

Scheme 23. *Asymmetric hydrogenation of alkene* ***14***

For safety reasons the reactor must not be filled to more than 50 % and the working pressure must not exceed the 50 % of the maximum design pressure. For this reason, the reaction mixture must be less than 30 L and the pressure must not exceed 15 bar.

In Moehs, the batch size has been increased in the synthesis of the alkene **14**. Consequently, concerning safety considerations, little changes were made to fit this new batch size in the same hydrogenation facilities.

To fit Moehs new batch size, the reaction volumes were decreased to around a half. The objective of this step was maintaining the results reported by Norchim when increasing the concentration. As mentioned at the beginning of the chapter, the time to reach the market was crucial for the success of the project. For this reason, an exhaustive study of different conditions of this reaction were performed.

2.4.1 Study of the influence of concentration in the asymmetric hydrogenation of alkene **14**

Firsts trials focused on the study of the influence of the concentration on the reaction conversion. The enantiomeric excess was not expected to vary. The reaction was controlled at 12 h and 24 h. Reaction volumes and results are shown in Table 9:

Table 9. *Results in the hydrogenation of alkene* ***14*** *at 45 – 50 ºC*

Entry	MeOH volumes	Conversion at 12 h (%)[a]	Conversion at 24 h (%)[a]	e.e. (%)[ab]
1	46	97,9	Quantitative	78,4
2	30	94,5	96,0	78,3
3	25	92,5	93,6	78,8
4	15	82,3	83,5	78,7

(a) Determined by CHPLC from the reaction crude. (b) Determine at the reaction crude at 24 h

When concentrating the reaction mixture, the reactivity decreased, and complete conversion was not reached. For this reason, reaction time was increased from 12 h to 16 h and also the reaction temperature from 45 – 50 ºC to 55 – 60 ºC. Reaction volumes and results for these new conditions are shown in Table 10:

Table 10. *Results of the alkene* ***14*** *hydrogenation at 55 – 60 ºC*

Entry	MeOH volumes	Conversion at 16 h (%)[a]	Conversion at 24 h (%)[a]	e.e. (%)[ab]
1	46	Quantitative	-	76,1
2	30	Quantitative	Quantitative	76,3
3	25	Quantitative	Quantitative	76,1
4	15	87,6	99,2	76,4

(a) Determined by CHPLC from the reaction crude. (b) Determine at the reaction crude at 24 h

From these trials, conditions chosen for next studies were 25 V of MeOH, 16 h of reaction at 55 – 60 ºC with 10 bar or H_2.

2.4.2 Study of the influence of temperature in the asymmetric hydrogenation of alkene **14**

With these conditions, the influence of temperature on the conversion, but specially on the enantioselectivity, was investigated by changing the temperature from 70 to 40 ºC

maintaining the previous described conditions. Reactions were stopped after 16 h and analyzed by CHPLC. With these trials, it was also studied the robustness by repeating several times trials at 55 ºC. Temperatures and results are shown in Table 11:

Table 11. *Study of the temperature influence in the alkene* ***14*** *hydrogenation*

Entry[a]	Temperature (ºC)	Conversion (%)[b]	e.e. (%)
1	70	Quantitative	73,5
2	65	Quantitative	75,7
3	60	Quantitative	76,1
4	55	Quantitative	77,3
5	55	Quantitative	77,6
6	55	Quantitative	77,5
7	55	Quantitative	77,6
8	55	Quantitative	77,3
9	50	99	78,1
10	45	98	79,3
11	40	98	80,5

(a) All reactions performed in 25 V of MeOH. (b) Determined by CHPLC from the reaction crude

According to the results, it can be stated that the hydrogenation procedure is robust (entries 4 to 8). As expected, a decrease of e.e. is observed when increasing the temperature. The enantiomeric excess expected to obtain from the hydrogenation is between 76,0 a 78,0 % according to previous data provided by Norchim.

Once this brief study of the influence of temperature on the result of the reaction was carried out, since it is a hydrogenation reaction, it was considered appropriate to also carry out a combined study of temperature and pressure influence. For this, a rationalization was first carried out through the design of experiment (DoE) tool.

2.4.3 Design of Experiments study

A design of experiment was performed in order to study the influence of the temperature and pressure together. A 2^2 full factorial DoE was performed with 3 central points ranging the temperature from 40 – 70 ºC and pressure from 5 to 15 bar. MeOH volumes were fixed to 25 V and reaction time to 16 h. Conditions and results are shown in table 12:

Table 12. *First DoE of the alkene* ***14*** *hydrogenation*

Experiment	Temperature (ºC)	Pressure (bar)	Conv. (%)[a]	e.e. (%)[a]
1	40	5	97,0	81,5
2	70	5	Quantitative	73,5
3	40	15	97,3	80,8
4	70	15	Quantitative	73,3
5	55	10	99,9	77,6
6	55	10	99,9	77,5
7	55	10	99,9	77,6

(a) Determined by CHPLC from the reaction crude

The software used for data analysis was Design Expert v.22.0.6. The temperature was the most significant factor whereas pressure had no significant effect. Both factors being directly proportional to the conversion and inversely proportional to enantiomeric excess (Figure 5).

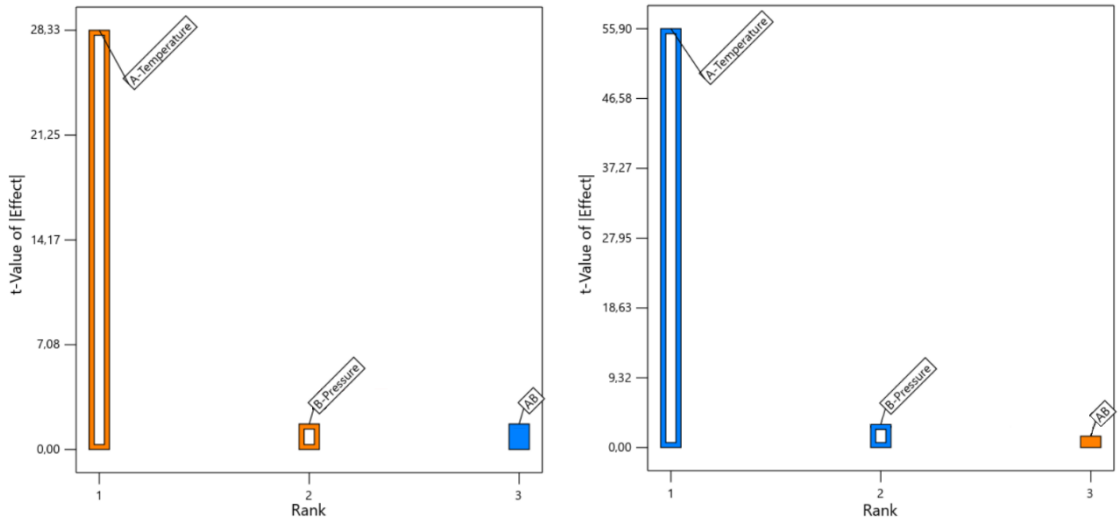


Figure 5. *Effect chart of conversion (left) and e.e. (right). In orange positive effects and in blue negative effects*

Finally, the alkene **14** hydrogenation was carried out with 1 % of catalyst in 25 V of MeOH at 55 – 60 ºC for at least 16 h under 10 bar of H_2. The expected e.e. is between 76,0 – 78,0 % which was further improved. A deeply study of upgrade is discussed in Chapter 4.

2.5 Obtention of the enantiopure alkane *S*-8

As described by Norchim, to achieve the resolution of enantioenriched alkane **8** from the hydrogenation crude (e.e. between 76,0 – 78,0 %), **8** was precipitated as diastereomeric salt with 1 eq of L-(+)-tartaric acid in acetone/H_2O mixture (Scheme 24). This tartrate salt **39** was recrystallized from an EtOH/H_2O mixture until ≥ 99,8 % e.e. crystals were collected. Finally, **39** is treated with NaOH in H_2O to recover by filtration enantiopure alkane *S*-**8**.

At this point, the 2 main critical quality attributes of the final product are of special relevance as they are determined in this step. These are:

- **Optical purity:** The e.e. must be higher than 99,8 %.

- **Residue on Ignition (RoI):** Inorganic impurities must be lower than 0,1 %.

The main goal for this step was to verify if the slightly decreased enantiomeric excess from the hydrogenation obtained by Moehs could be pure enough to achieve the isolated alkane *S*-**8** with the desired quality attributes following the process described by Norchim (99,8 % e.e.). In addition, it was also proposed to increase the concentration in the precipitation step to enhance the yield.

2.5.1 Studies on the precipitation of diastereomeric tartrate salt **39**

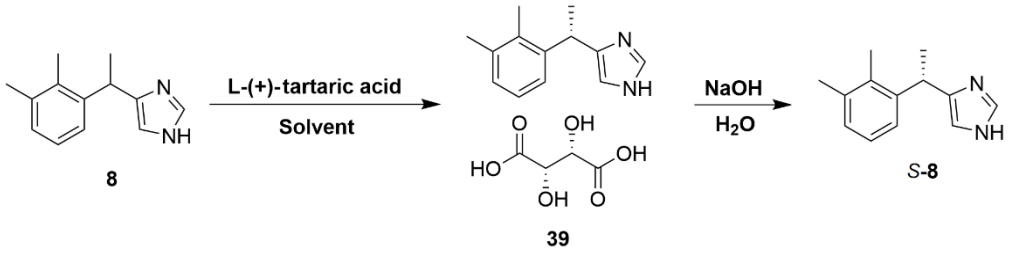
Norchim described the precipitation of the tartrate salt in 11 V of 10/1 acetone/H_2O mixture in the presence of 1 eq of L-(+)-tartaric acid (Scheme 24). There are three key features described in this step:

- **Resolving acid:** L-(+)-tartaric acid was reported to be the most efficient in terms of resolution between the most common acids used in the literature. Those acids studied by Norchim included Dibenzoyl L-(+)-tartaric acid, L-(-)-malic acid and L-(-)-camphorsulfonic acid.

- **Solvent system:** A compromise between yield and purity is achieved when carrying out the precipitation in acetone/H_2O mixture. The presence of water was reported to be very important for the resolution.

- **Resolving agent equivalents:** It was reported by Norchim that the use of less equivalents of resolving agent aiming to precipitate only the major and desired

enantiomer, *S*-**8** was not efficient as the increase in optical purity did not justify the drop in yield.



Scheme 24. *Formation of the diasteriomeric salt* ***39*** *and S-****8*** *obtention*

The study of the precipitation focused on solvent conditions maintaining L-(+)-tartaric acid as resolving agent and 1 eq for the salt formation. A selection of solvents was carried out as a verification of the information received by Norchim.

Table 13. *Solvent screening for* ***39*** *precipitation from hydrogenation of* ***8***

Entry	Organic solvent	H_2O (V)	Yield (%)	e.e. (%)[a]
1	Acetone, 10 V	1	84	91,3
2	Acetone, 10 V	0,5	90	87,3
3	Acetone, 10 V	-	99	80,6
4	Acetone, 8 V	2	74	93,9
5	MeOH, 10 V	1	47	97,7
6	MeOH, 10 V	0,5	56	96,2
7	EtOH, 10 V	1	73	94,9
8	EtOH, 10 V	0,5	79	91,8
9	EtOH, 8 V	2	66	95,9
10	iPrOH, 10 V	1	77	93,3
11	iPrOH, 10 V	0,5	85	90,1
12	iPrOH, 5 V	-	96	82,1
13	MeCN, 10 V	1	85	88,1
14	MeCN, 10 V	0,5	88	84,8
15	MeCN, 10 V	0,2	90	81,3
16	THF, 10 V	1	60	94,7
17	THF, 10 V	0,5	78	92,0
18	THF, 10 V	-	95	85,4
19	EtOAc, 10 V	0,2	99	82,7

(a) Determined by CHPLC

A hydrogenation reproducing the conditions pointed by Norchim was carried out with a 99,9 % conversion and 78,5 % e.e. The crude of this reaction was used as the starting material in the study summarized in table 13.

It was observed that bot entries 1 and 7 resent the best compromise between yield and e.e. being the mixture of acetone or EtOH in combination with H_2O (10:1) the best among the mixtures studied. This was easier to see when ploting % of yield vs % of e.e. of all trials and drawing a trend line (Figure 6). This line was moved parallely until the least number of points are placed above the line. The region above the line contains those points with higher yields and e.e. at the same time. This approximation was useful to easily identify the most promising conditions.

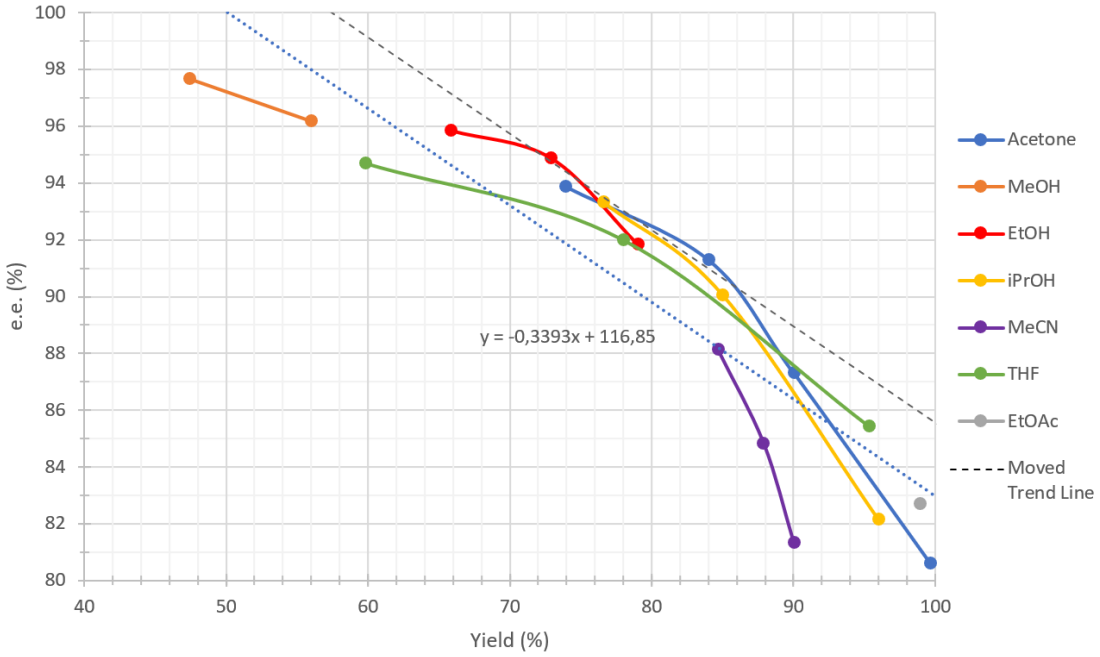


Figure 6. *e.e. (%) vs Yield (%) plot for precipitation of* ***39*** *screening*

As observed in figure 6, entries 1 (in blue) and 7 (in red) of table 13 are above the moved trend line indicating that these conditions provide the best yield and e.e. at the same time.

It was observed that MeOH increases dramatically the e.e. in detrimental of yield. EtOH had the same effect but lower. It was proposed to introduce MeOH or EtOH in the precipitation to increase the e.e. value. Also, in order not to decrease so much the yield, the solvent mixture amount was reduced to the half. With this, a tertiary solvent

mixture was proposed consisting of acetone, H_2O and an alcohol (EtOH / MeOH). The proportion of the alcohol was set to 3 V as it is the half of the mean between acetone and H_2O. With this, 2 trials were carried out and compared to entries 1 and 7 in table 13. Detailed solvent conditions and results are shown in table 14.

Table 14. *Solvent optimization for* ***39*** *precipitation from* ***8*** *hydrogenation crude*

Entry	Organic Solvent	Alcohol	H_2O (V)	Yield (%)	e.e. (%)[a]
1	Acetone, 10 V	-	1	84	91,3
2	EtOH, 10 V	-	1	73	94,9
3	Acetone, 5 V	MeOH, 3 V	0,5	85	93,2
4	Acetone, 5 V	EtOH, 3 V	0,5	88	91,4

(a) Determined by CHPLC

The tertiary mixture containing MeOH provide a higher e.e. but a lower yield than the mixture containing EtOH. Trend line was moved until only one point was right above the line (Figure 7).

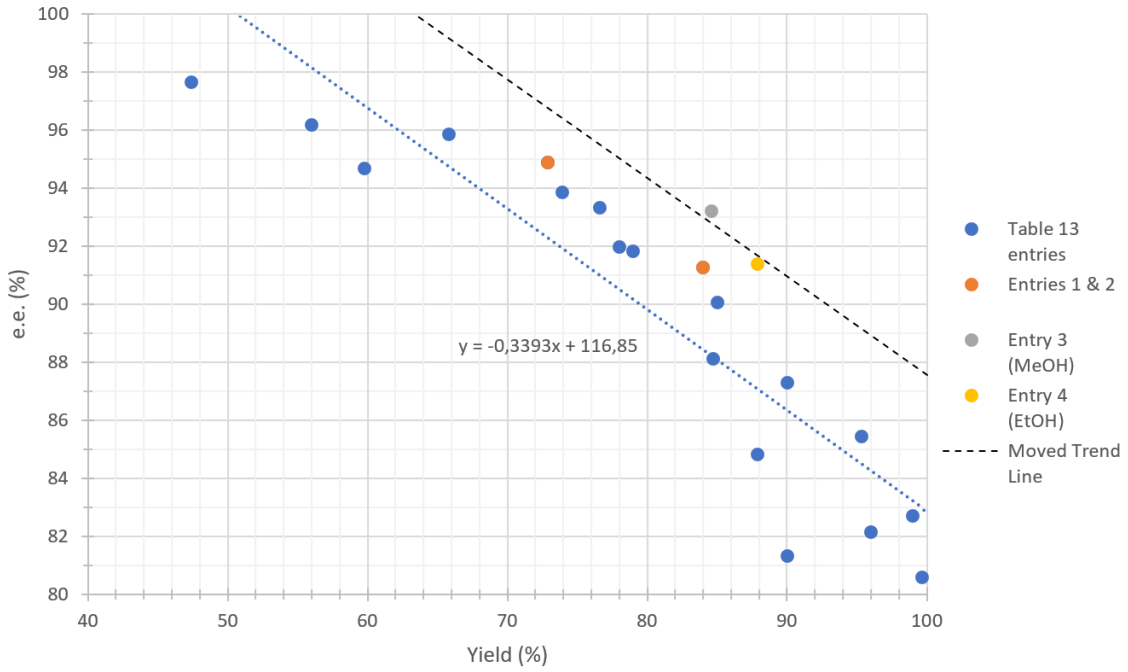


Figure 7. *e.e. (%) vs Yield (%) plot for the optimization of precipitation of* ***39***

As observed in figure 7, entry 3 is the only above the trend line indicating the best compromise between yield and e.e.

2.5.2 Study on the crystallization of diastereomeric tartrate salt **39**

Despite the improvement in e.e. any attempt reported in the last section achieved the desired e.e. of ≥ 99,8 %. Therefore, it was decided to crystallize the tartrate salt **39**, as described by Norchim. Tartrate salt **39** coming from entry 3 in table 14 was used to crystallize in a solvent screening. Detailed solvent conditions and results are shown in table 15.

Table 15. *Solvent screening for **39** 1st crystallization and 2nd crystallization*

Entry	Initial e.e. (%)[a]	Organic solvent	H_2O (V)	Yield (%)	e.e. (%)[a]
1	93,22	EtOH, 10 V	1	85	98,7
2		EtOH, 10 V	0,5	88	97,6
3		iPrOH, 10 V	1	82	96,7
4		Acetone, 10 V	1	89	96,5
5		MeCN, 10 V	1	87	95,4
6		Acetone, 5 V MeOH, 3V	1	82	99,3
7[b]	98,7[b]	EtOH, 10 V	1	90	99,9
8	95,9	EtOH, 10 V	1	93	99,2
9[c]	99,2[c]	EtOH, 10 V	1	93	99,9

(a) Determined by CHPLC. (c) Product from entry 1 was crystallized again. (d) Product from entry 8 was crystallized again

Crystallization of **39** with the studied conditions did not reach an e.e. ≥ 99,8 % when samples were only once crystallized. However, following the same methodology as in the precipitation, the only point above the trend line is entry 1 (Figure 8).

For this reason, the solid isolated in entry 1 were recrystallized in entry 7 and thus the desired optical purity was achieved. Following these conditions, a sample of **39** with higher e.e. was crystallized (Entry 8). Despite the higher e.e. of the starting sample, a recrystallization did not reach the desired optical purity. However, a second recrystallization gave finally the desired e.e. (Entry 9).

Finally, it was concluded that 3 purification steps (precipitation + 2 crystallizations) were needed in order to increase the e.e. obtained in the hydrogenation up to the desired optical purity. Despite this, a slight drop in performance must be assumed.

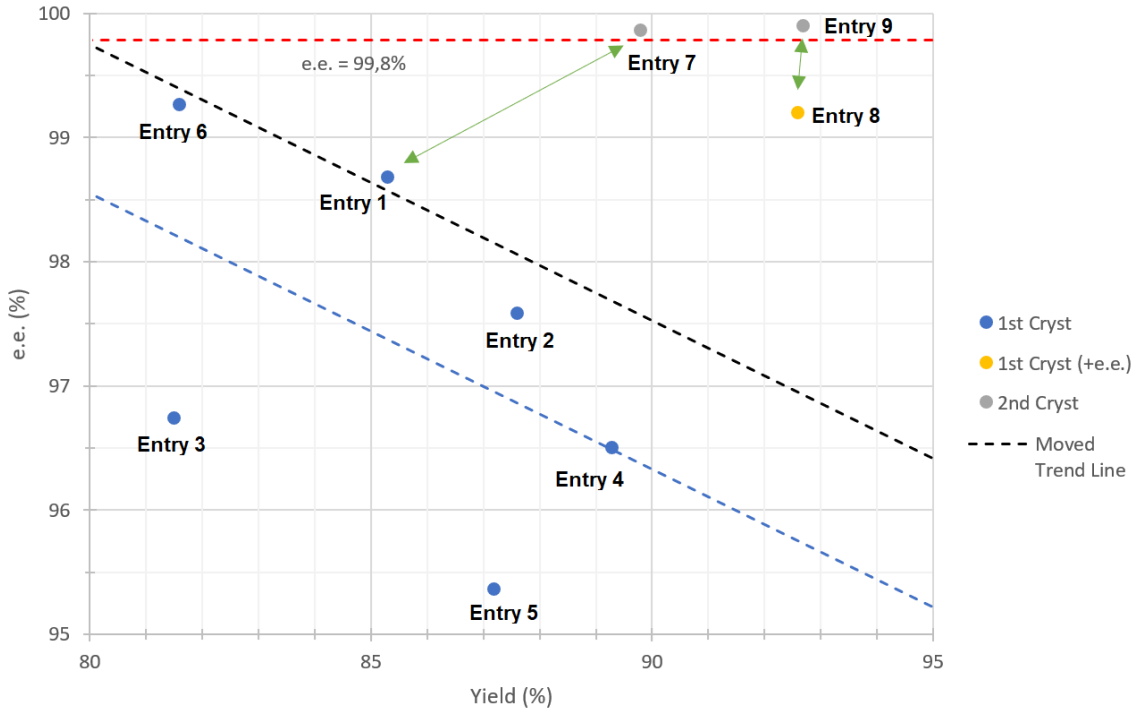


Figure 8. *e.e. (%) vs Yield (%) plot for* ***39*** *crystallization and recrystallization*

2.5.3 Study on the base release of enantiopure alkane *S*-**8**

The last step is the neutralization of the tartaric salt **39** to obtain the enantiopure alkane *S*-**8** as a base. Norchim performed this reaction in 10,4 V of H_2O with NaOH to pH > 10 at room temperature. At this temperature, **39** is not dissolved and *S*-**8** is not soluble in H_2O. It was observed that the tartrate salt was soluble at 50 ºC so the addition of NaOH was proposed to be done at this temperature. With that, *S*-**8** precipitates along the addition. This could lead to more homogeneous product.

Table 16. *S-**8** formation homogeneity and robustness study*

Entry	NaOH addition Temperature	Final pH (>10)	Yield (%)	RoI (%)[a]
1	20 – 25 ºC	12,0	93	0,0
2		12,6	97	0,2
3		11,6	88	0,4
4	50 ºC	14,0	92	0,1
5		11,8	92	0,0
6		12,1	94	0,0

(a) Determined by sulphated ash test

Some trials were carried out to proof the homogeneity and robustness of both processes focusing on the Residue on Ignition (RoI) values. Results of these trials are shown in table 16:

It was observed that neutralizations performed at 50 ºC (entries 4 - 6) present better results in terms of yield and RoI than those at 20 – 25 ºC (entries 1 - 3). The organic purity of *S*-**8** including optical purity remains the same as **39**.

The final conditions and expected yields and purities for each step in the obtention of enantiopure alkane *S*-**8** from the hydrogenation are summarized in *Table 17*:

Table 17. *Obtention of S-**8** process parameters from hydrogenation crude*

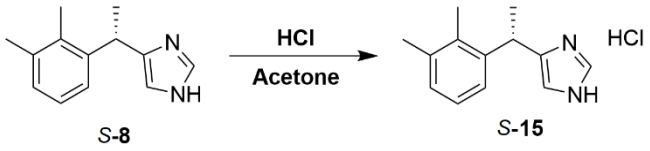
Step	Conditions	Purity[a]	Expected yield
Precipitation	5 V acetone 3 V MeOH 0,5 V H_2O	About 93 %	About 80 %
1st Crystallization	10 V EtOH	About 98 %	About 85 %
2nd Crystallization	1 V H_2O	> 99,8 %	About 90 %
Neutralization	10,4 V H_2O pH > 10 at 50 ºC		About 95 %
Global		> 99,8 %	About 58 %

(a) Determined by CHPLC

Norchim reported a global yield of the resolution of about 52 %. Our synthesis at Moehs increases slightly the yield despite the number of total purifications are the same. The time dedicated to the purification is very high. Considering that the work must be done into an isolator containment system, the manufacturing costs of this step are relatively high. For this reason, the resolution step can be further improved. A deeply study of this step and other alternatives are discussed in Chapter 4.

2.6 Obtention of the final product *S*-15

The formation of the hydrochloride salt was studied by Norchim starting from enanatiopure *S*-**8** and precipitating the salt *S*-**15** in acetone after the addition of aqueous HCl (Scheme 25). The dissolution of *S*-**8** in acetone with the subsequent addition of 1,2 eq of aqueous HCl turned the mixture from yellowish to brown and it was reported a low yield.



Scheme 25. *Obtention of the final product S-**15***

The salt *S*-**15** is known to be extremely water soluble. Its solubility is about 950 g/L. For this reason, the salt formation was first carried out in 5 V of EtOH and then the solvent was changed to acetone.

In order to eliminate completely the water from the reaction mixture, 6 distillations were performed by adding acetone followed by distillation removal. Finally, 4 V of acetone were added to the distillation residue and filtered at 0 – 5 ºC obtaining about 90 % yield.

Norchim also studied the solubility of *S*-**15** in acetone and EtOH being around 200 g/L and 400 g/L respectively. For this reason, the first optimization proposed by Moehs was to reduce the final acetone volumes to those necessary to obtain a fluid suspension.

In addition, as compound *S*-**15** is extremely soluble in H_2O, it was also proposed to change the use of aqueous HCl to HCl in EtOH. The commercial HCl in EtOH has a concentration of 1,25 M. This matched very well with the described conditions, as maintaining the 5 V of EtOH the equivalents of HCl were increased to from 1,2 to 1,25.

As the final product is still very soluble in EtOH and at least more than acetone, 2 distillations of acetone were maintained to successfully eliminate the amount of EtOH in the final suspension.

A screening considering the proposed improvements was carried out and the results obtained are shown in table 18.

Table 18. *Trials for the obtention of S-**15*** [ab]

	Entry 1	**Entry 2**
HCl used	Aqueous HCl	HCl in EtOH
Remaining after ethanol distillation	3,9 % of H_2O	0,6 % of H_2O
Remaining after acetone distillation 1	33,0 % of EtOH 3,3 % of H_2O	35,7 % of EtOH 0,01 % of H_2O
Remaining after acetone distillation 2	2,4 % of EtOH 3,1 % of H_2O	2,5 % of EtOH 0,01 % of H_2O
Remaining after acetone distillation 3	0,1 % of EtOH 1,9 % of H_2O	N/A
Remaining after acetone distillation 4	0,0 % of EtOH 1,1 % of H_2O	
Remaining after acetone distillation 5	0,6 % of H_2O	
Remaining after acetone distillation 6	0,4 % of H_2O	
Final suspension	4 V of acetone containing: 0,0 % of EtOH + 0,4 % of H_2O	3 V of acetone containing: 0,0 % of EtOH + 0,0 % of H_2O
Yield	91,4 %	96,9 %

(a) All % of H_2O given were determined by KF titration. (b) All % of EtOH given were determined by HS-GC

It was observed that the amount of water after the second distillation is considerably lower in when using HCl in EtOH (entry 2 vs entry 1). Thus, 2 distillations of acetone were enough to completely remove the EtOH from the mixture with this HCl source.

Table 18. *Optical purity evaluation in S-**15** obtention*

Trial	**Initial compound *S*-8**	**Initial e.e. (%)[a]**	**Yield (%)**	**Final e.e. (%)[a]**
82	100 % Compound *S*-**8**	99,9	95	> 99,9
83	99,5 % Compound *S*-**8** 0,5 % *R*-**8**	98,9	95	99,1

(a) Determined by CHPLC

The possible enantioenrichment of *S*-**8** in the hydrochloride formation was studied by contaminating the initial compound *S*-**8** with its enantiomer. The initial and final e.e. were evaluated using HCl in EtOH for the salt formation and results are shown in table

18. From these two experiments it can be observed that the e.e. and yield almost remain invariable.

With all these results, the optimizated Norchim process was scaled-up to industrial production scale in Moehs facilities. As a summary, Table 19 shows a compilation of the changes introduced in the initial process described by Norchim:

Table 19. *Improvements in Moehs process compared to Norchim's process*

Step	Norchim process	Moehs process
Grignard **20** formation	7 V of THF with Mg 1,2-dibromoethane at 45 ºC as initiator 17 V of THF with **33**	14 V of THF with Mg DIBALH at 20 – 25 ºC 3 V of THF with **33**
Imidazole **19** deprotonation	50 V of THF -5 ºC	17 V of THF -15 ºC
Imine-magnesium complex **54** formation	No THF washings in Grignard **20** transfer No residual Mg processing	THF washings in Grignard **20** transfer Systematization of Mg destruction
Imine-magnesium complex **54** hydrolysis	20 V of H_2O	10 V of H_2O
Ketone **21** obtention	18 V of *n*-heptane 13 V of H_2O	Salts filtration 9 V of *n*-heptane 6,5 V of H_2O
Tertiary alcohol **22** obtention	10 V of THF 3 eq of MeMgCl 2 h at reflux	8 V of THF 2,98 eq of MeMgCl 3 h at reflux
Alkene **14** obtention	Isolation of tertiary alcohol **22**	No isolation of tertiary alcohol **22**
Alkene **14** asymmetric hydrogenation	46 V of MeOH 45 - 50 ºC 12 h	25 V of MeOH 55 - 60 ºC 16 h
Tartrate **39** resolution	10 V of acetone + 1 V of H_2O	5 V of acetone + 3 V of MeOH + 0,5 V of H_2O
Alkane *S*-**8** obtention	Precipitation at 20 – 25 ºC	Precipitation at 50 ºC
Final product *S*-**15** obtention	Aqueous HCl 4 V of acetone	HCl in EtOH 3 V of acetone

Chapter 3.
Process Industrialization

Chapter 3. Process industrialization

After the study and optimization of the Norchim synthetic route, and its adaptation to the Moehs facilities, the whole process was scaled-up to an industrial production scale. A process validation was also performed.

Before starting the validation process, some prior considerations were taken into account. First of all, the process had to be studied to assess the safety regarding exothermic reactions and possible decompositions. If any risk is observed, some mitigation measures must be defined to minimize risks.

Although compound **8** is dissolved in the hydrogenation crude oil, it must be handled as an HPAPI, since a possible solution spill can eventually dry out and release the active substance in solid form into the environment.

The amounts of HPAPI to be handled in the manufacturing process are considerably higher than in the laboratory, for that reason contention measures must be defined. The key point to assure a proper containment of the process is to handle the HPAPI product in its solid form inside an isolation containment system. In solution it can be carefully handled outside the isolator containment system.

To ensure a total contention of the product, the analytical cabinets, the isolator and reactors must be placed inside a room with controlled negative pressure. Moehs called this room, HPAPI Unit and its design is crucial for the health safety of the workers involved in the project.

Finally, as the intention of Moehs is to reach the market with this HPAPI, some regulations aspect must be considered during this project. As this is not the main objective of the project but is strictly related, some keynotes about quality assurance and regulatory affairs and its implications into the project will be also described in this chapter.

3.1 Process Safety studies

To effectively assess the safety at Moehs production plants, every product produced is evaluated accordingly to its manufacturing process.

This evaluation covers two key aspects:

- Secondary Reactions: Thermal stability of compounds is rated according to structural alerts present in the molecule.

- Main Reaction: The potential danger of the reaction is rated with a number which considers its reaction heat.

3.1.1 Secondary reactions study

Initially, the thermal stability of all compounds present in the synthesis is evaluated by Differential Scanning Calorimetry (DSC). Despite this technique can be used to other purposes, in studies on process safety DSC evaluates the thermal decomposition in a temperature range, in case of Moehs from 30 ºC to 400 ºC.

The temperature of decomposition is evaluated with the ADT_{24}. This is the temperature under adiabatic conditions that the compound could be held without a runaway reaction during 24 h.[57]

In addition, the severity of the thermal decomposition can be classified by estimating the temperature increase due to the thermal decomposition of the compound under adiabatic conditions (ΔT_{atd}). The estimation of the ADT_{24} and ΔT_{atd} from the data obtained by DSC follows the formulas present in equations 1 and 2 respectively.[58]

Equation 1. *ADT_{24} approximation from DSC*

$$ADT_{24} = (Left\ Limit\ x\ 0{,}7) - 46$$

Equation 2. *ΔT_{atd} approximation from DSC*

$$\Delta T_{atd} = \frac{integral\ normalized}{C_P}$$

Left limit is initial temperature of the exothermic event which is taking place. Integral normalized is the thermal decomposition heat evolved per gram of product (J/g). C_p is the heat capacity of the reaction mixutre, generally approximated to 1,8 J/K·g. Depending on the ΔT_{atd} obtained, the thermal decomposition can be classified in the criteria shown in table 20.

Table 20. *Thermal decomposition severity criteria*

Severity	Criteria (ΔT_{atd})
Catastrophic	> 400 ºC
Critical	200 – 400 ºC
Medium	50 – 200 C
Negligible	< 50 ºC

Figure 9 is an example of a DSC thermogram. Endotherms are shown in blue downside and exotherms are shown in red upside. Generally, endotherms indicate melting points or glass transitions whereas exotherms are characteristic of degradation reactions. The thermogram shows the heat evolved from this reaction and can be used to calculate the increase of temperature due to this degradation. Both, left limit temperature and heat evolved are considered for the safety of the process.

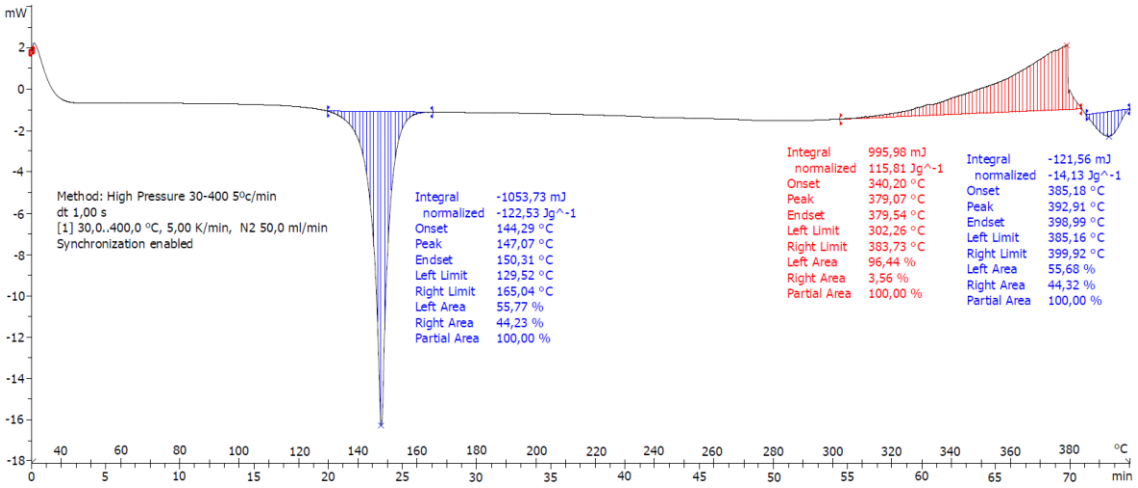


Figure 9. *Example of DSC thermogram*

Once the ADT_{24} is obtained for each material (product or reagent) and the severity of its thermal decomposition evaluated, the process is reviewed to check if at some point this ATD_{24} may be achieved, for example in distillation residues, drying, etc.

However, reaction heats of each step in the synthesis must be considered to properly assess the safety of the process. An uncontrolled reaction can cause an excessive increase in temperature and eventually rising above the ADT_{24}, potentially causing the decomposition of the compounds present at that moment. For this reason, the main reaction must be characterized and the data from this is evaluated together with the secondary reaction studies to properly assess the safety of the manufacturing process.

3.1.2 Main reaction study

It is important to know the heat produced by an exothermic reaction and the capacity of the reactor to release this heat. When studying exothermic reactions, in order to quantify the amount of heat generated, is useful to perform a calorimetry with a calorimetric reactor.

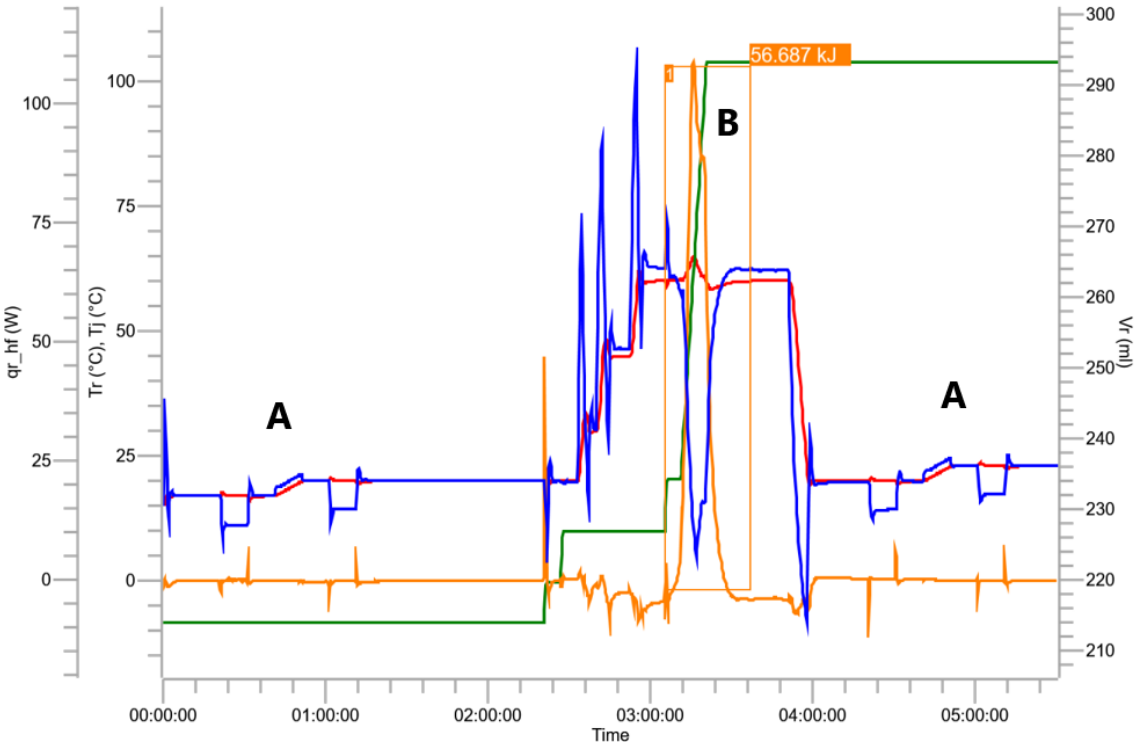


Figure 10. *Plot example of a reaction in a calorimetric reactor*

As an example, in figure 10 a calorimetry study is plotted. Green line is the total volume of the reaction. Blue line is the jacket temperature and red line reaction mixture temperature. Yellow line is the heat of the mixture. This heat is calculated by the equipment considering the difference between jacket and reaction mixture temperatures. Before and after the reaction, it is compulsory to perform a heat calibration shown as regions **A** in figure 10. This calibration calculates the heat capacity of the reaction mixture by applying small changes in jacket temperature and evaluating the changes in reaction mixture temperature. This parameter, heat capacity, is essential for the correct calculation of the reaction heat.

After the calibration, the heat is monitored during the exothermic event, shown as region **B** in figure 10. Generally, the reaction mixture temperature is set to a fixed point

and during heat evolving the jacket temperature changes to maintain the set point of the mixture.

Equation 3. *ΔT_{ad} calculation from calorimetric data*

$$\Delta T_{ad} = \frac{\Delta H_r \; x \; n}{m \; x \; C_p}$$

Then, the reaction heat obtained from the calorimetry is used to evaluate the safety of the reaction. Considering the total reaction mass (m), the moles of the limiting reagent (n) of the reaction and the heat capacity (C_p) obtained from the calorimetry, increase of temperature under adiabatic conditions (ΔT_{ad}) can be calculated, as shown in equation 3. This increase in temperature considers that heat is released at the same time without evolving heat to the outside.

Generally, reaction heat is progressively released or released when a reagent is added. The sum of ΔT_{ad} to the process temperature (T_p) gives the maximum temperature of the synthesis reaction (MTSR).

3.1.3 Process criticality assessment

Stoessel Diagram, shown in figure 11[58,59,60], is key to classify the criticality of a reaction. It correlates the main reaction with the values of T_p, MTSR and T_b obtained from the calorimetry with the ADT_{24} value obtained from the DSC.

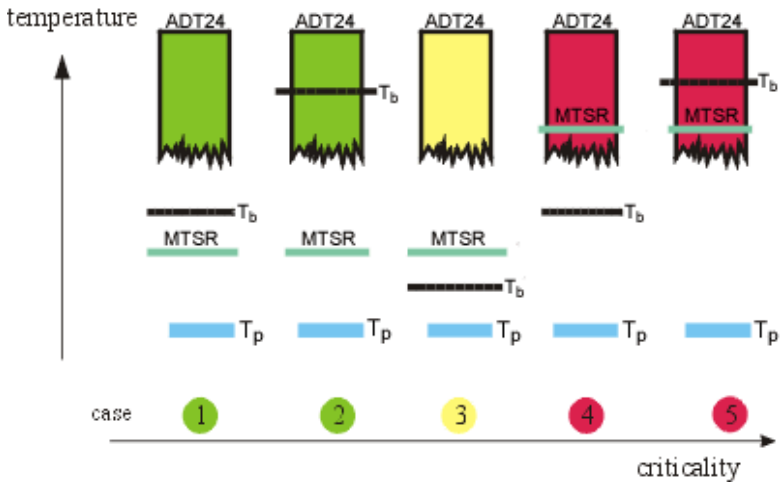


Figure 11. *Stoessel's Diagrams*[60]

Depending on the values of these 4 parameters, the criticality is determined regarding the order of the values.

All 5 different cases are explained more in detail:

- Case 1: If MTSR is achieved, it would not reach boiling temperature. However, neither MTSR nor T_b would not reach the ADT_{24} of the compounds, so no risk is present in this case.

- Case 2: MTSR did not reach boiling temperature but this last is above the ADT_{24} of the compounds. No risk is present because MTSR will never reach neither decomposition temperature nor boiling temperature.

- Case 3: MTSR is higher than T_b so there is risk of increased pressure because of solvent boiling. This could lead to reaction mixture spillage outside the reactor, breaking of the rupture disk. Generally, this risk can be mitigated by splitting the addition of a reagent, increasing solvent volumes or reducing process temperature, if possible. No more risk is expected as MTSR and T_b are lower than ADT_{24}.

- Case 4: MTSR is higher than T_b and all consideration of Case 3 applies also to Case 4. However, in this case, MTSR may reach ADT_{24}. The solvent, in this case, can act as temperature regulator and the temperature would not rise until there is still solvent present in the reaction mixture and the system has enough capacity to efficiently condensate the solvent. In the case that the whole solvent could be boiled and could not condense properly, there is risk of achieving ADT_{24} and a thermal decomposition may occur increasing the probability of a runaway reaction (Figure 12). If there is no other option to change the process, some technical mitigations can be applied and the calorimetric data and thermal stability of compounds must be more accurately studied.

- Case 5: MTSR reaches ADT_{24} and T_b is higher than MTSR. In this case, if the whole reaction heat is released at once, the temperature could rise too high that can produce the decomposition of compounds in the reaction mixture. In this case T_b does not act as temperature regulator in the main reaction but in the degradation process. Generally, degradation processes are self-accelerated and the runaway reaction is likely to produce an explosion (Figure 12).

In all scenarios, this case needs a process redefinition. A different solvent could be used or other intermediates must be considered.

Cases 1 and 2 does not require more safety measures than those general considerations as they are inherently safe. Cases 3 and 4 need to be revised and some measures must be applied in order to reduce the possible risk. Finally, case 5 should be further studied and the manufacturing process must be redesign.

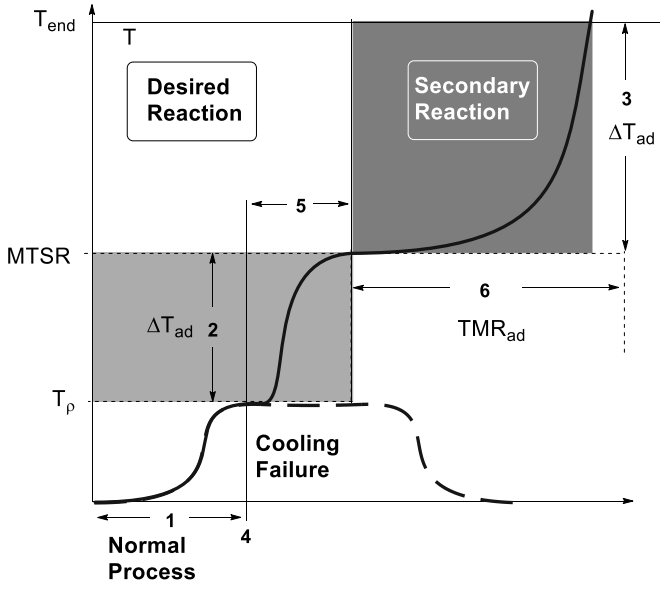


Figure 12. *Temperature diagram of a MTSR achieving ADT_{24} producing a thermal decomposition and a runaway reaction*[60]

After safety corrective measures are applied, the process criticality is reevaluated and should be reduced to cases 1 or 2.

3.1.4 Manufacturing process safety evaluation

Initially, the thermal stability of compounds is determined by DSC to study secondary reactions and the results are shown in table 21.

Table 21. *DSC results of compounds during the synthesis*

Synthetic Step	Compound	Left Limit T[a]	Integral normalized	ADT_{24}	ΔT_{atd}	Severity
1	**33**	Not exothermic		N/A		Negligible
	20 in 17 V of THF	Not exothermic		N/A		Negligible
	19	302 ºC	116 J/g	166 ºC	64 ºC	Medium
	53 in 17 V of THF	Not exothermic		N/A		Negligible
	54 in 35 V of THF	Not exothermic		N/A		Negligible
	21	Not exothermic		N/A		Negligible
2	**55** in 8 V of THF	203 ºC	43 J/g	96 ºC	24 ºC	Negligible
	22	267 ºC	149 J/g	141 ºC	83 ºC	Medium
	14	257 ºC	172 J/g	134 ºC	96 ºC	Medium
3	**39**	Not determined				
	9	Not determined				
4	*S*-**15**	Not exothermic		N/A		Negligible

The DSC analysis was not performed for tartrate **39** and enantiopure alkane *S*-**8**. These are the base and the tartrate salt of the final product *S*-**15**. As the core molecule is the same in all cases, *S*-**15** did not present degradation between 30 ºC and 400 ºC.

Regarding the manufacturing process, the temperature of distillation points is compared to ADT_{24} of the compounds present in that point to evaluate the risk of thermal decomposition (Table 22).

Table 22. *Distillation temperature and ADT_{24} comparison*

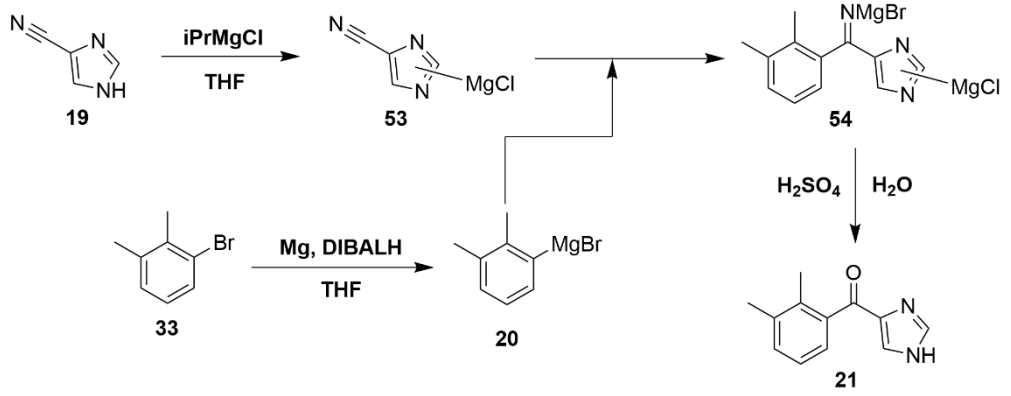
Compound	Distillation temperature	ADT_{24}	Risk
22	Max 60 ºC	141 ºC	No risk
8	Max 60 ºC	N/A (from compound *S*-**15**)	No risk
S-**15**	Max 40 ºC	N/A	No risk

Regarding the study of the key synthetical steps, reactions from alkene **14** to the final product *S*-**15** were discarded to be considered as low risk or no-risk processes. The

hydrogenation of compound **14** was very diluted and the calculations could be carried out with tabulated values. Furthermore, Moehs has not the proper equipment to perform the calorimetry study in high-pressure processes.

The following steps to yield hydrochloride *S*-**15** consist of crystallizations and precipitations which could be also studied using tabulated values of reaction heats. Moehs mainly focused in studying the safety of steps 1 and 2, which are the synthesis of ketone **21** and alkene **14**, involving Grignard reactions.

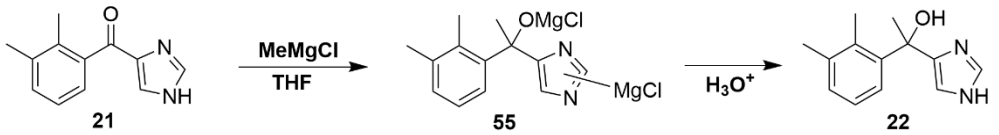
Table 23. *Calorimetric study of ketone **21** obtention*



	Obtention of compound			
	20	**53**	**54**	**21**
Reaction heat (kJ/mol)	270	89	88	147
Heat capacity (kJ/Kg·K)	1,41	1,69	1,69	1,69
ΔT_{ad} (ºC)	125	96	39	49
Process Temperature (ºC)	65	- 5	0	30
MTSR (ºC)	190	91	39	79

The synthesis of ketone **21** is divided in 4 reactions: Grignard formation, imidazole **19** deprotonation, imine-complex **54** formation and its corresponding hydrolysis. Each part is studied independently in the calorimetric reactor. Reaction heat, heat capacity and ΔT_{ad} obtained for each part of the synthesis are shown in table 23. The same calorimetric study was performed for the obtention of the tertiary alcohol **22** (Table 24).

Table 24. *Calorimetric study of tertiary alcohol **22** obtention*



21 55 22

	Obtention of compound	
	55	**22**
Reaction heat (kJ/mol)	315	1127 kJ/mol[a]
Heat capacity (kJ/Kg·K)	2,05	3,26
ΔT_{ad} (ºC)	54	99
Process Temperature (ºC)	65	10
MTSR (ºC)	119	109

(a) Not feasible data due to precipitation issues during the measurement

With all this data, the criticality of this reactions is evaluated by sorting different parameters in decreasing temperature and shown in table 25:

Table 25. *Criticality evaluation of process reaction*

20	**53**	**54**	**21**	**55**	**22**
ADT_{24} N/A	ADT_{24} N/A	ADT_{24} N/A	ADT_{24} N/A	MTSR 119 ºC	MTSR 109 ºC
MTSR 190 ºC	MTSR 91 ºC	T_b (THF) 66 ºC	MTSR 79 ºC	ADT_{24} 96 ºC	ADT_{24} 96 ºC
T_b (THF) 66 ºC	T_b (THF) 66 ºC	MTSR 39 ºC	T_b (THF) 66 ºC	T_b (THF) 66 ºC	T_b (THF) 66 ºC
T_p 65 ºC	T_p -5 ºC	T_p 0 ºC	T_p 30 ºC	T_p 65 ºC	T_p 10 ºC
Criticality evaluation (Stoessel's diagram)					
Case 3	Case 3	Case 1	Case 3	Case 4	Case 4

For the first reaction, the obtention of Grignard **20**, was difficult to assess its safety as the process is intrinsically risky. The Grignard formation is an exothermic reaction in which the mixture needs to be near to the reflux. The main risk in this step is the boiling

of the whole solvent. In this case, the criticality of the process cannot be decreased. However, other technical mitigations can be applied to assess its safety.

The first safety measure applied was the controlled addition of a solution of **33** to the Mg suspension in a given time. The addition was fixed to 1 h and the power of the reaction was calculated by dividing the reaction heat by the time obtaining a result of 2,5 kW. The refrigeration system had a power of 3,4 kW at 10ºC. This was considered enough to successfully condensate the solvent evaporated during the reaction boiling.

The second safety measure for **20** obtention implies the initiation of the reaction. If all **33** solution is added at 65 ºC, 75 % of the solvent would boil.[61a] So the amount of solution added to initiate the reaction must be limited. This limit was fixed to a maximum of 20 % of the solution. If this was added at 65 ºC, only a 15 % of the solvent would boil, which is a reasonable lower than the initial scenario. However, it is expected that the initiation takes place at a temperature between 25 ºC and 65 ºC. The midpoint, at 45 ºC, was used to calculate the MTSR considering a 20 % of the solution added obtaining a value of 70 ºC. This result indicates that almost no solvent would be boiled when initiating the reaction at 45 ºC with a 20 % of the solution added. To ensure the safety of the initiation, the initiation would be tried with 5 % portions of the solution to a maximum of 20 %.

The criticality of the compound **53** obtention was reduced from case 3 to case 1 by limiting the addition of iPrMgCl at 25 % of the total amount at once. This reduced the MTSR to 26 ºC which is lower than T_b. The same approach was applied to reduce the criticality in the obtention of compound **21**. In this case the amount of H_2SO_4 solution is limited to a 20 % of the total amount at once. This reduces the MTSR to 40 ºC. For further safety, the addition of H_2SO_4 solution is initialized at 0 ºC and can be raised up to 30 ºC.

In the case of the obtention of compound **55**, it was needed to limit the amount of MeMgCl to the 25 % of the total amount and also reduce the temperature of addition which was reduced from 65 ºC to 45 ºC. Limiting the amount of MeMgCl added prevents the accidental addition of the whole amount of the reagent. This reduced the MTSR to 59 ºC which is lower than T_b.

Finally, for the obtention of alcohol **22** the total amount of NH_4Cl solution was limited to 20 % at once, applying the same approach in its corresponding magnesium salt **55**, reducing the MTSR to 30 ºC. At the same time, for quality reasons, the maximum temperature permitted at this point is 30 ºC.

In these last cases, the criticality of the process was reduced from case 4 to case 1. All safety considerations of the whole process are shown in *Table 26*.

Table 26. *Safety considerations of the whole process*

20 (Grignard formation)	Initiation from 25 to 65 ºC with 5 % of solution added to a maximum of 20 % of solution added. Once the reaction is initiated, the rest of the solution is added in portions over 1 h.
53 (**19** deprotonation)	Controlled addition to a maximum of 25 % of iPrMgCl added at once.
21 (Hydrolysis)	Controlled addition to a maximum of 20 % of H_2SO_4 solution added at once.
55 (Methylation)	Addition of MeMgCl at 45 ºC and maximum of 25 % of solution added at once.
22 (Quenching)	Controlled addition to a maximum of 20 % of NH_4Cl solution added at once.
22 (Distillation)	Maximum 65 ºC jacket temperature
9 (Distillation)	Maximum 65 ºC jacket temperature (no thermal decomposition expected)
S-**15** (Distillation)	Maximum 40 ºC jacket temperature (no thermal decomposition expected)

3.2 HPAPI Unit design

Highly Potent APIs handling into a manufacturing scale presents a challenge to Moehs. As the product right after the generation of the stereogenic center (compound **8** and derivates) is considered to be an OEB5 HPAPI, the containment of the product to protect the workers from the possible toxic effect must be studied in detail. A cleanroom in which the manufacturing of the compound *S*-**15** will be carried out is designed and called HPAPI Unit.

3.2.1 HPAPI Unit facilities

This cleanroom may contain all the facilities for the manufacturing and for the analysis. However, the handling of higher amounts of HPAPI in solid form required an extra level of protection. Furthermore, compound *S*-**15** is sold as sterile injectables. This means that compound *S*-**15** must be handled in a sterile environment. For this reason, an isolator was planned to be placed inside the cleanroom. This isolator, also considered as a clean room, prevents the exposure of the operator to the HPAPI and provides an extra protection for the workers outside the room.

Inside the isolator, 2 Nutsche filters and a tray dryer would be placed in order to have the HPAPI in solid form contained. Reactor would be placed outside the isolator as it is expected to have the HPAPI in solution or in suspension inside them. The electrical equipment required for the well-functioning of the room and the heating and cooling system would be placed in an adjacent separated area.

For the area dedicated to the analysis, safety weighing analytical cabinets with a laminar airflow would be placed to prepare solutions or suspensions which could came out the HPAPI Unit. Those analysis that required the product to remain in solid form, would be performed in the analytical cabinets inside the HPAPI Unit.

With these initial considerations, the final design of the HPAPI Unit was establish as shown in figure 13.

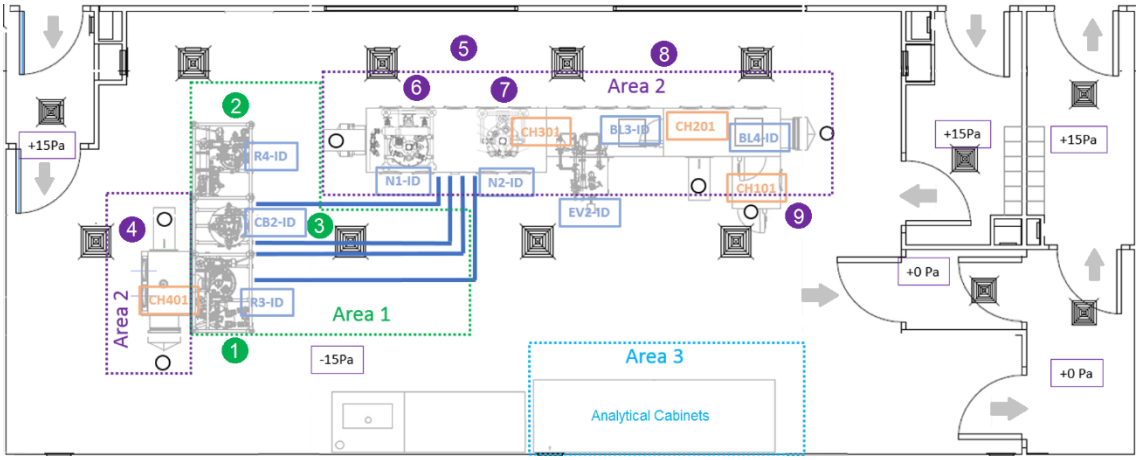


Figure 13. *HPAPI Unit layout*

Area 1 is the production area where the reactors are placed. Two reactors are placed: a 30 L glass reactor (1 in figure 13) mainly used for the process and a 10 L glass

reactor (2 in figure 13) used only for the final product. Additionally, a 30 L glass vessel (3 in figure 13) used to collect mother liquors from filtrations (Figure 14).

Area 2 is the clean room which contains 2 isolators. A small charging isolator connected to the 30 L glass reactor to be able to add solids directly to the reactor (4 in figure 13). The larger one is the main isolator. The main isolator is divided in 3 different chambers:

- Filtration chamber (5 in figure 13) where 2 Nutsche filters are placed: A 30 L glass Nutsche filter (6 in figure 13) directly connected to both reactors and a 10 L glass Nutsche filter (7 in figure 13) directly connected to 10 L reactor. Both Nutsche filters are also directly connected to the colleting vessel. The equipment outside the isolator is connected to the Nutsche filters with glass pipes.

- Dispensing chamber (8 in figure 13) where samples are weighted and packaged.

- Airlock chamber (9 in figure 13) is the entrance of materials to the isolator. It is specifically small to be decontaminated every time is opened to the outside the isolator.

To avoid further handling of the HPAPI, the tray dryer was designed to fit the 10 L Nutsche filter basket and placed into the filter chamber without any door in between.

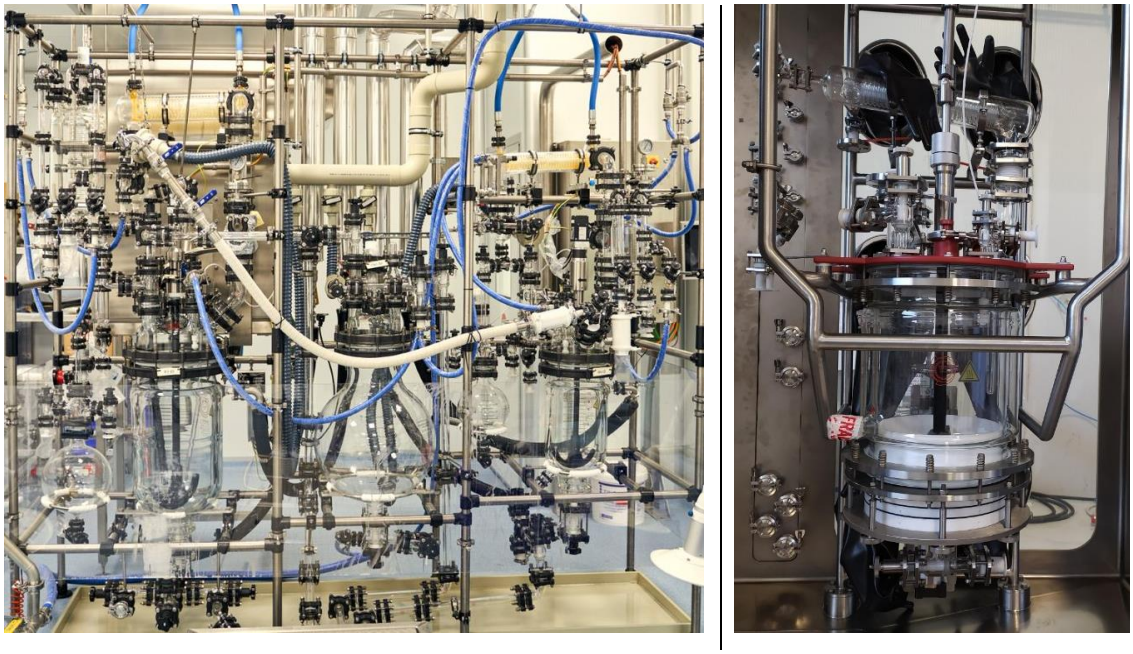


Figure 14. *Reactors (left) and 30 L Nutsche filter (right)*

Before removing any item from the isolator, it must be previously cleaned and taken out using the continuous liner system (CLS). This is a continuous plastic bag which is sealed with a safe-seal closure system, maintaining the inner part in contact with the isolator contained (Figure 15).

A rapid transport port (RTP) is used to transport rapidly any item from one chamber to another or to the charging isolator (Figure 15). This is a plastic cylinder equipped with double locked doors. One door is placed to the RTP and the other door is placed into the isolator wall. Only when both doors are fixed, the RTP is unlocked. With this system, the isolator and the RTP cannot be opened to the outside.

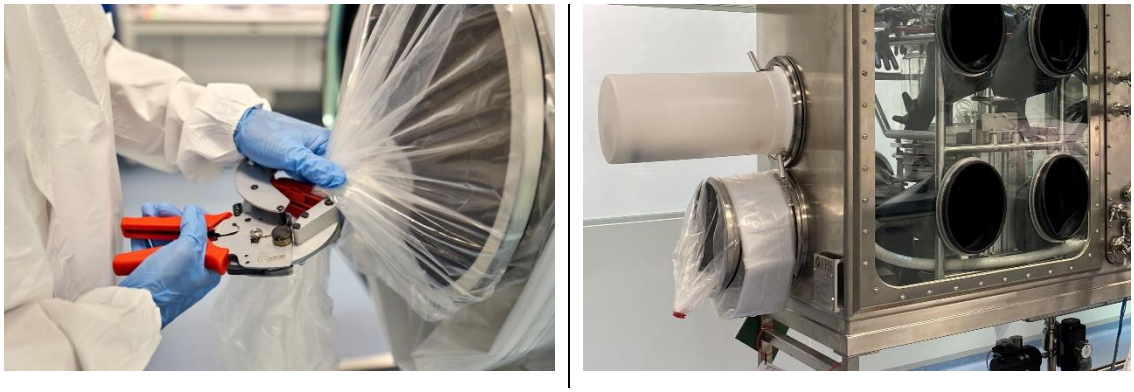


Figure 15. *CLS (left) and RTP (right)*

Different chambers into the isolator are placed at different pressures. Filtration chamber has the highest depression followed by the dispensing chamber. The airlock is the one with the lowest depression with the room. At the same time, the room is also in depression. However, to maintain the HPAPI inside the room and other contaminants outside the room, the entry and exit rooms are placed with overpressure.

3.2.2 HPAPI Unit Risk Management

To ensure the containment of the product inside the isolator, the Standardized Measurement of Equipment Particulate Airborne Concentration (SMEPAC) test is performed. Initially, the conditions of the manufacturing process and the accepted exposure outside the isolator must be set. The conditions of the manufacturing process consider up to 2 Kg of fine powder dried solid and the Containment Performance Target (CPT) is set to 100 ng/m^3. This CPT is the acceptable concentration exposure outside the isolator. It must be remembered that OEL of final product *S*-**15** is 600 ng/m$^{3[14]}$ and is much lower to have a safety gap in case of any problem.

The SMEPAC test was performed reproducing with a surrogate, a less toxic compound, typical operations that are supposed to be carried out during the manufacturing process. As a result of the SMEPAC test, most of the points reported a concentration of the surrogate below 20 ng/m^3. In other points, especially in the CLS it was revealed a higher concentration, about 80 ng/m^3, indicating the main weak points of containment. Despite that, the SMEPAC test was conform and the CPT of 100 ng/m^3 was successfully achieved.

Before the beginning of the manufacturing, a risk assessment was performed. Initially, all possible risks were identified and listed. These risks are mainly focused on the loss of contention due to leaking in glass pipes or reactor or a malfunction in the isolator. Every possible risk is rated with a number (RPN) considering its severity, its likelihood of occurrence, and its detectability. Depending on the criteria applied for each company or institution, every risk is evaluated with its RPN and classified as Negligible Risk, Acceptable Risk with some safety measures and Not Acceptable Risk. This last one needs strong mitigation actions and safety measures (Figure 16).

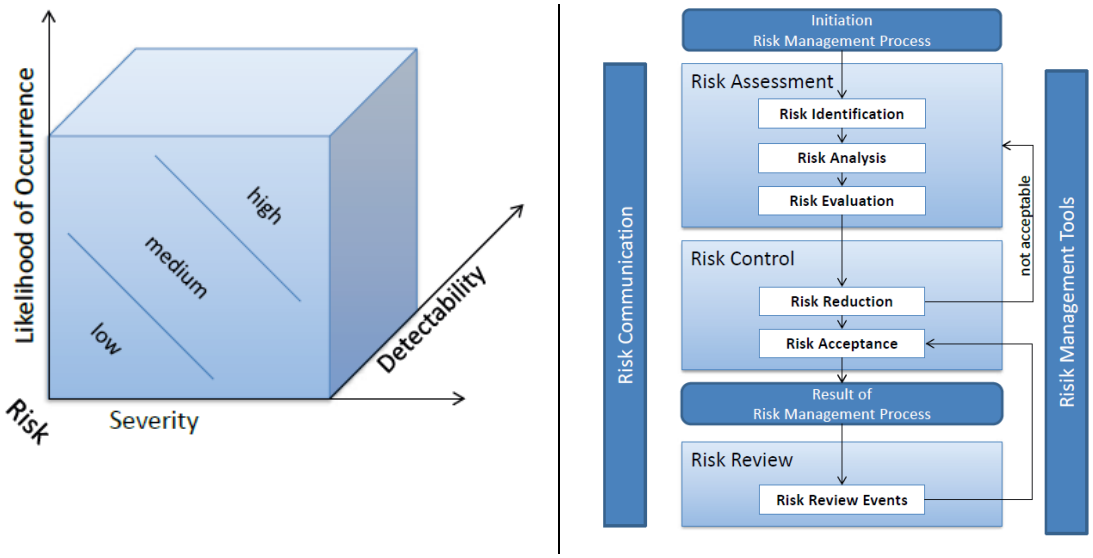


Figure 16. *Risk evaluation plot (left) and Risk management diagram (right)*

Then, mitigations and safety measures are applied to those risky situations. After that, the risk is re-evaluated and the obtained RPN must classify all situations as negligible risk or acceptable risk with measures.

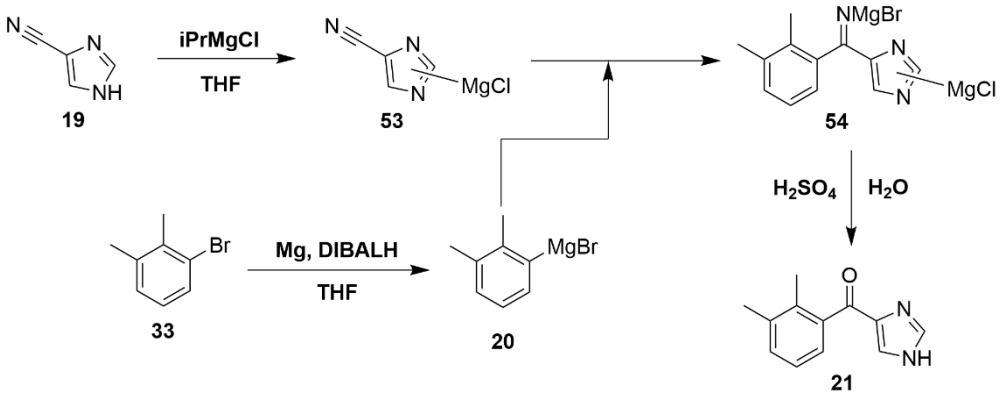
Finally, all risk and parameters used to classify them must be continuously re-evaluated with the real data obtained during the manufacturing process (Figure16).

3.3 Process validation

The process described in Chapter 2 was validated under Good Manufacturing Practices (GMP) regulations by manufacturing 3 batches of the target compound *S*-**15**. To increase the productivity, the batch size was doubled by using 2 batches of ketone **21** to subsequently manufacture as single batch of alkene **14**. From this point to the end of the process, the batch size was one batch of the previous intermediate.

3.3.1 Industrial obtention of ketone **21**

Six batches of ketone **21** were planned to manufacture three batches of the final product *S*-**15** for validation purposes. Each batch of ketone **21** had a batch size of 400 g of the starting material imidazole **19**.



Scheme 26. *Industrial obtention of ketone* ***21***

The first step in the synthesis was the obtention of Grignard **20**. Magnesium was suspended in THF and the whole system was inertized. After the addition of DIBALH, small foam was formed as observed in the laboratory but in less amount. Then, the jacket temperature was set to 65 ºC and at approximately at 35 – 40 ºC a 5 % of the aryl bromide **33** solution was added. Approximately 1 minute after the addition, the suspension turned black and a high exotherm was observed indicating the proper initiation of the reaction as shown in figure 17. All three validation batches exhibited the same behavior.

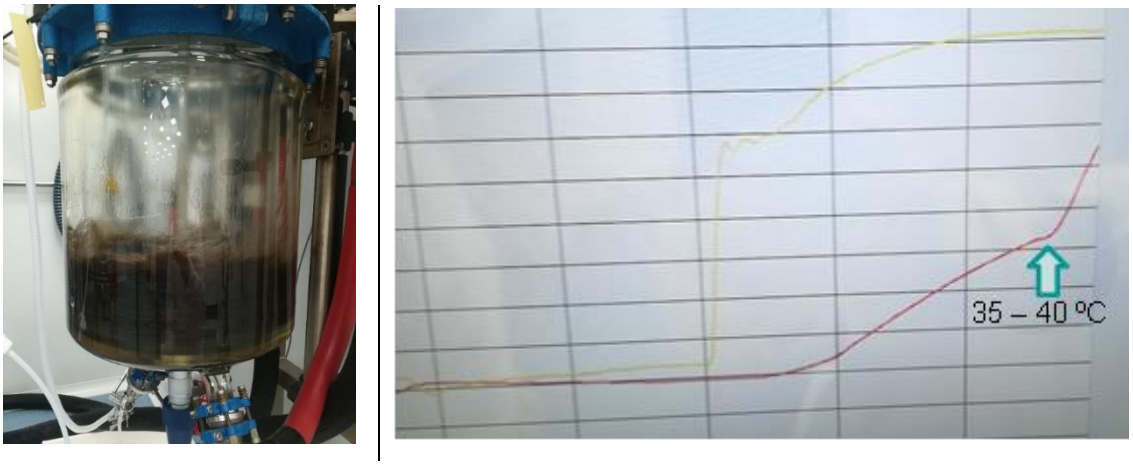


Figure 17. *Initiation of* ***20*** *formation. Reaction mixture (left) and temperatures plot (right): Jacket temperature in yellow and reaction temperature in red*

To reduce time and possible degradations, the deprotonation of imidazole **19** was carried out during the analysis of the conversion of the previous reaction by Quality Control (QC) laboratory. The addition of iPrMgCl to imidazole **19** was performed with 0,8 L bottles through a double tipped syringe with nitrogen pressure. For safety reasons, only a 25 % of the solution could be added at once. However, for technical

reasons, each bottle could be added in a minimum of 10 minutes so there was no risk in this procedure.

After the deprotonation and with the conform of QC laboratory, a solution of compound **20** was added to a suspension of compound **53**. To prevent air from entering the reactors, nitrogen overpressure was applied from the reactor containing the solution of compound **20** to the other reactor. A Polytetrafluoroethylene (PTFE) flexible tube was used for this purpose. Once the reaction was completed, the resulting suspension was analyzed by QC laboratory to evaluate the conversion.

With the approval of the QC laboratory, H_2SO_4 solution was added to hydrolyze the intermediate **54**. Considering the safety warning that only 20 % of the acidic solution could be added at once, this was added to the addition funnel. Although the addition was performed in approximately 1 h, the addition of 20 % portions into the addition funnel was carried out following the safety considerations in case of addition funnel malfunction.

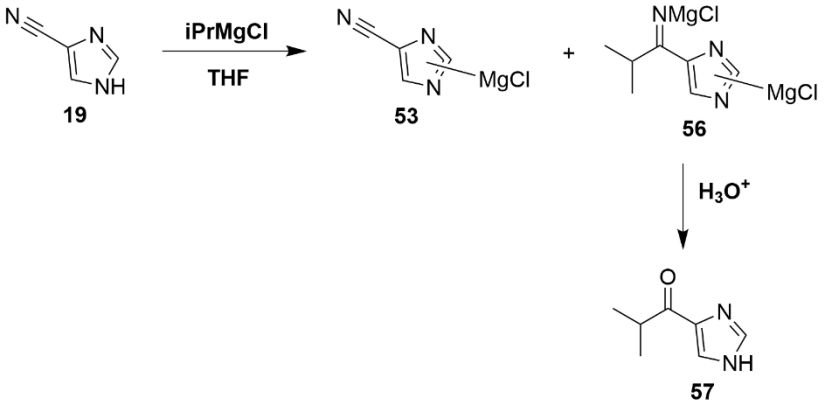
Work-up and precipitation of all six batches worked very similar to the laboratory, as it was expected (Table 27).

Table 27. *Process results of ketone **21** obtention*

Batch	**1**	**2**	**3**	**4**	**5**	**6**
20 conversion (min. 97 %)[a]	99,0	100	100	100	100	100
54 conversion (min. 96,5 %)[a]	100	99,4	97,8	99,7	99,5	99,4
21 conversion (min. 99 %)[a]	100	100	100	100	100	100
21 final assay (min 95 %)[b]	96	100	99	100	99	100
21 final purity (min. 98,5 %)[a]	99,8	99,8	99,7	99,6	99,9	99,9
21 yield (min 65 %)	71	65	79	61	67	58

(a) Determined by UHPLC. (b) Determined by potentiometric titration

As observed in table 27, the yield for some batches was very low, barely above the minimum expected yield of 65 %. However, even batch 4 and 6 had yields below the expected. The analysis by UHPLC-MS of the mother liquors revealed the presence of impurity **57**. This impurity was observed in higher values in the mother liquors of the lower yield batches.



Scheme 27. *Formation of* ***57*** *impurity*

Impurity **57** originates in the deprotonation step of imidazole **19** employing iPrMgCl as the base (Scheme 27). This impurity was observed in very low values during the development. It was known that this impurity could be formed at higher temperatures during the deprotonation. However, temperatures registered by the heating-cooling system were revised and revealed that all six batches maintained the temperature in the stablished range (from -15 ºC to -10 ºC). Further investigation revealed that the time between the addition of iPrMgCl and the addition of **20** was crucial for the formation of this impurity. For example, batch 3 (79 % yield) the time between additions was of 15 minutes whereas the time in batch 6 (58% yield) was of about 2 hours 30 minutes.

To prove this hypothesis, three trials were carried out to study how temperature and time affect to the impurity formation (Table 28). Entry 1 was the control reaction in which the temperature was maintained between -15 ºC and -10 ºC and the shortest time was maintained between additions. Entry 2 was performed at -5 ºC ± 5 ºC and the shortest time was maintained between additions as entry 1. Finally, entry 3 as carried between -15 ºC and -10 ºC and it was maintained for 16 h until the addition of **20**. All three reactions were carried on to completion to obtain ketone **21**.

Table 28. *Investigation at lab scale of* ***57*** *formation parameters*

Entry	Addition temperature of iPrMgCl	Time before addition of 20	% of 57 in reaction mixture[a]	21 final yield (%)
1	From -15 ºC to -10 ºC	No more than 15 minutes	1,1	70
2	From -10 ºC to 0 ºC	No more than 15 minutes	24,3	29
3	From -15 ºC to -10 ºC	16 h	22,2	33

(a) Determined by UHPLC-MS

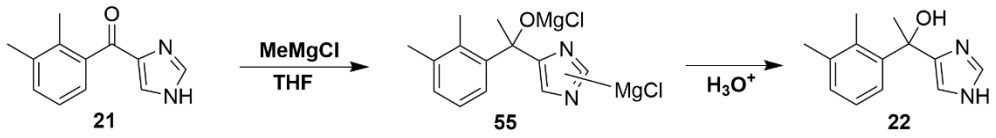
It was confirmed that not only temperature during the addition of iPrMgCl but also the time between the additions were relevant for the **57** formation. Whereas this impurity is observed to be more water soluble than **21** and the quality of it is no affected, the formation of this impurity is strongly related to the yield.

For future batches, the time between the end of iPrMgCl addition and the beginning of **20** addition will be reduced to the minimum. However, this reaction needs further investigation to solve this problem and gain robustness and yield. This issue will be further discussed in Chapter 4.

3.3.2 Industrial obtention of alkene **14**

For the obtention of alkene **14**, two consecutive batches of ketone **21** were used. The first part of the synthesis consisted of the formation of tertiary alcohol **22** (Scheme 28).

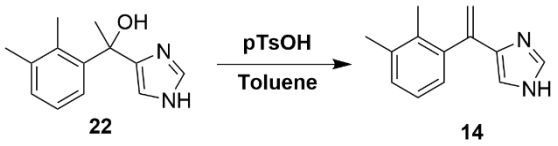
The addition of MeMgCl was performed at 45 ºC as established in the process safety study. It was added in 0,8 L and 0,1 L bottles through a double tipped syringe with nitrogen pressure. For safety reasons, only a 25 % of the solution could be added at once. However, for technical reasons, each 0,8 L bottle could be added in a minimum of 10 minutes so there was no risk in this procedure. The addition was performed in around 45 minutes and the temperature raised to about 50 ºC.



Scheme 28. *Industrial obtention of tertiary alcohol* ***22***

Initially, the reaction mixture had a pinkish color and after the reaction time, the color changed to orange, as observed in the laboratory scale. At this point, the reaction evolution was analyzed by QC laboratory and, with its approval, the mixture was cooled and quenched. Thus, NH_4Cl solution was added to quench the mixture. Considering the safety warning that only 20 % of the solution could be added at once, this percentage of the solution was added to the addition funnel. Although the addition was performed in approximately 1 h, the addition of 20 % portions into the addition funnel is carried out to keep the safety consideration in case of addition funnel malfunction.

It was calculated that around 4 % of the acidic solution was enough to quench the organomagnesium present in the reaction mixture. It was observed that with around 2-5 % of the solution was needed to quench the whole mixture which was consistent with the theoretical calculations. Furthermore, a very high reaction heat was observed the production of gas in this initial stage. This 2-5 % was added in around 30 minutes. The rest of the solution did not show much heat released and was added in around 30 minutes.



Scheme 29. *Industrial obtention of alkene* ***14***

The next step was the dehydration of the tertiary alcohol **22** (Scheme 29). The reaction proceeded as expected and all three batches crystalized around 38 ºC. Then the mixture was cooled to room temperature. This was systematized to 20 ºC ± 5 ºC. The maintenance temperature was different for each batch in order to study the influence of this in yield and purity of the final alkene **14**. The results and the final maintenance temperature of the industrial obtention of **14** is shown in table 28.

Table 28. *Process results of* ***14*** *obtention*

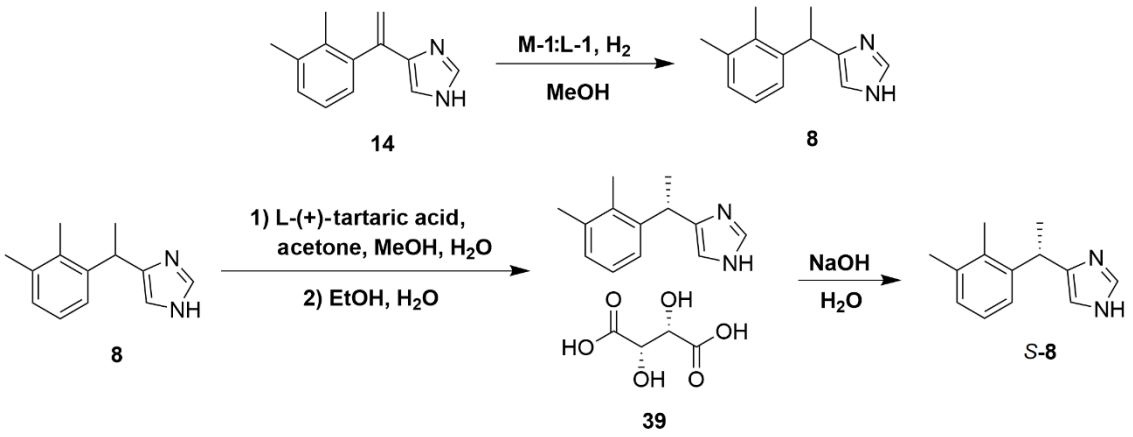
Batch	55 conversion (%) (min. 99,5)[a]	14 conversion (%) (min. 99,5)[a]	Final maintenance temperature	Final yield (%) (min. 80)	Final purity (%) (min. 98)[a]
1	99,7	99,9	25 ºC	90	99,9
2	99,9	99,9	20 ºC	92	99,8
3	99,7	99,8	15 ºC	93	99,9

(a) Determined by UHPLC

These results indicate that more yield could be obtained in the **14** obtention process by further studying the final crystallization. This will be further discussed in Chapter 4.

3.3.3 Industrial obtention of the enantiopure alkane *S*-**8**

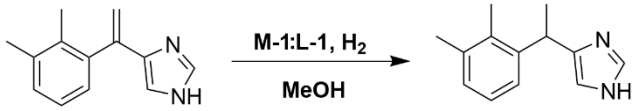
The obtention of compound *S*-**8** is divided in 3 steps: the asymmetric hydrogenation of alkene **14**, the resolution of the resulting alkane **8** through the corresponding tartare salt **39** and finally, the base release of compound *S*-**8** (Scheme 30).



Scheme 30. *Industrial obtention of enantiopure alkane S-**8***

The 3 hydrogenation reactions of the validation batches were carried out at 55 ºC whereas the range was 55 – 60 ºC to achieve que highest possible e.e. At the same time, to ensure the total conversion of the reaction, the reaction time in all three batches were 24 h which is in accordance with the time specified during the development (at least 16 h). The results obtained is this step are shown in table 29.

Table 29. *Process results of S-**8** obtention. First step: Asymmetric hydrogenation of **14***



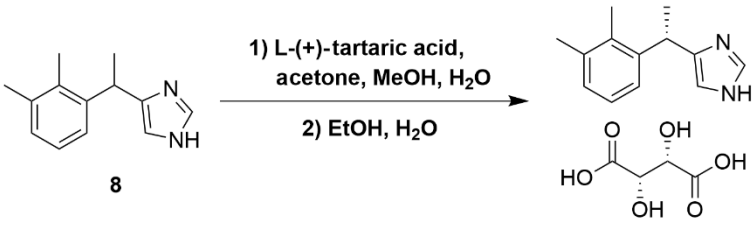
14 **8**

Batch	**1**	**2**	**3**
8 conversion (%) (min 99,9 %)[a]	Quantitative	Quantitative	99,9
8 e.e. (%)[a]	77,6	77,2	76,8

(a) Determined by CHPLC

After reaction completion, the hydrogenated solution was charged to the 30 L reactor inside the HPAPI Unit. THF was distilled and acetone and MeOH were added. Finally, L-(+)-tartaric acid was added through the charging isolator. The tartrate salt was filtered through a 30 L Nutsche filter and at this point, the isolated material was weighted and analyzed. Then, the precipitated tartrate **39** was dissolved in the Nutsche filter and recirculated to the 30 L reactor. After its crystallization, **39** was filtered. This last procedure was repeated one more time. The results obtained into the resolution are shown in table 30.

Table 30. *Results of the process of obtaining S-**8**. Second step: resolution with L-(+)-tartaric acid*



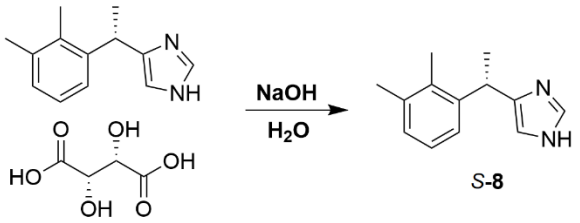
8 **39**

Batch	**1**	**2**	**3**
39 precipitation yield (%)	87	89	87
39 precipitation e.e. (%) (about 90)	91,1	93,6	92,8
39 1st crystallization yield (%)	83	84	82
39 1st crystallization e.e. (%) (about 98)	98,5	98,7	99,0
39 2nd crystallization yield (%)	90	87	92
39 2nd crystallization e.e. (%) (min. 99,8)	99,8	99,9	> 99,9

Once compound **39** had the desired e.e. (> 99,8 %), it was redissolved in H_2O and precipitated with NaOH 30 % solution. The suspension was filtered in the Nutsche filter and washed with warm H_2O. Then, to effectively eliminate the possible inorganic salts present in *S*-**8**, 5 V of H_2O were charged into the reactor and heated to 40 – 45 ºC. The

H_2O was transferred to the Nutsche filter and the resulting suspension was stirred for 1 h. After that, the water was filtered and alkane *S*-**8** was dried inside the Nutsche filter by applying heat under vacuum. The results obtained are shown in table 31.

Table 31. *Process results of S-**8** obtention. Third step: base release of S-**8***



Batch	1	2	3
S-**8 final yiled (%)**	93	96	95
S-**8 final purity (%)**[a]	Quantitative	99,9	99,9
S-**8 final e.e. (%)**[b]	99,8	99,9	> 99,9
S-**8 RoI (%) (max. 0,1 %)**[c]	0,1	0,1	0,1

(a) Determined by UHPLC. (b) Determined by CHPLC. (c) Determined by sulphated ash test

Obtaining compound *S*-**8** usually proceeded as expected and very similar to the laboratory scale. The evolution of the e.e. and the accumulated yield of every filtration step for each validation batch are plotted and shown in figure 18. When studying the evolution of the accumulated yield it can be observed that, despite each individual yield is very high (around 85 – 90 %), the accumulation of many filtrations reduced drastically the overall yield of the process. Furthermore, it was observed that the main improvements in e.e. are achieved in the earlier purification steps.

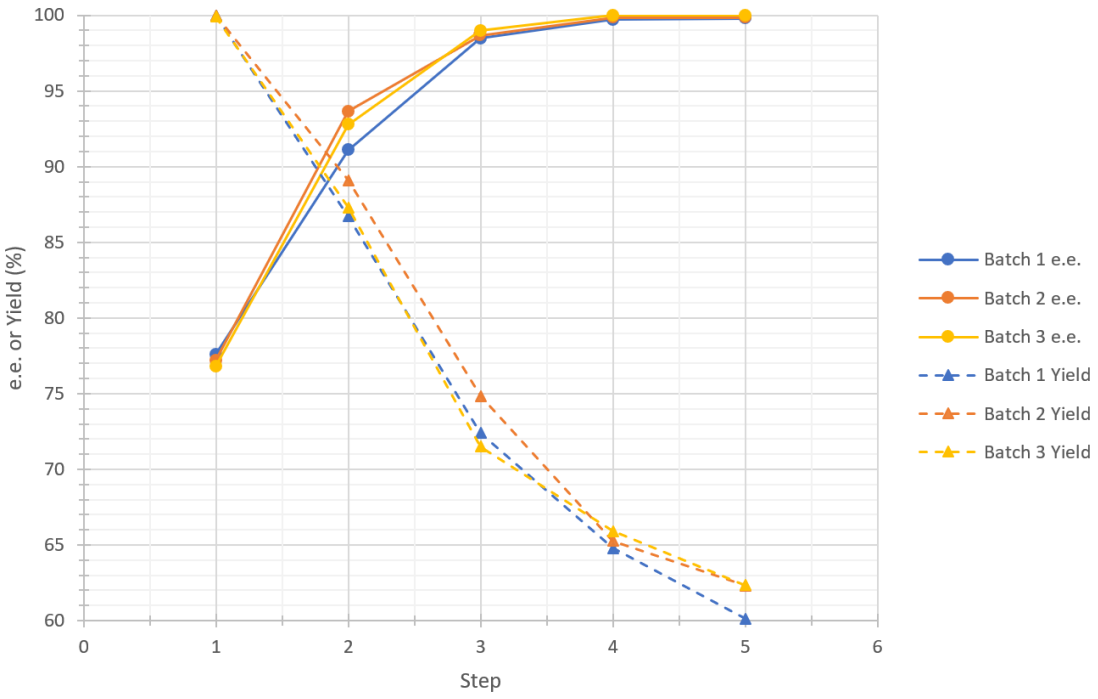


Figure 18. *% Yield and % e.e. evolution plot from alkene **14** to enantiopure alkane S-**8** in the validation batches*[a]

(a) Step 1 refers to Hydrogenation, Step 2 to **39** precipitation, Step 3 and 4 to **39** crystallization and recrystallization and Step 5 to *S*-**8** base obtention

As mentioned in Chapter 2, due to the low e.e. obtained in the hydrogenation, up to 3 purification steps must be performed to achieve the desired e.e. and a final step to release the desired compound *S*-**8** as a base. This procedure increases manufacturing times increasing also manufacturing costs. These 4 filtrations steps from compound **14** to compound *S*-**8** decreases dramatically the overall yield of this step to around 61 %. This drawback will be deeply studied in Chapter 4.

3.3.4 Industrial obtention of the final product *S*-**15**

The final step in the manufacturing process is the obtention of the hydrochloride salt *S*-**15**.



Scheme 31. *Industrial obtention of the final product S-**15***

Compound *S*-**8**, placed in the 30 L Nutsche filter, was redissolved by the addition of HCl in EtOH. The resulting solution was filtered and transferred to the 10 L reactor. In this reactor, the solution was distilled and acetone (previously filtered) was added for the precipitation. Any solvent that enters the reactor must be previously filtered.

The suspension containing compound *S*-**15** was filtered in the 10 L Nutsche filter. And washed with cold acetone. Resulting *S*-**15** in solid form was homogenized in the Nutsche filter basket and directly dried inside the tray dryer. The results obtained for all three batches are shown in table 32.

Table 32. *Process results of S-**15** obtention*

Batch	**1**	**2**	**3**
Yield (%)	85	86	85
Purity (%)[a]	100	100	100
e.e. (%)[b]	99,9	> 99,9	> 99,9

(a) Determined by UHPLC. (b) Determined by CHPLC

The yield obtained in all 3 validation batches was considerably lower than the obtained in the laboratory. This may be due to the volume of the glass pipe which connects the reactor with the Nutsche filter. Approximately, the volume of the glass pipe is around 2 L and the volume of the reaction mixture in to 10 L reactors was around 3 L. Despite the majority of the suspension reached the Nutsche filter, some product remains inside the system.

Given the results obtained, it can be concluded that the yield of the process at this scale is robust but lower to the expected (about 95 %) because the facilities are over-dimensioned for batch size of the process.

3.3.5 General results and conclusions of the process validation

Regarding all these results, the manufacturing process of final product *S*-**15** can be considered as successfully validated. After the manufacturing of all validation batches, it is demonstrated that *S*-**15** meets the expected quality and can be obtained in a consistent way with a high degree of assurance.

Despite that, some issues have to be remarked:

- The equipment used to manufacture the validation was qualified and adequate for this purpose. However, the equipment was a little oversized for the batch size at the end of the manufacturing process. This can be solved in further process optimization.

- The manufacturing process to obtain ketone **21** can be further improved since deficiencies have been observed with the process yield and robustness. At the same time, there are some signs that the process to obtain alkene **14** can also be slightly improved.

- The manufacturing process to obtain compound *S*-**8** revealed to be strongly robust. However, due to its high number of manufacturing steps, time, and costs, the productivity of the whole process is not as efficient as it could be expected.

With all the knowledge gained and with both the process and product ready for market launch, a further modification of the manufacturing process was conducted. The details of this will be discussed in Chapter 4.

3.4 Regulatory affairs

After the validation of the manufacturing process the Drug Master File was prepared. It follows the Common Technical Document guidelines stablished in the ICH M4.[62,63] This document is presented to the appropriate regulatory authority to which the drug, in this case *S*-**15**, is pretended to reach the market.

In the document it is listed all relevant information about the manufacturing of the drug as the description of the analytical procedures used to ensure the quality of the process, specifications, stability data, validation of analytical procedures and process manufacturing, elucidation of structure and properties. However, the most important parts for the change management during the whole lifecycle of the API and also the most relevant parts for this project are the impurities discussion section, the mutagenicity assessment, the description of the manufacturing process and its controls, the control of the starting materials and intermediates and finally the critical steps.

More in detail, every change in the manufacturing process must be evaluated and approved by the corresponding regulatory authority. This change must be accompanied of all those related documents. In case of a reagent change, it must be discussed its fate and purge along the process. Also, potential impurities must be evaluated and discussed.

One of the most important things to be considered when changing or optimizing a process is to maintain the starting materials and the relevant isolated intermediates. If those were changed, it can be considered by the authority that a new Drug Master File would be needed. If these compounds are not changed in the process improvement, the justification and discussion of all related parameters associated to the change can be enough to be approved.

Taking this into account, it is preferable not to change compounds **19** and **33** as starting materials and compounds **21**, **14** and *S*-**8** as key isolated intermediates (Figure 19). It must be considered that every new compound present in the synthesis must be evaluated in the control strategy of materials, especially for those mutagenic or potentially mutagenic compounds.

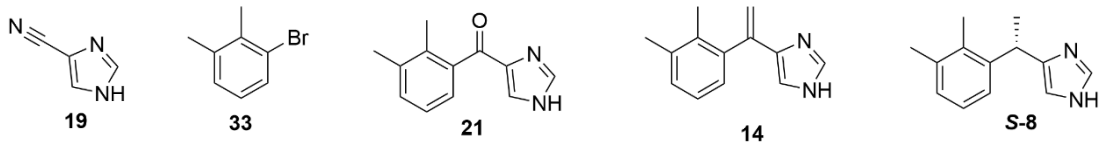


Figure 19. *Key regulatory compounds*

Chapter 4.
New synthetic approach

Chapter 4. New synthetic approach

The study of the synthesis of Norchim and its industrialization at Moehs facilities revealed some weaknesses in terms of productivity. In some cases, this productivity was lower because the obtained process yield could be increased. In other cases, the elevated number of manufacturing steps decreased the productivity.

In this chapter, the main objective was to improve both the yield and robustness of the process to obtain ketone **21** and alkene **14** within the required specification. The hydrogenation step and consequently the resolution was deeply studied in order to decrease production steps maintaining the yield and purity of the current process.

4.1 Route of synthesis improvements

The main problem arose during the industrialization of ketone **21** was the formation of impurity **57**, which lowered the yield and the robustness. The proposed solution for this problem was the elimination of iPrMgCl reagent and the synthesis of the double amount of Grignard **20** to be used as a base and as a nucleophile. The excess of arylbromide **33** and the remaining amounts of **20**, are expected to be removed in the work-up. This change prevents the formation of the isopropylketone **57** assuring the total conversion of imidazole **19** to the desired ketone **21**.

At the same time, the centrifugation of salts after the hydrolysis was proposed to be performed at 0 – 5 ºC in order to eliminate the maximum amount of these salts. This could provide an extra robustness in the final potentiometric assay of the ketone **21** regardless the use of iPrMgCl or Grignard **20** as a base.

Proposed changes in the obtention of the alkene **14** included to reduce the dehydration concentration and the centrifugation of the desire product at 0 – 5 ºC. This tendency to increase the yield lowering the centrifugation temperature was observed during the validation stage, indicating that it could be effective.

Regarding the hydrogenation, some other parameters could be studied in order to increase the e.e. of the reaction. Temperature, concentration and pressure were studied but the influence of different solvents and different catalyst remain unstudied. Specifically, the catalyst includes the use of different metal sources, different families of

ligands and in each family, different ligands. Also, a combination of different metals and ligands could be tested.

If the e.e. of the hydrogenation is increased, the resolution could be shortened by decreasing the number of filtrations of the tartrate salt **39**. The best scenario would be the direct obtention of enantiopure alkane *S*-**8** from the reaction crude. This could depend on the e.e. obtained from the hydrogenation. However, a different resolution approach could be studied.

Finally, for regulatory issues, it was preferable not to modify the last step in order not to alter the physicochemical properties of the final API. Despite that, this step seems to be optimized during the study in Chapter 2 and the lower yields obtained in the validation could be solved by increasing the batch size in a previous step of the manufacturing process.

4.2 Synthesis of ketone 21

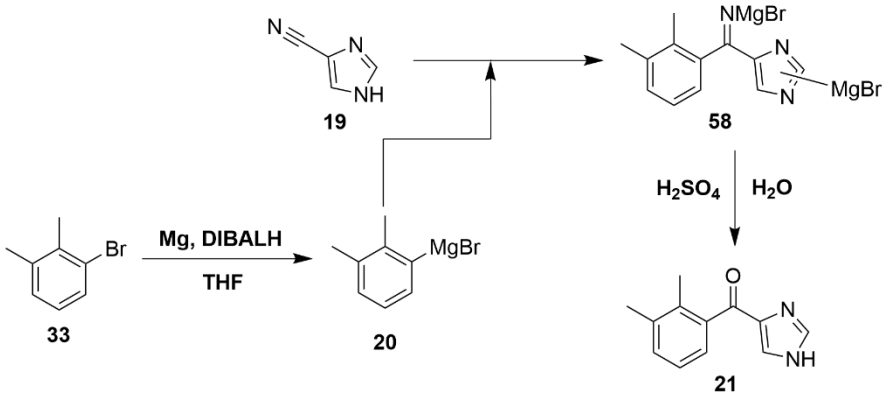
The proposed changes to further optimize this step and other studies to deeply understand the process are the following:

- Replacement of iPrMgCl by **20**
- Centrifugation of magnesium salts at 0 – 5 ºC
- Impurities determination
- Impurities fate and purge evaluation

As this step was observed to produce the main impurities of the process, the evaluation of them and the study of their fate and purge would help to further understand the whole manufacturing process.

4.2.1 Change proposal studies

In the first step of the synthesis, the reaction conditions for Grignard **20** formation, were maintained but with twofold quantities (Scheme 32). However, the increase in the total volume forced to reduce of the THF volumes in the imidazole **19** suspension.



Scheme 32. *New approach for ketone **21** obtention*

Considering that the amount of Grignard **20** was doubled and iPrMgCl was not present, imidazole **19** was suspended in 6,5 V of THF (from 17 V in the previous approach). With this, the total volume of the reaction mixture was maintained. As no impurities are expected, the reaction between **19** and **20** was carried out at different temperatures. Trials and results in the intermediate complex **58** obtention are shown in table 33 with different conditions.

Table 33. *Conditions and results of the trials for formation of **58***

Entry	Temperature	Conversion (%)[a] at				Yield (%)[a]
		30 min	45 min	1 h	2 h	
1	- 10ºC	98,2	Quantitative	Quantitative	Quantitative	85
2	0 ºC	Quantitative	Quantitative			86
3	25 ºC	Quantitative	Quantitative	Quantitative		85

(a) Determined by UHPLC

All reaction yields were ≥ 85 % which were much higher than the yields obtained when using iPrMgCl (65 – 85 %). At the same time, the reaction mixture looks much more fluid and homogeneous. It was also interesting to see that the reaction time could be reduced to about 45 minutes instead of the 2 h needed in the previous process.

Interestingly, it was observed less reaction heat than when using iPrMgCl. The deprotonation using iPrMgCl produces propane when deprotonating the imidazole **19**.

However, it produces the corresponding xylene when using **20** as a base. As the xylene is a liquid at the temperature of work, there was no problem of over-pressure in case of accidental quick addition.

Furthermore, the cost of the reagents is almost the same. The main cost of the **20** synthesis comes from the cost of the starting material **33**. This is around 600 € per batch less expensive than the cost of iPrMgCl. If THF, DIBALH and magnesium are considered when calculating costs, they are almost the same.

Generally, the reaction works much more efficiently, cost economically and much safer when using Grignard **20** as a base than iPrMgCl and even more remarkable, formation of isopropylketone **57** is avoided. At the same time, there is no significant regulatory impact on this change.

Finally, the elimination of salts at different temperatures was also studied. Entry 4 in table 34 was performed using iPrMgCl and filtrating the salts at 0 – 5 ºC. Conditions and results are shown in table 34.

Table 34. *Conditions and results in the study of salts filtration in ketone **21** synthesis*

Entry	Base	Temperature of salts filtration (ºC)	Amount of salts filtered (w/w ratio)[a]	Assay of 21 (%)[b]
1	**20**	20 – 25	7,2	100
2	**20**	20 – 25	7,1	100
3	**20**	0 – 5	8,2	100
4	iPrMgCl	0 – 5	7,9	100

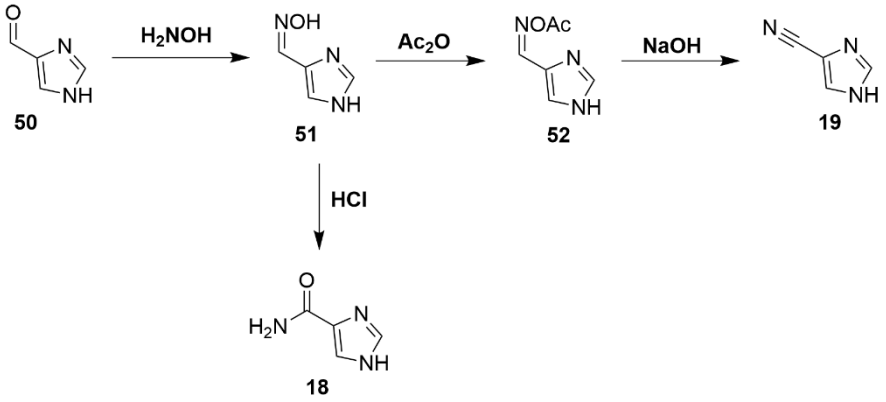
(a) w/w ratio calculated as: g of salts / g of **19**. (b) Determined by potentiometric titration

As observed, all potentiometric assays gave 100 % regardless of the filtration temperature of the salts, the amount of salts filtrated are higher at lower temperature. The base used for the deprotonation seems not to have an effect on the amount of salts filtrated. At laboratory scale, the potentiometric assay is generally better than at higher scale. Probably this effect would be more visible at the production scale.

4.2.2 Evaluation of ketone **21** related compounds

All related compounds present in the synthesis were studied and its fate and purge evaluated.

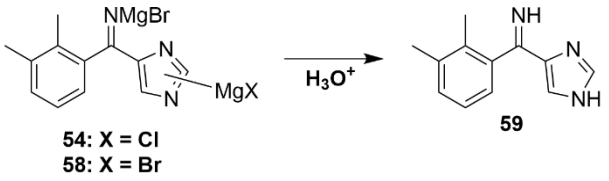
Initially, impurities present in the starting materials were evaluated. The UHPLC-MS analysis of imidazole-nitrile **19** revealed the presence of imidazole-aldehyde **50** and an unknown impurity. The MS spectrum revealed a m/z ratio of 112 consistent with aldoxime **51** (Scheme 33).



Scheme 33. *Norchim's synthesis of imidazole **19** starting material*

To check the structure of the peak with m/z ratio of 112, **51** was synthesized. Surprisingly, aldoxime **51** did not elute at the same retention time in UHPLC-MS as the 112 m/z impurity. A possible explanation for the formation of the 112 m/z impurity was thought to be due to the fact that the remaining not acetylated aldoxime, **51**, in combination with the acidic medium could undergo a Beckmann rearrangement to give amide **18**.[64] To confirm this hypothesis, amide **18** was synthesized and characterized and finally confirmed as the unknown impurity in imidazole **19**.

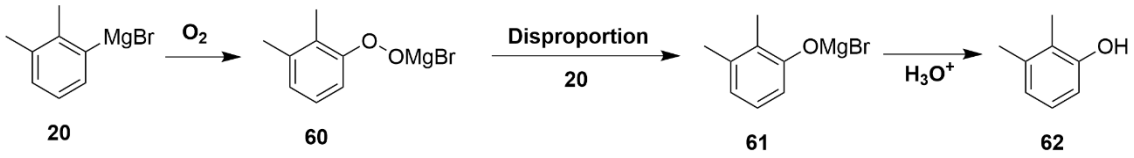
Then, from Grignard **20**, the real molecule observed by UHPLC-MS is its hydrolysis corresponding xylene. This impurity is purged in the work-up with *n*-heptane washes at the same time as arylbromide **33**.



***Scheme 34. 54** and **58** protonation carry over impurity*

Imine **59** is obtained from the magnesium salts **54** or **58**, after hydrolysis (Scheme 34). Imine **59** was observed to be converted straightforward into ketone **21** even without acid media. Besides, it was observed that in alkaline aqueous media **59** could last for around 48 hours. In summary, imine **59** was not expected to be present in ketone **21** as an impurity.

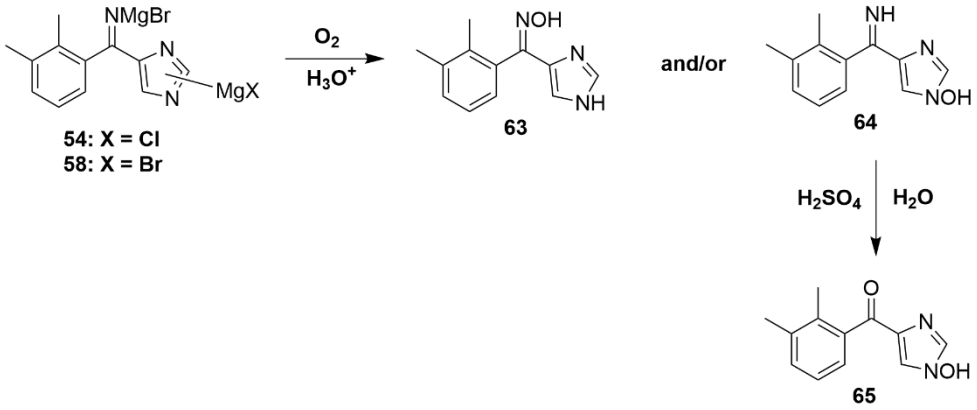
Another impurity related with Grignard **20**, the product of oxygenation of the Grignard reagent, **65**, is expected if the reaction mixture is not properly inertized.



***Scheme 35.** Grignard **20** oxygenation*

According to the literature, the oxygenation of Grignard reagents occurs through a radical mechanism. The initial contact of **20** with oxygen leads to the peroxide **60**. This is transformed to compound **61** through disproportion of the peroxide with another equivalent of **20** (Scheme 35).[65,66] Impurity **62** was found during the development stage and removed in the work-up, at the same point as compound **33**.

Imine **54** or **58** can also undergo oxygenation as Grignard **20**. This leads to the ketoxime **63** or to the hydroxylimidazole **64** (Scheme 36).



Scheme 36. *Imine **54** or **58** oxygenation*

After compounds **63** and **64** formation the next step is the corresponding hydrolysis. Therefore, **64** would convert into ketone **65** whereas compound **63** would remain unreacted. During the development stage, compound **65** never has been observed after the hydrolysis. Although, ketoxime **63** has been observed by UHPLC-MS in the imine formation and after the hydrolysis steps.

Fortunately, although most of the impurities are formed at this step, most of them are eliminated during the work-up or in the mother liquors.

4.3 Synthesis of alkene 14

The synthesis of alkene **14** was previously due optimized. However, some easy improvements and changes could be applied to enhance even more the yield. For this, the amount of toluene in the crystallization was reduced and also temperature of centrifugation was decreased. All these changes are summarized in table 35.

Table 35. *Conditions and results of alkene **14** obtention optimization*

Trial	Toluene Volumes	Temperature (ºC)	Yield (%)	Purity (%)[a]
19	10	20 – 25	89	99,7
91	5	20 – 25	91	99,9
92	10	0 – 5	95	99,6
93	5	0 – 5	96	99,9

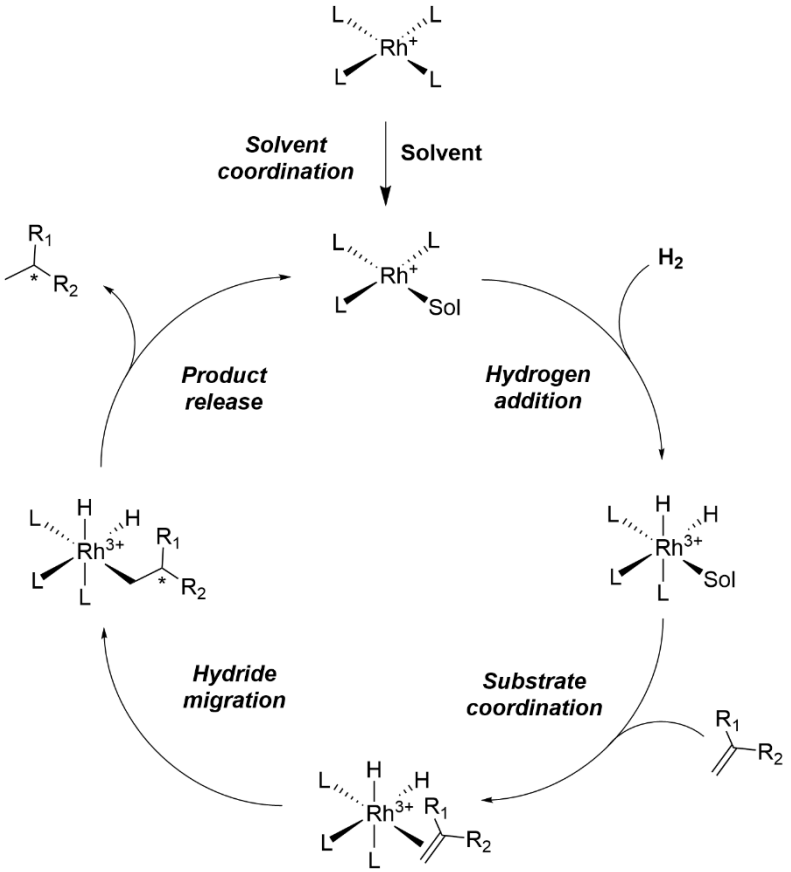
(a) Determined by UHPLC

It was observed that decreasing the temperature of centrifugation the yield increased remarkably. Also, when reducing toluene volumes yield and purity increased.

Besides, the main impurity in alkene **14** is the residual presence of pTsOH at about 0,2 %. When reducing toluene volumes, less amount of pTsOH is dissolved in the organic phase with **14** and more is dissolved in the aqueous phase with $NaHCO_3$. Moreover, these changes would not only increase the yield but also the purity of the alkene **14**.

4.4 Asymmetric hydrogenation of alkene 14

Homogeneous catalyzed hydrogenation reactions are not relevantly used in the industry with the exception of their asymmetric version. Most of the knowledge in this field has been derived from the most popular homogeneous catalyst for hydrogenations: chloridotris(triphenylphosphine)rhodium(I), $RhCl(PPh_3)_3$, knonw as the Wilkinson's Catalyst.[67]



Scheme 37. *Olefin hydrogenation mechanism catalyzed by the Wilkinson's catalyst*

The mechanistic sequence has been deeply studied and the discussions derived from this contributed to the understanding of the catalyst role. The reaction mechanism depicted in scheme 37 consists in the is the following steps:

- **Solvent coordination:** Solvent coordinates to the metal center by a ligand exchange.

- **Hydrogen oxidative addition:** The activation of hydrogen gas proceeds through the oxidative addition of this. The step occurs in *cis* position and can be promoted by the presence of more electron-rich ligands on the metal complex.[68]

- **Substrate coordination:** The coordination of the substrate to the metal center is carried out by a ligand or solvent exchange.

- **Hydride migration:** A rearrangement takes place by the migration of a hydride to the double bond. However, strong electron donating ligands could stabilize the dihydride trivalent metal complex such that the complex is no longer active to undergo the hydride migration. [68]

- **Product release (reductive elimination):** The final product obtained is released by means of a reductive elimination of the alkyl group and the hydride of the metal center. The rate of this step could be increased by the presence of an electron withdrawing ligands. [68] The catalyst recovers its initial state and the cycle is restarted.

The evolution of the homogeneous catalysis leads to the use of chiral metal complexes composed by a metal atom bound to chiral ligands which can discriminate between enantiotopic faces of a prochiral substrate. The industry has interest in these chiral complexes for the production of a broad range of enantiopure or enantioenriched compounds. As both enantiomers of chiral ligands can be accessible, in principle, it is possible to synthetize both enantiomers of the desired target compound.

When the prochiral alkene coordinates to the metal center, a chiral reactive complex is formed. However, the presence of a chiral ligand leads to diastereomeric complexes. Each of these diastereomeric complexes would yield to a different enantiomer. The most stable diastereomeric reactive complex is not the one that lead to the major

observed enantiomer. [69,70] This indicates that the less stable diastereomeric complex reacts faster. It is also known that the oxidative addition of hydrogen to the metal center is irreversible. After the addition of hydrogen and substrate coordination (in any order) the position of the compounds in the complex determines the enantioselectivity of the reaction.[68] Electron-poor ligands can undergo the oxidative addition of H_2 after the substrate coordination.[68]

The migration of the hydride locks the configuration of the resulting chiral product. Generally, this step is the rate-determining step and can also be considered to be reversible. However, further studies are needed in every specific case.

The asymmetric hydrogenation described by Norchim is carried out with a rhodium bis-alkadiene complex containing a weakly coordinating counterion and an asymmetric Josiphos-type ligand. Diene ligands are rapidly exchanged *in situ* by the phosphine added.[68] Commonly used solvents for this are DCM or MeOH.

Initially, all parameters involved in the hydrogenation are listed and their impact in conversion and enantioselectivity is studied theoretically.

- **Temperature**: Enantioselectivity is determined by the difference in energy barriers between the transition states leading to the diastereomeric reactive complexes formed. By increasing the temperature, both enantiomers would be accessible and thus reducing the e.e. However, increasing the energy of the system could speed up the reaction and increase the conversion.

- **Pressure**: The amount of hydrogen available to react depends on the solubility of this in the reaction solvent. By increasing hydrogen pressure, the amount of hydrogen dissolved is also increased. This would increase the reaction rate in the oxidative addition step and thus increase the conversion.[71]

- **Time**: It is clear that longer reaction times could lead to higher conversions. However, the influence of time on e.e. is not clear and depends on the reaction kinetics.

- **Reaction volumes**: Higher reaction volumes could increase the amount of hydrogen dissolved but reduce the probability of the substrate to find the

catalyst. Lowering reaction volumes increase the probability of substrate-catalyst interaction but reducing the amount of hydrogen dissolved. This indicates that a compromise must be assumed regarding reaction volumes.

- **Solvent**: Reaction solvent is important to effectively dissolve all reagents to perform the catalytic reaction. At the same time, solvents can participate in the catalytic cycles and thus affect the stereochemical outcome of the reaction.

- **Reaction pH**: The pH can affect the energy required to bind hydrogen influencing the conversion. At the same time, the pH can favor or disfavor the coordination of other parts of the substrate affecting the e.e.[72]

- **Metal catalyst**: The metal has a key role in the catalytic process. The outcome of the reaction strongly depends on the metal catalyst and its fitting with the substrate.

- **Chiral ligand**: The ligand modifies the stereoelectronics around the metal center. Although some hypothesis can be done based on previous knowledge, the influence of a determined ligand must be experimentally studied.

- **Substrate**: The fitting of the substrate with the metal catalyst is crucial for the success of the catalysis. Auxiliary functionalization into the substrate can dramatically change final result of the reaction.

Each parameter will be studied separately and those with best results could be mixed and deeply studied in order to achieve the best possible results in the hydrogenation among all the parameters and regions studied.

4.4.1 Effect of solvent in the asymmetric hydrogenation of alkene **14**

Reaction solvent participates as a labile ligand in the catalytic cycle. Solvent also must dissolve the reagents and intermediates in a way that does not inhibit the catalysis. The effect that a specific solvent can have in the result of the catalysis is difficult to predict.

The first assumption done to evaluate the effect of the solvent is about the solubility. Those solvents that could dissolve better both catalyst and substrate could have better conversions.

[redacted]

[redacted]

[redacted]	[redacted]	[redacted]	[redacted]	[redacted]
[redacted]	[redacted]	[redacted]	[redacted]	[redacted]
[redacted]	[redacted]	[redacted]	[redacted]	[redacted]
[redacted]	[redacted]	[redacted]	[redacted]	[redacted]
[redacted]	[redacted]	[redacted]	[redacted]	[redacted]
[redacted]	[redacted]	[redacted]	[redacted]	[redacted]
[redacted]	[redacted]	[redacted]	[redacted]	[redacted]
[redacted]	[redacted]	[redacted]	[redacted]	[redacted]
[redacted]	[redacted]	[redacted]	[redacted]	[redacted]

[redacted]

[redacted]

[redacted]

[redacted]

[redacted]

[redacted]

[redacted]

[redacted]

[redacted]

[redacted]

[redacted]

[redacted]	[redacted]	[redacted]	[redacted]	[redacted]
[redacted]	[redacted]	[redacted]	[redacted]	[redacted]
[redacted]	[redacted]	[redacted]	[redacted]	[redacted]
[redacted]	[redacted]	[redacted]	[redacted]	[redacted]
[redacted]	[redacted]	[redacted]	[redacted]	[redacted]
[redacted]	[redacted]	[redacted]	[redacted]	[redacted]
[redacted]	[redacted]	[redacted]	[redacted]	[redacted]
[redacted]	[redacted]	[redacted]	[redacted]	[redacted]
[redacted]	[redacted]	[redacted]	[redacted]	[redacted]
[redacted]	[redacted]	[redacted]	[redacted]	[redacted]
[redacted]	[redacted]	[redacted]	[redacted]	[redacted]
[redacted]	[redacted]	[redacted]	[redacted]	[redacted]
[redacted]	[redacted]	[redacted]	[redacted]	[redacted]
[redacted]	[redacted]	[redacted]	[redacted]	[redacted]
[redacted]	[redacted]	[redacted]	[redacted]	[redacted]

[redacted]

[redacted]

[redacted]

[redacted]

[redacted]

[redacted]

[redacted]	[redacted]	[redacted]	[redacted]
[redacted]	[redacted]	[redacted]	[redacted]
[redacted]	[redacted]	[redacted]	[redacted]
[redacted]	[redacted]	[redacted]	[redacted]
[redacted]	[redacted]	[redacted]	[redacted]
[redacted]	[redacted]	[redacted]	[redacted]
[redacted]	[redacted]	[redacted]	[redacted]
[redacted]	[redacted]	[redacted]	[redacted]

[redacted]

[redacted]

[redacted]

4.4.2 Effect of pH in the asymmetric hydrogenation of alkene **14**

The pH could affect the energy required to bind hydrogen affecting the conversion.[68] Therefore, this could influence the final performance of the reaction. [redacted]

[redacted]

[redacted]	[redacted]	[redacted]	[redacted]	[redacted]
[redacted]	[redacted]	[redacted]	[redacted]	[redacted]
[redacted]	[redacted]	[redacted]	[redacted]	[redacted]
[redacted]	[redacted]	[redacted]	[redacted]	[redacted]

[redacted]

[redacted]

<u>4.4.3 Effect of the metal source in the asymmetric hydrogenation of alkene **14**</u>

The performance of the reaction strongly depends on the metal catalyst and its fitting with the substrate.

[redacted]

[redacted]

[redacted]

[redacted]

[redacted]

[redacted]	[redacted]	[redacted]	[redacted]
[redacted]	[redacted]	[redacted]	[redacted]
[redacted]	[redacted]	[redacted]	[redacted]
[redacted]	[redacted]	[redacted]	[redacted]
[redacted]	[redacted]	[redacted]	[redacted]

[redacted]

[redacted]

[redacted]

[redacted]

[redacted]

[redacted]	[redacted]	[redacted]	[redacted]	[redacted]
[redacted]	[redacted]	[redacted]	[redacted]	[redacted]
[redacted]	[redacted]	[redacted]	[redacted]	[redacted]
[redacted]	[redacted]	[redacted]	[redacted]	[redacted]
[redacted]	[redacted]	[redacted]	[redacted]	[redacted]

[redacted]

[redacted]

[redacted]

4.4.4 Effect of ligand in the asymmetric hydrogenation of alkene **14**

Chiral ligands alter both the esterics of the metal enviroment and its electronic properties. While certain hypotheses can be formulated based on prior knowledge, the impact of a specific ligand should be investigated through experimental study.

[redacted]



[redacted]

[redacted]	[redacted]	[redacted]	[redacted]	[redacted]
[redacted]	[redacted]	[redacted]	[redacted]	[redacted]
[redacted]	[redacted]	[redacted]	[redacted]	[redacted]
[redacted]	[redacted]	[redacted]	[redacted]	[redacted]
[redacted]	[redacted]	[redacted]	[redacted]	[redacted]
[redacted]	[redacted]	[redacted]	[redacted]	[redacted]
[redacted]	[redacted]	[redacted]	[redacted]	[redacted]
[redacted]	[redacted]	[redacted]	[redacted]	[redacted]
[redacted]	[redacted]	[redacted]	[redacted]	[redacted]

[redacted]

[redacted]

[redacted]

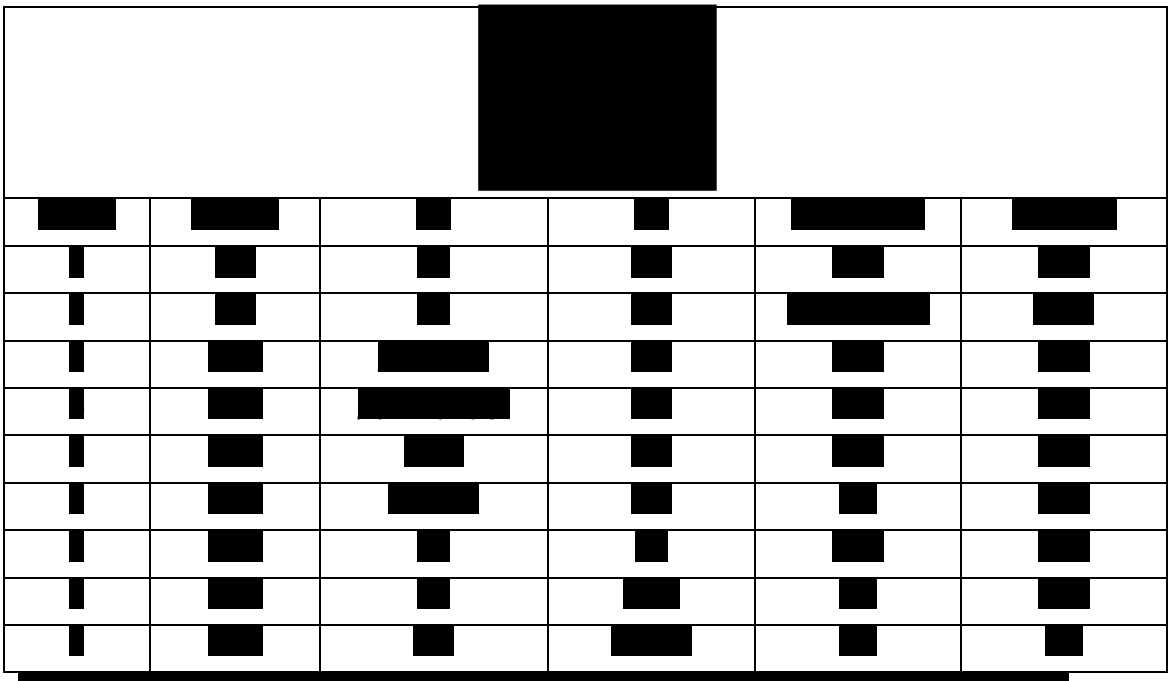
[redacted]

[redacted]

[redacted]

[redacted]

[redacted]



[redacted]

[redacted]

[redacted]

[redacted]

[redacted]

[redacted]



[redacted]



[redacted]							

[redacted]

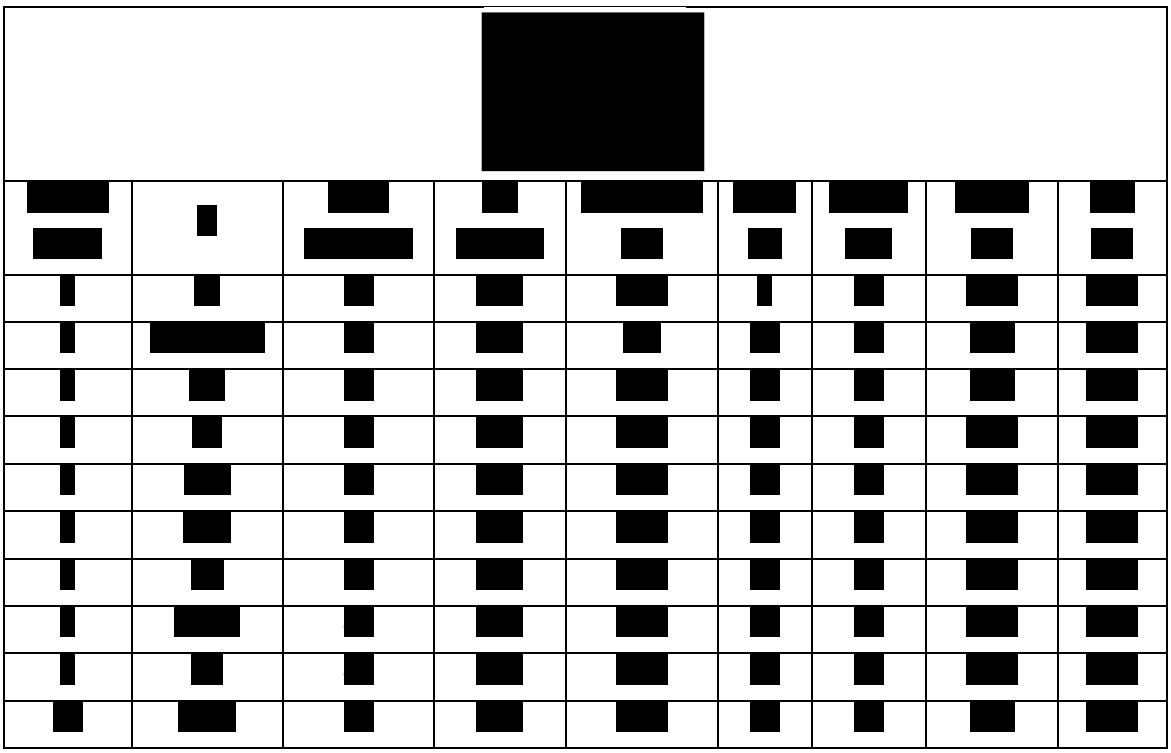
[redacted]

4.4.5 Effect of imidazole substitution in the asymmetric hydrogenation of alkene **14**

[redacted]



[redacted]



[redacted]

[redacted]				
[redacted]	[redacted]	[redacted]	[redacted]	[redacted]
[redacted]	[redacted]	[redacted]	[redacted]	[redacted]
[redacted]	[redacted]	[redacted]	[redacted]	[redacted]
[redacted]	[redacted]	[redacted]	[redacted]	[redacted]
[redacted]	[redacted]	[redacted]	[redacted]	[redacted]
[redacted]	[redacted]	[redacted]	[redacted]	[redacted]
[redacted]	[redacted]	[redacted]	[redacted]	[redacted]
[redacted]	[redacted]	[redacted]	[redacted]	[redacted]

[redacted]

[redacted]

[redacted]

[redacted]

[redacted]

[redacted]

[redacted]

[redacted]

[redacted]

[redacted]

[redacted]	[redacted]	[redacted]	[redacted]	[redacted]
[redacted]	[redacted]	[redacted]	[redacted]	[redacted]
[redacted]	[redacted]	[redacted]	[redacted]	[redacted]
[redacted]	[redacted]	[redacted]	[redacted]	[redacted]

[redacted]

[redacted]

[redacted]

[redacted]

[redacted]



[redacted]	[redacted]	[redacted]	[redacted]	[redacted]	[redacted]	[redacted]
[redacted]	[redacted]	[redacted]	[redacted]	[redacted]	[redacted]	[redacted]
[redacted]	[redacted]	[redacted]	[redacted]	[redacted]	[redacted]	[redacted]
[redacted]	[redacted]	[redacted]	[redacted]	[redacted]	[redacted]	[redacted]
[redacted]	[redacted]	[redacted]	[redacted]	[redacted]	[redacted]	[redacted]
[redacted]	[redacted]	[redacted]	[redacted]	[redacted]	[redacted]	[redacted]
[redacted]	[redacted]	[redacted]	[redacted]	[redacted]	[redacted]	[redacted]
[redacted]	[redacted]	[redacted]	[redacted]	[redacted]	[redacted]	[redacted]
[redacted]	[redacted]	[redacted]	[redacted]	[redacted]	[redacted]	[redacted]

[redacted]

[redacted]

[redacted]

[redacted]

[redacted]

[redacted]

[redacted]

[redacted]

[redacted]

[redacted]

[redacted]

[redacted]



[redacted]

[redacted]

[redacted]

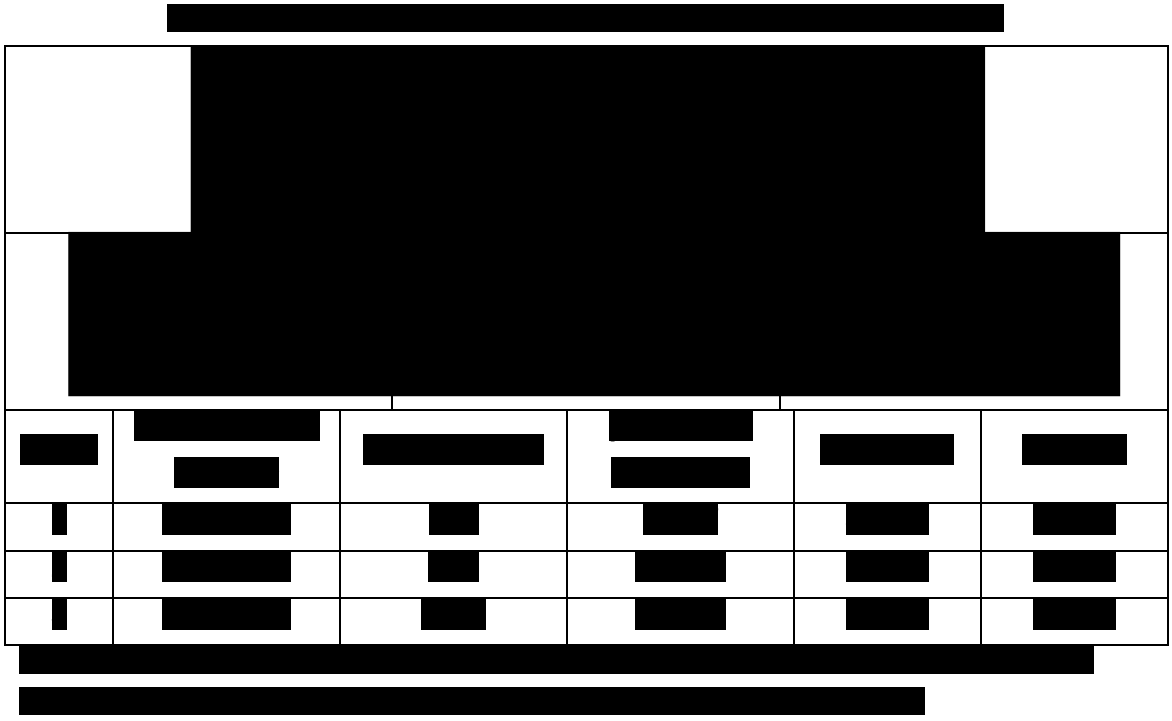
3.4.6 Effect of metal cocatalyst in the asymmetric hydrogenation of alkene **68**

[redacted]

[redacted]

[redacted]

[redacted]



[redacted]

[redacted]

[redacted]

[redacted]

[redacted]	[redacted]	[redacted]	[redacted]	[redacted]	[redacted]
[redacted]	[redacted]	[redacted]	[redacted]	[redacted]	[redacted]
[redacted]	[redacted]	[redacted]	[redacted]	[redacted]	[redacted]

[redacted]

[redacted]

[redacted]



[redacted]

[redacted]

[redacted]

[redacted]

[redacted]	[redacted]	[redacted]	[redacted]	[redacted]
[redacted]	[redacted]	[redacted]	[redacted]	[redacted]
[redacted]	[redacted]	[redacted]	[redacted]	[redacted]
[redacted]	[redacted]	[redacted]	[redacted]	[redacted]
[redacted]	[redacted]	[redacted]	[redacted]	[redacted]
[redacted]	[redacted]	[redacted]	[redacted]	[redacted]

[redacted]

[redacted]

[redacted]

[redacted]

4.4.7 Study on the functionalization of imidazole regioselectivity

In some cases [redacted] impurities with the same molecular weight were observed at a very close retention time in the UHPLC-MS analysis. [redacted] This may indicate the presence of isomers [redacted]

[redacted]

In an imidazole ring, both nitrogen atoms are close in reactivity due to tautomerism (Figure 27). As the proton at N_τ is moderately acidic and it can react with a strong base to yield a nucleophilic anion.[90,91] As a result, nucleophilic substitution can be performed in both nitrogen atoms.

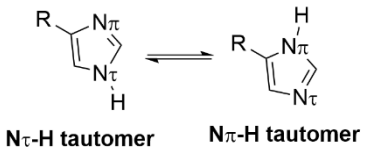


Figure 27. *Tautomerism of imidazole ring*

[redacted]



The analysis by ^{1}H-NMR revealed that the obtained regioisomer was almost pure (99,7 %) . However, the product obtained , was a mixture of compounds . The major regioisomer was about 81 %. The ^{1}H NMR spectrum of the product obtained is shown in figure 28.

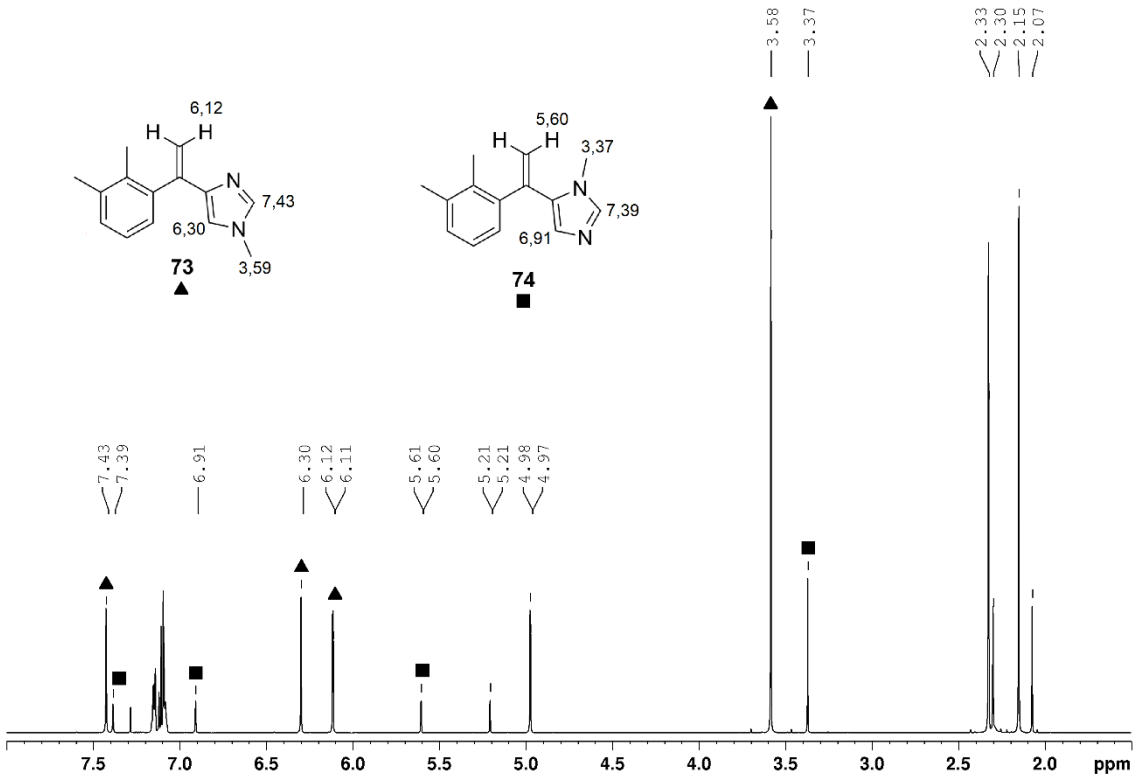


Figure 28. *[1]H-NMR spectra of product **73** and **74** mixture resulting from the methylation reaction of **14***

Selective NOE [1]H-NMR experiment was carried out for 3,37 and 3,59 ppm signals which correspond to the methylic protons

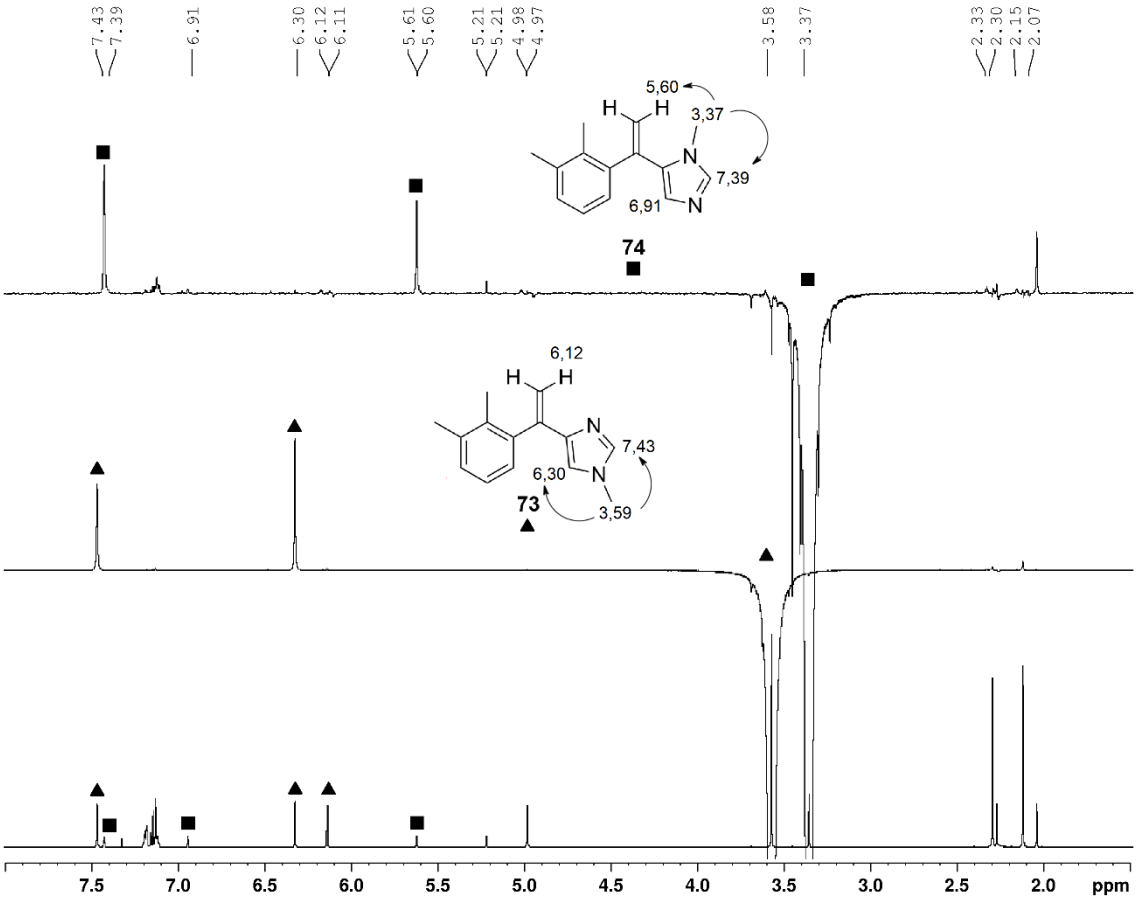
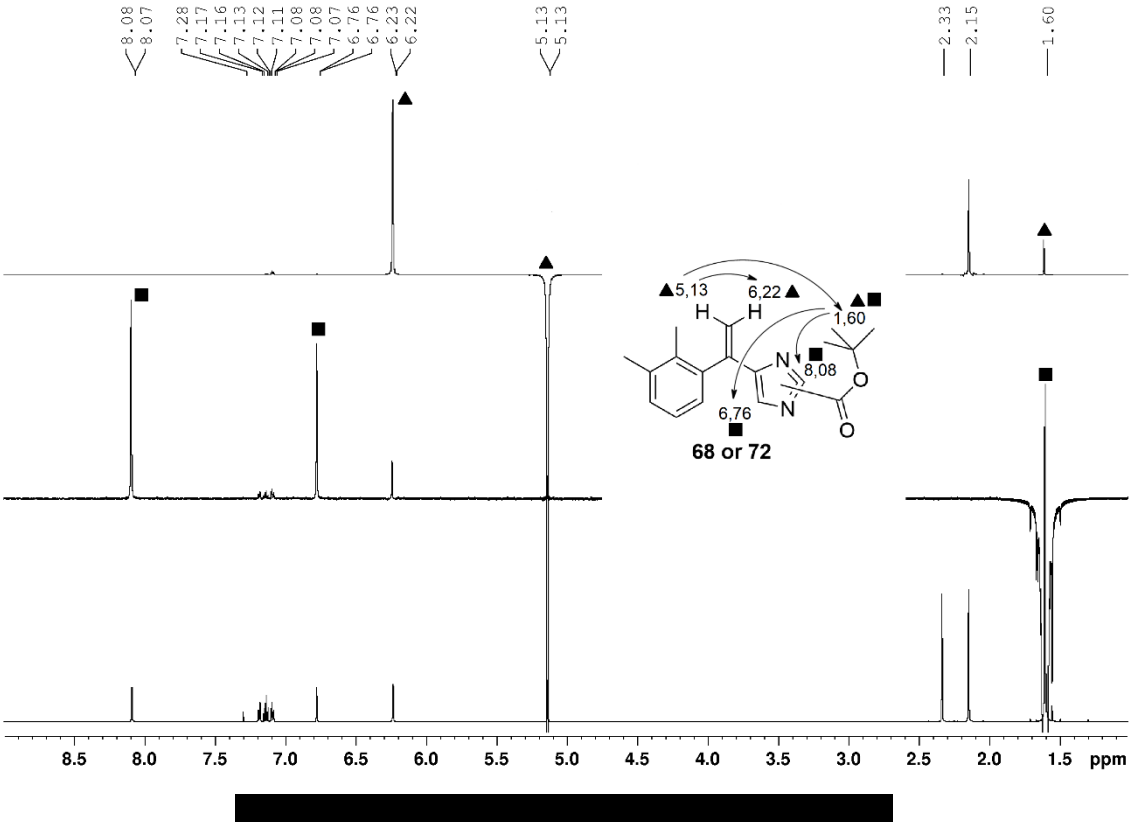


Figure 29. *Selective NOE in a) [1]H NMR spectrum of imidazole **73** and (b) imidazole **74**. c) [1]H NMR spectrum of a **73**/**74**, ~4/1 mixture*

[redacted]



[redacted]

[redacted]

Fortunately, after an exhaustive crystallization study, [redacted] imidazole crystals with sufficient quality to resolve the structure by SC-XRD could be obtained [redacted]

[redacted]

[redacted] The structures obtained by SC-XRD are shown in figure 31.



[redacted] Finally, the structure [redacted] was unequivocally found.

4.4.8 Synthesis optimization of Boc functionalized alkene **68**

[redacted]



[redacted]

[redacted]

[redacted]

[redacted]

[redacted]	[redacted]	[redacted]	[redacted]	[redacted]	[redacted]
[redacted]	[redacted]	[redacted]	[redacted]	[redacted]	[redacted]
[redacted]	[redacted]	[redacted]	[redacted]	[redacted]	[redacted]
[redacted]	[redacted]	[redacted]	[redacted]	[redacted]	[redacted]
[redacted]	[redacted]	[redacted]	[redacted]	[redacted]	[redacted]
[redacted]	[redacted]	[redacted]	[redacted]	[redacted]	[redacted]
[redacted]	[redacted]	[redacted]	[redacted]	[redacted]	[redacted]
[redacted]	[redacted]	[redacted]	[redacted]	[redacted]	[redacted]

[redacted]

[redacted]

[redacted]



[redacted] With that, the regulatory impact of this change in the manufacturing process would be lower and easier to be approved by the regulatory agencies.

4.4.9 Summary of asymmetric hydrogenation of Boc functionalized alkene **68**

Initially, the asymmetric synthesis of *S*-**8** was described through the asymmetric hydrogenation [redacted]

[redacted]

[redacted]	[redacted]	[redacted]
[redacted]	[redacted]	[redacted]
[redacted]	[redacted]	[redacted]
[redacted]	[redacted]	[redacted]
[redacted]	[redacted]	[redacted]
[redacted]	[redacted]	[redacted]
[redacted]	[redacted]	[redacted]
[redacted]	[redacted]	[redacted]
[redacted]	[redacted]	[redacted]
[redacted]	[redacted]	[redacted]

The new proposed process has some advantages in addition to those already mentioned:

It must be noted that the new proposed process must be compatible with process, which will be studied in the following section.

4.5 Synthesis of enantiopure alkane *S*-8

The resolution of enantioenriched *S*-**8** was previously performed following the same approach reported by Norchim.

A new purification approach was needed to further improve the enantioselectivity. This new purification approach was focused on the reduction of the manufacturing steps maintaining or improving the yield and purity.

4.5.1 Direct resolution of alkene *S*-**8**

The obtention of the enantiopure alkane *S*-**8** was attempted



[redacted]

[redacted]				
[redacted]	[redacted]	[redacted]	[redacted]	[redacted]
[redacted]	[redacted]	[redacted]	[redacted]	[redacted]
[redacted]	[redacted]	[redacted]	[redacted]	[redacted]
[redacted]	[redacted]	[redacted]	[redacted]	[redacted]
[redacted]				
[redacted]	[redacted]		[redacted]	
[redacted]	[redacted]		[redacted]	

[redacted]

[redacted]

[redacted]

[redacted]

[redacted]

[redacted]	[redacted]	[redacted]	[redacted]	[redacted]	[redacted]
[redacted]	[redacted]	[redacted]	[redacted]	[redacted]	[redacted]
[redacted]	[redacted]	[redacted]	[redacted]	[redacted]	[redacted]
[redacted]	[redacted]	[redacted]	[redacted]	[redacted]	[redacted]
[redacted]	[redacted]	[redacted]	[redacted]	[redacted]	[redacted]

[redacted]

[redacted]

[redacted]

[redacted]

[redacted]

[redacted]	[redacted]	[redacted]	[redacted]	[redacted]
[redacted]	[redacted]	[redacted]	[redacted]	[redacted]
[redacted]	[redacted]	[redacted]	[redacted]	[redacted]
[redacted]	[redacted]	[redacted]	[redacted]	[redacted]
[redacted]	[redacted]	[redacted]	[redacted]	[redacted]
[redacted]	[redacted]	[redacted]	[redacted]	[redacted]

[redacted]

[redacted]



[redacted]

[redacted]

[redacted]

[redacted]

[redacted]	[redacted]	[redacted]	[redacted]	[redacted]
[redacted]	[redacted]	[redacted]	[redacted]	[redacted]
[redacted]	[redacted]	[redacted]	[redacted]	[redacted]
[redacted]	[redacted]	[redacted]	[redacted]	[redacted]
[redacted]	[redacted]	[redacted]	[redacted]	[redacted]
[redacted]	[redacted]	[redacted]	[redacted]	[redacted]
[redacted]	[redacted]	[redacted]	[redacted]	[redacted]
[redacted]	[redacted]	[redacted]	[redacted]	[redacted]
[redacted]	[redacted]	[redacted]	[redacted]	[redacted]
[redacted]	[redacted]	[redacted]	[redacted]	[redacted]
[redacted]	[redacted]	[redacted]	[redacted]	[redacted]
[redacted]	[redacted]	[redacted]	[redacted]	[redacted]
[redacted]	[redacted]	[redacted]	[redacted]	[redacted]
[redacted]	[redacted]	[redacted]	[redacted]	[redacted]

[redacted]

[redacted]







[redacted]

[redacted]

[redacted]	[redacted]	[redacted]	[redacted]
[redacted]	[redacted]	[redacted]	[redacted]
[redacted]	[redacted]	[redacted]	[redacted]
[redacted]	[redacted]	[redacted]	[redacted]

[redacted]

[redacted]

[redacted]

[redacted]

[redacted]

[redacted]

[redacted]

4.5.2 New resolution strategy from Boc functionalized alkene **68** hydrogenation

From the previous section, it was concluded that a higher [redacted] was needed to achieve the required yield and e.e. [redacted]

[redacted]

[redacted]

[redacted]

[redacted]

[redacted]	[redacted]	[redacted]	[redacted]
[redacted]	[redacted]	[redacted]	[redacted]
[redacted]	[redacted]	[redacted]	[redacted]
[redacted]	[redacted]	[redacted]	[redacted]
[redacted]	[redacted]	[redacted]	[redacted]

[redacted]

[redacted]

[redacted]

[redacted]

[redacted]

[redacted]

[redacted]	[redacted]	[redacted]	[redacted]
[redacted]	[redacted]	[redacted]	[redacted]
[redacted]	[redacted]	[redacted]	[redacted]
[redacted]	[redacted]	[redacted]	[redacted]

[redacted]

[redacted]

4.5.3 Resolution mechanism of the direct crystallization method

The resolution of alkane **8** can be easily explained by the tartrate **39** formation, as a diastereomer is formed.

To prove that, a SC-XRD analysis was carried out,



Distances and bond angle are shown in table 66.

[redacted]

The PXRD of *rac*-**8** and *S*-**8** shown in figure 37, [redacted]

[redacted]

4.6 Scale-up trial

A scaled-up trial was planned to consolidate all the changes proposed along the whole process. The scaled trial was performed to a 10 % of the final commercial batch scale. [redacted]

[redacted]

[redacted]	[redacted]	[redacted]	[redacted]
[redacted]	[redacted]	[redacted]	[redacted]
[redacted]	[redacted]	[redacted]	[redacted]
[redacted]	[redacted]	[redacted]	[redacted]
[redacted]	[redacted]	[redacted]	[redacted]
[redacted]	[redacted]	[redacted]	[redacted]

[redacted]

[redacted]



[redacted]

[redacted]

[redacted]		
[redacted]	[redacted]	[redacted]
[redacted]	[redacted]	[redacted]
[redacted]	[redacted]	[redacted]
[redacted]	[redacted]	[redacted]
[redacted]	[redacted]	[redacted]

[redacted]

[redacted]

[redacted]

[redacted]





[redacted]

[redacted]

[redacted]

[redacted]	[redacted]	[redacted]
[redacted]	[redacted]	[redacted]
[redacted]	[redacted]	[redacted]
[redacted]	[redacted]	[redacted]
[redacted]	[redacted]	[redacted]
[redacted]	[redacted]	[redacted]

[redacted]

[redacted]

[redacted]

[redacted]

[redacted]

[redacted]

[redacted]	[redacted]	[redacted]
[redacted]	[redacted]	[redacted]
[redacted]	[redacted]	[redacted]
[redacted]	[redacted]	[redacted]
[redacted]	[redacted]	[redacted]

[redacted]

[redacted]

[redacted]

4.6.1 Summary of the new optimized process

The comparison between the initial Norchim's process, Moehs validated process and the new process proposal (described in Chapter 4), is shown in table 73.

Table 73. *Yield comparison between S-**15** manufacturing processes*

Yield (%) of	Norchim's Process	Moehs Validated Process	New process proposal
Ketone **21**	73	67	87
Alkene **14**	93	92	97
Asymmetric Hydrogenation	100 % conv. 78,0 % e.e.	100 % conv. 77,0 % e.e.	99,8 % conv. 98,5 % e.e.
Alkane *S*-**8**	51	61	62
Final product *S*-**15**	85	85	85
Global yield (about)	29	32	44

Although the performance of the validated Moehs process is higher than that obtained by Norchim, the new process proposal further increases the overall yield, maintaining the quality of the final product.

Besides, the productivity has also been increased. The duration of the whole manufacturing process and the amount of final product obtained, based on the batch size and process yield, are compared between the 3 manufacturing processes in table 74.

Table 74. *Productivity comparison between S-**15** manufacturing processes*

Time and amount of *S*-**15**	Norchim's Process	Moehs Validated Process	New process proposal
Batch size (g) (per batch of *S*-15)	396,5	800	1600
Global yield (%)	29	32	44
Manufacturing time (weeks) (per batch of *S*-15)	9	9	7
***S*-15 final amount per batch (g)**	292	650	1800
Productivity (g/week)	33	72	257

The increase in batch size and yield of the Moehs validated process respect from the initial Norchim's process, provide a huge improvement in the productivity. However, the new proposed process dramatically increases the productivity as more amount of final

product is expected with the reduction of manufacturing steps, playing a key role in the final increased productivity.

With the results shown, it is clear that Moehs' validated process provides several benefits over the initial method. Even so, the new process proposal presents even more advantages, which could provide a strategic position for the company in the market with this product.

4.7 Nitrosamines Drug Substance Related Impurities (NDSRIs)

N-Nitrosamines are carcinogenic impurities present in common consumable products. Nitrosamines were discovered more than 100 years ago and begin to be visible when their carcinogenicity was detected. However, it was not until mid-2018 that regulatory agencies detected unacceptable levels of *N*-nitrosodimethylamine (NMDA) impurity in Valsartan, which represented a big challenge to the Pharmaceutical Industry. Immediately, further testing revealed presence of NDMA also in both Ranitidine and Metformin medicines.[93]

Numerous batch recalls beginning to threaten the global supply of essential drugs and huge efforts were initiated to assess the potential risks posed by nitrosamines in the currently marketed drugs.

Common and well-studied small nitrosamines were first limited, leading to the relatively swift establishment of acceptable limits. However, the much more challenging task was the control of a *N*-nitrosamines from an amine-containing API (also called Nitrosamines Drug Substance Related Impurities), which carcinogenicity had not been previously studied. A recent update of regulatory guidelines have set a procedure to establish a more accurate limit for the majority of nitrosamines found in the drug substance and to develop and implement a control strategy.

Regulatory agencies required extensive reviews of all human medications to evaluate the possible presence of nitrosamines through a risk assessment. Also, they published a guide and general recommendations on the mitigation and prevention of the presence of nitrosamines in human medicinal products.

The risk assessment evaluation focuses on limiting of the possible nitrosable compounds (amines and generally secondary amines) and the absence demonstration

of the possible nitrosating agents (generally nitrites). However, as the toxicological limits known for some nitrosamines are really low (ppb levels) the negligibility is not usually accepted. [93]

As the HPAPI of this project contains an NH moiety in the imidazole ring, a risk assessment evaluation of the potential presence of nitrosamines during the manufacturing process was performed.

To demonstrate the absence of any potential nitrosamine, a reference standard of the relevant impurity is needed. Diverse synthetic procedures are described in the literature for the nitrosation of nitrogen-containing compounds.[95] However, these procedures can be summarized in 2 different conditions depending on reagents used:

- The most common use synthesis consist in the reaction of the nitrogen-containing compound with $NaNO_2$ in aqueous acid medium.[96]

- The second methodology consist in the reaction of assessed compound with *tert*-butyl nitrite (TBN) as nitrosating agent.[97]

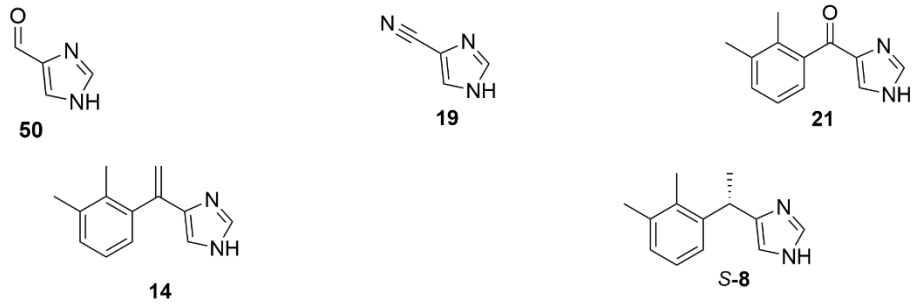
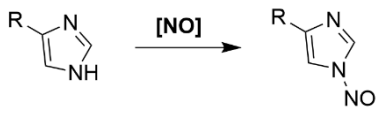


Figure 37. *Imidazole compounds present in the synthesis of S-**15** and could react under nitrosation conditions*

Those imidazole compounds present in the synthesis of *S*-**15** were reacted under nitrosating conditions and the formation of *N*-nitroso compounds were studied. Imidazoles **52** and **19**, ketone **21**, alkene **14** and alkane *S*-**8** were reacted with $NaNO_2$ and TBN. The results obtained are shown in table 75.

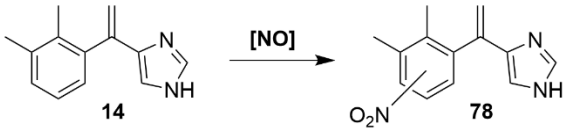
Table 75. *Imidazole compounds present in the synthesis of S-**15** nitrosation trials*



Entry	Compound	Conditions	Results[a]
1	**52**	$NaNO_2$, HCl	No reaction
2	**52**	TBN	No reaction
3	**19**	$NaNO_2$, HCl	No reaction
4	**19**	TBN	No reaction
5	**21**	$NaNO_2$, HCl	No reaction
6	**21**	TBN	No reaction
7	**14**	$NaNO_2$, HCl	Reaction
8	**14**	TBN	Reaction
9	**9**	$NaNO_2$, HCl	No reaction
10	**9**	TBN	No reaction

(a) Analyzed by UHPLC-MS from the reaction crude

In most of cases, no reaction was observed when reacted the imidazole containing compound under nitrosating conditions. However, alkeneimidazole **14** showed the formation of 2 unknow compounds (entries 7 and 8). The analysis by UHPLC-MS reported that these new compounds had an m/z ratio corresponding to a nitrobenzene-analog. This was reported in the literature to be possible in aromatic rings.[98]

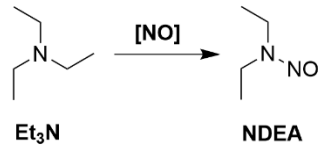


Scheme 46. *Nitro-compound **78** formation under nitrosation conditions*

Despite alkene **14** generates new impurities when reacted under nitrosation conditions, these nitro compounds **78** were considered not to be potential under the usual synthetic conditions in the manufacturing process. The exact structure of the 2 impurities were not elucidated. The NO_2^- group could be bonded in 3 different positions in the aromatic ring so this can explain the appearance of 2 different compounds with the exact same molecular weight.

The presence of secondary amine generally ends up with the possibility of *N*-nitrosamine impurity formation. However, in the most recent literature, it has been

reported that *N*-nitrosamine impurities can be formed from tertiary amine, among others (Scheme 47).[94]



Scheme 47. *Nitrosation of Et_3N*

The nitrosative dealkylation[93,94] of Et_3N could lead to the formation of *N*-nitrosodiethylamine (NDEA) impurity which was one of the first reported. Because of that, the use of Et_3N was changed to K_2CO_3 to prevent the possibility of *N*-nitrosamine impurities formation.

During the development of an analytical method,[99] a reference standard of the relevant nitrosamine impurity is generally needed. If synthesis of the nitrosamine impurity is difficult, this could be an indication that nitrosamine either does not exist or that there is no risk of its formation. In such cases, it may not be necessary to conduct confirmatory testing if it is thoroughly justified.

In summary, it could be considered that, despite extensive efforts, it becomes apparent that the nitrosamines under study could not be obtained. Thus, *S*-**15** manufacturing process reported in this project is not likely to form *N*-nitrosamine impurities.

4.8 General conclusions

The main objective of this project was to optimize the manufacturing process for the obtention of a HPAPI, reducing costs and increasing productivity. Furthermore, the final scope of this project was to validate a manufacturing process meeting regulatory requirements in the market.

In Chapters 1 and 2, an optimized process has been validated and industrialized. The process initially reported by Norchim was adapted to Moehs facilities and the process studied in detail and optimized. The global yield was slightly increased from 29 % to 32 % and the productivity was doubled. Despite these good results, the process still presented some deficiencies. The obtention of ketone **21** was reported not to be robust enough. The asymmetric hydrogenation achieved a low enantiomeric excess which

forces to carry out a resolution via tartrate salt, **39**. This, significantly increases the manufacturing time. Considering that from this step in the manufacturing process the products are considered as a HPAPI, the manufacturing must be carried out inside the isolator. The cost of the operations in the isolator is considerably higher than in a regular process. It was clear that the validated manufacturing process, which is used to obtain marketable product, can be improved.

In Chapter 4,further optimization of the process has been performed. The change of the base used in the synthesis of ketone **21** from iPrMgCl to the Grignard **20** provided excellent yields and robustness. However, more studies, specifically in terms of process safety, are needed to fully implement these improvements.

Moreover, the asymmetric hydrogenation has been deeply investigated. The enantiomeric excess has been remarkably improved from 77,0 to 98,5 % e.e. At the same time, a new resolution approach has been investigated to reduce the manufacturing steps. The direct crystallization of the enantiopure alkane *S*-**8** from the hydrogenation crude has been successfully achieved. Despite the yield remains the same, quality is maintained while the purification steps had been reduced from 4 to 1.

The combination of these 2 approaches, increased the yield from 32 % to 44 % and the productivity by more than 3 times. Even with these improvements achieved in Chapter 4, some aspects have to be further investigated. The effect on e.e. of the Boc functionalization specifically together with the ligand used for the hydrogenation. Also the regioselectivity of the imidazole functionalization remains challenging.

The objectives of this project had been successfully accomplished. Even so, more work has to be done. The next most relevant step that has to be next done is the validation of the new process proposal to fully optimize the process yield and productivity.

4.9 Next steps

Some work has been left pending after the 3 years of this thesis. The main point that has been left is the implementation of the new process described in Chapter 4. Implementation depends on strategic factors of the Company, which can take a few years.

Another aspect that has been left due to lack of time is the understanding of the regioselectivity of the imidazole functionalization, specifically involving alkene **14**. Maybe, the contradictory results obtained could be due to the improper structural assignment of alkene **14**. This compound could be analyzed by SC-XRD and more functional groups can be tried and study its regioselectivity.

The exact mechanism of the asymmetric hydrogenation that could give and explanation to the improvements observed by using Boc functionalized alkene **68** and Josiphos ligand **L-10** remains unstudied.

A kinetic study of the hydrogenation at 0 – 5 ºC could be performed in order to be able to achieve a compromise between reaction time and amount of catalyst that best fits the company interests.

Moreover, the study of the resolution could be extended to the optimization of the resolution agent with different solvents. The direct crystallization of alkane *S*-**8** can also be deeply studied with a DoE from the Boc functionalized alkeneimidazole **68** hydrogenation crude as has been performed for alkene **14**.

Finally, the process safety for the synthesis of ketone **21** must be carefully studied. The safety of the whole new process must be assessed before it will be validated at commercial scale.

4.10 Bibliography

[1] - Hill, R. G. Drug Discovery and Development, *2nd Ed*, **2012**. ISBN: 978-0-7020-4299-7

[2] - *European Medicines Agency*. ICH Q7 Good manufacturing practice for active pharmaceutical ingredients - Scientific guideline. Page: ema.europa.eu/en/ich-q7-good-manufacturing-practice-active-pharmaceutical-ingredients-scientific-guideline. Accessed February **2024**

[3] - *Moehs Fine Chemicals*. Brief history. Page: moehs.com/company/brief-history/. Accessed March **2024**

[4] - *Royal Society of Chemistry*. Highly Potent Active Pharmaceutical Ingredients (HPAPI). Page: rsc.org/events/detail/30385/highly-potent-active-pharmaceutical-ingredients-hpapi. Event of 21-23 May **2018**

[5] - *PharmaTech*. High-Potency APIs: Containment and Handling Issues. Page: pharmtech.com/view/high-potency-apis-containment-and-handling-issues. Accessed March **2024**

[6] - *Escopharma*. Fine Chemicals and HPAPIs. Page: escopharma.com/solutions/fine-chemicals-and-hpapis. Accessed March **2024**

[7] - *European Chemicals Agency*. Occupational exposure limits. Page: echa.europa.eu/en/oel. Accessed March **2024**

[8] - *Medisca*. Safety Data Sheet for Ibuprofen. Page: files.medisca.com/ProductFiles/0299/Medisca%20Document/SDS/EN/0299.pdf. Accessed March **2024**.

[9] - *Esco Lifesciences*. Active Pharmaceutical Ingredients (API) surrogate containment testing on Esco powdermax™ powder weighing balance enclosure. Page: escolifesciences.com/pdf/PW1_surrogate.pdf. Accessed March **2024**

[10] - *Gilead Science*. Submital to the National Institute For Occupational Safety and Health (NIOSH) to request that NIOSH not list Tenefovir Disoproxil Fumarate (Viread®) as a "Hazardous Drug". Page: cdc.gov/niosh/docket/archive/pdfs/niosh-105/0105-092607-mchugh_sub.pdf. Accessed March **2024**

[11] - *Pharmacyclics*. Safety Data Sheet of Ibrutinib - Drug Product. Page: obaid.info/pdf/MSDS/I/Ibrutinib.pdf. Accessed March **2024**

[12] - Garg, M. K.; Aggrawal, S.; Srivastava, A. Pharmaceutical composition comprising apixaban. **2017**, WO Patent nº 2017163170A1

[13] - *Genetech*. Safety Data Sheet of Erivedge® Capsules (150mg). Page: gene.com/download/pdf/ErivedgeCapsules150mgMSDS.pdf. Accessed March **2024**

[14] - *Hospira a Pfizer company*. Safety Data Sheet of Precedex®. Page: safetydatasheets.pfizer.com/DirectDocumentDownloader/Document?prd=PZ02986~~PDF~~MTR~~HSP~~EN~~PFIZER&DocType=DOC. Accessed March **2024**

[15] - Ciccarelli, M.; Sorriento, D.; Coscioni, E.; Iaccarino, G.; Santulli, G. Endocrinology of the Heart in Health and Disease. Integrated, Cellular, and Molecular Endocrinology of the Heart, *1st Ed*, **2017**. *Chapter 11 - Adrenergic Receptors*, 285-315. ISBN: 978-0-12-803111-7. DOI: 10.1016/c2014-0-04170-6

[16] - Giovannitti, J. A.; Thoms, S. M.; Crawford, J. J. α_2 adrenergic receptor agonists: a review of current clinical applications. *Anesth. Prog.*, **2015**, *62*, 31-38. DOI: 10.2344/0003-3006-62.1.31. PMID: 25849473; PMCID: PMC4389556.

[17] - Kossel, A. Über das Agmatin. *Biol. Chem.*, **2009**, *66*, 257-261. DOI: 10.1515/bchm2.1910.66.3.257

[18] - Mc Pherson, R. The curious stories of drugs with two lives: a new paradigm in drug development. J. R. Soc. Med., **2015**, *108*, 255–258. DOI: 10.1177/0141076815578653, PMCID: PMC4530410, PMID: 25827907

[19] - K.W. Clarke, C.M. Trim, L.W. Hall. Veterinary Anaesthesia, *11th Ed*, **2014**. *Chapter 4 - Principles of sedation, anticholinergic agents, and principles of premedication*, 79-100. ISBN: 978-0-7020-2793-2. DOI: 10.1016/C2009-0-45620-4

[20] - Jnoff, E.; Christophe, B.; Collart, P.; Coloretti, F.; Debeuckelaere, A.; Ryck, M.; Fuks, B.; Genicot, C.; Gillard, M.; Guyaux, M.; Price, N.; Vandergeten, M. C.; Vermeiren, C. Discovery of Selective α_{2C} Adrenergic Receptor Agonists. *ChemMedChem Special Issue: Neuroscience Drug Discovery*, **2012**, *7*, 385-390. DOI: 10.1002/cmdc.201100528

[21] - *Orion Pharma*. Achievements. Page: web.archive.org/web/20130315082255 /http://orion.fi/en/Research-and-developement/Achievements/. Accesses April **2024**

[22] - Virtanen R. Pharmacological profiles of medetomidine and its antagonist, atipamezole. *Acta Vet. Scand. Suppl.*, **1989**, *85*, 29-37. PMID: 2571275.

[23] – Kuusela, E.; Vainio, O.; Kaistinen, A.; Kobylin, S.; Raekallio, M. Sedative, analgesic, and cardiovascular effects of levomedetomidine alone and in combination with dexmedetomidine in dogs. *Am. J. Vet. Res.*, **2001**, *62*, 616-21. DOI: 10.2460/ajvr.2001.62.616. PMID: 11327474

[24] – Virtanen, R. Antinociceptive activity and mechanism of action of detomidine. *J. Vet. Pharmacol. Ther.*, **1986**, *9*, 286-292. DOI: 10.1111/j.1365-2885.1986.tb00043.x

[25] - *Zoetis*. Safety Data Sheet for Domosedan®. Page: zoetis.ca/sds/technical-documents/dormosedan-gel-canadian-english-sds.pdf. Accessed April **2024**

[26] - *Dechra*. Safety Data Sheet for Zenalpha®. Page: dechra-us.com/Files/Files/ProductDownloads/US/07SS-ZEN22006-0622-Zenalpha-Medetomidine-and-Vatinoxan_US-SDS_November2021.pdf. Accessed April **2024**

[27] - Karjalaynen, A. J.; Kurkela, K. O. A. 4-Benzyl- and 4-benzoylimidazole derivatives, processes for their preparation and pharmaceutical compositions comprising the same. **1980**, EP Patent nº 0024829A1

[28] - Karjalainen, A. J.; Virtanen, R. E.; Savolainen, E. J. Optical isomer of an imidazole derivative. **1988**, EP Patent nº 0300652B1

[29] - Reine, I.; Zandersons, A. Method for preparing medetomidine and its salts. **2007**, EP Patent nº 2079706B1

[30] - Ziegler, D. S.; Wei, B.; Knochel, P. Improving the Halogen–Magnesium Exchange by using New Turbo-Grignard Reagents. *Chem. Eur. J.*, **2019**, *25*, 2695-2703. DOI: 10.1002/chem.201803904

[31] - Wei, C.; Kejie, O.; Jianjun, Y. Method for preparing dexmedetomidine. **2009**, CN Patent nº 101921234B

[32] - Bin, L. Y.; Jianhang, W.; Zhifang, Z. Preparation of dexmedetomidine hydrochloride key intermediate. **2010**, CN Patent nº 101805294B

[33] - Thanukrishnan, K.; Balaraman, S. Process for preparation of medetomidine. **2010**, WO Patent nº 2011070069A1

[34] - Doerwald, F. Z.; Kulesza, A.; Elzner, S; Bujok, R.; Wrobel, Z.; Wojciechowski, K. Method for preparation of 2-(2,3-dimethylphenyl)-1-propanal. **2012**, WO Patent nº 2013011156A2

[35] - Doerwald, F. Z.; Kulesza, A.; Elzner, S; Bujok, R.; Wrobel, Z.; Wojciechowski, K. Method for preparation of medetomidine. **2012**, WO Patent nº 2013011155A2

[36] - Doerwald, F. Z.; Kulesza, A.; Elzner, S; Bujok, R.; Wrobel, Z.; Wojciechowski, K. Method for preparation of 2-(2,3-dimethylphenyl)-1-propanal with chloroacetone. **2012**, WO Patent nº 2013011158A2

[37] - Doerwald, F. Z.; Kulesza, A.; Elzner, S; Bujok, R.; Wrobel, Z.; Wojciechowski, K. Method for preparation of 2-(2,3-dimethylphenyl)-1-propanal with chloroacetone. **2012**, WO Patent nº 2013011157A1

[38] - Jürgens, E.; Wucher, B.; Rominger, F.; Törnroos, K. W.; Kunz, D. Selective rearrangement of terminal epoxides into methylketones catalysed by a nucleophilic rhodium–NHC–pincer complex. *Chem. Commun.*, **2015**, *51*, 1897-1900. DOI: 10.1039/c4cc07154a

[39] - Oldenziel, O. H.; Van Leusen, D.; Van Leusen, A. M. A general one-step synthesis of nitriles from ketones using tosylmethyl isocyanide. Introduction of a one-carbon unit. *J. Org. Chem.*, **1977**, *42*, 3114-3118. DOI: 10.1021/jo00439a002

[40] - Alzieu, T.; Lehmann, J.; Naidu, A. B.; Martin, R. E.; Britton, R. Converting oxazoles into imidazoles: new opportunities for diversity-oriented synthesis. *Chem. Commun.*, **2014**, *50*, 1867-1870. DOI: 10.1039/c3cc48467j

[41] - Zacche, M.; Gerli, F.; Gatti, P. A. Process for the resolution of medetomidine and recovery of the unwanted enantiomer. **2013**, US Patent nº 8877941B2

[42] - Yong, X.; Lie, L.; Xuehai, W.; Jie, L.; Yang, L.; Xi, J.; Quanwu, F.; Zhongwen, Y.; Qiang, X.; Hua, T.; Jing, Y. Prepare the method for dexmedetomidine. **2013**, CN Patent nº 103664788B

[43] - Aiwei, W.; Wenjuan, D.; Bihua. New method for preparing dexmedetomidine hydrochloride. **2013**, CN Patent nº 103694175A

[44] - Heng, M. Y.; Lai, J.; Zhou, Z. A kind of dexmedetomidine pharmaceutical co-crystals and preparation method thereof. **2014**, CN Patent nº 103880753B

[45] - Daofei, H.; Jin, Z.; Dongming, L.; Ji, X. New method for preparing dexmedetomidine hydrochloride key intermediate. **2014**, CN Patent nº 104447562A

[46] - Honghai, S.; Zhicun, S.; Haiping, H.; Chao, Z. Method for preparing medetomidine intermediate. **2013**, WO Patent nº 2015078235A1

[47] – Kui, X.; Li, L. Medetomidine industrialization method for splitting. **2014**, CN Patent nº 104151249B

[48] - Fei, S. S.; Xiulian, L.; Zhenxin, D.; Zuopeng, H.; Pin, S.; Zhongjing, L. Method for preparing dexmedetomidine hydrochloride. **2015**, CN Patent nº 105175339A

[49] - Dan, Y.; Zhenglin, D.; Zhen, S.; Zhen, X.; Yuxi, L.; Long, C. Method for preparing high-purity dexmedetomidine hydrochloride crystal from high-purity intermediate crystal. **2015**, CN Patent nº 105175340A

[50] - Shifeng, M.; Xiaofei, W.; Haibo, Z.; Changquan, Y; Shikang, W.; Yuefan, Y.; Chen, H.; Wu, L.; Xianfeng, L. Method for preparing dexmedetomidine hydrochloride key intermediate. **2015**, CN Patent nº 105254567A

[51] - Dong, W.; Liang, C.; Chen, D.; Chao, H.; Weijuan, P.; Ming, L.; Guisen, Z. Dexmedetomidine hydrochloride crystal form C and preparation method thereof. **2016**, CN Patent nº 105481774A

[52] - Eklund, L.; Eek, M.; Ekambaram, R.; Maasalu, A. Processes for the preparation of compounds, such as 3-arylbutanals, useful in the synthesis of medetomidine. **2019**, WO Patent nº 2016120635A1

[53] - Xianshan, H.; Zhian, W.; Yan, X.; Yongjiang, C. A kind of method for preparing Dexmedetomidine and its intermediate. **2016**, CN Patent nº 105884691B

[54] - Xianshan, H.; Junyan, W.; Zhian, W.; Xinguang, Z. A kind of preparation method of dexmedetomidine. **2016**, CN Patent nº 106083724A

[55] - Wakefield, B. J. Grignard Reagents — New Developments. *Appl. Organomet. Chem.*, **2000**, *14*, 396. DOI: 10.1002/1099-0739(200007)14:7<396::AID-AOC3>3.0.CO;2-8. A review from book ISBN: 0-471-99908-3

[56] - Tilstam, U.; Weinmann, H. Activation of Mg Metal for Safe Formation of Grignard Reagents on Plant Scale. *Org. Process Res. Dev.*, **2002**, *6*, 906-910. DOI: 10.1021/op025567

[57] - Allian, A. D.; Shah, N. P.; Ferretti, A. C.; Brown, D. B.; Kolis, S. P.; Sperry, J. B. Process Safety in the Pharmaceutical Industry—Part I: Thermal and Reaction Hazard Evaluation Processes and Techniques. *Org. Process Res. Dev.*, **2020**, *24*, 2529-2548. DOI: 10.1021/acs.oprd.0c00226

[58] - Pastre, J.; Wörsdörfer, U.; Keller, A.; Hungerbühler, K. Comparison of different methods for estimating TMR_{ad} from dynamic DSC measurements with ADT_{24} values obtained from adiabatic Dewar experiments. *J. Loss Prev. Process Ind.*, **2000**, *13*, 7-17. DOI: 10.1016/S0950-4230(99)00061-3

[59] - Allian, A. D.; Shah, M. P.; Ferretti, A. C.; Brown, D. B.; Kolis, S. P.; Sperry, J. B. Process Safety in the Pharmaceutical Industry—Part I: Thermal and Reaction Hazard Evaluation Processes and Techniques. *Org. Process Res. Dev.*, **2020**, *24*, 2529-2548. DOI: 10.1021/acs.oprd.0c00226

[60] – Stoessel, F. Thermal Safety of Chemical Processes: Risk Assessment and Process Design, *1st Ed*, **2020**. ISBN: 9783527339211. DOI: 10.1002/9783527696918

[61] – (A) - Majer, V.; Svoboda, V.; Kehiaian, H. V. Enthalpies of vaporization of organic compounds : a critical review and data compilation, **1985**, 300. ISBN: 9780632015290
(B) – Calculation was performed by the relation between reaction heat and enthalpy of vaporization to know the amount of solvent boiled

[62] - *US Food and Drug Administration*. Drug Master Files: Guidelines. Page: fda.gov/drugs/guidances-drugs/drug-master-files-guidelines. Accessed April **2024**

[63] - *European Medicines Agency*. ICH M4 Common technical document (CTD) for the registration of pharmaceuticals for human use - organisation of CTD - Scientific guideline. Page: ema.europa.eu/en/ich-m4-common-technical-document-ctd-registration-pharmaceuticals-human-use-organisation-ctd-scientific-guideline. Accessed April **2024**

[64] - Sharghi, H.; Hosseini, M. Solvent-Free and One-Step Beckmann Rearrangement of Ketones and Aldehydes by Zinc Oxide. *Synth.*, **2002**, *8*, 1057-1060. DOI: 10.1055/s-2002-31964

[65] - Dowson, G. R. M.; Dimitriou, I.; Owen, R. E.; Reed, D. G.; Allen, R. W. K.; Styring, P. Kinetic and economic analysis of reactive capture of dilute carbon dioxide with Grignard reagents. *Faraday Discuss.*, **2015**, *183*, 47-65. DOI: 10.1039/C5FD00049A

[66] - Nobe, Y.; Arayama, K.;Urabe, H. Air-Assisted Addition of Grignard Reagents to Olefins. A Simple Protocol for a Three-Component Coupling Process Yielding Alcohols. *J. Am. Chem. Soc.*, **2005**, *127*, 18006-18007. DOI: 10.1021/ja055732b

[67] – Osborn, J. A.; Jardine, F. H.; Young, J. F.; Wilkinson, G. The preparation and properties of tris(triphenylphosphine)halogenorhodium(I) and some reactions thereof including catalytic homogeneous hydrogenation of olefins and acetylenes and their derivatives. *J. Chem. Soc.*, **1966**, 1711-1732. DOI: 10.1039/J19660001711

[68] - Van Leeuwen, P. W. N. M. Homogeneous Catalysis. Understanding the Art, *1st Ed*, **2004**. *Chapter 4: Hydrogenation*, 75-101. ISBN:978-1-4020-1999-9. DOI: 10.1007/1-4020-2000-7

[69] - Halpern, J. Mechanism and Stereoselectivity of Asymmetric Hydrogenation. *Science*, **1982**, *217*, 401-407. DOI: 10.1126/science.217.4558.401

[70] - Brown, J. M.; Chaloner, P. A. The mechanism of asymmetric homogeneous hydrogenation. Rhodium(I) complexes of dehydroamino acids containing asymmetric ligands related to bis(1,2-diphenylphosphino)ethane. *J. Am. Chem. Soc.*, **1980**, *102*, 3040-3048. DOI: 10.1021/ja00529a029

[71] - Konkol, M.; Wrobel, W.; Bicki, R.; Gołębiowski, A. The Influence of the Hydrogen Pressure on Kinetics of the Canola Oil Hydrogenation on Industrial Nickel Catalyst. *Catalysts*, **2016**, 6 (*4*), 55. DOI: 10.3390/catal6040055

[72] - Singh, N.; Lee, M.; Akhade, S. A.; Cheng, G.; Camaioni, D. M.; Gutierrez, O. Y.; Glezakou, V. A.; Rousseau, R.; Lercher, J. A.; Campbell, C. T. Impact of pH on Aqueous-Phase Phenol Hydrogenation Catalyzed by Carbon-Supported Pt and Rh. *ACS Catal.*, **2019**, *9*, 1120-1128. DOI: 10.1021/acscatal.8b04039

[73] – Zhong, H. Cobalt-Catalyzed Asymmetric Hydrogenation of Alkenes: Catalyst Developments and Mechanistic Investigations, *Princeton University NJ*, **2021**. Page: dataspace.princeton.edu/handle/88435/dsp01n870zt88w. A Doctoral Dissertation

[74] - Verendel, J. J.; Pamies, O.; Dieguez, M.; Andersson, P. G. Asymmetric Hydrogenation of Olefins Using Chiral Crabtree-type Catalysts: Scope and Limitations. *Chem. Rev.*, **2014**, *114*, 2130-2169. DOI: 10.1021/cr400037u

[75] - Pamies, O.; Dieguez, M.; Andersson, P. G. Asymmetric Hydrogenation of Minimally Functionalised Terminal Olefins: An Alternative Sustainable and Direct Strategy for Preparing Enantioenriched Hydrocarbons. *Chem. Eur. J.*, **2010**, *16*, 14232-14240. DOI: 10.1002/chem.201001909

[76] - Yan, Y.; RajanBabu, T. V. Ligand Substituent Effects on Asymmetric Induction. Effect of Structural Variations of the DIOP Ligand on the Rh-Catalyzed Asymmetric Hydrogenation of Enamides. *Org. Lett.*, **2000**, *2*, 4137-4140. DOI: 10.1021/ol006591f

[77] - Etayo, P.; Vidal-Ferran, A. Rhodium-catalysed asymmetric hydrogenation as a valuable synthetic tool for the preparation of chiral drugs. *Chem. Soc. Rev.*, **2013**, *42*, 728-754. DOI: 10.1039/C2CS35410A

[78] - Biosca, M.; Magre, M.; Pamies, O.; Dieguez, M. Asymmetric Hydrogenation of Disubstituted, Trisubstituted, and Tetrasubstituted Minimally Functionalized Olefins and Cyclic β-Enamides with Easily Accessible Ir–P,Oxazoline Catalysts. *ACS Catal.*, **2018**, *8*, 10316-10320. DOI: 10.1021/acscatal.8b03170

[79] - Duan, Z.; Wang, L.; Song, X.; Hu, X.; Zheng, Z. Enantioselective synthesis of optically active alkylphosphonates via Rh-catalyzed asymmetric hydrogenation of β-substituted α,β-unsaturated phosphonates. *Tetrahedron: Asymmetry*, **2012**, *23*, 508-514. DOI: 10.1016/j.tetasy.2012.03.024

[80] - Iacobini, G. P.; Porterb, D. W.; Shipman, M. Chemo- and enantioselective Rh-catalysed hydrogenation of 3-methylene-1,2-diazetidines: application to vicinal diamine synthesis. *Chem. Commun.*, **2012**, *48*, 9852-9854. DOI: 10.1039/C2CC35445D

[81] - Lölsberg, W.; Werle, S.; Neudörfl, J.; Schmalz, H. An Enantioselective Total Synthesis of Helioporins C and E. *Org. Lett.*, **2012**, *14*, 5996-5999. DOI: 10.1021/ol302898h

[82] - Landert, H.; Spindler, F.; Wyss, A.; Blaser, H.; Pugin, B.; Ribourduoille, Y.; Gschwend, B.; Ramalingam, B.; Pfaltz, A. Chiral Mixed Secondary Phosphine-Oxide–Phosphines: High-Performing and Easily Accessible Ligands for Asymmetric Hydrogenation. *Angew. Chem.*, **2010**, *49*, 6873-6876. DOI: 10.1002/anie.201002225

[83] - Hayashida, Y.; Umeda, Y. Method for producing imidazole derivative. **2016**, JP Patent nº 2018039757A

[84] - Gutmann, B.; Cantillo, D.; Kappe, C. O. Continuous-Flow Technology-A Tool for the Safe Manufacturing of Active Pharmaceutical Ingredients. *Angew. Chem.*, **2015**, *54*, 6688-6728. DOI: 10.1002/anie.201409318

[85] - Johnson, M. D.; May, S. A.; Calvin, J. R.; Remacle, J.; Stout, J. R.; Diseroad, W. D.; Zaborenko, N.; Haeberle, B. D.; Sun, W.; Miller, M. T.; Brennan, J. Development and Scale-Up of a Continuous, High-Pressure, Asymmetric Hydrogenation Reaction, Workup, and Isolation. *Org. Process Res. Dev.*, **2012**, *16*, 1017-1038. DOI: 10.1021/op200362h

[86] - *PubChem*. Tetrafluoroboric acid. Page: pubchem.ncbi.nlm.nih.gov/compound/Tetrafluoroboric-acid#section=Dissociation-Constants. Accessed April **2024**

[87] - Trummal, A.; Lipping, L.; Kaljurand, I.; Koppel, I. A.; Leito, I. Acidity of Strong Acids in Water and Dimethyl Sulfoxide. *J. Phys. Chem. A*, **2016**, *120*, 3663-3669. DOI: 10.1021/acs.jpca.6b02253

[88] - Olah, G. A.; Prakash, G. K. S.; Molnar, A.; Sommer, J. Superacid Chemistry, *2nd Ed*, **2009**. ISBN: 978-0-471-59668-4

[89] - Petrucci, R. H.; Harwood, W. S.; Herring, G. F.; Madura, J. D. General chemistry : principles and modern applications, *9th Ed*, **2007**. ISBN: 9780131493308

[90] - Tolomeu, H. V.; Fraga, C. A. M. Imidazole: Synthesis, Functionalization and Physicochemical Properties of a Privileged Structure in Medicinal Chemistry. *Molecules*, **2023**, *28*, 838. DOI: 10.3390/molecules28020838

[91] - Zhang, H.; Wu, W.; Mo, Y. Tautomerism of protonated imidazoles: A perspective from ab initio valence bond theory. *Tetrahedron*, **2018**, *74*, 4791-4798. DOI: 10.1016/j.tet.2018.07.037

[92] - Paliwoda, D.; Dziubek, K. F.; Katrusiak, A. Imidazole Hidden Polar Phase. *Cryst. Growth Des.*, **2012**, *12*, 4302–4305. DOI: 10.1021/cg300852t

[93] – Spek, A. L. Structure validation in chemical crystallography. *Acta Crystallogr. D. Biol. Crystallogr.*, **2009**, 65, 148-55. DOI: 10.1107/S090744490804362X

[94] - Akkaraju, H.; Tatia, R.; Mane, S. S.; Khade, A. B.; Dengale, S. J. A comprehensive review of sources of nitrosamine contamination of pharmaceutical substances and products. *Regul. Toxicol. Pharmacol.*, **2023**, *139*, 105355. DOI: 10.1016/j.yrtph.2023.105355

[95] - López-Rodríguez, R.; McManus, J. A.; Murphy, N. S.; Ott, M. A.; Burns, M. J. Pathways for N-Nitroso Compound Formation: Secondary Amines and Beyond. *Org. Process Res. Dev.*, **2020**, *24*, 1558-1585. DOI: 10.1021/acs.oprd.0c00323

[96] - Ashworth, I. W.; Blanazs, A.; Byrne, J. J.; Dirat, O.; Fennell, J. W.; Kuhl, N.; Wells, S. L.; Whiting, M. P. Approaches and Considerations for the Investigation and Synthesis of N-Nitrosamine Drug Substance-Related Impurities (NDSRIs). *Org. Process Res. Dev.*, **2023**, *27*, 1784-1791. DOI: 10.1021/acs.oprd.3c00084

[97] - Chaudhary, P.; Gupta, S.; Muniyappan, N.; Sabiah, S.; Kandasamy, J. An efficient synthesis of N-nitrosamines under solvent, metal and acid free conditions using tert-butyl nitrite. *Green Chem.*, **2016**, *18*, 2323-2330. DOI: 10.1039/C5GC02880A

[98] - Chaudhary, P.; Gupta, S.; Muniyappan, N.; Sabiah, S.; Kandasamy, J. Regioselective Nitration of N-Alkyl Anilines using tert-Butyl Nitrite under Mild Condition. *J. Org. Chem.*, **2019**, *84*, 104–119. DOI: 10.1021/acs.joc.8b02377

[99] - Marles, A.; López, R.; Bessa, S.; Galan, C. Ultra-high-speed liquid chromatography combined with mass spectrometry detection analytical methods for the determination of nitrosamine drug substance-related impurities. *J. Sep. Sci.*, **2023**, *46*. DOI: 10.1002/jssc.202300125

[100] - Liu, D.; Zhang, X. Practical P-Chiral Phosphane Ligand for Rh-Catalyzed Asymmetric Hydrogenation. *Eur. J. Org. Chem.*, **2005**, *4*, 646–649. DOI: 10.1002/ejoc.200400690

Chapter 5.
Experimental Methodologies

Chapter 5. Experimental methodologies

Because in many cases the procedures have consisted of the optimizations of various reaction conditions, usually a general experimental procedure will be shown. Only most relevant and representative methodologies will be reported for each synthetized compound.

The purity of solvents and reagents used for the synthesis of compounds have not been considered if its purity is higher than 98 %. Solvents and reagents used for chromatography have been previously filtered through a 0,2 µm filter and degassed.

5.1 Analytical procedures

5.1.1 Ultra-High Performance Liquid Chromatography

Ultra-High Performance Liquid Chromatography (UHPLC) and **Ultra-High Performance Liquid Chromatography coupled with Mass Spectrometry (UHPLC-MS)** were carried out with a Waters ACQUITY™ UPLC™ H-Class equipped with a photodiode array (PDA) detector ACQUITY™ UPLC™ PDA and a single quadrupole mass detector ACQUITY™ QDa™ with an integrated electrospray ionization (ESI) probe. The mobile phase is a gradient from 5 % of ACN to 95 % over 12 minutes and 25 mM ammonium formate at pH 4,8. The stationary phase was a BEH C_{18} column 100 mm x 2,1 mm x 1,7 µm. This equipment was used to study reaction kinetics and coupled with the MS module, to identify new molecules or impurities along the project.

5.1.2 High Performance Liquid Chromatography

High Performance Liquid Chromatography (HPLC) was carried out with a Waters ACQUITY™ UPLC™ H-Class equipped with a Tungsten ultraviolet-visible (TUV) detector ACQUITY™ TUV. The mobile phase is 15 % of ACN and 85 % of 0,03 M phosphate buffer at pH 7. The stationary phase is a Chiralpak AGP column 150 mm x 4,0 mm x 5 µm. This equipment was used to determine enantiomeric purities of the samples during this project. The analytical method used was validated and the uncertainty obtained was ± 0,006 %. The equipment reported the results with two decimals and rounding the uncertainty, the results was ± 0,01 %. The conversions and enantiomeric excesses in this project are given with one decimal to assure the accuracy and the precision of the reported results.

5.1.3 High-Resolution Mass spectrometry

High-Resolution Mass spectrometry (HRMS) was performed with a Waters ACQUITY™ UPLC™ H-Class equipped with a photodiode array (PDA) detector ACQUITY™ UPLC™ PDA in tandem with Time-of-Flight High-Resolution Mass spectrometer Xevo™ G2 ToF equipped with an electrospray ionization (ESI) probe LockSpray. The mobile phase is a gradient from 5 % of ACN to 95 % and 25 mM ammonium formate at pH 4,8. The stationary phase is an ACQUITY™ UPLC™ HSS T3 column 100 mm x 2,1 mm x 1,8 µm. This equipment was used to characterize molecules obtained its molecular weight with precision.

5.1.4 Nuclear Magnetic Resonance

Nuclear Magnetic Resonance (NMR) spectra were obtained with a BRUKER 600 UltraShield™ of 14T magnetic field equipped with AVANCE II console and BCU II unit for sample temperature control. The spectra collection has been conducted by the *Servei de Ressonància Magnètica Nuclear (SeRMN)* at *Universitat Autònoma de Barcelona (UAB)*. This equipment was used to characterize molecules by running ^{1}H, ^{13}C, COSY, HSQC, HMBC, NOE and NOESY experiments at 600 MHz.

5.1.5 Differential Scanning Calorimetry

Differential scanning calorimetry (DSC) thermograms were obtained with a Mettler Toledo Differential Scanning Calorimeter DSC 882e using gold Crucibles from 30 ºC to 400 ºC at 10 ºC/min rate. This equipment was used to study the safety of the process by characterizing the possible temperatures of degradation of the different molecules or reaction mixtures.

5.1.6 Potentiometric titration

Potentiometric titration (Assay) was carried out with a Mettler Toledo T50 titrator equipped with an Inmotion Flex Autosampler. This equipment was used to determine the purity of the intermediates synthetized along the project.

5.1.7 Single Crystal X-Ray Diffraction

Single Crystal X-Ray Diffraction (SC-XRD) structure were obtained with a Bruker SMART-APEX diffractometer using a Mo Kα of λ = 0,71073 Å. A SADABS empirical absorption correction was applied for the area detector data. The structures had been resolved by SHELXS-86 direct methods and had been refined using least square methods in the complete matrix using all reflexions (SHELXL-2016). The non-hydrogen atoms have been tuned with anisotropic displacement parameters. Hydrogen atoms bonded to carbon atoms have been placed in positions calculated with isotropic displacement parameters set to 1,5 (CH_3) or 1,2 (CH_2 and CH) times the U_{eq} of the corresponding carbon atoms. Hydrogen bonded to a nitrogen atom has been located on a difference Fourier map and tuned with an isotropic shift parameter. The analysis and the data processing have been conducted by the *Servei de Difracció de Raigs X (SDRX)* at *Universitat Autònoma de Barcelona (UAB)*. This equipment was used to determine the structure of some compound synthetized along the project.

5.1.8 Powder X-Ray Diffraction

Powder X-Ray Diffraction (PXRD) difractograms were obtained with a Panalytical X'Pert Powder diffractometer equipped with a Cu-tube (λ = 1,5419 Å), graphite secondary monochromator and a PIXcel^{1D} detector. The analysis and the data processing have been conducted by the *Servei de Difracció de Raigs X (SDRX)* at *Universitat Autònoma de Barcelona (UAB)*. This equipment was used to determine the crystalline properties of some compound synthetized along the project.

5.1.9 Head-Space Gas Chromatography

Head-Space Gas Chromatography (HS-GC) was carried out with an Agilent 7890B equipped with a Gerstel external injector. The carrier gas was He which flows at 2 mL/min from 30 ºC to 210 ºC in a 30 ºC/min of slope with 1,5 split ratio and 30 min of incubation at 60 ºC. The stationary phase is a RTx-1301 column 30 m x 0,53 mm x 3,0 µm. This equipment was used to quantify the amount of volatile components into a sample, generally, residual solvents or volatile impurities.

5.2 Synthesis and characterization of ketone 21 and its related compounds

5.2.1 Synthesis of ketone **21**

37,60 g (1,6 mol; 3,6 eq) of Magnesium turnings were suspended in 1,1 L (27,5 V) of THF. The resulting suspension was stirred and inertized with nitrogen. To the mixture was added 30 mL (d. 0,866 g/mL; 25,97 g; 1 M; 30 mmol; 0,06 eq) of DIBALH in THF and bubbling was observed.

At the same time, a solution of 150 mL (d. 1,365 g/mL; 204,76 g; 1,1 mol; 1,3 eq) of **33** in 125 mL (3 V) of THF was prepared. Then, 20 mL of the solution was added to the magnesium suspension. Reaction heat was checked as the initiation of the reaction and the rest of the **33** solution was added dropwise. The mixture was heated to 60 – 65 ºC and maintained for 1 h. Then, the mixture was cooled to 20 – 25 ºC and maintained under nitrogen.

Then, 40 g (430 mmol; 1 eq) of **19** was suspended in 250 mL (6 V) of THF. The suspension was cooled to -5 ºC the **20** solution was added. Then, the mixture was maintained at 0 ºC for 1 h.

A solution of 96 mL (d. 1,82 g/mL; 172 g; 1,7 mol; 4 eq) of H_2SO_4 in 400 mL (10 V) of H_2O was prepared and added dropwise to the reaction mixture. The mixture turned yellow over 5 h. The mixture turned yellow over 5h. The mixture was filtered and the cake washed with 40 mL (1 V) of THF twice.

To mother liquors, 350 mL (9 V) of *n*-heptane and 250 mL (6 V) of H_2O were added and phases were separated. The lower aqueous phase was washed with 350 mL (9 V) of *n*-heptane and phases were separated. To the aqueous phase 400 mL (10 V) of H_2O was added.

The aqueous phase was cooled to 0 – 5 ºC and aqueous NH_3 (d. 0,904 g/mL; 20,5 wt.%) was added to pH 10. At approximately pH 3 some turbulence was observed and at pH 7 the precipitate was abundant. The suspension was maintained at 0 – 5 ºC for at least 1 h.

The product was recovered by filtration and the solid was washed with 500 mL (12,5 V) of H_2O 4 times and then with 300 mL (7,5 V) of *n*-heptane 2 times. The solid was dried

under vacuum at 50 ºC for at least 16 h to give **21** as an off-white powder (74,41 g; 87 %).

NMR data for 21:

^{1}H NMR (600 MHz, DMSO-d_6): δ 12,90 (br s; 1H; NH); 7,91 (br s; 1H; N=CH-N); 7,50 (br s; 1H; C=CH-N); 7,30 (d; 1H; $C_{Ar}H$; ^{3}J = 7,1 Hz); 7,22 (d; 1H; $C_{Ar}H$; ^{3}J = 7,1 Hz); 7,18 (t; 1H; $C_{Ar}H$; ^{3}J = 7,1 Hz); 2,29 (s; 3H; CH_3); 2,14 (s; 3H; CH_3).

^{13}C NMR (600 MHz, DMSO-d_6): δ 193,8 (1C; CO); 140,3 (1C; C_{Ar}); 139,5 (1C; C-C=CH); 137,2 (1C; C_{Ar}); 135,8 (1C; N=CH-N); 134,2 (1C; C_{Ar}); 131,5 (1C; $C_{Ar}H$); 125,9 (1C; $C_{Ar}H$); 125,9 (1C; C=CH-N); 125,4 (1C; $C_{Ar}H$); 20,2 (1C; CH_3); 16,6 (1C; CH_3).

MS data for 21:

UHPLC-HRMS (ESI-TOF): *m/z* = 201,1024 (201,1022 calculated) $[M+H]^+$; *m/z* = 199,0875 (199,0877 calculated) $[M-H]^-$ ($C_{12}H_{12}N_2O$).

5.2.2 Synthesis of ketone **57**

5 g (54 mmol; 1 eq) of **19** was suspended in 250 mL (50 V) of THF. The suspension was cooled to -5 ºC and added dropwise 70 mL (d. 0,975 g/mL; 71,62 g; 2 M; 140 mmol; 2,6 eq) iPrMgCl in THF. At the end of the addition, the suspension was maintained 0 ºC for 2 h.

A solution of 12 mL (d. 1,82 g/mL; 21,5 g; 214,85 mmol) of H_2SO_4 in 50 mL (10 V) of H_2O was prepared and added dropwise to the reaction mixture. The mixture turned yellow over 5 h. After the reaction was completed, aqueous NH_3 (d. 0,904 g/mL; 20,5 wt.%) was added to pH 7 and phases separated.

The aqueous phase was washed with 10 mL of EtOAc (2 V) twice and the combined organic phases were washed with a previously prepared solution of 15,44 g of NaCl (264 mmol; 4,9 eq) in 26 mL of H_2O (5,15 V). The resulting organic phase was distilled under vacuum to dryness and charged 25 mL of *n*-heptane (5 V).

The product was recovered by filtration and the solid was washed with 5 mL (1 V) of *n*-heptane twice. The solid was dried under vacuum at 40 ºC for 16 h to give **57** as an off-white powder (4, 87 g; 65 %).

NMR data for 57:

^{1}H NMR (600 MHz, $CDCl_3$): δ 12,62 (br s; 1H; NH); 8,04 (s; 1H; N=CH-N); 7,87 (s; 1H; C=CH-N); 3,36 (Hept; 1H; CH; ^{3}J = 7,0 Hz); 1,24 (d; 6H; CH_3; ^{3}J = 7,0 Hz).

^{13}C NMR (600 MHz, $CDCl_3$): δ 197,5 (1C; CO); 138,6 (1C; N=CH-N); 135,1 (1C; CO-C=CH); 128,8 (1C; C=CH-N); 36,9 (1C; CH); 19,3 (1C; CH_3).

MS data for 57

UHPLC-HRMS (ESI-TOF): *m/z* = 139,0859 (139,0866) calculated) $[M+H]^+$; *m/z* = 137,0717 (137,0720 calculated) $[M-H]^-$ ($C_7H_{10}N_2O$).

5.2.3 Synthesis of imine **59**

9,40 g (0,4 mol; 3,6 eq) of Magnesium turnings were suspended in 275 mL (27,5 V) of THF. The resulting suspension was stirred and inertized with nitrogen. To the mixture was added 7,5 mL (d. 0,866; 6,50 g; 1 M; 7,5 mmol; 0,06 eq) of DIBALH in THF and bubbling was observed.

At the same time, a solution of 37,5 mL (d. 1,365 g/mL; 51,19 g; 275 mmol; 1,3 eq) of **33** in 30 mL (3 V) of THF was prepared. Then, 10 mL of the solution was added to the magnesium suspension. Reaction heat was checked as the initiation of the reaction and the rest of the **33** solution was added dropwise. The mixture was heated to 60 – 65 ºC and maintained for 1 h. Then, the mixture was cooled to 20 – 25 ºC and maintained under nitrogen.

Then, 10 g (107,5 mmol; 1 eq) of **19** was suspended in 60 mL (6 V) of THF. The suspension was cooled to -5 ºC the **20** solution was added. Then, the mixture was maintained at 0 ºC for 1 h. After the reaction was completed, 200 mL (20 V) of MeOH was added and the resulting suspension was filtered. The recovered solid was suspended in 500 mL (50 V) of H_2O and the pH was adjusted to 7 with HCl (37 wt. %; d. 1,19 g/mL). The suspension was stirred for 10 min.

The product was recovered by filtration and the solid was washed with 50 mL (5 V) of *n*-heptane twice. H_2O twice. The solid was dried at 40 ºC under vacuum for 16 h to give **57** as an off-white powder (18,21 g; 85 %).

MS data for 59

UHPLC-HRMS (ESI-TOF): *m/z* = 200,1173 (200,1182 calculated) $[M+H]^+$; *m/z* = 198,1031 (198,1026 calculated) $[M-H]^-$ ($C_{12}H_{13}N_3$).

5.2.4 Synthesis of imidazole **19**

7 g (73 mmol; 1 eq) of aldehyde **50** and 5,2 g (73 mmol; 1 eq) of hydroxylamine hydrochloride were suspended in 14 mL (2 V) of pyridine. The mixture was heated to 60 – 65 ºC and maintained for 90 min. After the reaction was completed, 12,7 mL (d. 1,080 g/mL; 13,7 g; 134 mmol; 1,8 eq) of acetic anhydride were added and heated to 70 – 85 ºC. The mixture was maintained for 2 h and cooled to 20 – 25 ºC. The mixture was distilled under vacuum to dryness.

To the residue, 14,6 mL (2,1 V) of H_2O, 21 mL (3 V) of EtOAc and 9,3 mL of NaOH (30 wt. %; d. 1,330 g/mL; 12,4 g; 95 mmol, 1,3 eq) were added and phases separated. The aqueous phase was washed with 21 mL (3 V) of EtOAc twice. The combined organic phases were distilled under vacuum to dryness. To the residue, 28 mL (4 V) of *n*-heptane were added.

The solid was recovered by filtration and washed with a 14 mL (2 V) of a 1:1 mixture of *n*-heptane / EtOAc, 14 mL (2 V) of a mixture of 4:1 mixture *n*-heptane / EtOAc and 14 mL (2 V) of *n*-heptane. The solid was dried at 40 ºC under vacuum for 16 h to give **19** as a white to yellowish powder (6,35 g; 94 %).

NMR data for 19

^{1}H NMR (600 MHz, DMSO-d_6): δ 13,00 (br s; 1H; NH); 8,09 (s; 1H; N=CH-N); 7,90 (s; 1H; C=CH-N).

^{13}C NMR (600 MHz, DMSO-d_6): δ 138,5 (1C; C=CH-N); 127,5 (1C; N=CH-N); 116,4 (C-C=C); 112,1 (1C; CN).

MS data for 19

UHPLC-HRMS (ESI-TOF): *m/z* = 94,0403 (94,0400 calculated) $[M+H]^+$; *m/z* = 92,0249 (92,0243 calculated) $[M-H]^-$ ($C_4H_3N_3$).

5.2.5 Synthesis of aldoxime **51**

7 g (73 mmol; 1 eq) of aldehyde **50** and 5,2 g (73 mmol; 1 eq) of hydroxylamine hydrochloride were suspended in 14 mL (2 V) of pyridine. The mixture was heated to 60 – 65 ºC and maintained for 90 min. After the reaction was completed, the mixture was distilled under vacuum to dryness.

To the residue, 14,6 mL (2,1 V) of H_2O, 21 mL (3 V) of EtOAc and 9,3 mL (30 wt. %; d. 1,330 g/mL; 12,4 g; 95 mmol, 1,3 eq) were added and phases separated. The aqueous phase was washed with 21 mL (3 V) of EtOAc twice. The combined organic phases were distilled under vacuum to dryness. To the residue, 28 mL (4 V) of *n*-heptane were added.

The solid was recovered by filtration and washed with a 14 mL (2 V) of a 1:1 mixture of *n*-heptane / EtOAc, 14 mL (2 V) of a mixture of 4:1 mixture *n*-heptane / EtOAc and 14 mL (2 V) of *n*-heptane. The solid was dried at 40 ºC under vacuum for 16 h to give **51** as a white powder (5,45g; 67 %)

NMR data for 51

^{1}H NMR (600 MHz, DMSO-d_6): δ 12,38 (br s; 1H; NH); 11,43 (br s; 1H; OH); 7,80 (br s; 1H; CHN); 7,72 (s; 1H; N=CH-N); 7,42 (s; 1H; C=CH-N).

^{13}C NMR (600 MHz, DMSO-d_6): δ 141,7 (1C; C=CH-N); 135,7 (1C; N=CH-N); 132,4 (1C; C-C=C); 121,9 (1C; CHN).

MS data for 51

UHPLC-HRMS (ESI-TOF): *m/z* = 112,0513 (112,0505 calculated) $[M+H]^+$; *m/z* = 94,0403 (94,0400 calculated) $[M+H-H_2O]^+$; *m/z* = 110,0346 (110,0349 calculated) $[M-H]^-$ ($C_4H_5N_3O$).

5.2.6 Synthesis of amide **18**

7 g (73 mmol; 1 eq) of aldehyde **50** and 5,2 g (73 mmol; 1 eq) of hydroxylamine hydrochloride were suspended in 14 mL (2 V) of pyridine. The mixture was heated to 60 – 65 ºC and maintained for 90 min. After the reaction was completed, the mixture was distilled under vacuum to dryness.

To the residue, 14,6 mL (2,1 V) of H_2O and 7,9 mL (37 wt. %; d. 1,190 g/mL; 9,37 g; 95 mmol; 1,3 eq) of HCl were added and heated to 60 – 65 ºC for 2 h. The mixture was cooled to 20 – 25 ºC and 21 mL (3 V) of EtOAc and 18,6 mL (30 wt. %; d. 1,330 g/mL; 24,8 g; 190 mmol, 2,6 eq) were added. The phases were separed and the aqueous phase was washed with 21 mL (3 V) of EtOAc twice. The combined organic phases were distilled under vacuum to dryness. To the residue, 28 mL (4 V) of *n*-heptane were added.

The solid was recovered by filtration and washed with a 14 mL (2 V) of a 1:1 mixture of *n*-heptane / EtOAc, 14 mL (2 V) of a mixture of 4:1 mixture *n*-heptane / EtOAc and 14 mL (2 V) of *n*-heptane. The solid was dried at 40 ºC under vacuum for 16 h to give **18** as a brownish powder (5,98 g; 74 %).

NMR data for 18

^{1}H NMR (600 MHz, DMSO-d_6): δ 12,50 (br s; 1H; NH); 7,71 (s; 1H; N=CH-N); 7,62 (br s; 1H; C=CH-N); 7,43 + 7,13 (br s; 2H; NH_2).

^{13}C NMR (600 MHz, DMSO-d_6): δ 164,6 (1C; $CONH_2$); 136,3 (1C; N=CH-N); 136,2 (1C; C=CH-N); 120,2 (1C; CO-C=CH).

MS data for 18

UHPLC-HRMS (ESI-TOF): *m/z* = 112,0513 (112,0505 calculated) $[M+H]^+$; *m/z* = 95,0233 (95,0240 calculated) $[M+H-NH_3]^+$; *m/z* = 110,0346 (110,0349 calculated) $[M-H]^-$ ($C_4H_5N_3O$).

5.2.7 Characterization of aryl bromide **33**

Colorless transparent liquid

NMR data for 33

^{1}H NMR (600 MHz, $CDCl_3$): δ 7,43 (d; 1H; $C_{Ar}H$; ^{3}J = 7,6 Hz); 7,11 (d; 1H; $C_{Ar}H$; ^{3}J = 7,6 Hz); 6,97 (t; 1H; $C_{Ar}H$; ^{3}J = 7,6 Hz); 2,40 (s; 3H; CH_3); 2,36 (s; 3H; CH_3).

^{13}C NMR (600 MHz, $CDCl_3$): δ 138,5 (1C; C_{Ar}); 136,2 (1C; C_{Ar}); 130,3 (1C; $C_{Ar}H$); 128,9 (1C; $C_{Ar}H$); 126,8 (1C; $C_{Ar}H$); 125,6 (1C; $C_{Ar}Br$); 21,3 (1C; CH_3); 19,4 (1C; CH_3).

MS data for 33

UHPLC-HRMS (ESI-TOF): *m/z* = 105,0703 (105,0699 calculated) $[M+H-HBr]^+$ (C_8H_9) from (C_8H_9Br).

5.2.8 Characterization of phenol **62**

White to yellowish crystalline solid

NMR data for 62

^{1}H NMR (600 MHz, $CDCl_3$): δ 7,00 (t; 1H; $C_{Ar}H$; ^{3}J = 7,6 Hz); 6,87 (d; 1H; $C_{Ar}H$; ^{3}J = 7,6 Hz); 6,80 (t; 1H; $C_{Ar}H$; ^{3}J = 7,6 Hz); 4,72 (s; 1H; OH); 2,31 (s; 3H; CH_3); 2,20 (s; 3H; CH_3).

^{13}C NMR (600 MHz, $CDCl_3$): δ 153,5 (1C; $C_{Ar}OH$); 138,4 (1C; C_{Ar}); 126,0 (1C; $C_{Ar}H$); 122,5 (1C; C_{Ar}); 122,4 (1C; $C_{Ar}H$); 112,6 (1C; $C_{Ar}H$); 20,1 (1C; CH_3); 11,5 (1C; CH_3).

MS data for 62

UHPLC-HRMS (ESI-TOF): *m/z* = 121,0659 (121,0648 calculated) $[M-H]^-$ ($C_8H_{10}O$).

5.3 Synthesis of alkene 14 and its related compounds

5.3.1 Synthesis of tertiary alcohol **22**

15 g (75 mmol; 1 eq) of ketone **21** were suspended in 150 mL (10 V) of THF. The suspension was inertized with nitrogen and added dropwise 75 mL (3 M; d. 1,112 g/mL; 83,4 g; 225 mmol; 3 eq) of MeMgCl. Once the addition was completed, the suspension was heated to 60 – 65 ºC and maintained for 3 h. Then, the solution was cooled to 0 – 10 ºC and a solution, previously prepared, of 22,32 g of NH_4Cl (417 mmol; 5,57 eq) in 75 mL of H_2O (5 V) was added dropwise. Then, the suspension was heated to 20 – 25 ºC, added 60 mL of H_2O (4 V), the pH was adjusted to 7 with HCl (37 wt. %; d. 1,190 g/mL) and phases were separated.

The aqueous phase was washed with 30 mL of EtOAc (2 V) twice and the combined organic phases were washed with a previously prepared solution of 21,45 g of NaCl (4,9 eq) in 77,5 mL of H_2O (5,15 V). The resulting organic phase was distilled under vacuum to dryness and charged of 75 mL of *n*-heptane (5 V).

The solid was recovered by filtration and washed with 15 mL of *n*-heptane (1 V) twice. The solid was dried at 40 ºC under vacuum for 16 h to give **22** as an off-white powder (15,39 g; 95 %).

NMR data for 22

^{1}H NMR (600 MHz, DMSO-d_6): δ 11,81 (br s; 1H; NH); 7,48 (s; 1H; N=CH-N); 7,41 (d; 1H; $C_{Ar}H$; ^3J = 4,6 Hz); 7,05 (t; 1H; $C_{Ar}H$; ^3J = 4,6 Hz); 7,02 (d; 1H; $C_{Ar}H$; ^3J = 4,6 Hz); 6,70 (s; 1H; C=CH-N); 5,23 (br s; 1H; OH); 2,18 (s; 3H; CH_3); 2,01 (s; 3H; CH_3); 1,80 (d; 3H; CH_3).

^{13}C NMR (600 MHz, DMSO-d_6): δ 149,3 (1C; C-C=CH); 146,3 (1C; C_{Ar}); 137,5 (1C; C_{Ar}); 134,9 (1C; C_{Ar}); 134,8 (1C; N=CH-N); 128,8 (1C; $C_{Ar}H$); 124,8 (1C; $C_{Ar}H$); 124,5 (1C; $C_{Ar}H$); 112,3 (1C; C=C-N); 72,0 (1C; C-OH); 30,3 (1C; CH_3); 21,0 (1C; CH_3); 17,2 (1C; CH_3).

MS data for 22

UHPLC-HRMS (ESI-TOF): *m/z* = 217,1354 (217,1335 calculated) $[M+H]^+$; *m/z* = 199,1217 (199,1230 calculated) $[M+H-H_2O]^+$; *m/z* = 215,1190 (215,1179 calculated) $[M-H]^-$ ($C_{13}H_{16}N_2O$).

5.3.2 Synthesis of alkene **14**

75 g (375 mmol; 1 eq) of ketone **21** were suspended in 600 mL of THF (8 V). The suspension was inertized with nitrogen and added dropwise 370 mL of MeMgCl (3 M; d. 1,112 g/mL; 413 g; 1,114 mol; 2,97 eq). Once the addition was completed, the suspension was heated to 60 – 65 ºC and maintained for 3 h. Then, the solution was cooled to 0 – 10 ºC and a solution, previously prepared, of 111,6 g of NH_4Cl (2,086 mol; 5,57 eq) in 375 mL of H_2O (5 V) was added dropwise. Then, the suspension was heated to 20 – 25 ºC, added 300 mL of H_2O (4 V), the pH was adjusted to 7 with HCl (37 wt. %; d. 1,190) and phases were separated.

The aqueous phase was washed with 150 mL of EtOAc (2 V) twice and the combined organic phases were washed with a previously prepared solution of 107,25 g of NaCl (1,835 mol; 4,9 eq) in 386 mL of H_2O (5,15 V). The resulting organic phase was distilled under vacuum to dryness.

To the residue, 412,5 mL of Toluene (5,5 V) and 7,12 g of $pTsOH \cdot H_2O$ (37 mmol; 0,1 eq) were charged. The mixture was heated to reflux (about 111 ºC) for 2 h. Then, the mixture was cooled to 50 ºC, added a previously prepared solution of 15,73 g of $NaHCO_3$ (187 mmol; 0,5 eq) in 210 mL of H_2O (2,8 V). The mixture resulting mixture was cooled to 38 ºC and let to crystalize. Once the mixture starts to crystalize, was cooled to 0 – 5 ºC and maintained for between 1 - 3 h.

The solid was recovered by filtration and washed with 82,5 mL of H_2O (1,1 V) twice and 82,5 mL of *n*-heptane (1,1 V) twice. The solid was dried at 40 ºC under vacuum for 16 h to give **14** as an off-white powder (71,65 g; 97 %).

NMR data for 14

^{1}H NMR (600 MHz, $CDCl_3$): δ 10,18 (br s; 1H; NH); 7,60 (s; 1H; N=CH-N); 7,15 (d; 1H; $C_{Ar}H$; ^{3}J = 6,7 Hz); 7,10 (t; 1H; $C_{Ar}H$; ^{3}J = 6,7 Hz); 7,09 (d; 1H; $C_{Ar}H$; ^{3}J = 6,7 Hz); 6,62 (s; 1H; C=CH-N); 5,91 + 5,01 (d; 2H; CH_2; ^{2}J = 1,3 Hz); 2,31 (s; 3H; CH_3); 2,12 (s; 3H; CH_3).

^{13}C NMR (600 MHz, $CDCl_3$): δ 140,7 (1C; $C=CH_2$); 140,5 (1C; C_{Ar}); 138,2 (1C; C-C=CH); 137,0 (1C; C_{Ar}); 135,6 (1C; N=CH-N); 134,6 (1C; C_{Ar}); 129,2 (1C; $C_{Ar}H$); 127,4 (1C; $C_{Ar}H$); 125,3 (1C; $C_{Ar}H$); 119,6 (1C; C=CH-N); 111,7 (1C; CH_2); 20,5 (1C; CH_3); 16,6 (1C; CH_3).

MS data for 14

UHPLC-HRMS (ESI-TOF): *m/z* = 199,1217 (199,1230 calculated) $[M+H]^+$; *m/z* = 197,1084 (197,1073 calculated) $[M-H]^-$ ($C_{13}H_{14}N_2$)

5.3.3 Synthesis of Bn functionalized alkene **32**

[redacted] to give **32** as an off-white powder [redacted]

NMR data for 32

^{1}H NMR (600 MHz, $CDCl_3$): 7,58 (s; 1H; N=CH-N); 7,35 (m; 2H; $C_{Ar}H$; ^3J = 7,3 Hz); 7,32 (m; 1H; $C_{Ar}H$; ^3J = 7,3 Hz); 7,14 (m; 1H; $C_{Ar}H$; ^3J = 4,6 Hz); 7,11 (m; 2H; $C_{Ar}H$; ^3J = 7,3 Hz); 7,10 (m; 1H; $C_{Ar}H$; ^3J = 4,6 Hz); 7,09 (m; 1H; $C_{Ar}H$; ^3J = 4,6 Hz); 6,37 (s; 1H; C=CH-N); 6,17 + 5,02 (d; 2H; CH_2; ^2J = 2,1 Hz); 2,31 (s; 3H; CH_3); 2,14 (s; 3H; CH_3).

^{13}C NMR (600 MHz, $CDCl_3$): δ 143,2 (1C; C-C=CH); 141,8 (1C; C=CH_2); 141,0 (1C; C_{Ar}); 137,7 (1C; N=CH-N); 136,9 (1C; C_{Ar}); 136,1 (1C; C_{Ar}); 134,6 (1C; C_{Ar}); 129,0 (2C; $C_{Ar}H$); 128,9 (1C; $C_{Ar}H$); 128,2 (1C; $C_{Ar}H$); 127,4 (1C; $C_{Ar}H$); 127,1 (2C; $C_{Ar}H$); 125,4 (1C; $C_{Ar}H$); 118,0 (1C; C=CH-N); 112,0 (1C; CH_2=C); 50,8 (1C; N-CH_2-Ph); 20,5 (1C; CH_3); 16,7 (1C; CH_3).

MS data for 32

UHPLC-HRMS (ESI-TOF): *m/z* = 289,1725 (289,1699 calculated) $[M+H]^+$ ($C_{20}H_{20}N_2$).

SC-XRD data for 32

Empirical formula	$C_{20}H_{20}N_2$	
Formula weight	288,38	
Temperature	296 K	
Wavelength	0,71073 Å	
Crystal system	Monoclinic	
Space group	P 2_1/c	
Unit cell dimensions	a = 14,6436 Å	α = 90°
	b = 6,2291 Å	β = 103,389°
	c = 18,7812 Å	γ = 90°
Volume	1666,59 Å3	
Z	4	
Density (calculated)	1,149 Mg/m^3	
Absorption coefficient	0,068 mm^{-1}	
F(000)	616	
Crystal size	0,4 x 0,3 x 0,1 mm^3	
Theta range for data collection	1,429 to 28,770°	
Index ranges	-19 ≤ h ≤ 19	
	-8 ≤ k ≤ 8	
	-24 ≤ l ≤ 25	
Reflections collected	12740	
Independent reflections	4018 [R(int) = 0,0389]	
Completeness to θ = 25,000°	100,0 %	
Absorption correction	Semi-empirical from equivalents	
Max, and min, transmission	1 and 0,6140	
Refinement method	Full-matrix least-squares on F^2	
Data / restraints / parameters	4018 / 0 / 201	
Goodness-of-fit on F^2	1,033	
Final R indices [I > 2σ (I)]	R_1 = 0,0603, wR_2 = 0,1511	
R indices (all data)	R_1 = 0,1003, wR_2 = 0,1734	
Extinction coefficient	n/a	
Largest diff, peak and hole	0,219 and -0,186 e, $Å^{-3}$	

5.3.4 Synthesis of Ms functionalized alkenes **66** and **79** (Mixture)

[redacted]

[redacted] to give **66** and **79** [redacted]

NMR data for 66

^{1}H NMR (600 MHz, $CDCl_3$): δ 7,99 (s; 1H; N=CH-N); 7,18 (d; 1H; $C_{Ar}H$; ^{3}J = 7,3 Hz); 7,11 (t; 1H; $C_{Ar}H$; ^{3}J = 7,3 Hz); 7,06 (d; 1H; $C_{Ar}H$; ^{3}J = 7,3 Hz); 6,71 (s; 1H; C=CH-N); 6,27 + 5,20 (d; 2H; CH_2; ^{2}J = 1,7 Hz); 3,24 (s; 3H; CH_3); 2,33 (s; 3H; CH_3); 2,13 (s; 3H; CH_3).

MS data for 66

UHPLC-HRMS (ESI-TOF): *m/z* = 277,1027 (277,1005 calculated) $[M+H]^+$; *m/z* = 275,0860 (275,0849 calculated) $[M-H]^-$ ($C_{14}H_{16}N_2O_2S$).

NMR data for 79

^{1}H NMR (600 MHz, $CDCl_3$): δ 8,86 (s; 1H; N=CH-N); 7,14 (d; 1H; $C_{Ar}H$; ^{3}J = 7,3 Hz); 7,11 (t; 1H; $C_{Ar}H$; ^{3}J = 7,3 Hz); 7,00 (d; 1H; $C_{Ar}H$; ^{3}J = 7,3 Hz); 6,60 (s; 1H; C=CH-N); 6,18 + 5,33 (d; 2H; CH_2; ^{2}J = 1,7 Hz); 2,87 (s; 3H; CH_3); 2,31 (s; 3H; CH_3); 2,07 (s; 3H; CH_3).

MS data for 79

UHPLC-HRMS (ESI-TOF): *m/z* = 277,1027 (277,1005 calculated) $[M+H]^+$; *m/z* = 275,0860 (275,0849 calculated) $[M-H]^-$ ($C_{14}H_{16}N_2O_2S$).

5.3.5 Synthesis of Cbz functionalized alkene **67**

[redacted] to give **67** as a transparent to yellowish sticky oil [redacted]

NMR data for 67

^{1}H NMR (600 MHz, $CDCl_3$): 8,17 (s; 1H; N=CH-N); 7,43 (m; 5H; $C_{Ar}H$); 7,18 (d; 1H; $C_{Ar}H$; ^{3}J = 7,4 Hz); 7,13 (t; 1H; $C_{Ar}H$; ^{3}J = 7,4 Hz); 7,08 (d; 1H; $C_{Ar}H$; ^{3}J = 7,4 Hz); 6,83 (s; 1H; C=CH-N); 6,25 + 5,16 (d; 2H; CH_2; ^{2}J = 1,8 Hz); 5,39 (s; 3H; CO-CH_2-Ph); 2,34 (s; 3H; CH_3); 2,14 (s; 3H; CH_3).

^{13}C NMR (600 MHz, $CDCl_3$): δ 148,6 (CO); 144,2 (1C; C-C=CH); 140,9 (1C; C=CH_2); 140,0 (1C; C_{Ar}); 137,4 (1C; N=CH-N); 137,1 (1C; C_{Ar}); 134,5 (1C; C_{Ar}); 134,0 (1C; C_{Ar}); 129,2 (1C; $C_{Ar}H$); 129,2 (1C; $C_{Ar}H$); 128,9 (4C; $C_{Ar}H$); 127,3 (1C; $C_{Ar}H$); 125,3 (1C; $C_{Ar}H$); 114,9 (1C; CH_2=C); 114,4 (1C; C=CH-N); 69,8 (1C; CO-CH_2-Ph); 20,5 (1C; CH_3); 16,6 (1C; CH_3).

MS data for 67

UHPLC-HRMS (ESI-TOF): *m/z* = 333,1614 (333,1598 calculated) $[M+H]^+$ ($C_{21}H_{20}N_2O_2$).

5.3.6 Synthesis of Boc functionalized alkene **68**

[redacted]

[redacted]

[redacted] to give **68** as an off-white powder [redacted]

NMR data for 68

^{1}H NMR (600 MHz, $CDCl_3$): 8,08 (s; 1H; N=CH-N); 7,17 (d; 1H; $C_{Ar}H$; ^{3}J = 7,6 Hz); 7,12 (t; 1H; $C_{Ar}H$; ^{3}J = 7,6 Hz); 7,07 (d; 1H; $C_{Ar}H$; ^{3}J = 7,6 Hz); 6,76 (s; 1H; C=CH-N); 6,22 + 5,13 (d; 2H; CH_2; ^{2}J = 2,0 Hz); 2,33 (s; 3H; CH_3); 2,15 (s; 3H; CH_3); 1,60 (s; 9H; CH_3).

^{13}C NMR (600 MHz, $CDCl_3$): δ 147,6 (CO); 143,7 (1C; C-C=CH); 141,1 (1C; C=CH_2); 140,2 (1C; C_{Ar}); 137,2 (1C; N=CH-N); 137,0 (1C; C_{Ar}); 134,5 (1C; C_{Ar}); 129,2 (1C; $C_{Ar}H$); 127,3 (1C; $C_{Ar}H$); 125,3 (1C; $C_{Ar}H$); 114,5 (1C; CH_2=C); 114,4 (1C; C=CH-N); 85,7 (1C; CO-C-CH_3); 20,5 (1C; CH_3); 16,6 (1C; CH_3).

MS data for 68

UHPLC-HRMS (ESI-TOF): *m/z* = 299,1742 (299,1754 calculated) $[M+H]^+$ ($C_{18}H_{22}N_2O_2$).

SC-XRD data for 68

Empirical formula	$C_{18}H_{22}N_2O_2$	
Formula weight	298,37	
Temperature	296 K	
Wavelength	0,71073 Å	
Crystal system	Triclinic	
Space group	P -1	
Unit cell dimensions	a = 7,6829 Å	α = 68,671°
	b = 10,6669 Å	β = 78,627°
	c = 11,8888 Å	γ = 71,207°
Volume	855,66 Å^3	
Z	2	
Density (calculated)	1,158 Mg/m^3	
Absorption coefficient	0,076 mm^{-1}	
F(000)	320	

Crystal size	0,6 x 0,5 x 0,2 mm^3
Theta range for data collection	1,846 to 28,607°
Index ranges	-10 ≤ h ≤ 10
	-13 ≤ k ≤ 13
	-15 ≤ l ≤ 15
Reflections collected	6752
Independent reflections	3924 [R(int) = 0,0132]
Completeness to θ = 25,000°	99,2 %
Absorption correction	Semi-empirical from equivalents
Max, and min, transmission	1 and 0,8561
Refinement method	Full-matrix least-squares on F^2
Data / restraints / parameters	3924 / 0 / 204
Goodness-of-fit on F^2	1,037
Final R indices [I > 2σ (I)]	R_1 = 0,0479, wR_2 = 0,1317
R indices (all data)	R_1 = 0,0564, wR_2 = 0,1403
Extinction coefficient	N/A
Largest diff, peak and hole	0,158 and -0,230 e, $Å^{-3}$

5.3.7 Synthesis of Fmoc functionalized alkene **69**

[redacted] to give **69** as a transparent to brownish sticky oil [redacted]

NMR data for 69

^{1}H NMR (600 MHz, $CDCl_3$): 8,07 (s; 1H; N=CH-N); 7,78 (d; 2H; $C_{Ar}H$; ^3J = 7,6 Hz); 7,53 (d; 2H; $C_{Ar}H$; ^3J = 7,6 Hz); 7,44 (t; 2H; $C_{Ar}H$; ^3J = 7,6 Hz); 7,33 (t; 2H; $C_{Ar}H$; ^3J = 7,6 Hz); 7,21 (d; 1H; $C_{Ar}H$; ^3J = 7,5 Hz); 7,16 (t; 1H; $C_{Ar}H$; ^3J = 7,5 Hz); 7,09 (d; 1H; $C_{Ar}H$; ^3J = 7,5 Hz); 6,75 (s; 1H; C=CH-N); 6,26 + 5,18 (d; 2H; CH_2; ^2J = 2,0 Hz); 4,70 (d; 2H; O-CH_2-C; ^3J = 6,7 Hz); 4,35 (t; 1H; C-CH-Ar_2; ^3J = 6,7 Hz); 2,37 (s; 3H; CH_3); 2,15 (s; 3H; CH_3).

^{13}C NMR (600 MHz, $CDCl_3$): δ 148,6 (CO); 144,2 (1C; C-C=CH); 142,7 (2C; C_{Ar}); 141,4 (2C; C_{Ar}); 140,9 (1C; $C=CH_2$); 140,0 (1C; C_{Ar}); 137,2 (1C; N=CH-N); 137,1 (1C; C_{Ar}); 134,4 (1C; C_{Ar}); 129,3 (1C; $C_{Ar}H$); 128,2 (2C; $C_{Ar}H$); 127,3 (2C; $C_{Ar}H$); 127,3 (1C; $C_{Ar}H$); 125,4 (1C; $C_{Ar}H$); 124,7 (2C; $C_{Ar}H$); 120,3 (2C; $C_{Ar}H$); 114,8 (1C; $CH_2=C$); 114,4 (1C; C=CH-N); 69,7 (1C; $CO-CH_2-C$); 46,6 (1C; $C-CH-Ar_2$); 20,5 (1C; CH_3); 16,6 (1C; CH_3).

MS data for 69

UHPLC-HRMS (ESI-TOF): *m/z* = 421,1926 (421,1911 calculated) $[M+H]^+$ ($C_{28}H_{24}N_2O_2$)

5.3.8 Synthesis of MC functionalized alkene **70**

[redacted] to give **70** as an off-white powder [redacted]

NMR data for 70

^{1}H NMR (600 MHz, $CDCl_3$): 8,15 (s; 1H; N=CH-N); 7,17 (d; 1H; $C_{Ar}H$; ^3J = 7,5 Hz); 7,12 (t; 1H; $C_{Ar}H$; ^3J = 7,5 Hz); 7,07 (d; 1H; $C_{Ar}H$; ^3J = 7,5 Hz); 6,79 (s; 1H; C=CH-N); 6,24 + 5,16 (d; 2H; CH_2; ^2J = 1,7 Hz); 3,99 (s; 3H; $O-CH_3$); 2,33 (s; 3H; CH_3); 2,13 (s; 3H; CH_3).

^{13}C NMR (600 MHz, $CDCl_3$): δ 149,1 (CO); 144,1 (1C; C-C=CH); 140,9 (1C; $C=CH_2$); 140,0 (1C; C_{Ar}); 137,3 (1C; N=CH-N); 137,1 (1C; C_{Ar}); 134,5 (1C; C_{Ar}); 129,2 (1C; $C_{Ar}H$); 127,3 (1C; $C_{Ar}H$); 125,3 (1C; $C_{Ar}H$); 114,8 (1C; $CH_2=C$); 114,1 (1C; C=CH-N); 54,6 (1C; $O-CH_3$); 20,5 (1C; CH_3); 16,5 (1C; CH_3).

MS data for 70

UHPLC-HRMS (ESI-TOF): *m/z* = 257,1274 (257,1285 calculated) $[M+H]^+$ ($C_{15}H_{16}N_2O_2$).

5.3.9 Synthesis of N_I-Me functionalized alkene **73**

[redacted] to give **73** as an off-white powder [redacted]

NMR data for 73

^{1}H NMR (600 MHz, $CDCl_3$): δ 7,44 (s; 1H; N=CH-N); 7,15 (d; 1H; $C_{Ar}H$; ^3J = 6,6 Hz); 7,11 (t; 1H; $C_{Ar}H$; ^3J = 6,6 Hz); 7,09 (d; 1H; $C_{Ar}H$; ^3J = 6,6 Hz); 6,30 (s; 1H; C=CH-N); 6,12 + 4,98 (d; 2H; CH_2; ^2J = 2,0 Hz); 3,59 (s; 3H; CH_3); 2,33 (s; 3H; CH_3); 2,15 (s; 3H; CH_3).

MS data for 73

UHPLC-HRMS (ESI-TOF): *m/z* = 213,1374 (213,1386 calculated) $[M+H]^+$ ($C_{14}H_{16}N_2$).

5.3.10 Synthesis of N_{II}-Me functionalized alkene **74** (From mixture)

[redacted]

[redacted]

[redacted] to give **74** (part from a mixture) as an off-white powder [redacted]

NMR data for 74

^{1}H NMR (600 MHz, $CDCl_3$): δ 7,39 (s; 1H; N=CH-N); 7,15 (d; 1H; $C_{Ar}H$; ^3J = 6,6 Hz); 7,11 (t; 1H; $C_{Ar}H$; ^3J = 6,6 Hz); 7,09 (d; 1H; $C_{Ar}H$; ^3J = 6,6 Hz); 6,91 (s; 1H; C=CH-N); 5,60 + 5,21 (d; 2H; CH_2; ^2J = 2,0 Hz); 3,37 (s; 3H; CH_3); 2,30 (s; 3H; CH_3); 2,07 (s; 3H; CH_3).

MS data for 74

UHPLC-HRMS (ESI-TOF): *m/z* = 213,1374 (213,1386 calculated) $[M+H]^+$ ($C_{14}H_{16}N_2$).

5.3.11 Synthesis of N_τ-Et and N_π-Et functionalized alkenes **75** and **76** HCl (Mixture)

[redacted]

[redacted]

[redacted] give **75** and **76** HCl as a white crystals [redacted]

NMR data for 75

^{1}H NMR (600 MHz, $CDCl_3$): δ 15,73 (br s; 1H; NH^+); 9,84 (s; 1H; N=CH-N); 7,18 (d; 1H; $C_{Ar}H$; ^3J = 7,6 Hz); 7,11 (t; 1H; $C_{Ar}H$; ^3J = 7,6 Hz); 7,01 (d; 1H; $C_{Ar}H$; ^3J = 7,6 Hz); 6,68 (s; 1H; C=CH-N); 6,38 + 5,40 (s; 2H; CH_2); 4,32 (q; 2H; N-CH_2; ^3J = 7,3 Hz); 2,30 (s; 3H; CH_3); 2,09 (s; 3H; CH_3); 1,50 (t; 3H; CH_3; ^3J = 7,3 Hz).

MS data for 75

UHPLC-HRMS (ESI-TOF): *m/z* = 227,1549 (227,1543 calculated) $[M+H]^+$ ($C_{15}H_{18}N_2$) from ($C_{15}H_{19}N_2Cl$).

NMR data for 76

^{1}H NMR (600 MHz, $CDCl_3$): δ 15,54 (br s; 1H; NH^+); 9,73 (s; 1H; N=CH-N); 7,27 (s; 1H; C=CH-N); 7,18 (d; 1H; $C_{Ar}H$; ^3J = 7,6 Hz); 7,11 (t; 1H; $C_{Ar}H$; ^3J = 7,6 Hz); 7,01 (d; 1H; $C_{Ar}H$; ^3J = 7,6 Hz); 5,81 + 5,54 (s; 2H; CH_2); 3,97 (q; 2H; N-CH_2; ^3J = 7,3 Hz); 2,28 (s; 3H; CH_3); 2,06 (s; 3H; CH_3); 1,33 (t; 3H; CH_3; ^3J = 7,3 Hz).

MS data for 76

UHPLC-HRMS (ESI-TOF): *m/z* = 227,1549 (227,1543 calculated) $[M+H]^+$ ($C_{15}H_{18}N_2$) from ($C_{15}H_{19}N_2Cl$).

5.4 Synthesis of the enantiopure alkane *S*-8 and its related compounds

5.4.1 Boc functionalized alkene **68** asymmetric hydrogenation

[redacted]

5.4.2 Synthesis of tartrate **39**

[redacted]

[redacted] to give **39** as white to yellowish crystals [redacted]

NMR data for 39

^{1}H NMR (600 MHz, DMSO-d_6): δ 9,32 (br s; 5H; NH, OH and COOH); 7,88 (s; 1H; N=CH-N); 6,99 (d; 2H; 2xC_{Ar}H; ^{3}J = 4,6 Hz); 6,90 (t; 1H; C_{Ar}H; ^{3}J = 4,6 Hz); 6,89 (s; 1H; C=CH-N); 4,37 (q; 1H; CH; ^{3}J = 7,1 Hz); 4,23 (s; 1H; CH); 2,25 (s; 3H; CH_3); 2,22 (s; 3H; CH_3); 1,47 (d; 3H; CH_3; ^{3}J = 7,1 Hz).

^{13}C NMR (600 MHz, DMSO-d_6): δ 174,0 (2C; COO); 143,6 (1C; C_{Ar}); 140,9 (1C; C-C=CH); 136,6 (1C; C_{Ar}); 135,0 (1C; N=CH-N); 134,0 (1C; C_{Ar}); 128,0 (1C; C_{Ar}H); 124,8 (1C; C_{Ar}H); 124,7 (1C; C_{Ar}H); 117,0 (1C; C=CH-N); 72,5 (2C; CHOH); 33,6 (1C; CH); 21,3 (1C; CH_3); 21,1 (1C; CH_3); 14,7 (1C; CH_3).

MS data for 39

UHPLC-HRMS (ESI-TOF): *m/z* = 201,1382 (201,1386 calculated) $[M+H]^+$; *m/z* = 199,1241 (199,1230 calculated) $[M-H]^-$ ($C_{13}H_{16}N_2$) and *m/z* = 149,0092 (149,0081 calculated) $[M-H]^-$ ($C_4H_6O_6$).

5.4.3 Synthesis of enantiopure alkane *S*-**8**

[redacted]

[redacted] to give *S*-**8** as an off-white powder [redacted]

NMR data for *S*-8

^{1}H NMR (600 MHz, $CDCl_3$): δ 11,33 (br s; 1H; NH); 7,26 (s; 1H; N=CH-N); 7,05 (t; 1H; C_{Ar}H; ^{3}J = 7,3 Hz); 7,03 (d; 1H; C_{Ar}H; ^{3}J = 7,3 Hz); 6,97 (d; 1H; C_{Ar}H; ^{3}J = 7,3 Hz); 6,67 (s; 1H; C=CH-N); 4,41 (q; 1H; CH; ^{3}J = 7,0 Hz); 2,29 (s; 3H; CH_3); 2,22 (s; 3H; CH_3); 1,59 (d; 3H; CH_3; ^{3}J = 7,0 Hz).

^{13}C NMR (600 MHz, $CDCl_3$): δ 143,5 (1C; C_{Ar}); 141,3 (1C; C-C=CH); 136,8 (1C; C_{Ar}); 134,7 (1C; N=CH-N); 134,1 (1C; C_{Ar}); 127,9 (1C; $C_{Ar}H$); 125,6 (1C; $C_{Ar}H$); 124,7 (1C; $C_{Ar}H$); 117,4 (1C; C=CH-N); 34,3 (1C; CH); 21,0 (1C; CH_3); 20,8 (1C; CH_3); 14,7 (1C; CH_3).

MS data for *S*-8

UHPLC-HRMS (ESI-TOF): *m/z* = 201,1373 (201,1386 calculated) $[M+H]^+$; *m/z* = 199,1241 (199,1230 calculated) $[M-H]^-$ ($C_{13}H_{16}N_2$).

SC-XRD data for *S*-8

Empirical formula	$C_{13}H_{16}N_2$	
Formula weight	200,28	
Temperature	296 K	
Wavelength	0,71073 Å	
Crystal system	Orthorhombic	
Space group	P 2_1 2_1 2_1	
Unit cell dimensions	a = 8,8953 Å	α = 90°
	b = 9,5263 Å	β = 90°
	c = 13,8647 Å	γ = 90°
Volume	1174,89 Å^3	
Z	4	
Density (calculated)	1,132 Mg/m^3	
Absorption coefficient	0,068 mm^{-1}	
F(000)	432	
Crystal size	0,7 x 0,6 x 0,3 mm^3	
Theta range for data collection	2,594 to 28,606°	
Index ranges	-11 ≤ h ≤ 11	
	-12 ≤ k ≤ 12	
	-18 ≤ l ≤ 18	
Reflections collected	9226	
Independent reflections	2811 [R(int) = 0,0128]	
Completeness to θ = 25,000°	100,0 %	
Absorption correction	Semi-empirical from equivalents	
Max, and min, transmission	1 and 0,8943	
Refinement method	Full-matrix least-squares on F^2	
Data / restraints / parameters	2811 / 0 / 143	
Goodness-of-fit on F^2	1,043	
Final R indices [I > 2σ (I)]	R_1 = 0,0431, wR_2 = 0,1187	

R indices (all data)	R_1 = 0,0465, wR_2 = 0,1219
Absolute structure parameter	0,8
Extinction coefficient	N/A
Largest diff, peak and hole	0,131 and -0,156 e, $Å^{-3}$

5.4.4 Synthesis of N_π-Me enantiopure alkane **77**

[redacted]

[redacted] to give **77** as a white powder [redacted]

NMR data for 77

^{1}H NMR (600 MHz, $CDCl_3$): δ 7,45 (s; 1H; N=CH-N); 7,03 (d; 1H; $C_{Ar}H$; ^3J = 7,5 Hz); 7,02 (d; 1H; $C_{Ar}H$; ^3J = 7,5 Hz); 6,98 (t; 1H; $C_{Ar}H$; ^3J = 7,5 Hz); 6,68 (s; 1H; C=CH-N); 4,28 (q; 1H; CH; ^3J = 7,2 Hz); 3,19 (s; 3H; N-CH_3); 2,35 (s; 3H; CH_3); 2,55 (s; 3H; CH_3); 1,56 (d; 3H; CH_3; ^3J = 7,2 Hz).

MS data for 77

UHPLC-HRMS (ESI-TOF): *m/z* = 215,1550 (215,1543 calculated) $[M+H]^+$ ($C_{14}H_{18}N_2$).

5.4.5 Synthesis of N_π-Et enantiopure alkane **80** (HCl)

[redacted]

[redacted]

[redacted] to give **80** as a white crystals [redacted]

NMR data for 80

^{1}H NMR (600 MHz, $CDCl_3$): δ 8,56 (br s; 1H; NH^+); 7,38 (s; 1H; N=CH-N); 7,00 (d; 1H; $C_{Ar}H$; ^3J = 7,5 Hz); 6,93 (t; 1H; $C_{Ar}H$; ^3J = 7,5 Hz); 6,60 (d; 1H; $C_{Ar}H$; ^3J = 7,5 Hz); 4,70 (s; 1H; C=CH-N); 4,43 (q; 1H; CH; ^3J = 7,0 Hz); 3,71 + 3,54 (m; 2H; CH_2; ^3J = 7,1 Hz); 2,25 (s; 3H; CH_3); 2,19 (s; 3H; CH_3); 1,44 (d; 3H; CH_3; ^3J = 7,0 Hz); 1,08 (t; 3H; CH_3; ^3J = 7,4 Hz).

MS data for 80

UHPLC-HRMS (ESI-TOF): *m/z* = 229,1662 (229,1699 calculated) $[M+H]^+$ ($C_{15}H_{20}N_2$) from ($C_{15}H_{21}N_2Cl$).

5.5 Synthesis of the final product *S*-15

[redacted]

[redacted] to give *S*-**15** as a white crystals [redacted]

NMR data for *S*-15

^{1}H NMR (600 MHz, $CDCl_3$): δ 14,49 (br s; 1H; NH^+); 14,27 (br s; 1H; NH); 8,74 (s; 1H; N=CH-N); 7,01 (m; 1H; $C_{Ar}H$; ^{3}J = 5,2 Hz); 7,00 (m; 1H; $C_{Ar}H$; ^{3}J = 5,2 Hz); 6,95 (m; 1H; $C_{Ar}H$; ^{3}J = 5,2 Hz); 6,71 (s; 1H; C=CH-N); 4,53 (q; 1H; CH; ^{3}J = 7,2 Hz); 2,23 (s; 3H; CH_3); 2,17 (s; 3H; CH_3); 1,63 (d; 3H; CH_3; ^{3}J = 7,2 Hz).

^{13}C NMR (600 MHz, $CDCl_3$): δ 139,5 (1C; C_{Ar}); 138,7 (1C; C-C=CH); 137,3 (1C; C_{Ar}); 134,2 (1C; C_{Ar}); 132,7 (1C; N=CH-N); 129,0 (1C; $C_{Ar}H$); 125,9 (1C; $C_{Ar}H$); 123,9 (1C; $C_{Ar}H$); 115,1 (1C; C=CH-N); 32,2 (1C; CH); 22,2 (1C; CH_3); 20,6 (1C; CH_3); 14,9 (1C; CH_3).

MS data for *S*-15

UHPLC-HRMS (ESI-TOF): *m/z* = 201,1374 (201,1386 calculated) $[M+H]^+$; *m/z* = 199,1240 (199,1230 calculated) $[M-H]^-$ ($C_{13}H_{16}N_2$) from ($C_{13}H_{17}N_2Cl$).

5.6 NMR spectra

5.6.1 NMR spectra of **18**

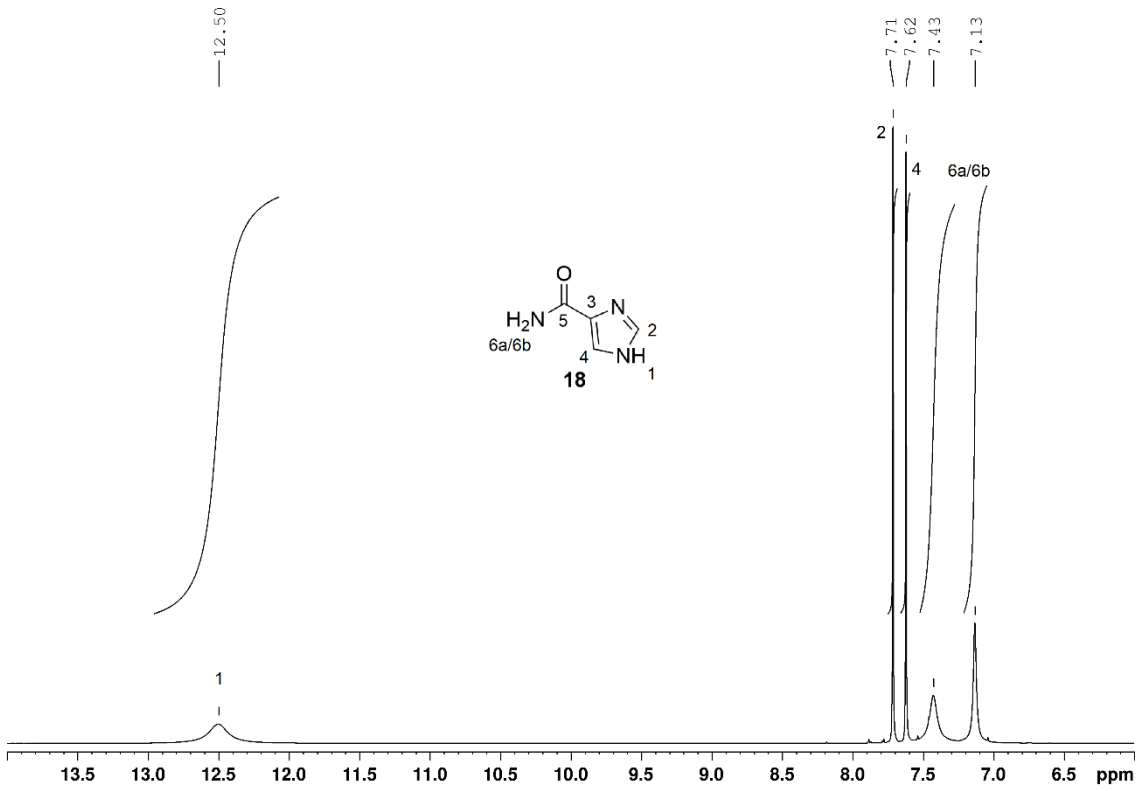


Figure 38. *[1]H-NMR spectrum of* ***18***

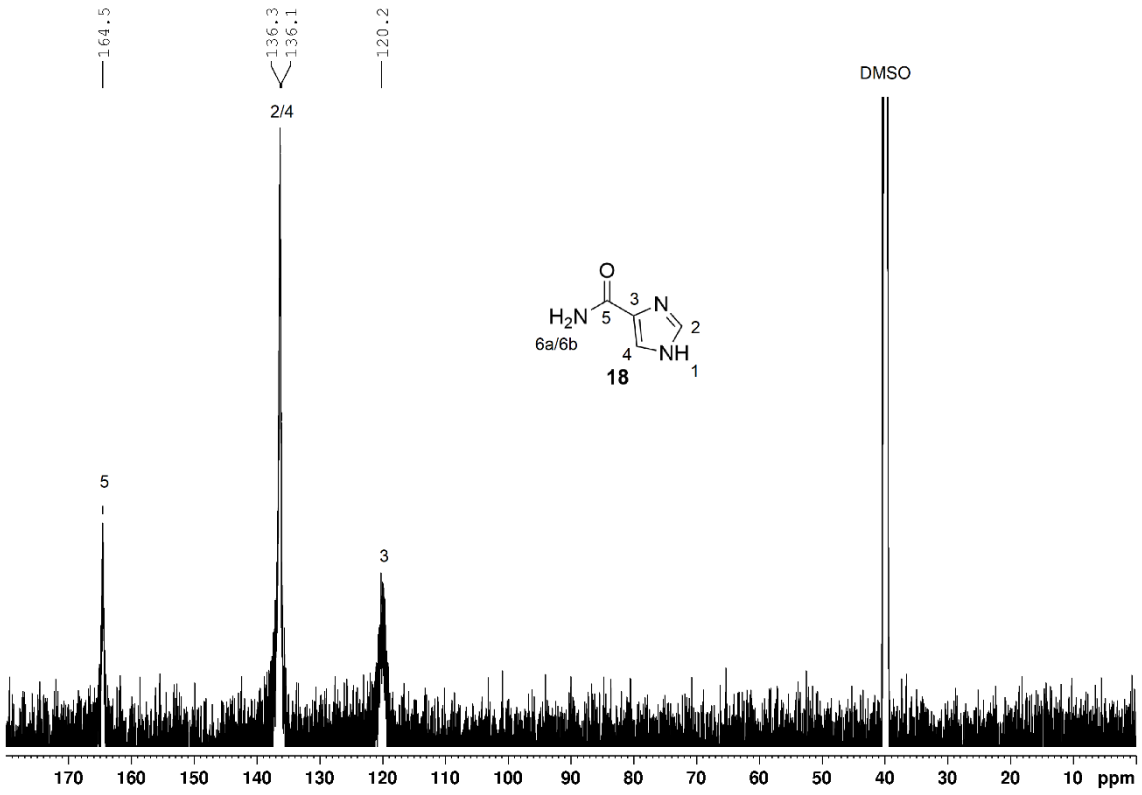


Figure 39. *[13]C-NMR spectrum of* ***18***

5.6.2 NMR spectra of **19**

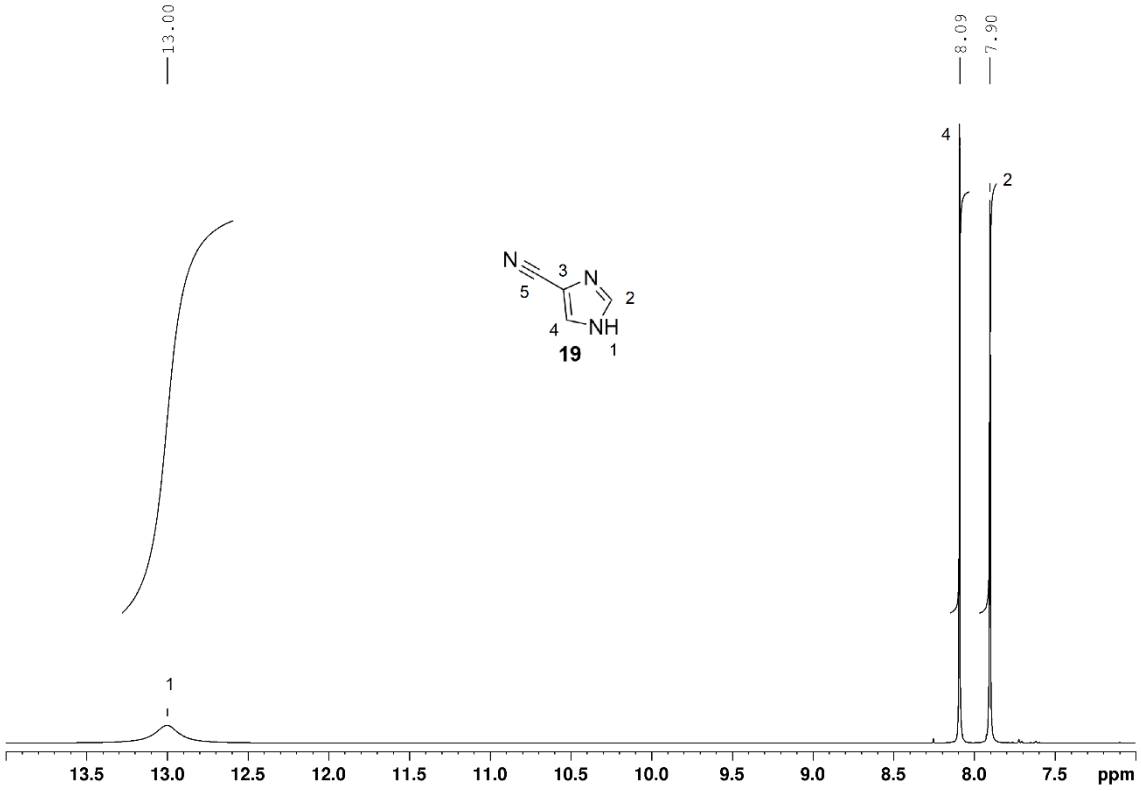


Figure 40. *^{1}H-NMR spectrum of* ***19***

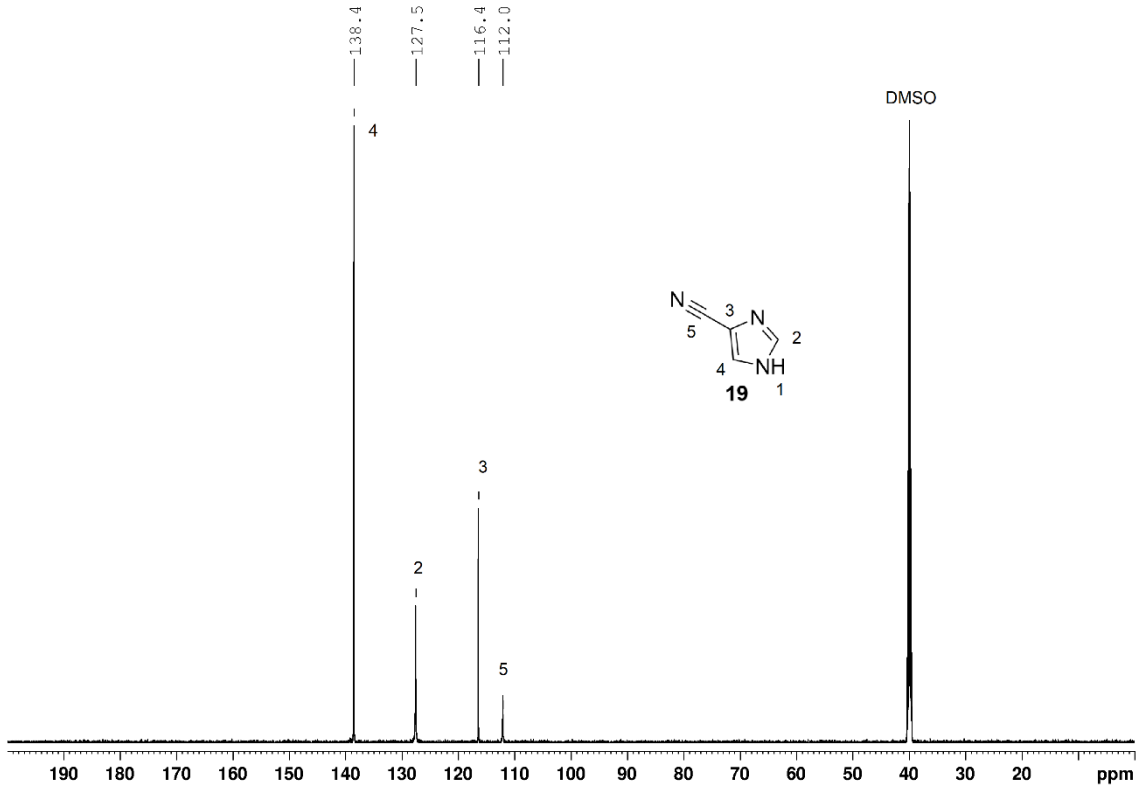


Figure 41. *^{13}C-NMR spectrum of* ***19***

5.6.3 NMR spectra of **33**

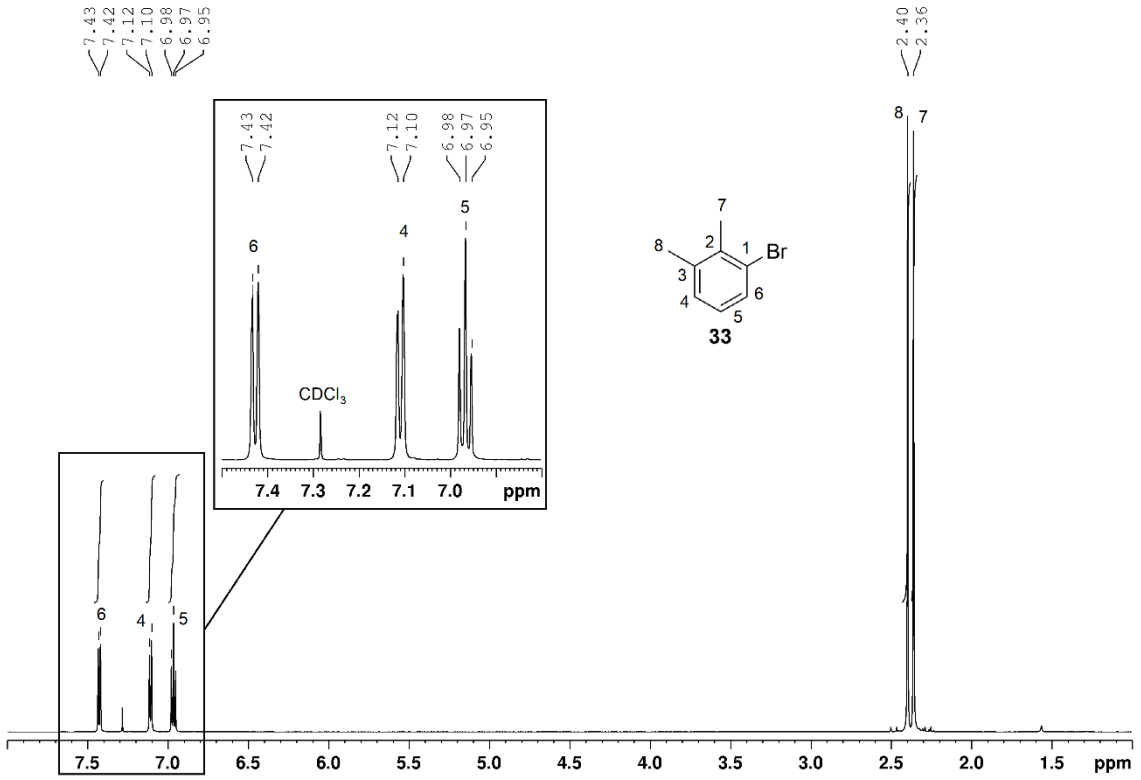


Figure 42. *[1]H-NMR spectrum of **33***

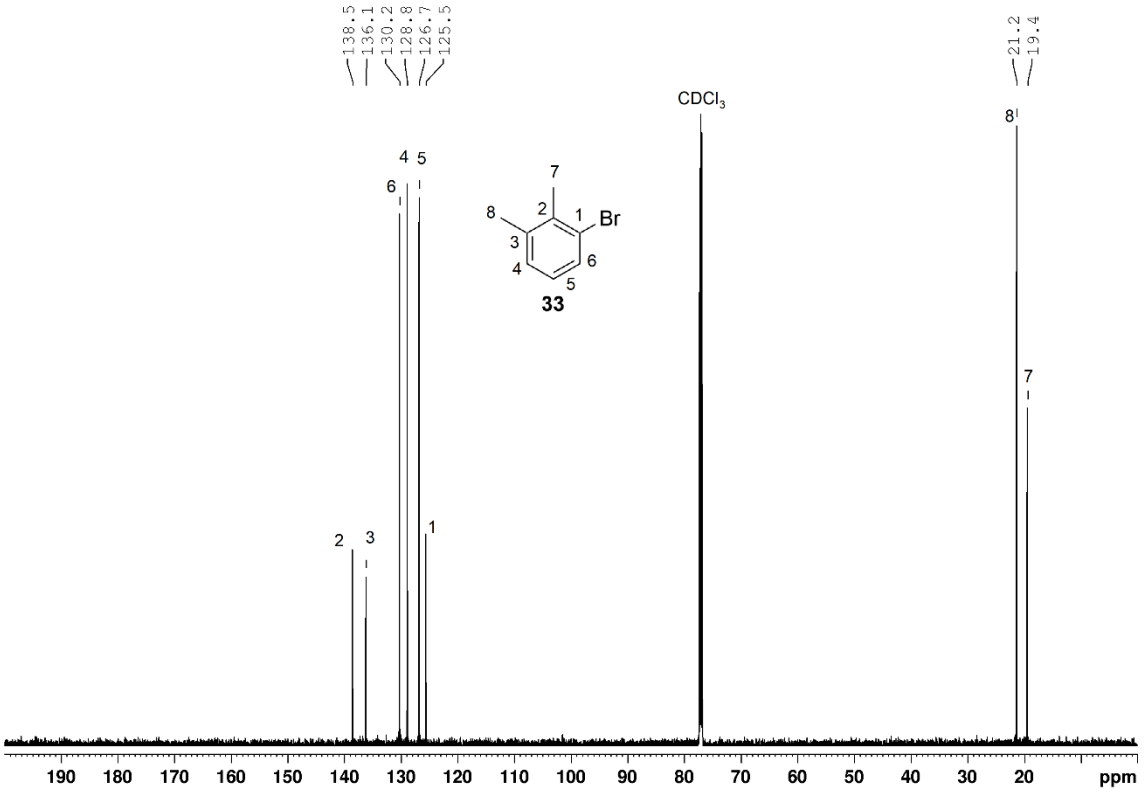


Figure 43. *[13]C-NMR spectrum of **33***

5.6.4 NMR spectra of **51**

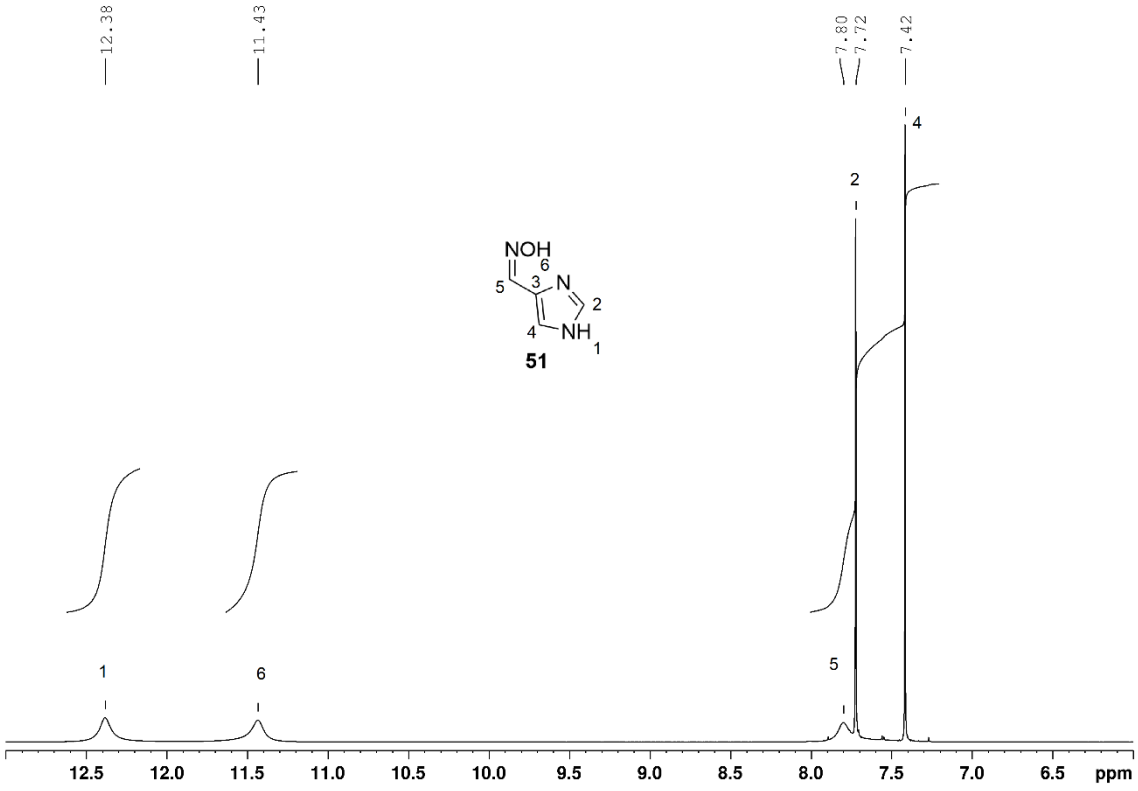


Figure 44. *^{1}H-NMR spectrum of* ***51***

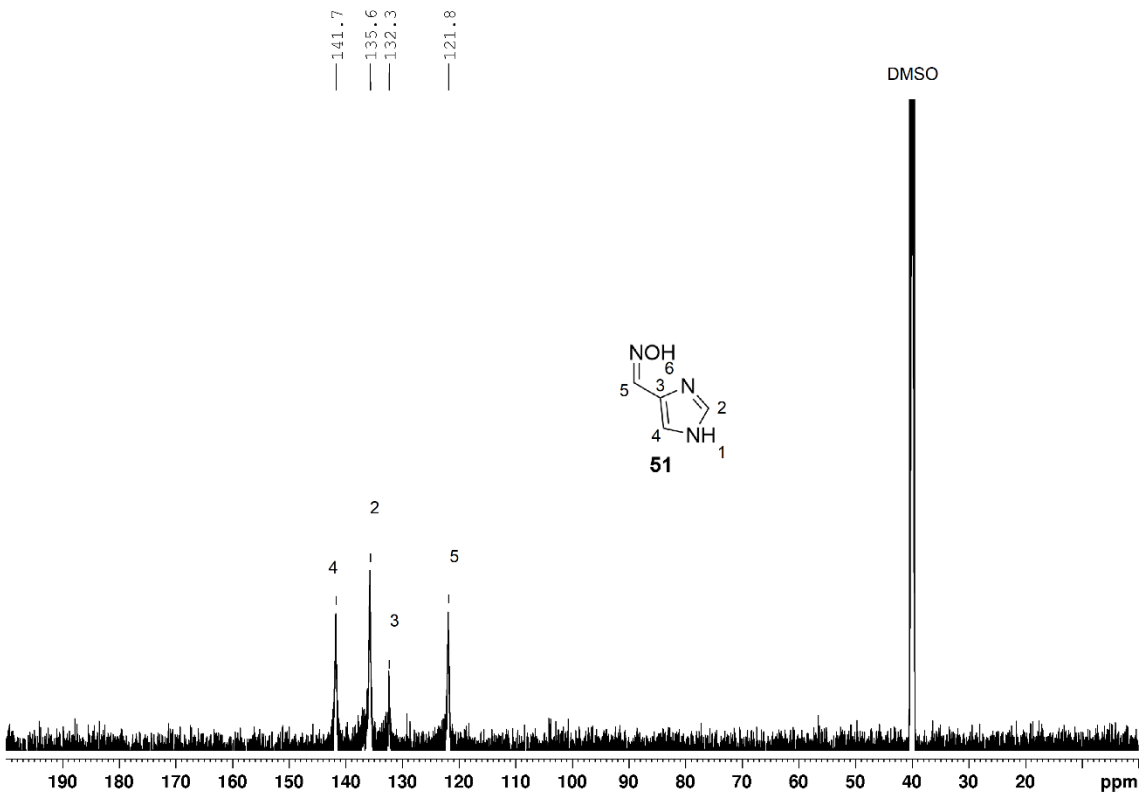


Figure 45. *^{13}C-NMR spectrum of* ***51***

5.6.5 NMR spectra of **21**

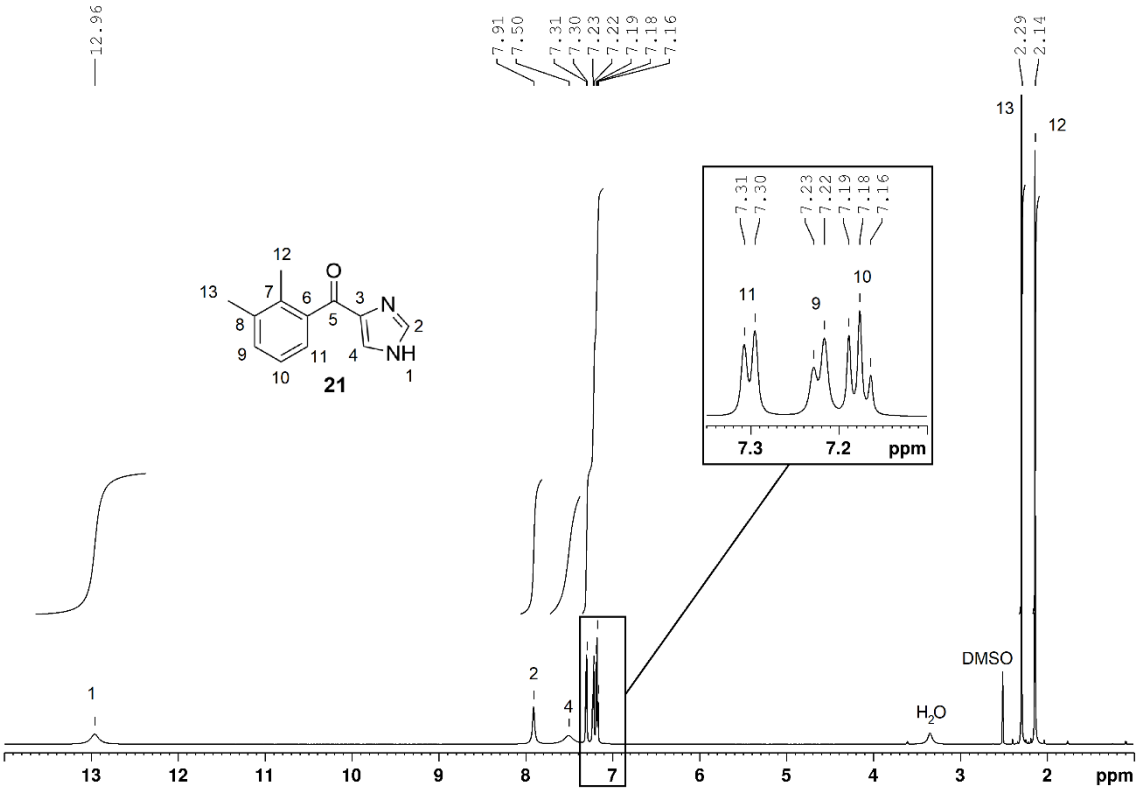


Figure 46. *^{1}H-NMR spectrum of **21***

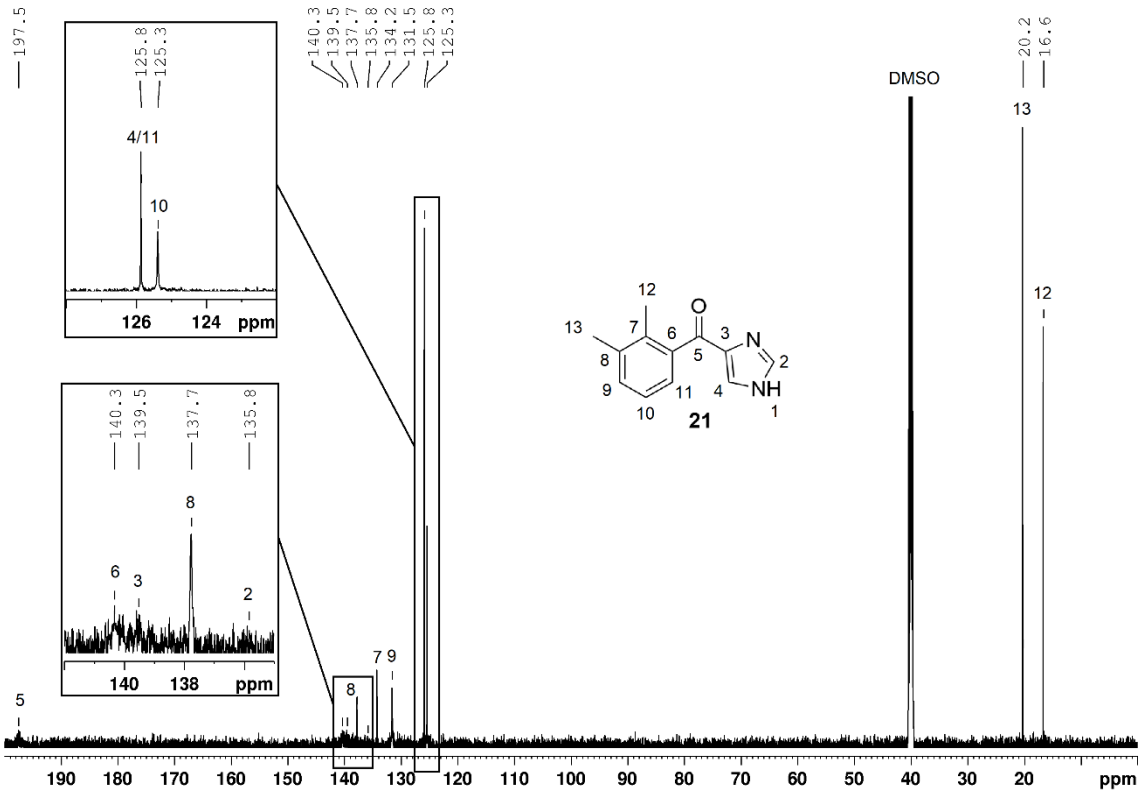


Figure 47. *^{13}C-NMR spectrum of **21***

5.6.6 NMR spectra of **57**

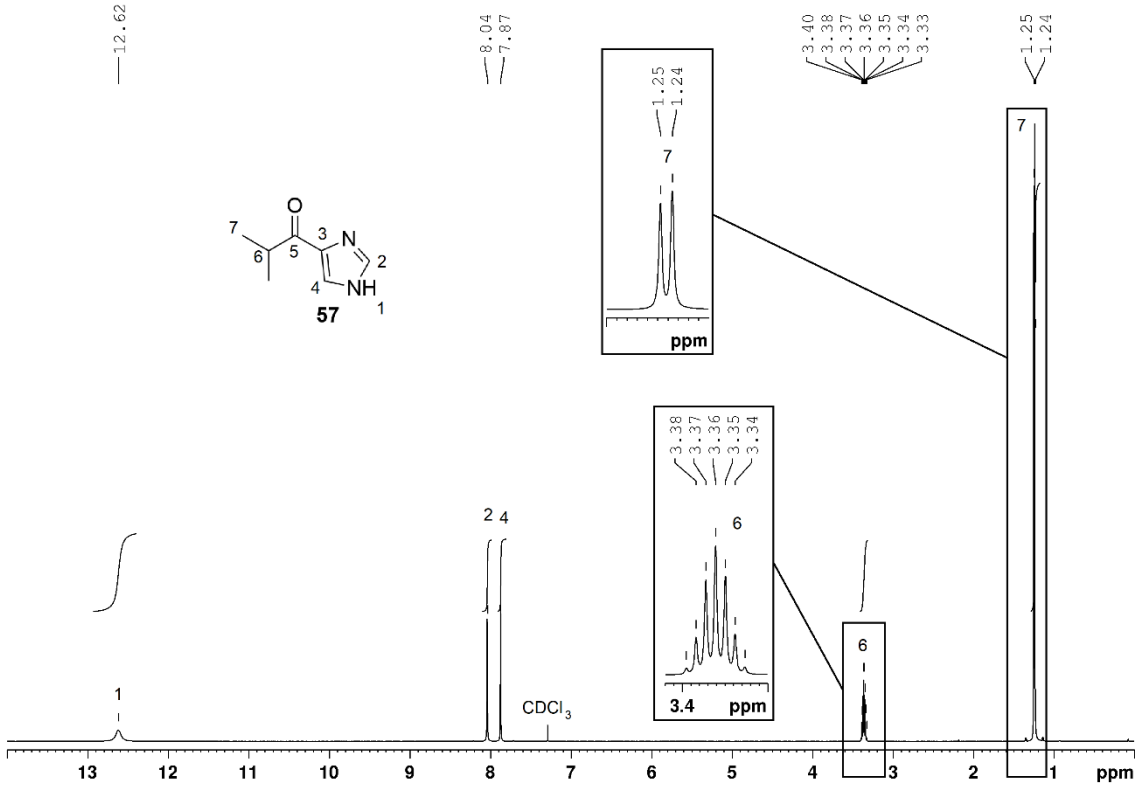


Figure 48. *[1]H-NMR spectrum of* ***57***

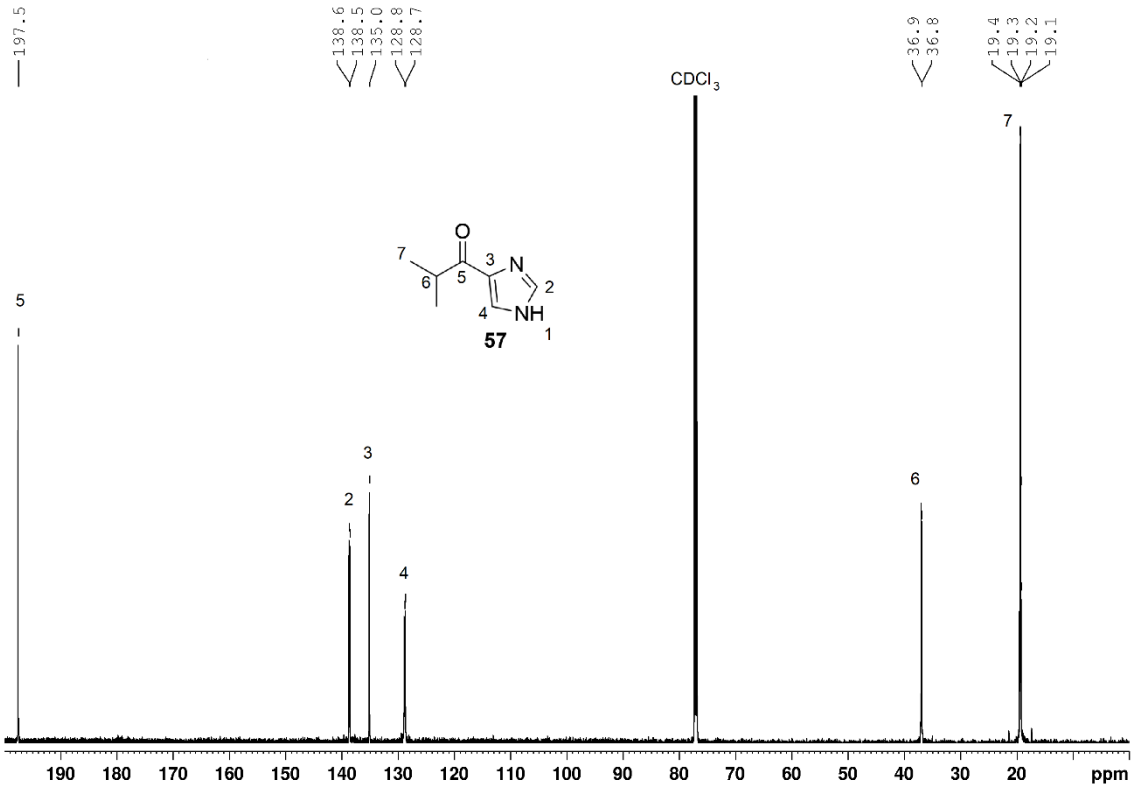


Figure 49. *[13]C-NMR spectrum of* ***57***

5.6.7 NMR spectra of **62**

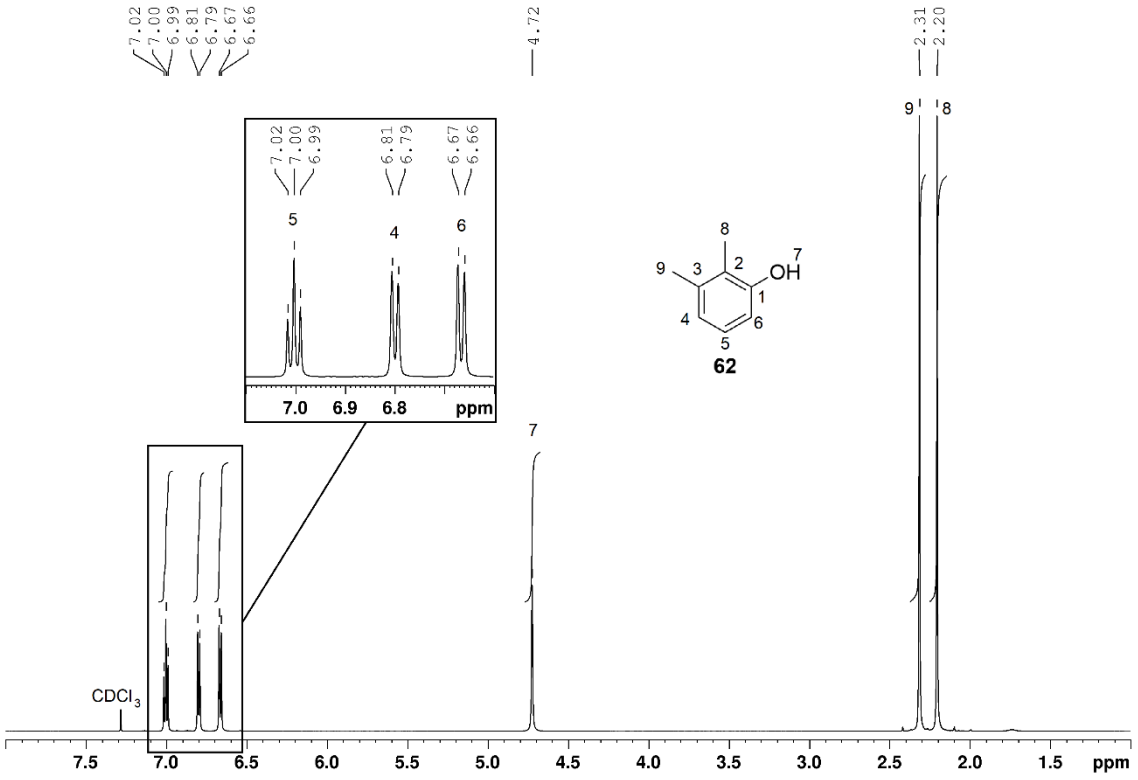


Figure 50. *^{1}H-NMR spectrum of **62***

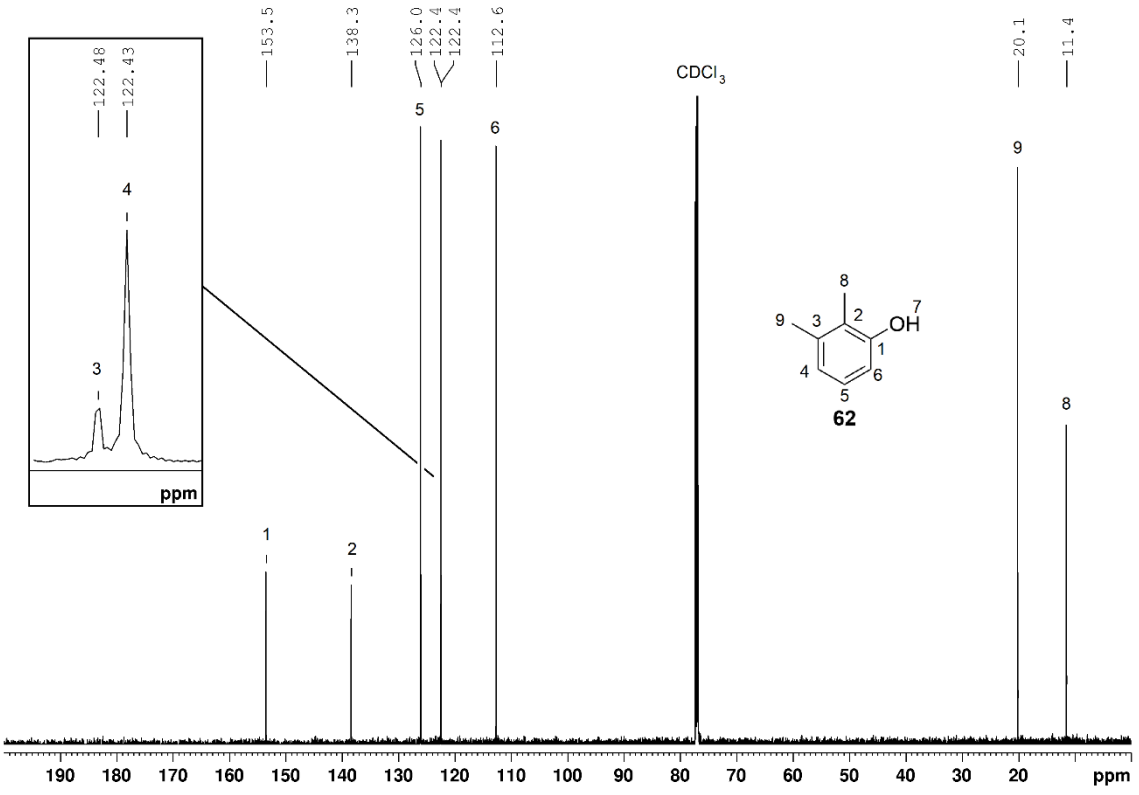


Figure 51. *^{13}C-NMR spectrum of **62***

5.6.8 NMR spectra of **14**

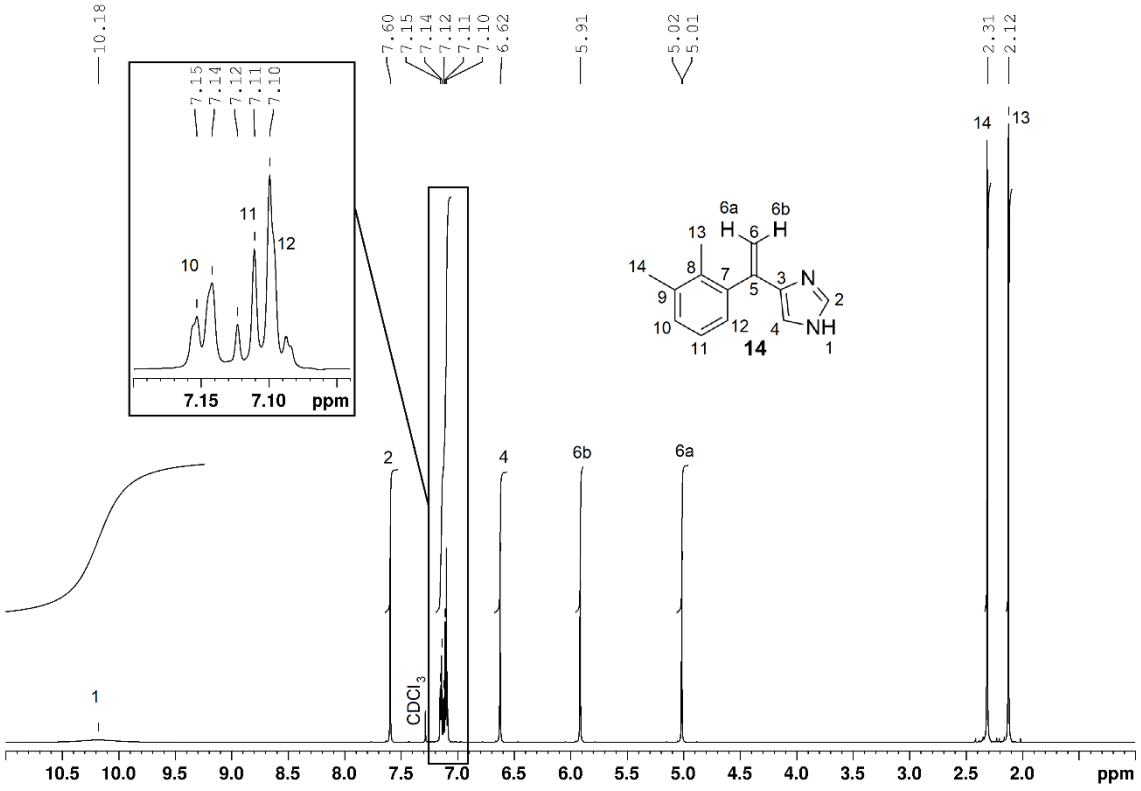


Figure 52. *[1]H-NMR spectrum of* ***14***

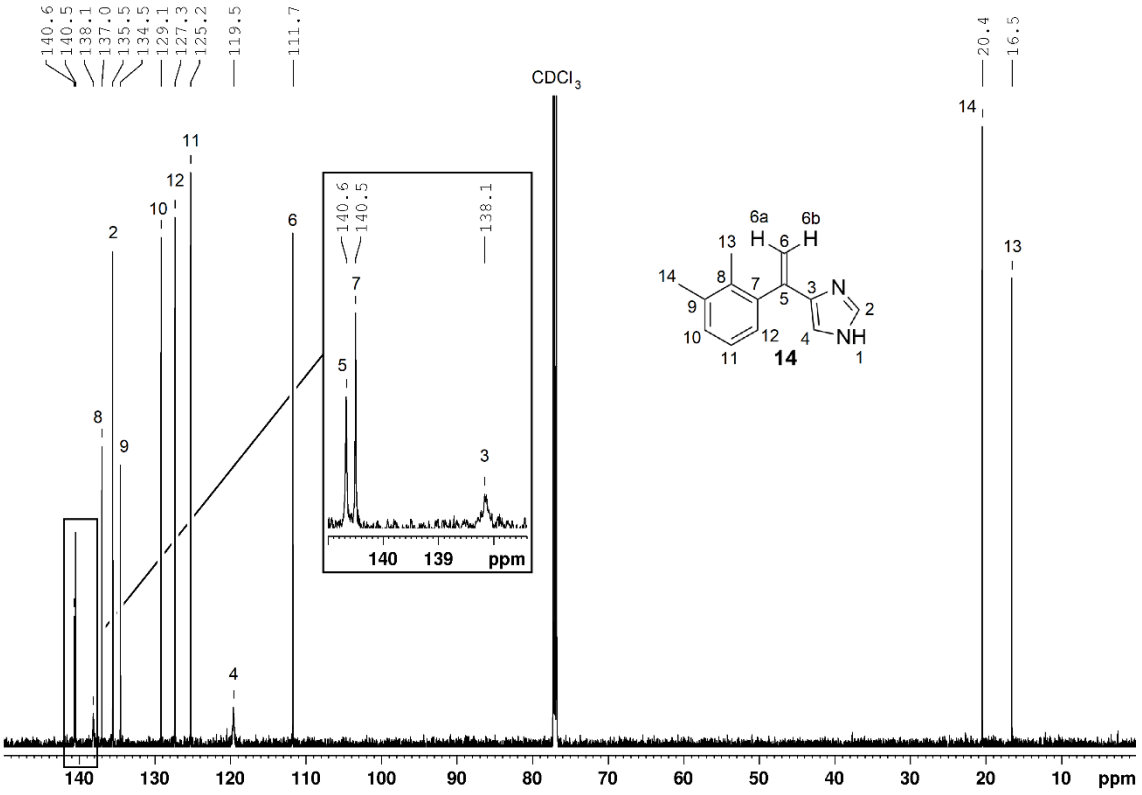


Figure 53. *[13]C-NMR spectrum of* ***14***

5.6.9 NMR spectra of **22**

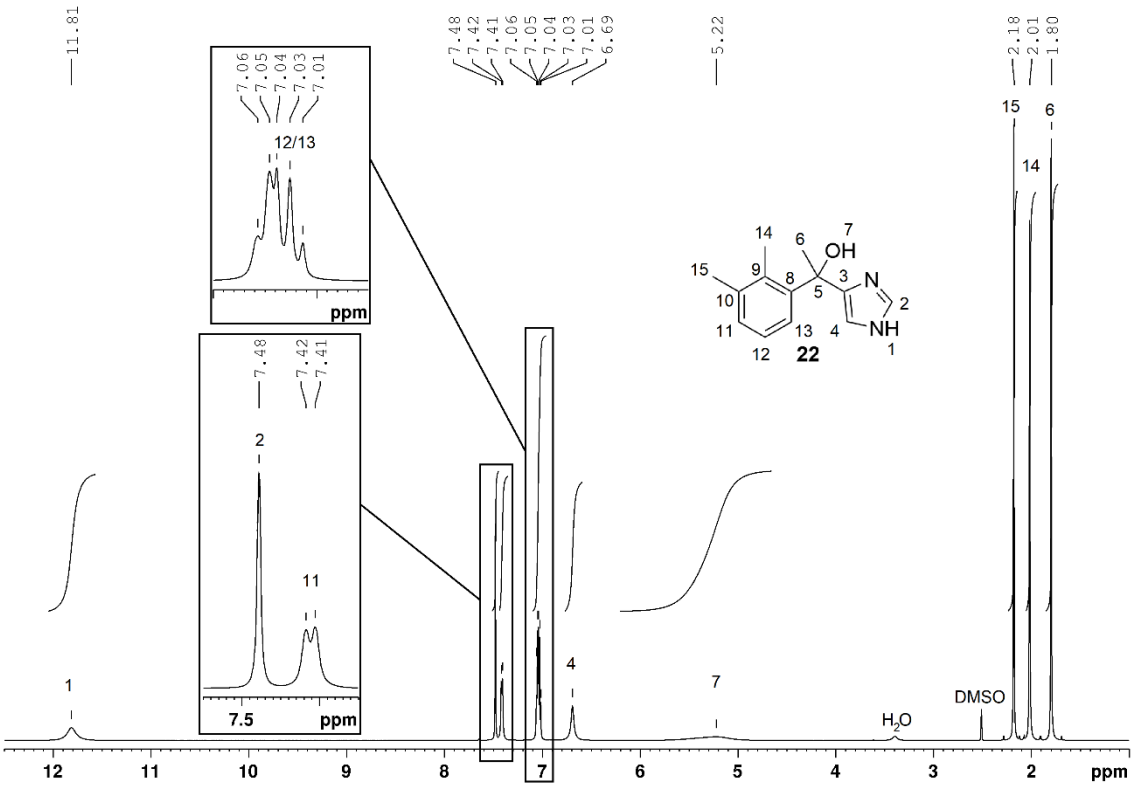


Figure 54. *[1]H-NMR spectrum of **22***

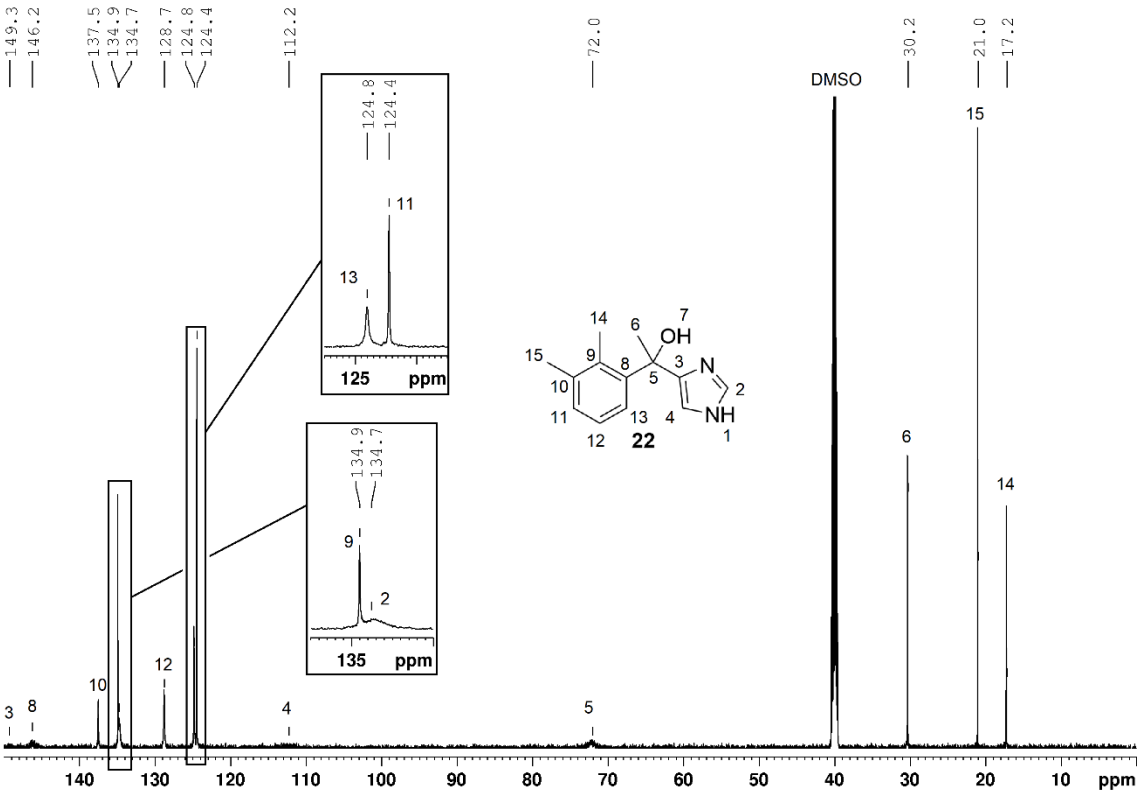


Figure 55. *[13]C-NMR spectrum of **22***

5.6.10 NMR spectra of **32**

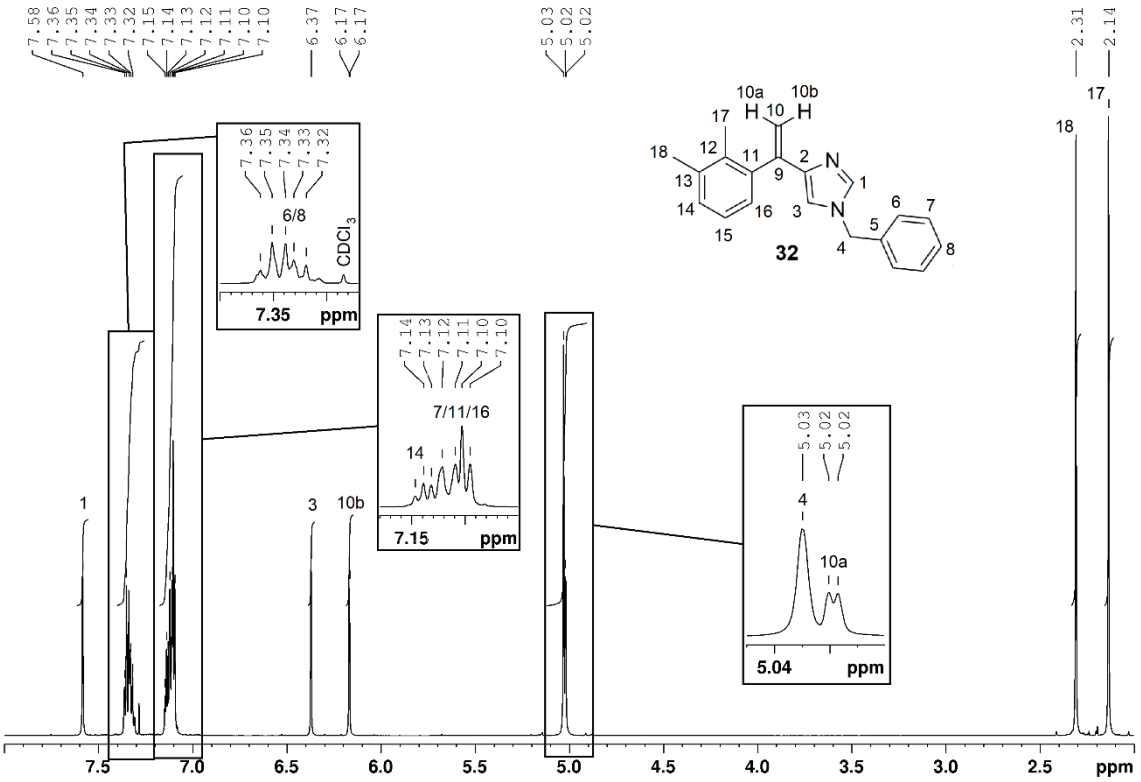


Figure 56. *[1]H-NMR spectrum of* ***32***

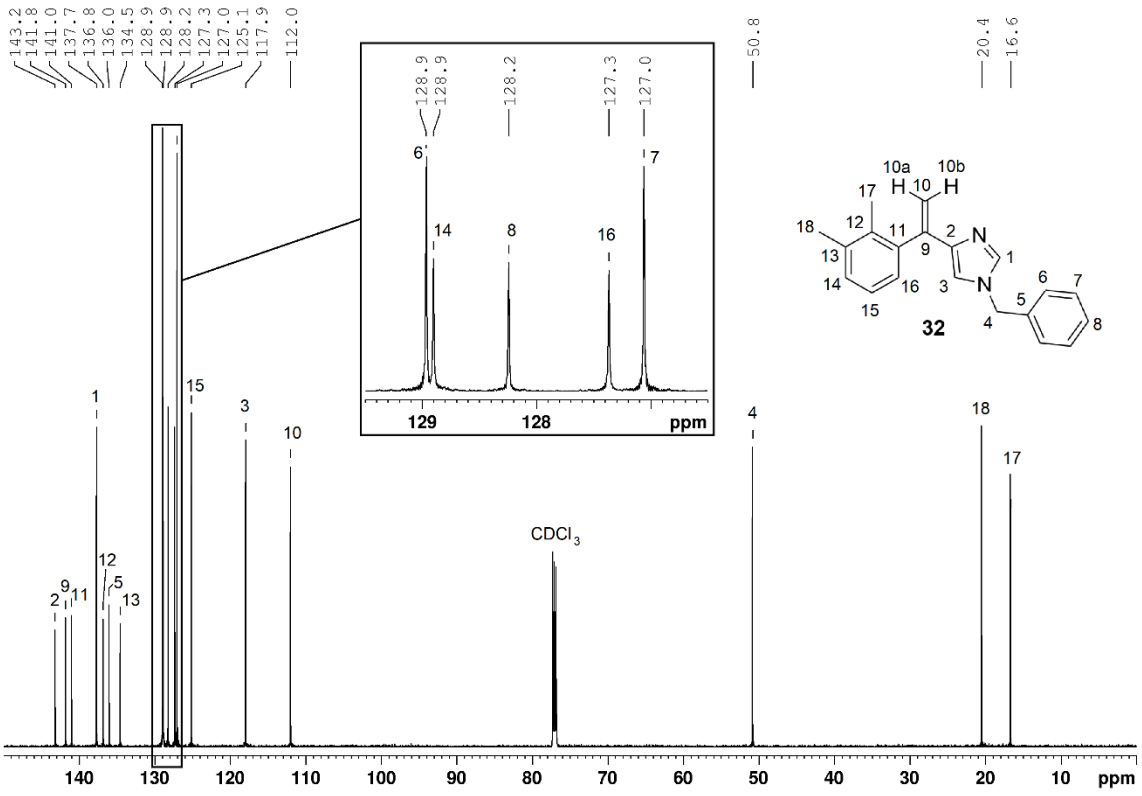


Figure 57. *[13]C-NMR spectrum of* ***32***

5.6.11 NMR spectrum of **66**

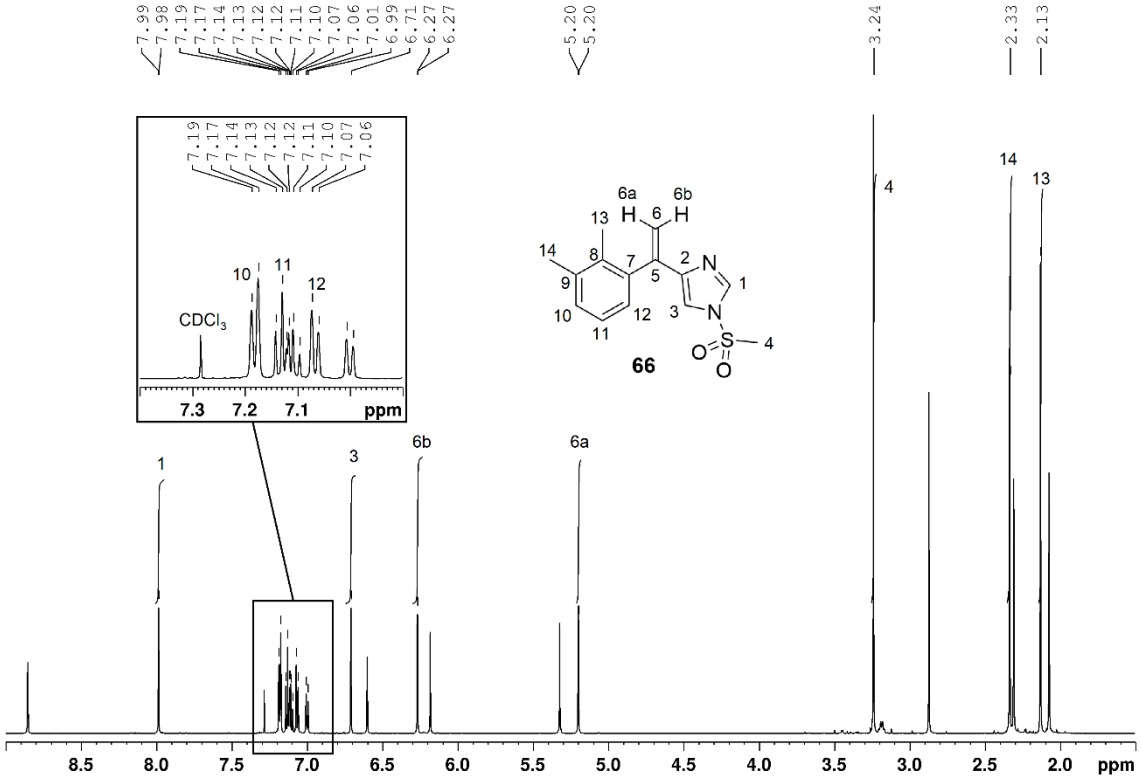


Figure 58. *[1]H-NMR spectrum of* ***66***

5.6.12 NMR spectrum of **79**

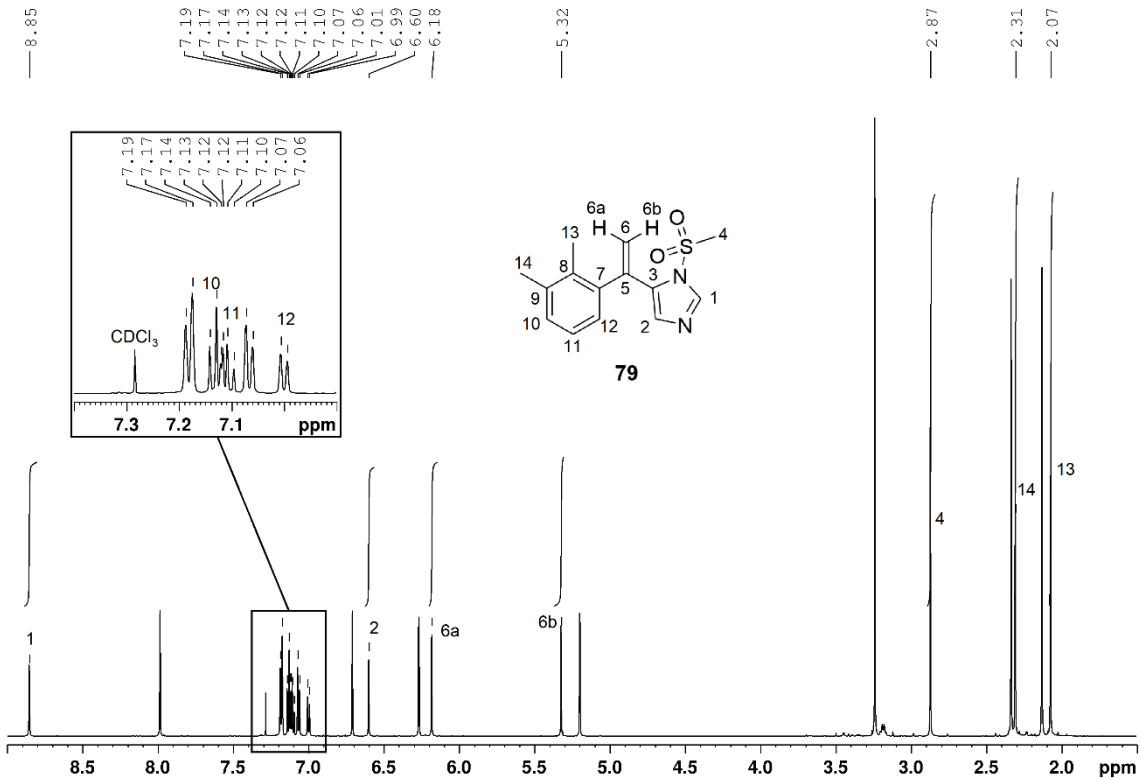


Figure 59. *[1]H-NMR spectrum of* ***79***

5.6.13 NMR spectra of **67**

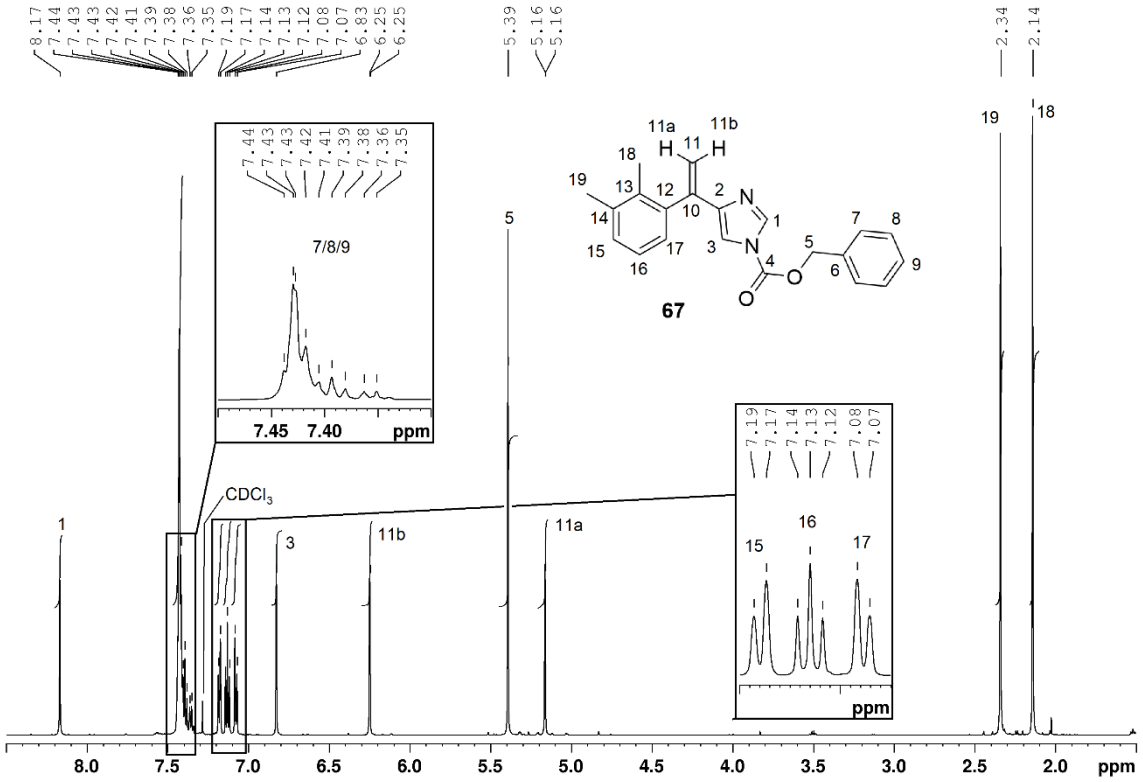


Figure 60. *^{1}H-NMR spectrum of **67***

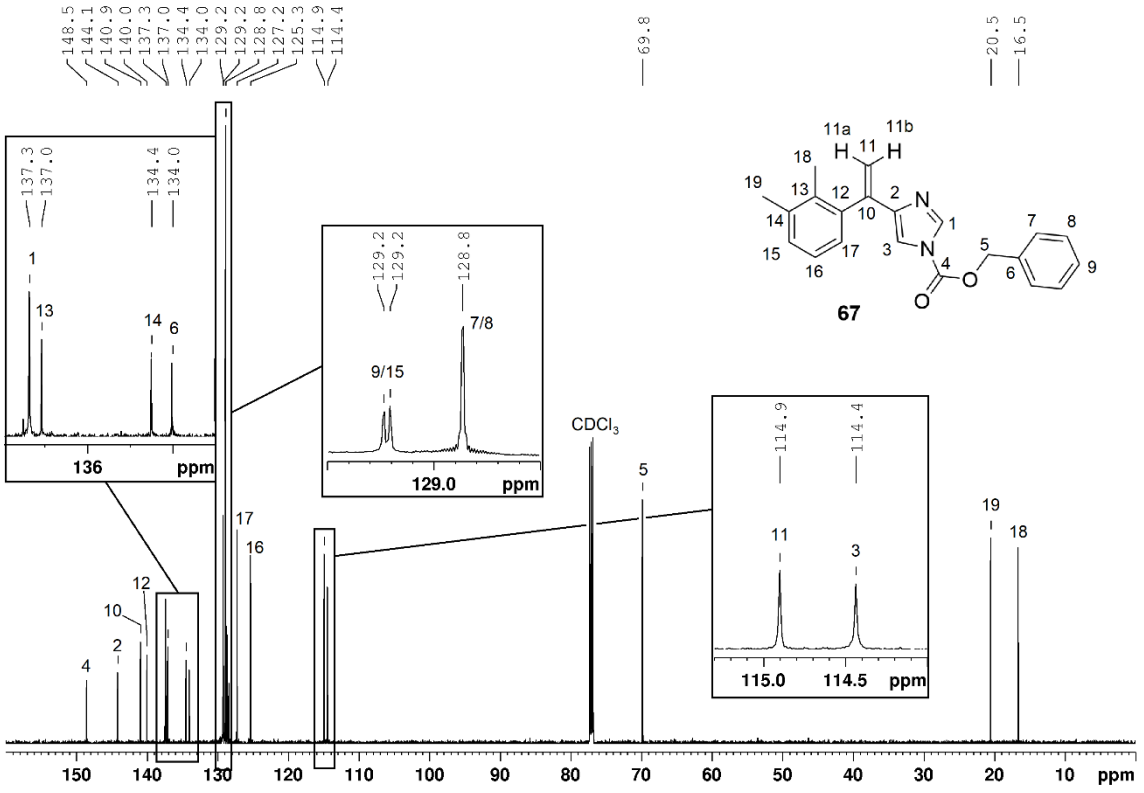


Figure 61. *^{13}C-NMR spectrum of **67***

5.6.14 NMR spectra of **68**

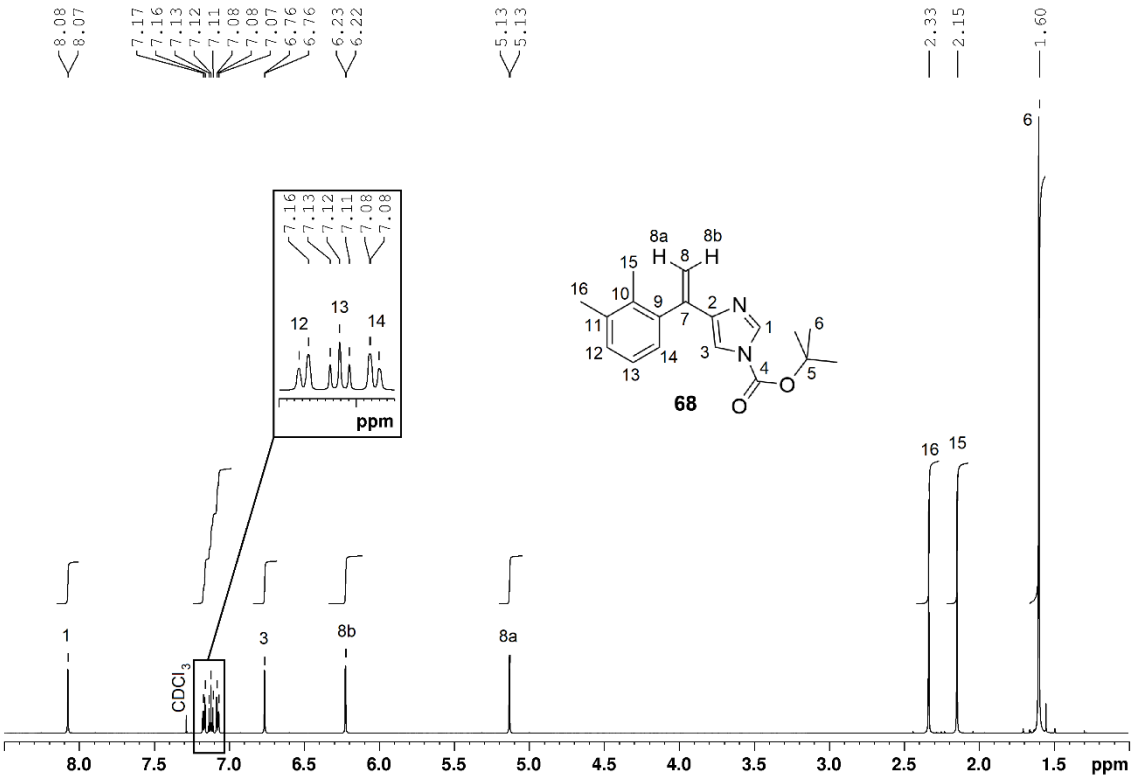


Figure 62. *^{1}H-NMR spectrum of **68***

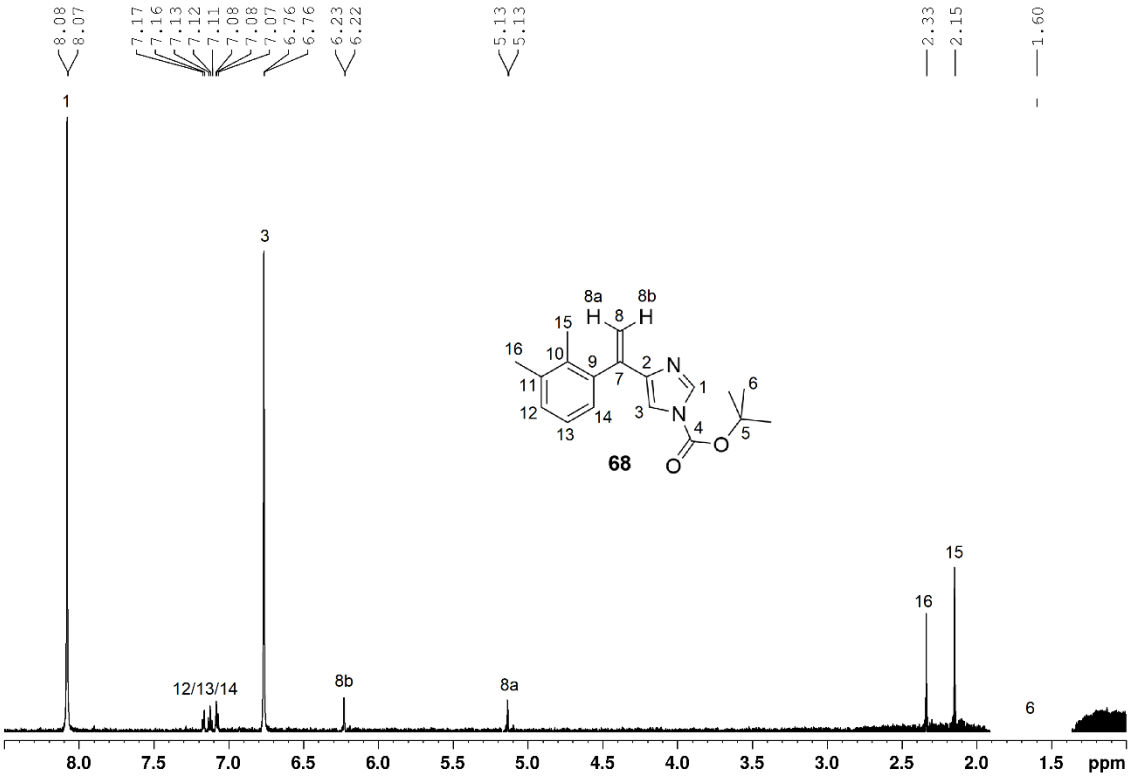


Figure 63. *^{1}H-NOE NMR at 1,60 ppm spectrum of **68***

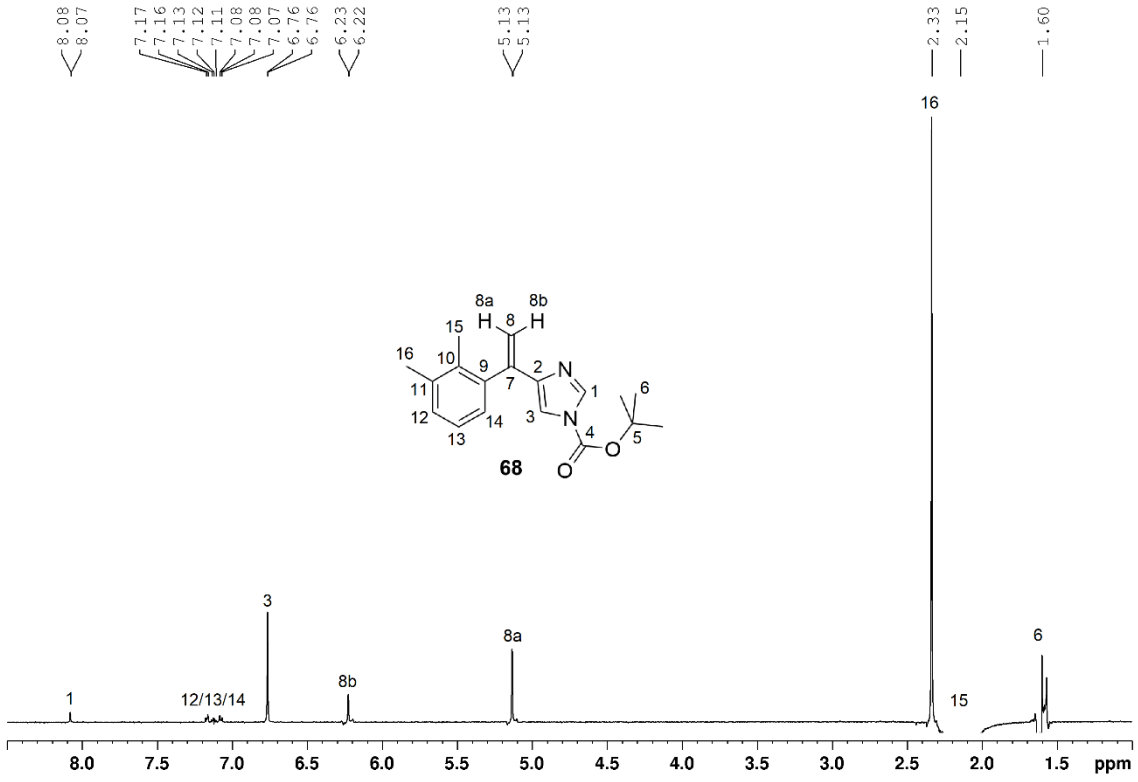


Figure 64. *^{1}H-NOE NMR at 2,15 ppm spectrum of* ***68***

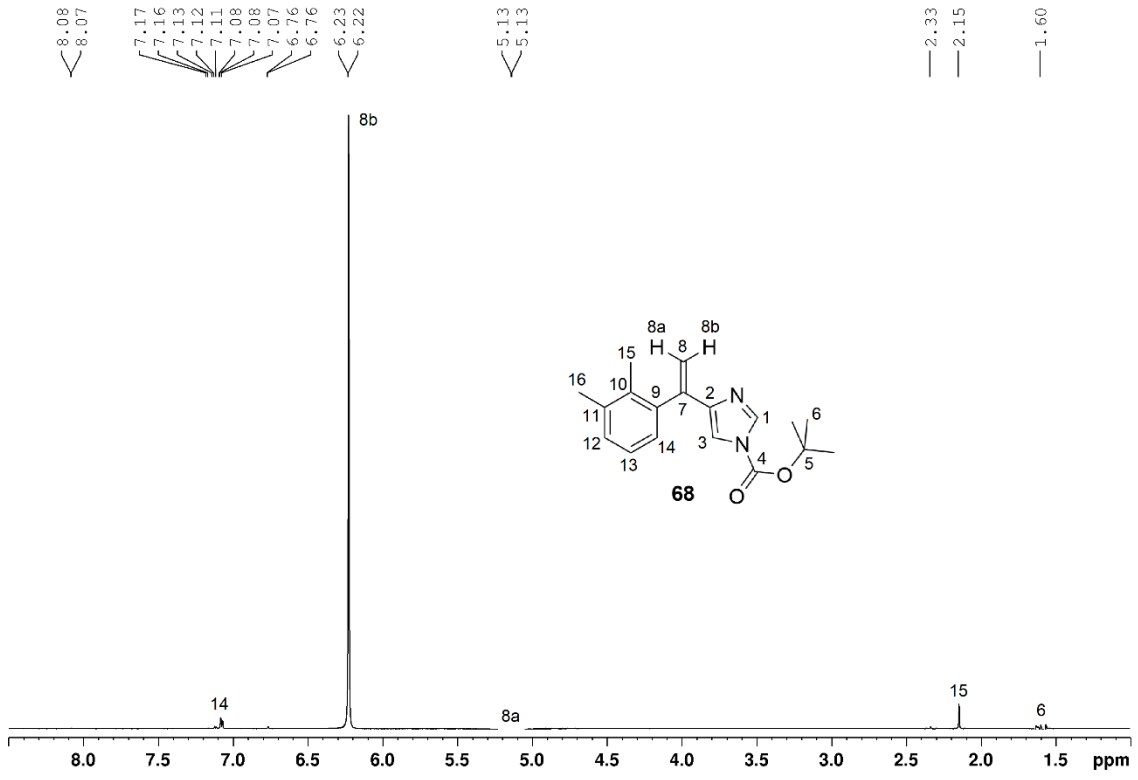


Figure 65. *^{1}H-NOE NMR at 5,13 ppm spectrum of* ***68***

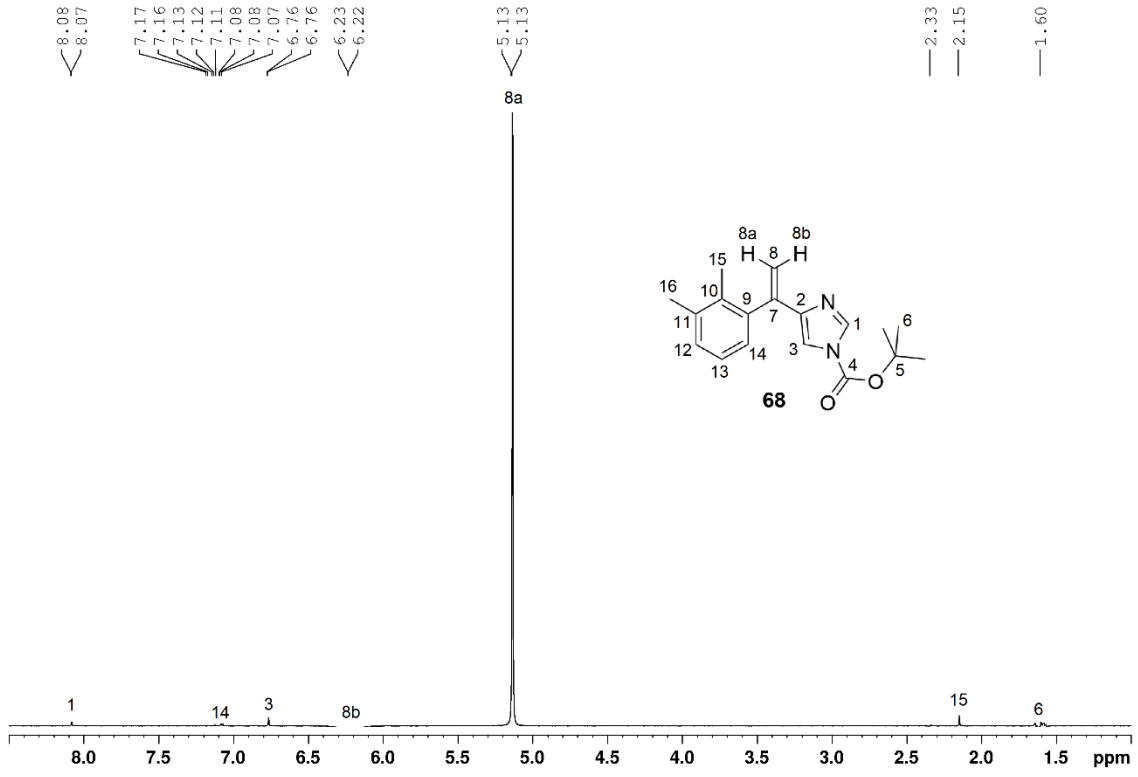


Figure 66. *^{1}H-NOE NMR at 6,23 ppm spectrum of* ***68***

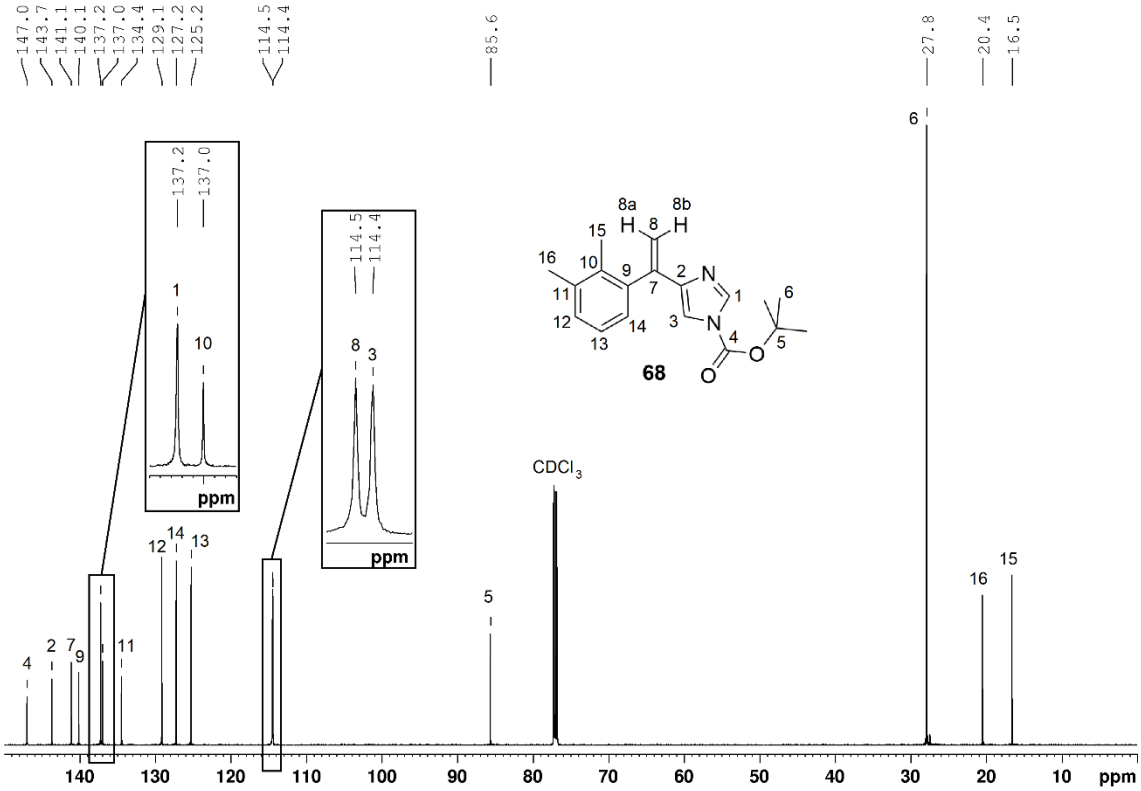


Figure 67. *^{13}C-NMR spectrum of* ***68***

5.6.15 NMR spectra of **69**

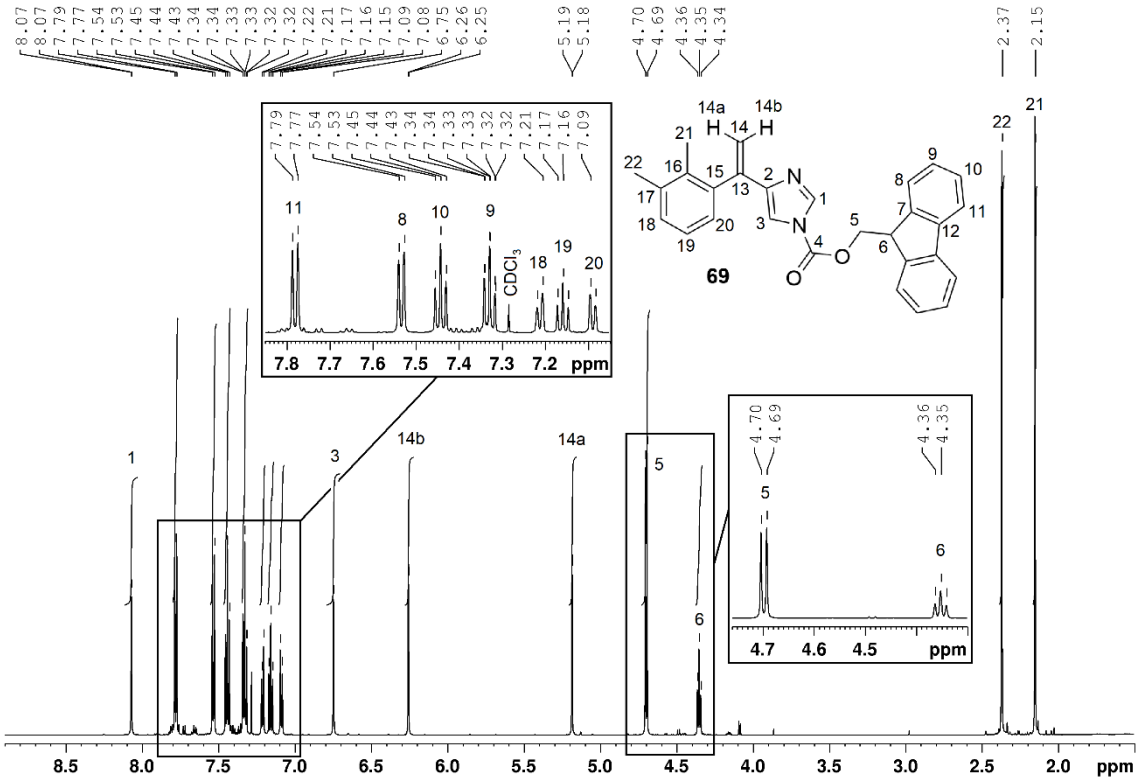


Figure 68. *[1]H-NMR spectrum of **69***

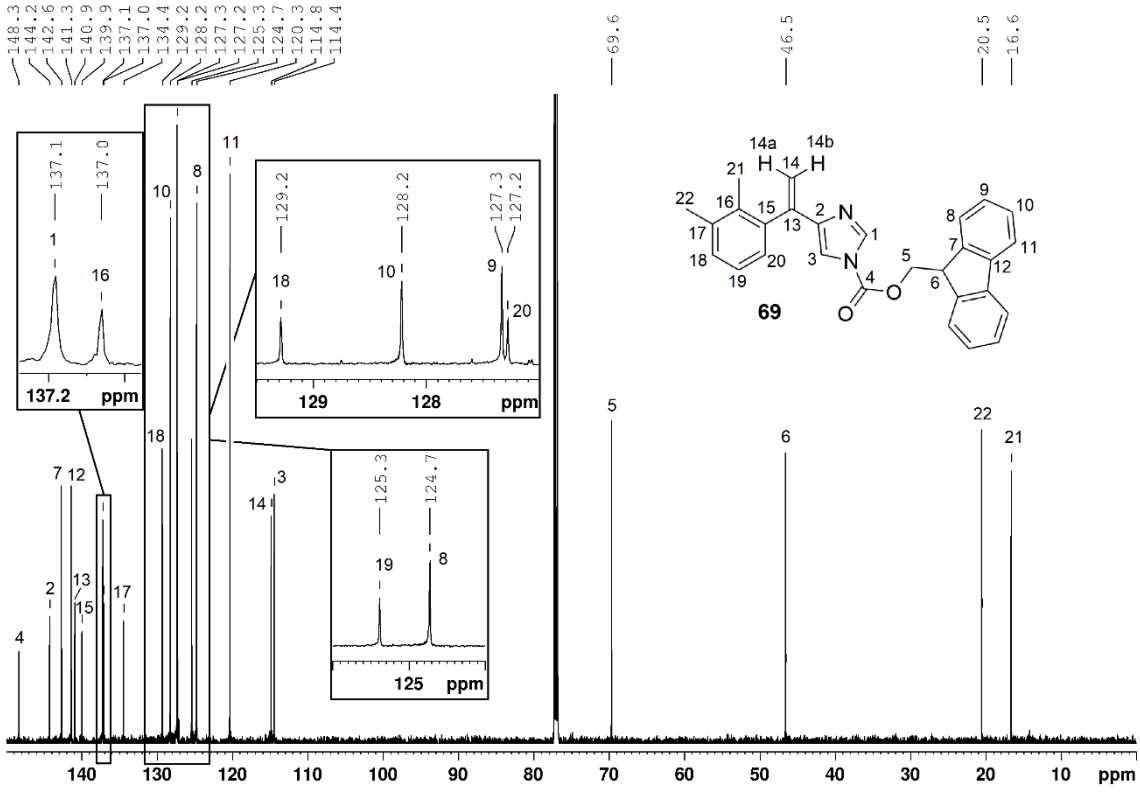


Figure 69. *[13]C-NMR spectrum of **69***

5.6.16 NMR spectra of **70**

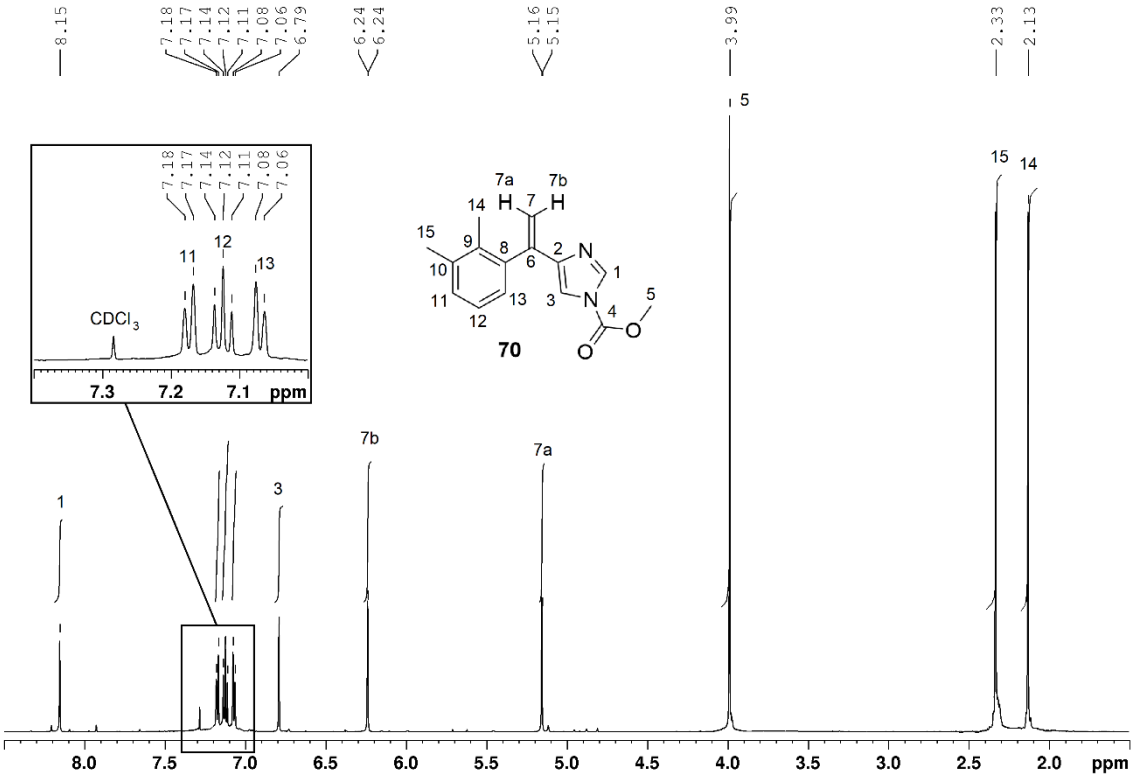


Figure 70. *[1]H-NMR spectrum of* ***70***

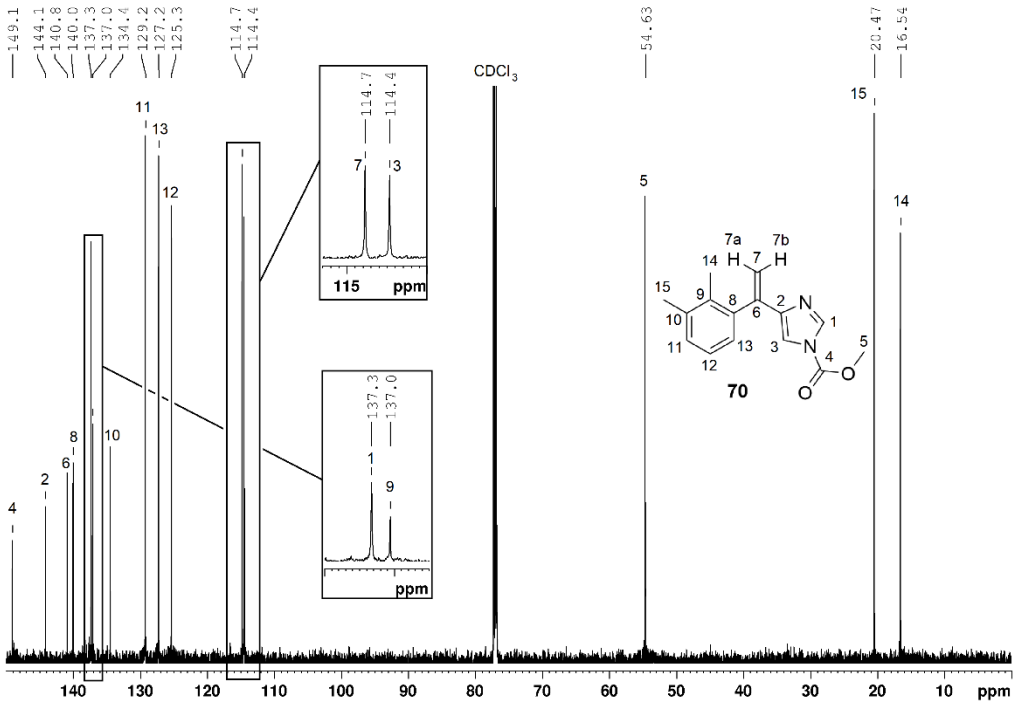


Figure 71. *[13]C-NMR spectrum of* ***70***

5.6.17 NMR spectra of **73**

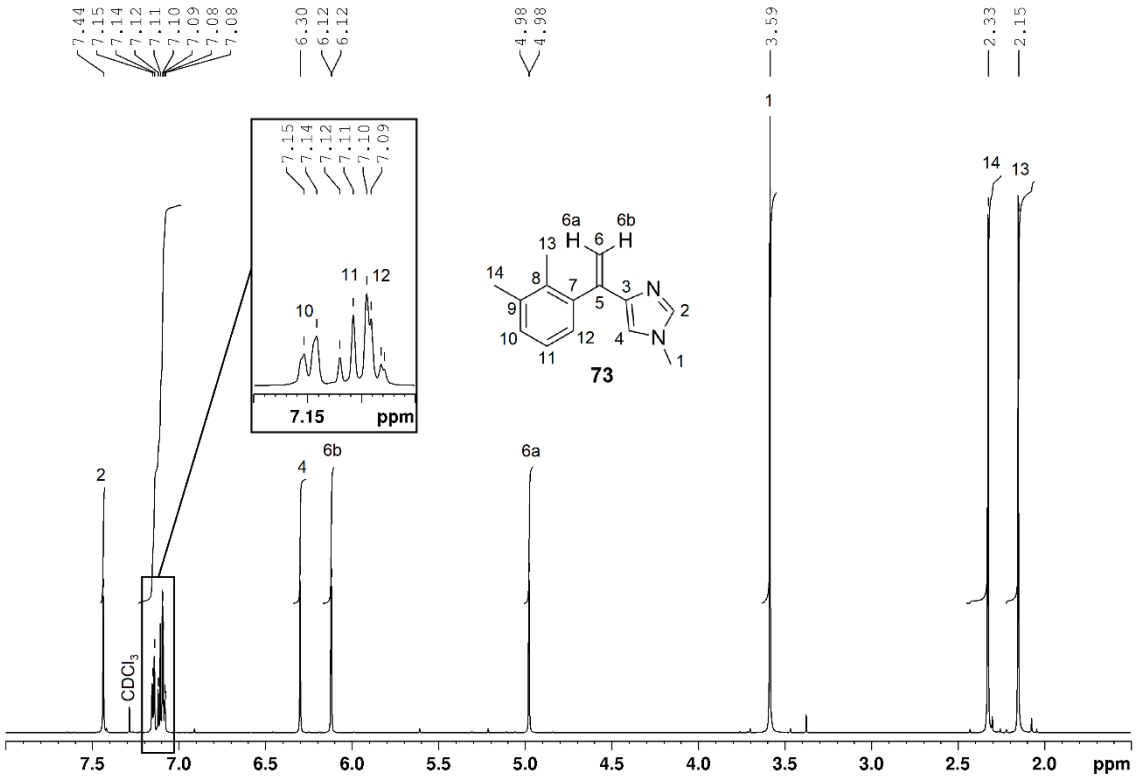


Figure 72. *^{1}H-NMR spectrum of **73***

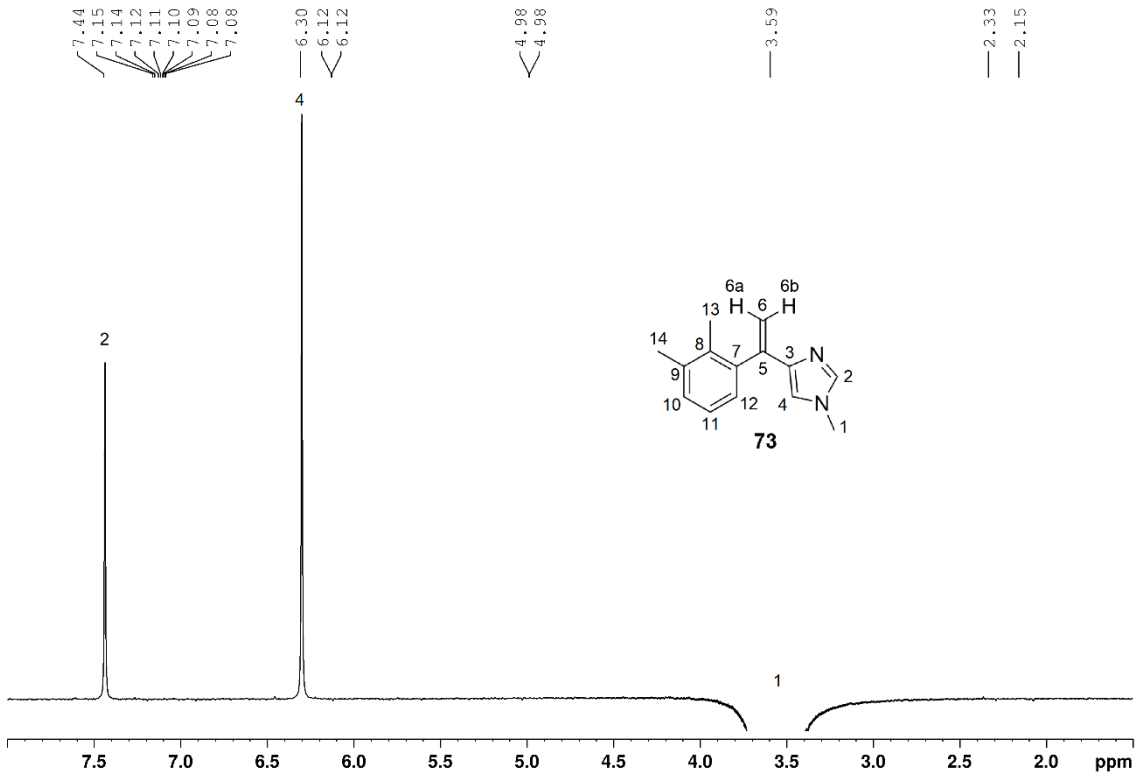


Figure 73. *^{1}H-NOE NMR at 3,59 ppm spectrum of **73***

5.6.18 NMR spectra of **74**

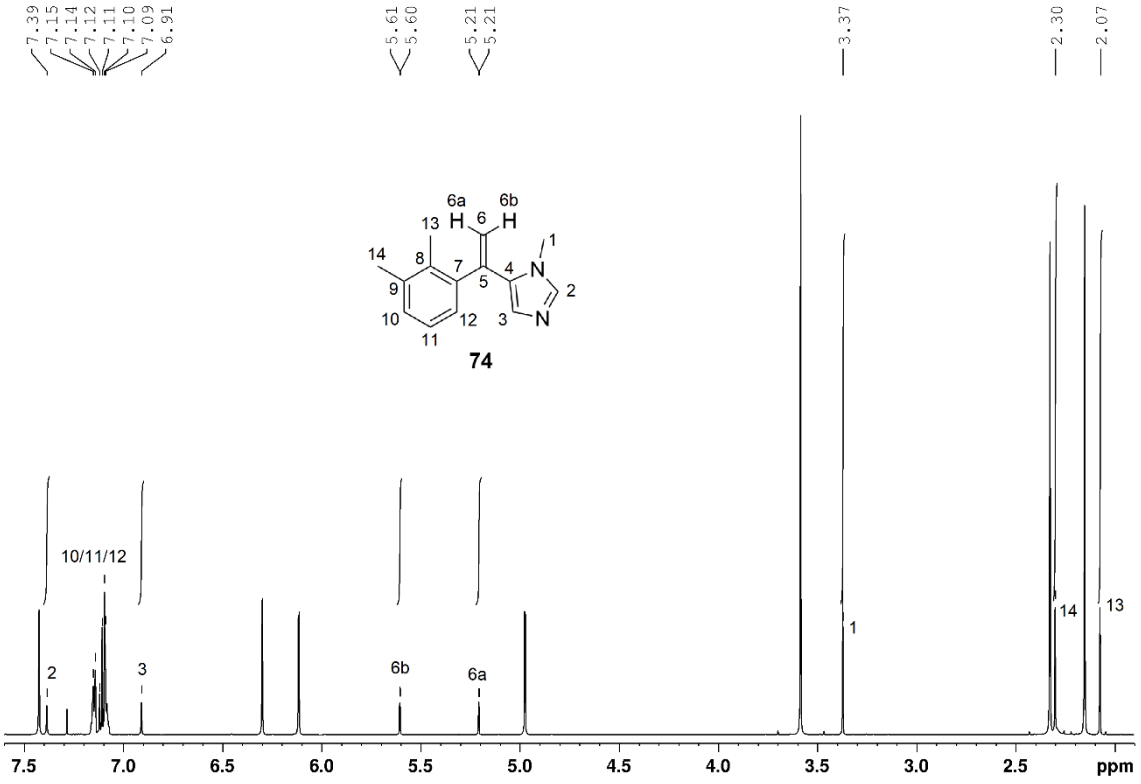


Figure 74. *^{1}H-NMR spectrum of **74***

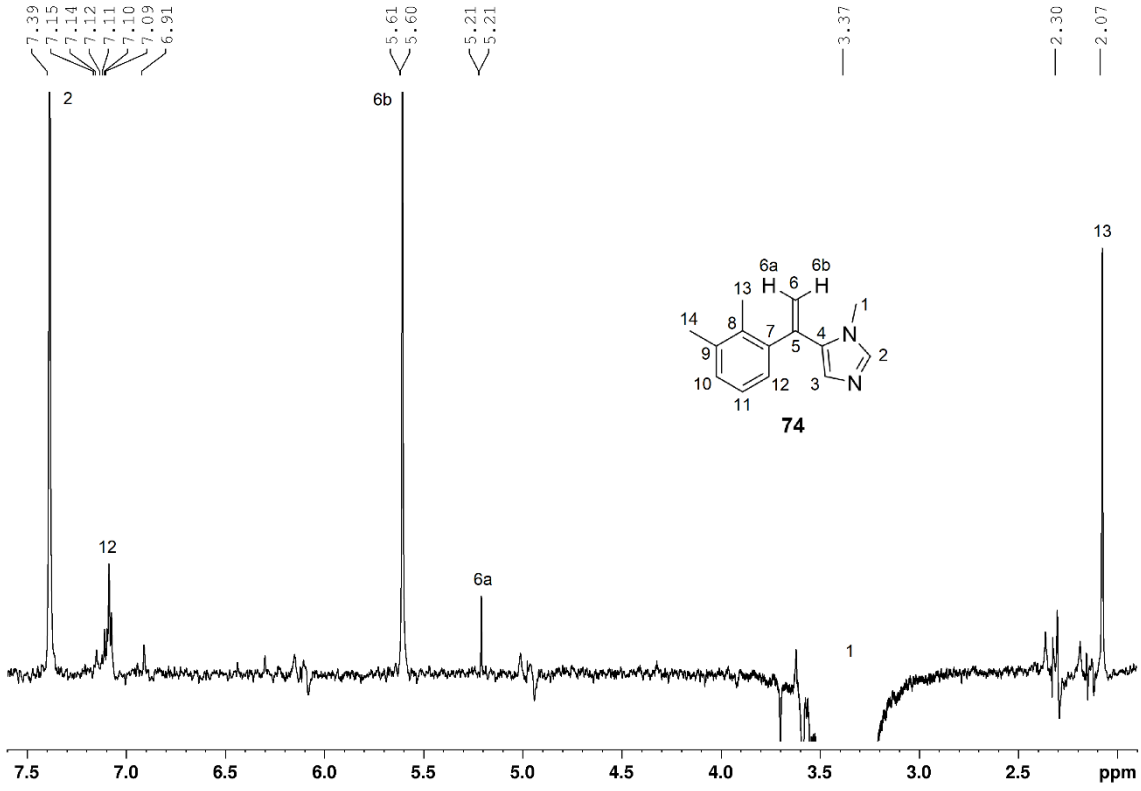


Figure 75. *^{1}H-NOE NMR at 3,59 ppm spectrum of **74***

5.6.19 NMR spectra of **75**

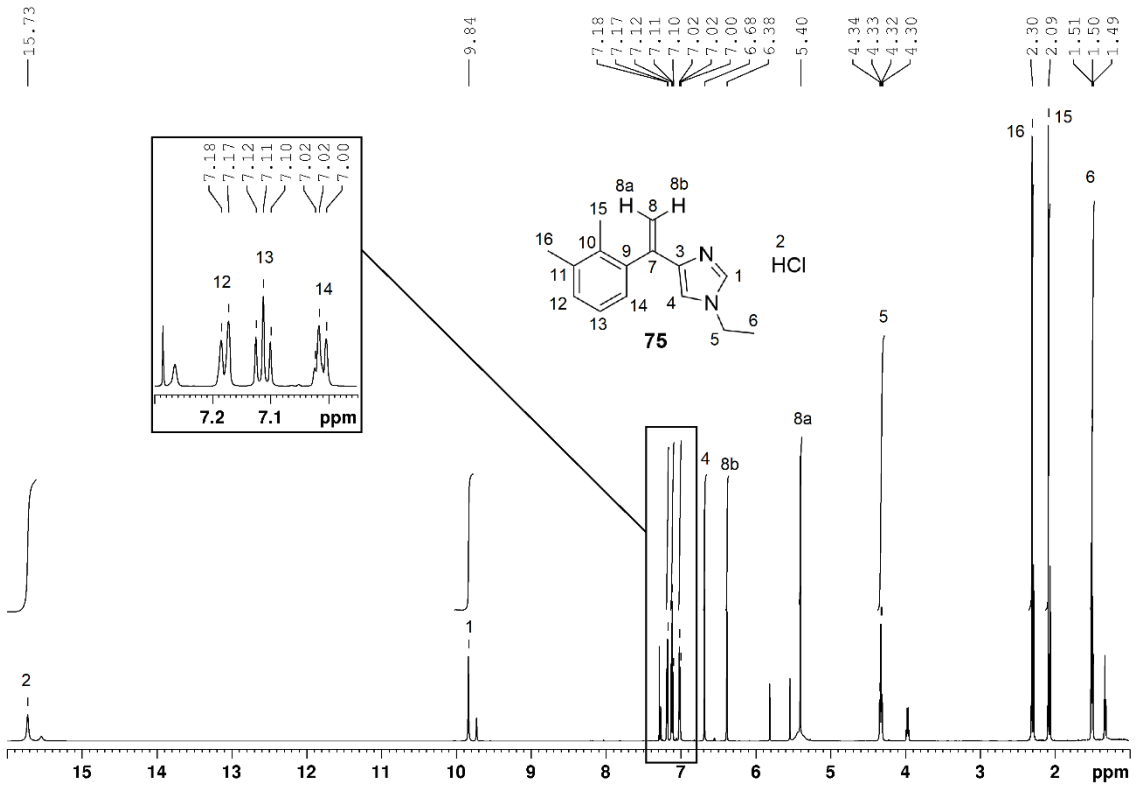


Figure 76. *^{1}H-NMR spectrum of **75***

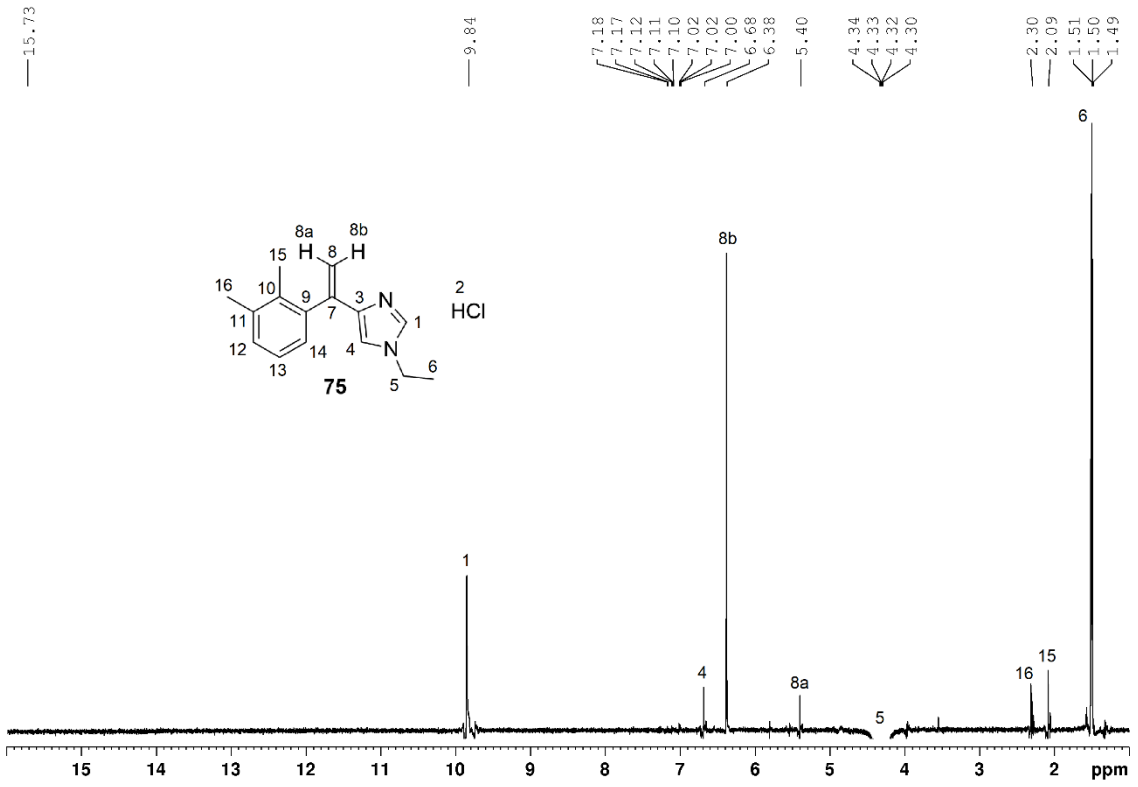


Figure 77. *^{1}H-NOE NMR at 4,32 ppm spectrum of **75***

5.6.20 NMR spectra of **76**

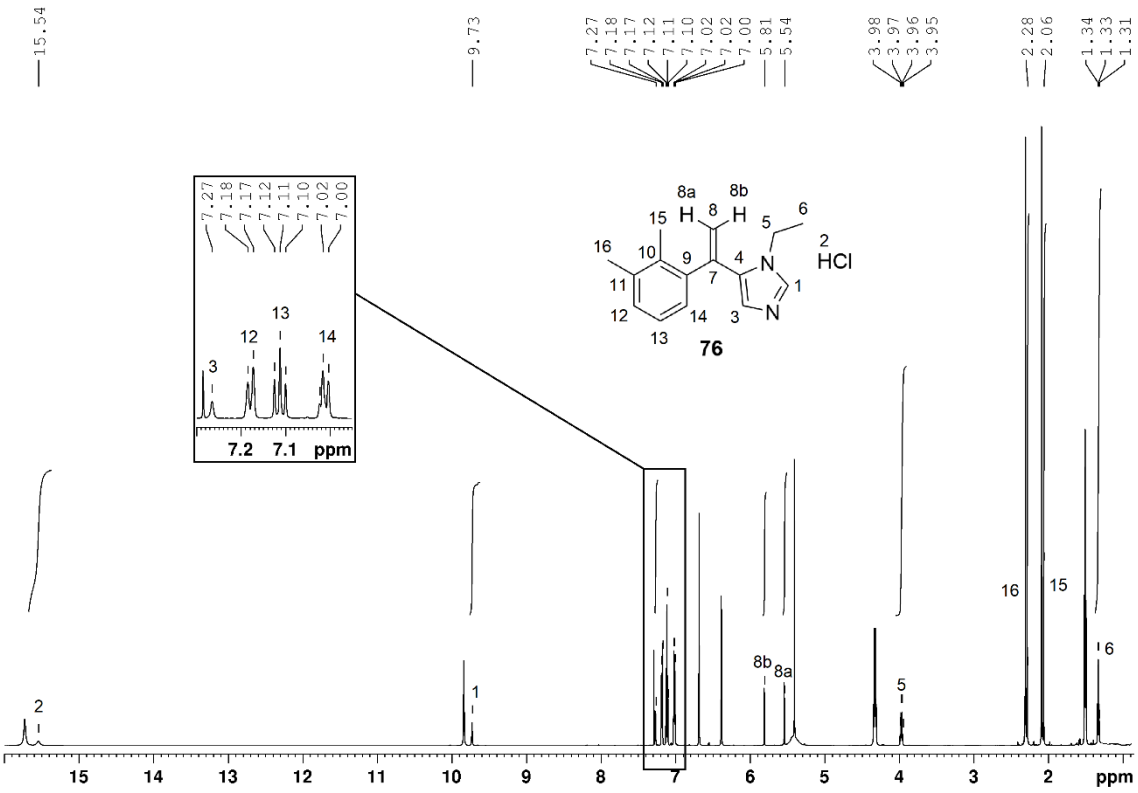


Figure 78. *[1]H-NMR spectrum of* ***76***

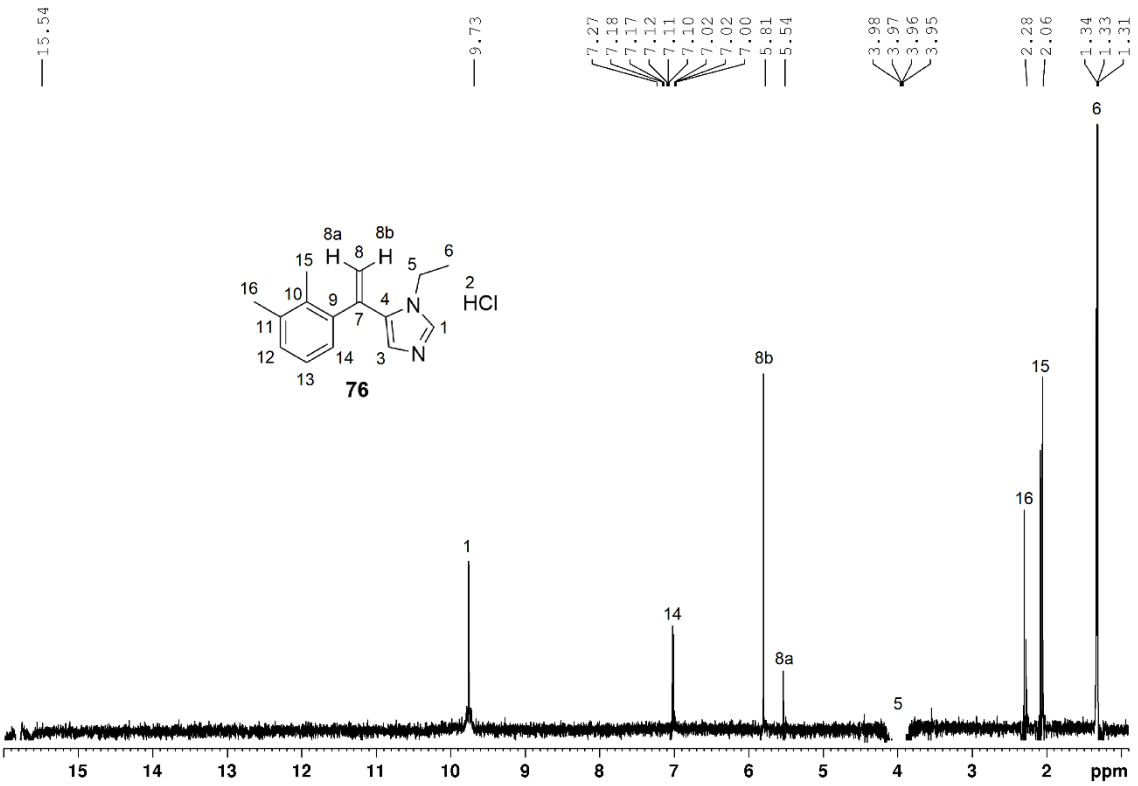


Figure 79. *[1]H-NOE NMR at 3,97 ppm spectrum of* ***76***

5.6.21 NMR spectra of *S*-**8**

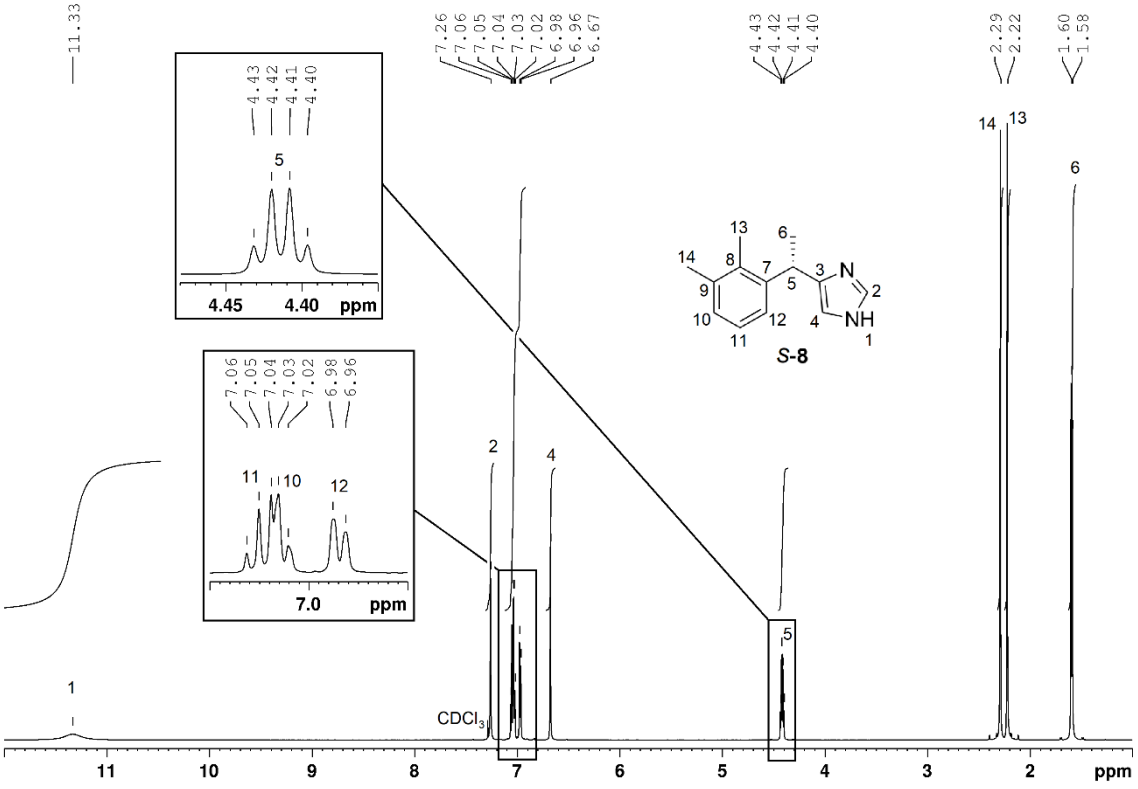


Figure 80. *[1]H-NMR spectrum of S-**8***

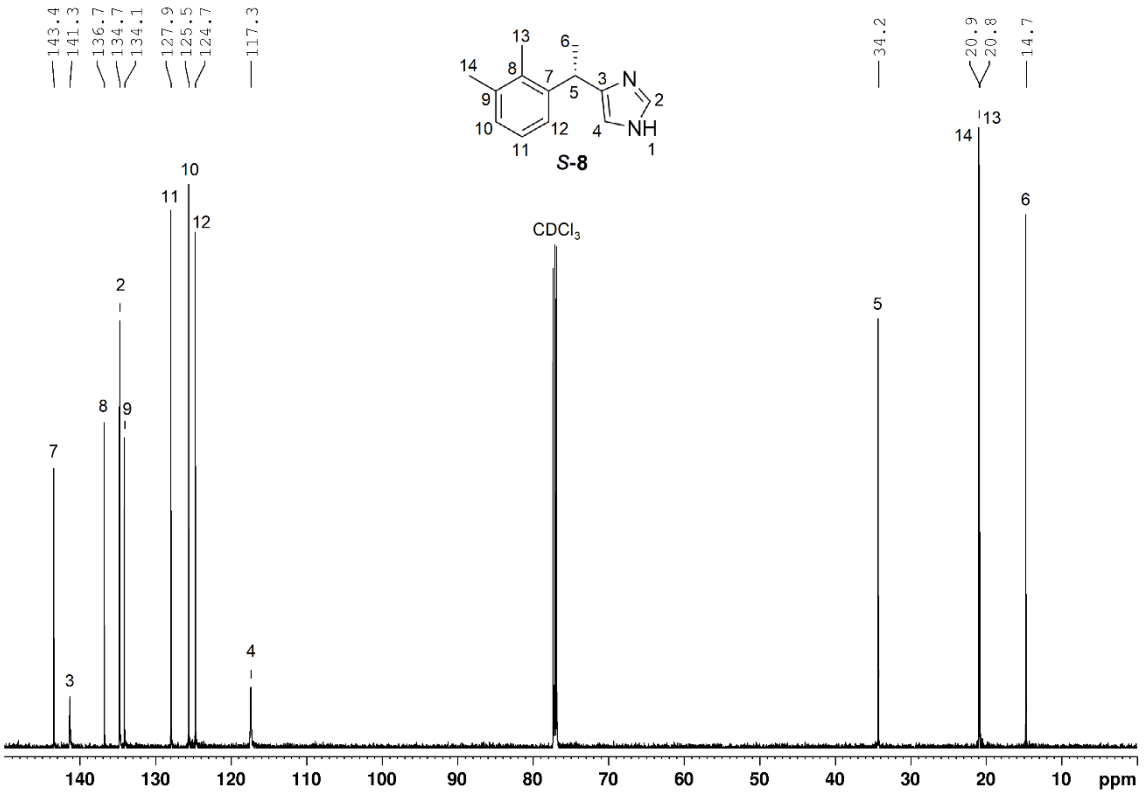


Figure 81. *[13]C-NMR spectrum of S-**8***

5.6.22 NMR spectra of **39**

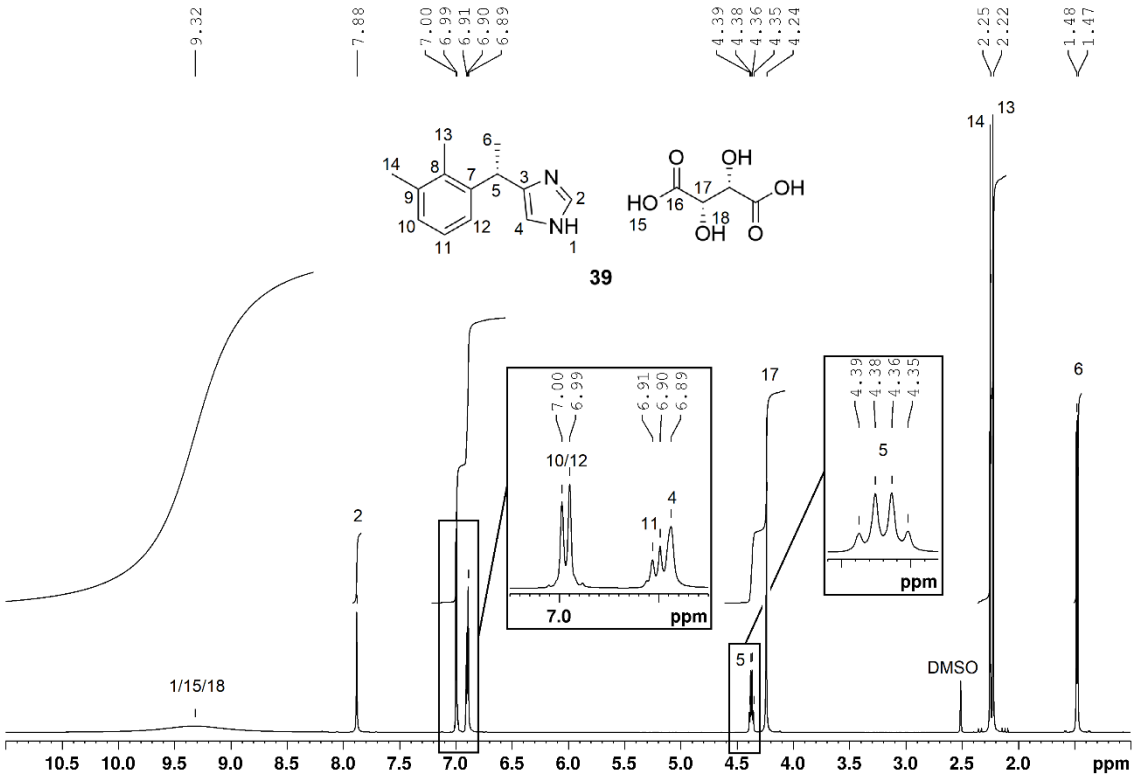


Figure 82. *^{1}H-NMR spectrum of **39***

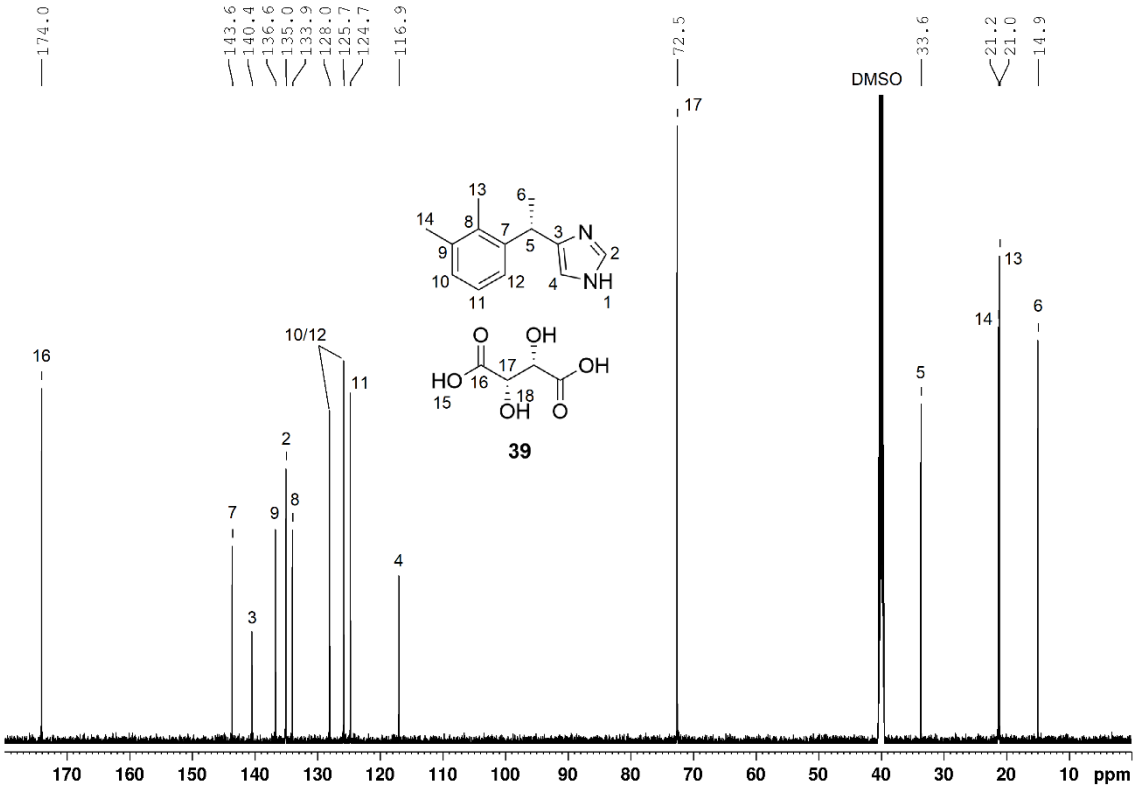


Figure 83. *^{13}C-NMR spectrum of **39***

5.6.23 NMR spectra of **77**

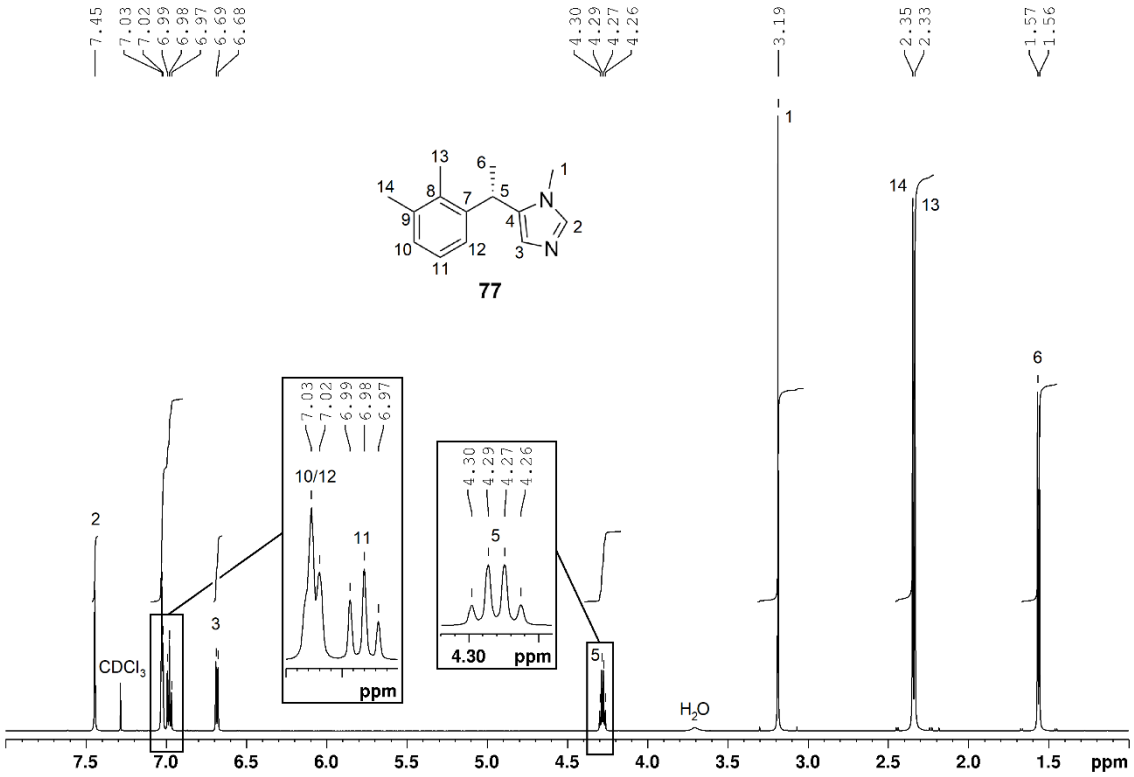


Figure 84. *[1]H-NMR spectrum of **77***

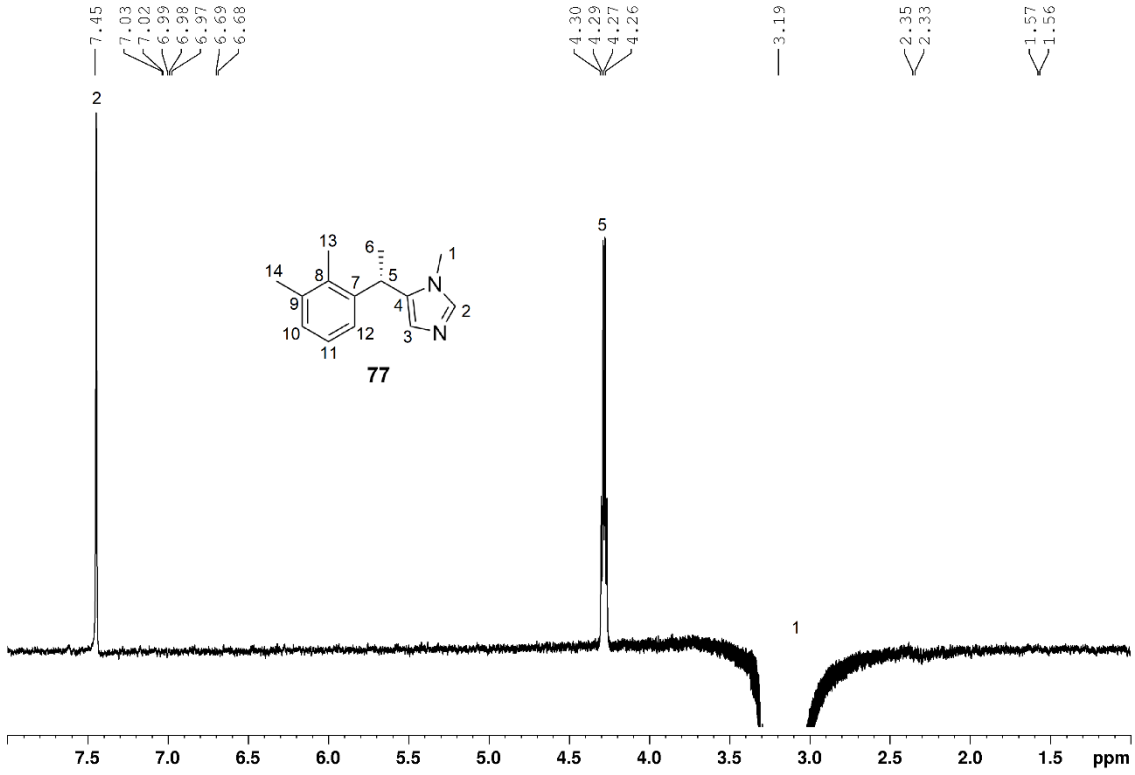


Figure 85. *[1]H-NOE NMR at 3,19 ppm spectrum of **77***

5.6.24 NMR spectra of **80**

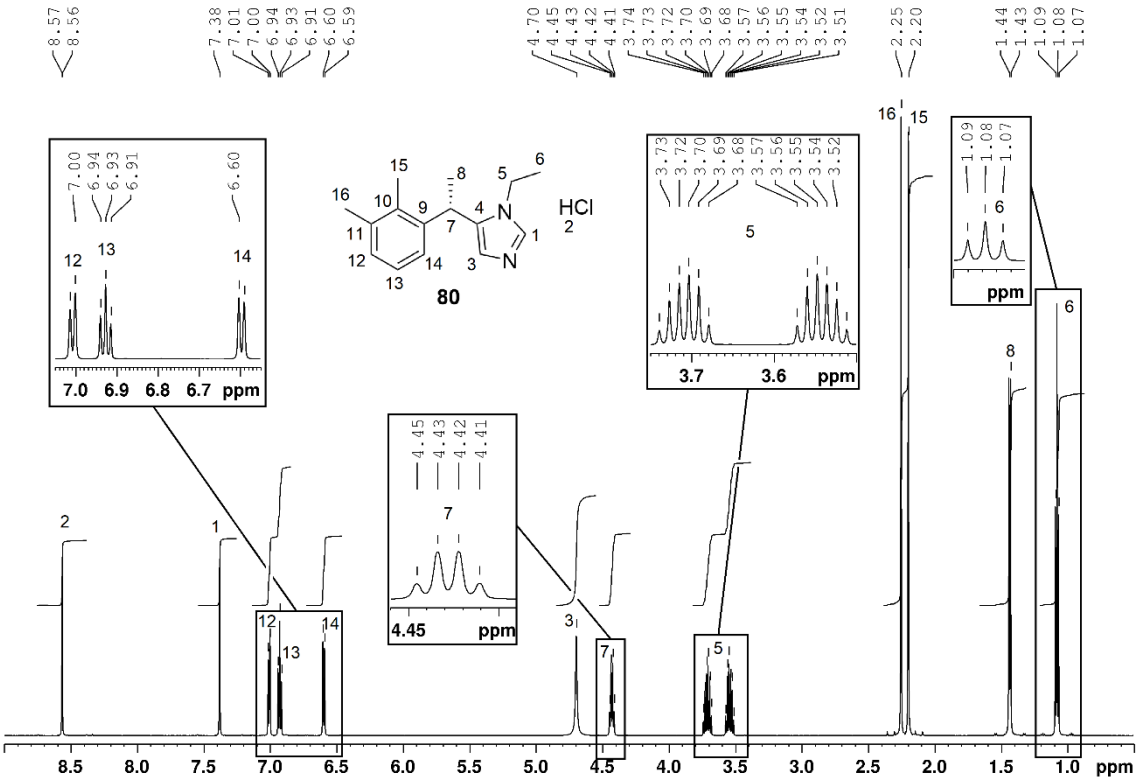


Figure 86. *^{1}H-NMR spectrum of **80***

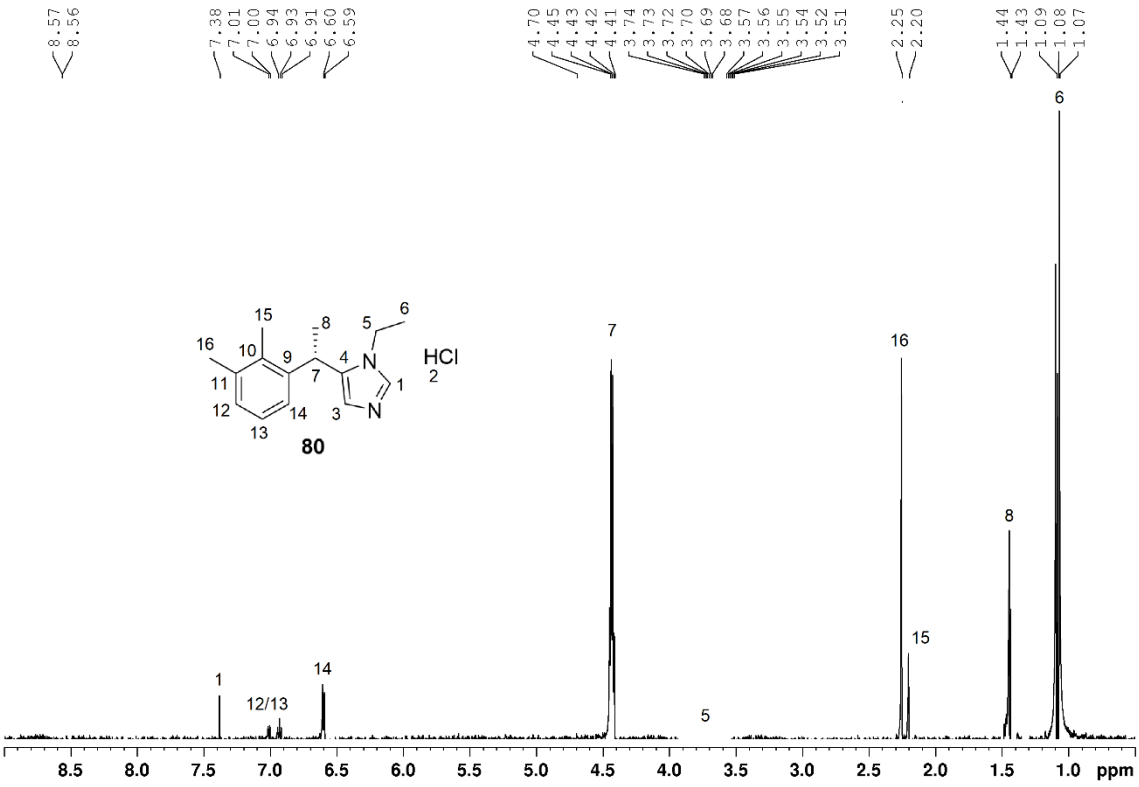


Figure 87. *^{1}H-NOE NMR at 3,71 ppm spectrum of **80***

5.6.25 NMR spectra of *S*-**15**

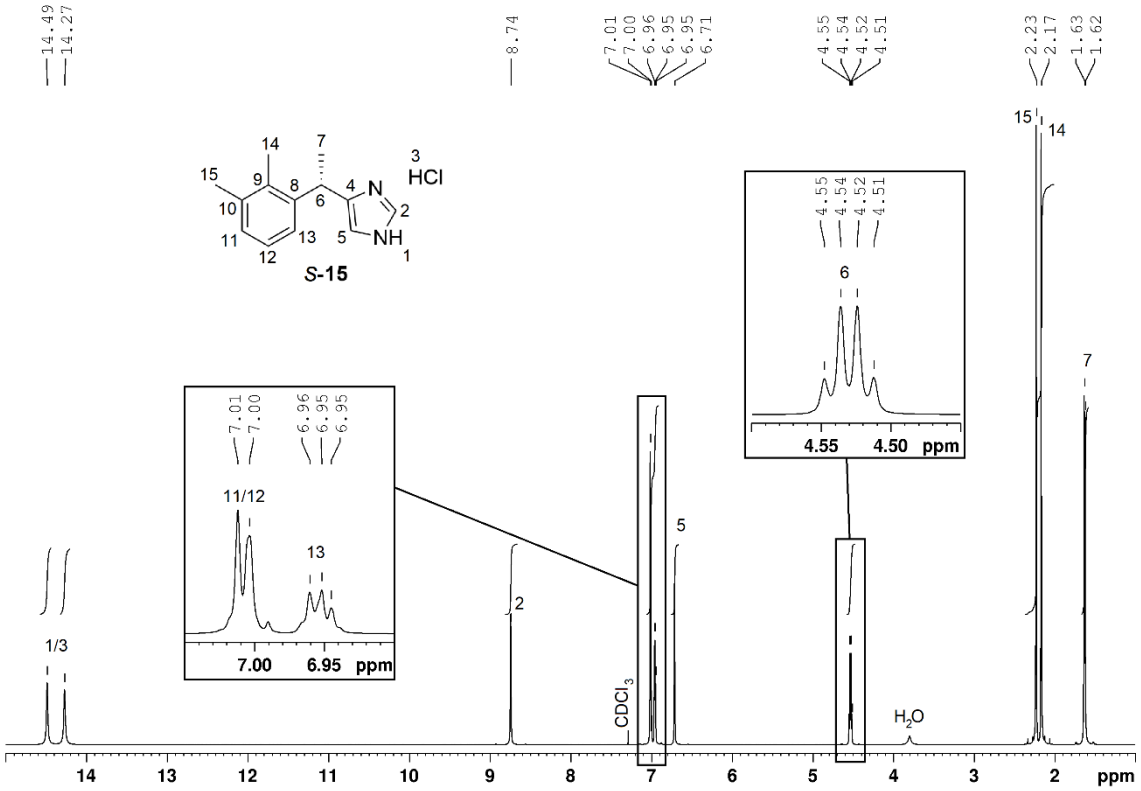


Figure 88. *[1]H-NMR spectrum of S-**15***

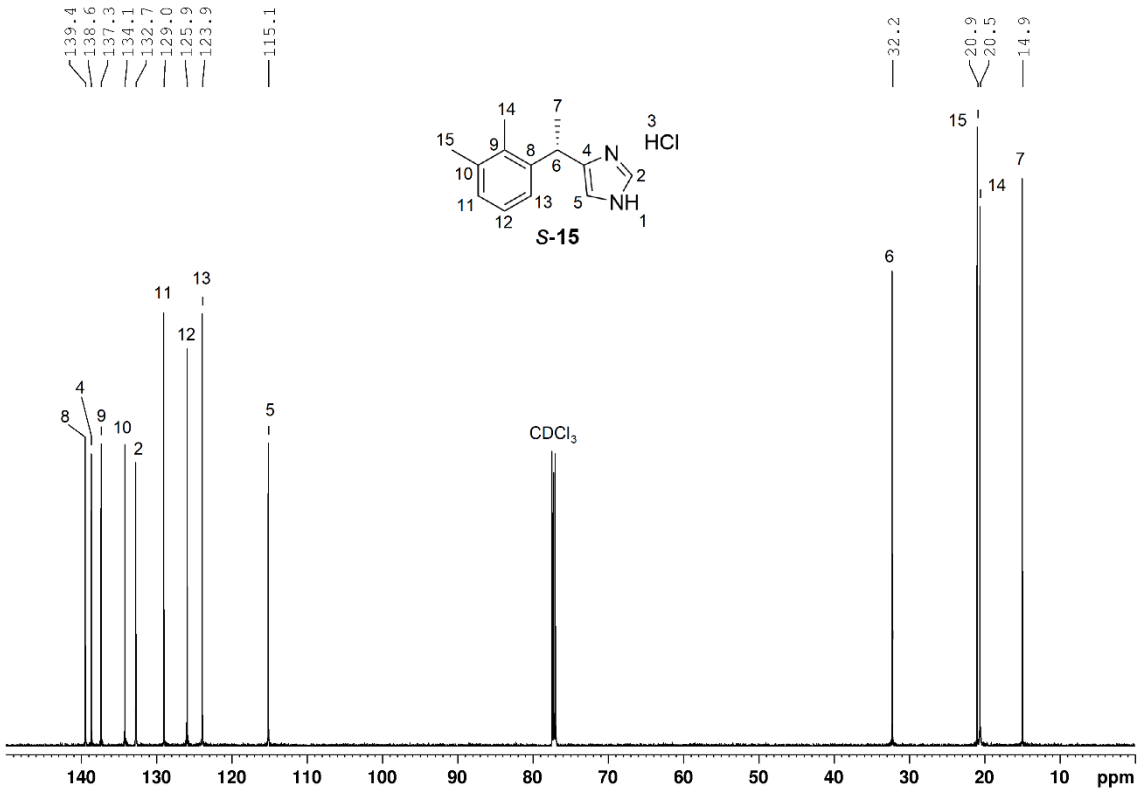


Figure 89. *[13]C-NMR spectrum of S-**15***